



**UCL**

# **Development of novel topical formulations of 5-fluorouracil for treatment of skin cancer and actinic keratosis**

**Shibo Wu**

**Thesis submitted in accordance with the requirements of UCL School of Pharmacy for the degree of Doctor of Philosophy**

**March 2024**

**UCL SCHOOL OF PHARMACY**

29-39 Brunswick Square

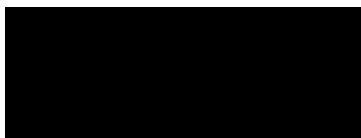
London WC1N 1AX

## Declaration

This thesis describes the research conducted in the School of Pharmacy, University College London between 2019 and 2024 under the supervision of Dr. Majella E. Lane, and Professor Micheal Heinrich. The RNA sequencing was carried out with BGI LTD, which provide raw data for my experimental work.

I certify that the research described is original and that any parts of the work that have been conducted by collaboration are clearly indicated. I also certify that I have written all the text herein and have clearly indicated by suitable citation any part of this dissertation that has already appeared in publications.

Signature: \_\_\_\_\_

A solid black rectangular box used to redact the signature.

Date: 31/07/2024

## Abstract

This study explores improved topical formulations of 5-fluorouracil (5-FU) combined with berberine chloride for enhanced skin cancer and actinic keratosis treatment. 5-FU is a standard therapy for these conditions, but its effectiveness is hindered by systemic toxicity, resistance, and suboptimal pharmacokinetics. Our objective was to develop formulations optimizing 5-FU delivery to, rather than through, the skin, enhancing treatment efficacy while minimizing side effects and resistance.

**Methodology:** Our approach utilized in vitro assays and RNA sequencing to assess cell cytotoxicity and understand the molecular effects of 5-FU and berberine chloride. The synergy of these compounds was evaluated through their impact on cancer cell viability, inflammation, and drug resistance. Pre-formulation studies assessed 5-FU solubility and skin permeation, aiming for high drug retention and minimal systemic absorption.

**Results:** The study found that 5-FU and berberine chloride exhibited a strong synergistic effect in reducing cancer cell viability, notably lowering IC<sub>50</sub> values. RNA sequencing revealed significant gene expression modulation, highlighting the downregulation of inflammation markers and upregulation of apoptosis pathways. Formulation efforts identified propylene glycol/Transcutol (PG/TC) binary systems as superior for 5-FU delivery, further enhanced by isopropyl myristate (IPM) to improve skin retention. The novel Carbopol® ETD 2020 gel formulation demonstrated promising results, outperforming conventional treatments in permeation efficiency and skin retention of 5-FU.

**Conclusion:** This investigation underscores the potential of combining 5-FU with berberine chloride in novel topical formulations to combat skin cancer and actinic keratosis. By enhancing drug delivery and efficacy while reducing adverse effects and resistance, these findings contribute significantly to the field of dermatological oncology treatment.

# Acknowledgments

First and foremost, I would like to extend my deepest gratitude to my lab colleagues. Your daily assistance, guidance, and camaraderie have been invaluable throughout my research journey. Your support and cooperation not only facilitated my work but also made the lab a welcoming and stimulating environment. I am incredibly thankful for the knowledge shared, the teamwork exhibited, and the friendships formed.

Special thanks go to my two supervisors, Dr. Majella Lane and Professor Michael Heinrich. Your long-standing help both academically and personally has been the cornerstone of my development. Your patience, encouragement, and unwavering support have taught me so much. From academic excellence to developing the ability to face and solve problems with persistence and resilience, your mentorship has been instrumental in my growth. I deeply appreciate the time and effort you invested in guiding me through every challenge and milestone.

I am also immensely grateful for your understanding and support during the pandemic and my personal challenges. The unprecedented times brought about by the pandemic posed numerous obstacles, but your flexibility and compassion allowed me to navigate these difficulties. Despite the hardships, including the disruptions to regular lab activities and my own psychological struggles, I have managed to complete this arduous journey, and for that, I am profoundly thankful. Your support has been a beacon of hope during the most trying times.

Lastly, I want to express my deepest appreciation to my wife. Your unwavering trust and encouragement, especially during my low points, have been my anchor. Your constant companionship and belief in me have been crucial in helping me persevere through the toughest times. Your patience, love, and understanding have provided me with the strength and motivation to push forward. Thank you for being my steadfast supporter and for sharing this journey with me. Your presence has made all the difference.

To everyone who has been a part of this journey, your contributions, whether big or small, have collectively brought me to this point. This accomplishment is as much yours as it is mine. Thank you.



Declaration.....	2
Abstract.....	3
Acknowledgments .....	4
Chapter 1: Comprehensive Introduction.....	6
1.1 Anatomy and functionality of human skin.....	6
1.2 Skin permeation .....	11
1.3 Physicochemical factors affecting permeation across human skin .....	13
1.4 Strategies for passive permeation enhancement.....	15
1.5 Skin cancer.....	19
1.6 Topical 5- fluorouracil formulation .....	22
1.7 Improvement of topical formulations of 5-FU .....	24
1.8 Berberine in topical anti-cancer and anti-inflammatory treatment ....	26
1.9 Aims and objectives .....	28
Chapter 2. <i>In vitro</i> cell culture experiments .....	29
2.1 Introduction .....	29
2.2 Aims.....	33
2.3 Materials and methods .....	34
2.4 Results.....	42
2.5 Discussion .....	62
2.6 Conclusion .....	70
Chapter 3. Development of analytical methods and characterisation of model compounds.....	71
3.1 Introduction .....	71
3.2 Materials and methods .....	78
3.3 Results.....	87
3.4 Discussion .....	99
3.5 Conclusions .....	102
Chapter 4. Development of topical formulations containing 5-FU .....	104
4.1 Introduction .....	104
4.2 Aims.....	107
4.3 Materials and methods .....	108
4.4 Results and Discussion .....	113
4.5 Conclusion .....	126
Chapter 5 Conclusions and future work.....	127
5.1 Conclusions .....	127
5.2 Limitations of this work.....	131
5.3 Future work .....	135
References:.....	136
Appendix .....	143

# Chapter 1: Comprehensive Introduction

## 1.1 Anatomy and functionality of human skin

The skin, universally acknowledged as the most substantial organ of the human body, contributes to approximately 10% of an individual's total body weight and encompasses a surface area of nearly 1.7 m<sup>2</sup> (Benson, 2011). It is an intricate organ imbued with multifaceted functions that directly impact several physiological activities.

Primarily, the skin serves as a robust protective barrier, safeguarding the internal body systems from various external perils. These threats encompass harmful microorganisms, ultraviolet (UV) radiation, aggressive chemicals, potential allergens, and excessive water loss (Prescott et al., 2017). Moreover, the skin plays an integral role in the regulation of body temperature and blood pressure, demonstrating its importance beyond mere surface-level protection (Johnson et al., 2016). Another significant function of the skin pertains to its sensory capabilities, mediating external stimuli such as pressure, pain, and shifts in temperature and humidity, thereby allowing the body to respond and adapt accordingly (Filingeri & Havenith, 2015).

Despite being a formidable barrier to the majority of external compounds, the skin simultaneously provides a pathway for the therapeutic administration of agents, allowing for both localized and systemic effects. Human skin is composed of three distinct layers, namely, the epidermis, the dermis, and the subcutaneous tissue or hypodermis, each fulfilling a unique set of functions (Figure 1.1). The skin is also associated with several appendages, including hair follicles, eccrine sweat glands, and apocrine sweat glands.

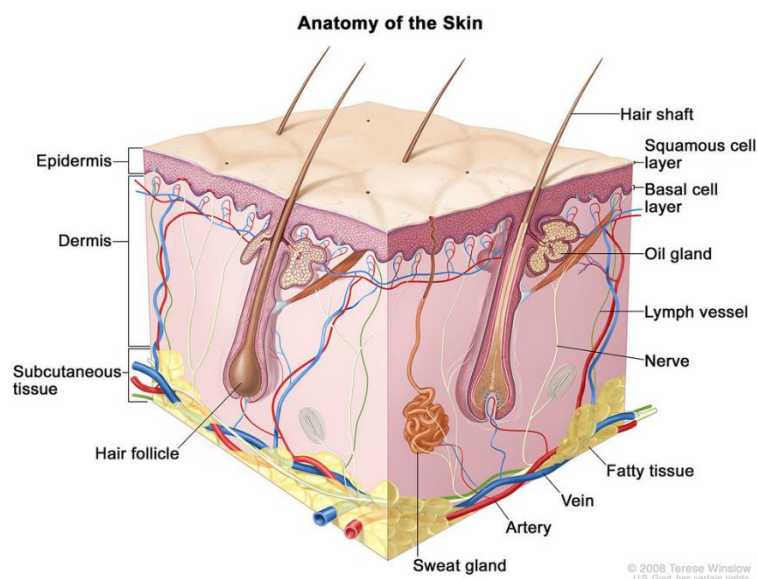


Figure 1.1. A schematic illustration of human skin. Skin anatomy; drawing shows layers of the epidermis, dermis, and subcutaneous tissue including hair shafts and follicles, oil glands, lymph vessels, nerves, fatty tissue, veins, arteries, and a sweat gland. Adapted from Winslow (2008).

### 1.1.1 The epidermis

Characterized as a stratified tissue, the epidermis exhibits variances in thickness contingent on its anatomical location. It extends from 0.8 mm in areas such as the palms and soles to a mere 0.06 mm on the eyelids. This layer is devoid of blood vessels; hence, the epidermal cells source nutrients and discard waste through diffusion across the epidermal-dermal junction. The keratinocyte, which constitutes the predominant cell type in the epidermis, undergoes a maturation process involving migration from the proliferative basal layer to the outermost stratum of the epidermis (Cichorek et al., 2013). The human epidermis is segmented into two regions: the viable epidermis and the stratum corneum (SC). The viable epidermis is further classified into the *stratum lucidum*, *stratum granulosum*, *stratum spinosum*, and *stratum basale* (Figure 1.2). The epidermis maintains a state of constant renewal. Newly formed cell layers of keratinocytes originate at the *stratum basale*. As the cell journeys towards the outer layers, it undergoes a transformation that results in the loss of the nucleus and other organelles to form desiccated, proteinaceous corneocytes before desquamation. This process indicates the transformation of the epidermal cells from the *stratum basale*, through the *stratum spinosum*, *stratum granulosum*, and *stratum lucidum*, culminating in the outermost stratum corneum (Figure 1.2).

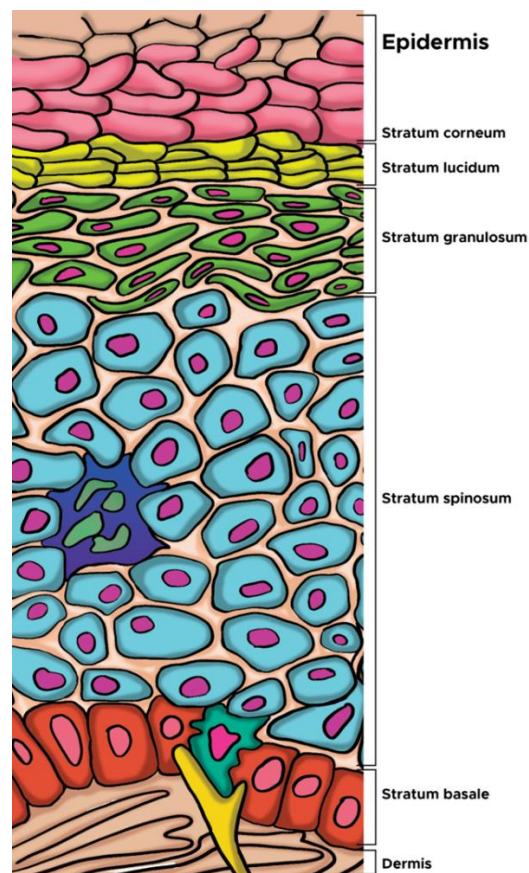


Figure 1.2: Anatomical Layers of the epidermis. Illustration of cells of the epidermis. *Stratum corneum* (Pink Layer at the top), *stratum lucidum* (Clear Yellow Layer beneath the Stratum Corneum), *stratum granulosum* (Green Layer with Darker Green Granules), *stratum spinosum* (Red Layer at the bottom of the Epidermis), *stratum basale* (Red Layer at the bottom of the Epidermis), *dermis* (Brown Area below the Epidermis). Adapted from Rowe (2022).

### 1.1.1.1 Stratum basale

The *stratum basale*, also known as the *stratum germinativum* or the basal layer, is fundamentally the foundation of the epidermis and is positioned as the deepest layer. This is the only active mitotic layer of the epidermis, teeming with an assortment of cells such as Langerhans cells, melanocytes, Merkel cells, and keratinocytes (Yousef et al., 2017). Langerhans cells, which are dendritic cells, predominantly act as the first line of defence in the skin, serving as major antigen-presenting cells. Originating from the bone marrow, they relocate to the *stratum basale* region of the epidermis. Melanocytes, on the other hand, are crucial for the production of the pigment melanin. This pigment acts as a protective shield against ultraviolet (UV) radiation, thus minimizing the release of harmful free radicals in the basal layer (Benson, 2011). Melanocytes are pigment-producing cells located in the basal layer of the epidermis, responsible for colouring our skin, hair, and eyes. While most remain static, a subset actively proliferates. During this process, these cells become rounded before dividing, and the newly formed cells move away from each other. This process is crucial for skin health and potential pathological states. Errors in division could lead to melanocyte clumps, possibly resulting in benign growths like moles, or in more severe cases, melanoma, a serious skin cancer (Taylor et al., 2011). Merkel cells, which are primarily associated with nerve endings, are predominantly found in the touch-sensitive regions of the body such as the hands, lips, and feet. Their strategic positioning suggests a primary role in cutaneous sensation (Haeberle & Lumpkin, 2008). Keratinocytes, the primary cells undergoing cell division in this layer, are responsible for the production of keratin. This keratin helps form the epidermal water barrier by creating and secreting lipids (Yousef et al., 2017). As new cells are generated, existing cells are progressively propelled outward from this layer.

### 1.1.1.2 Stratum spinosum

Following the basal layer is the *stratum spinosum*, also known as the prickly cell layer. This layer, composed of two to six rows of keratinocytes, is situated directly above the basal layer (Fig. 1.2). The morphology of these cells alters from columnar to polygonal, with an enlarged cytoplasm rich with various organelles and filaments. The cells in this layer, which are interconnected by desmosomes, contain keratin tonofilaments. The production of keratin by keratinocytes commences in the stratum spinosum layer. The size of the cell nuclei begins to diminish as the cells migrate away from the *stratum basale* (Benson, 2011).

### 1.1.1.3 Stratum Granulosum

Ascending from the *stratum spinosum*, one encounters the stratum granulosum, where the keratinocytes continue to differentiate. The keratinocytes in this layer appear granular, hence the name *stratum granulosum*. These cells are filled with intracellular keratohyalin granules and membrane-coating granules, which contain lamellar subunits arranged in parallel stacks. These are believed to be the precursors of the intercellular

lipid lamellae of the stratum corneum. The cells generate keratohyalin granules and fibrous keratin proteins. As a result of the accumulation of keratohyalin granules, the cytoplasm of the cells appears granular in this layer. Concurrently, the cells extrude lamellar bodies, which contain lipids and proteins, into the extracellular space and lose their nuclei. This process signifies the death of all other cellular organelles within the cells (Benson, 2011).

#### **1.1.1.4 Stratum Lucidum**

The *stratum lucidum*, distinguishing itself as a thin, transparent layer, is composed chiefly of dead keratinocytes. It earns its name from the unique translucent appearance it exhibits. Within this narrow layer, the nuclei and other organelles of the cells disintegrate, and the cells themselves assume a flattened, compressed form. This layer is generally confined to areas of thick skin, such as the palms of hands and the soles of feet, signifying its particular physiological purpose in these regions (Yousef et al., 2022).

#### **1.1.1.5 Stratum Corneum**

The outermost layer, the *stratum corneum*, is a tightly organized, multilayered structure consisting of 10 to 15 layers of flattened, stacked, and keratinized dead cells. Despite being only 10 to 30  $\mu\text{m}$  thick, this layer, characterized by high density and low hydration cell layers, plays a vital role in skin health and function (Crowther et al., 2008). The *stratum corneum* acts as the first barrier preventing the internal body from losing excessive water, simultaneously shielding us from the external environment. The corneocytes within this layer comprise 70 to 80% protein (primarily keratin) and 20% lipids. This unique structure has often been likened to a “brick and mortar” model, with the “bricks” representing the keratinized dead cells (corneocytes) and the “mortar” referring to the intercellular lipids (Benson, 2011; Kubo et al., 2012). Each “brick” measures about 34 - 46  $\mu\text{m}$  in length, 25 - 36  $\mu\text{m}$  in width, and 0.5 - 1  $\mu\text{m}$  in thickness (Walters & Brain, 2002). The lipid content within these layers is composed of 41% ceramides, 27% cholesterol, 10% cholesterol esters, 9% fatty acids, and 2% cholesterol sulfate (Wertz et al., 1987). Despite the average hydration of the human body being around 70%, the stratum corneum exhibits a much lower hydration level of approximately 15 to 20% w/w. Water present within the stratum corneum is primarily associated with the keratin in the corneocytes (Alexander et al., 2012). Moreover, the density of the stratum corneum is relatively high, about 1.4  $\text{g}/\text{cm}^3$  in the dry state, with a low hydration of 15%–20% (Walters, 2002). Contrary to the high-water permeability of other biological membranes, which show about 1000 times higher permeability, the *stratum corneum* exhibits significantly lower permeability (Potts & Francoeur, 1991). This attribute further underscores its crucial role in barrier function. The exterior of the corneocytes is covered by a cornified cell envelope, a protein/lipid polymer structure that forms just beneath the cytoplasmic membrane (Nemes & Steinert, 1999). This feature-rich envelope further enhances the barrier function of this outermost layer of the skin.

### **1.1.2 The dermis**

The dermis, a supportive and resilient layer, consists of collagen and elastin fibres embedded within an amorphous ground substance primarily composed of mucopolysaccharides. Approximately 30 times thicker than the overlying epidermis, it ranges from 1 to 5 mm in thickness (James, 2006).

Contrasting with the epidermis, the dermis hosts fewer cells, predominantly fibroblasts, which are responsible for secreting most of the dermal components. This layer also houses immune and inflammation-related cells such as macrophages, lymphocytes, and mast cells. Moreover, melanocytes, which participate in pigment production, are also located in this layer (Benson, 2011).

The dermis is anatomically complex and richly supplied with blood vessels and nerves. It is also the origin point for skin appendages such as sweat and sebaceous glands. Its structural composition, however, results in a barrier property that is less efficient than the stratum corneum for most drugs. Since the environment of the dermis is very hydrophilic, it may hinder the permeation of lipophilic drugs (Benson, 2011).

Owing to the extensive vascular network within the dermis, this layer plays a pivotal role in regulating skin temperature, blood pressure, and nutrient supply. It also contributes to the waste regulation of the skin (Powell, 2006). For a topically applied drug to be systemically absorbed, it must reach this vascular network in the dermis (Walters, 2002).

### **1.1.3 Subcutaneous Tissue**

The subcutaneous tissue, also known as the hypodermis, represents the deepest layer of the skin, situated immediately adjacent to muscle tissue. This layer comprises a network of fat cells interconnected by collagen and elastin fibres (Lancerotto et al., 2011). The subcutaneous tissue's primary roles include the absorption of mechanical shocks, providing thermal insulation, and serving as an energy storage depot. These functions underscore the critical role this layer plays in maintaining overall skin health and body homeostasis (Benson, 2011).

## 1.2 Skin permeation

Topical delivery of compounds for medical and personal care has been practiced for centuries, and the last six decades have seen significant advances in the understanding of the mechanistic process of skin permeation (Hadgraft & Lane, 2005). Topical delivery has many advantages over oral administration, including bypassing the potentially harmful gastrointestinal environment and minimising first-pass metabolism. In addition, drug release can be more easily controlled and prolonged with dermal administration.

The stratum corneum, the outermost layer of the skin, is generally considered to be the primary barrier to permeation of externally applied chemicals and moisture loss, known as trans-epidermal water loss (TEWL). Increased permeability has been demonstrated through tape stripping, which removes the stratum corneum, and in conditions like psoriasis where the stratum corneum barrier integrity is compromised (Schaefer et al., 1977). Thus, the stratum corneum provides primary protection against external pollutants, but it also restricts the potential therapeutic effects of topically administered drugs. In addition, therapeutic target sites within the skin must be considered when discussing skin permeation pathways, including whether the drug should permeate to deeper skin tissues for systemic uptake or target the skin surface or appendages.

### 1.2.1 Pathways of percutaneous absorption

Two major pathways for percutaneous absorption are currently recognized: the trans-appendageal and trans-epidermal routes (Figure 1.3). The trans-appendageal route involves permeation through sebaceous and sweat glands and hair follicles. Although solutes may diffuse through the skin more easily via the trans-appendageal route than by the trans-epidermal route, the former route contributes insignificantly to total skin permeation because the skin appendages occupy only a small area of skin surface, namely less than 0.1% of the total skin surface area (Schaefer & Redelmeier, 1996). The trans-epidermal route includes two pathways: the transcellular and intercellular routes. The transcellular route, the shortest pathway for a molecule, involves permeation through the dead keratinocytes and surrounding intercellular lipids. However, this route is highly resistant to solute permeation and requires sequential diffusion of the molecule through the relatively hydrophilic corneocytes, the hydrophobic lipid envelope surrounding the corneocytes and the intercellular matrix. These pathways are not mutually exclusive; most compounds likely permeate the skin via a combination of pathways, with the relative contribution of each being related to the physicochemical properties of the permeating molecule. In particular, many studies suggest that the intercellular route is the principal route for the penetration of lipophilic molecules (Albery & Hadgraft, 1979; Senel et al., 2001; Supe & Takudage, 2021). For instance, Albery and Hadgraft (1979) confirmed through *in-vivo* studies that the diffusional pathlength of methyl nicotinate is 20 times longer than the actual thickness of the stratum corneum. Within the intercellular domains, transport can take place by both lipid (diffusion through the lipid core) and polar (diffusion through the polar head

groups) pathways. The physicochemical characteristics of the permeant are critical in determining the relative contribution of these pathways to skin permeation.

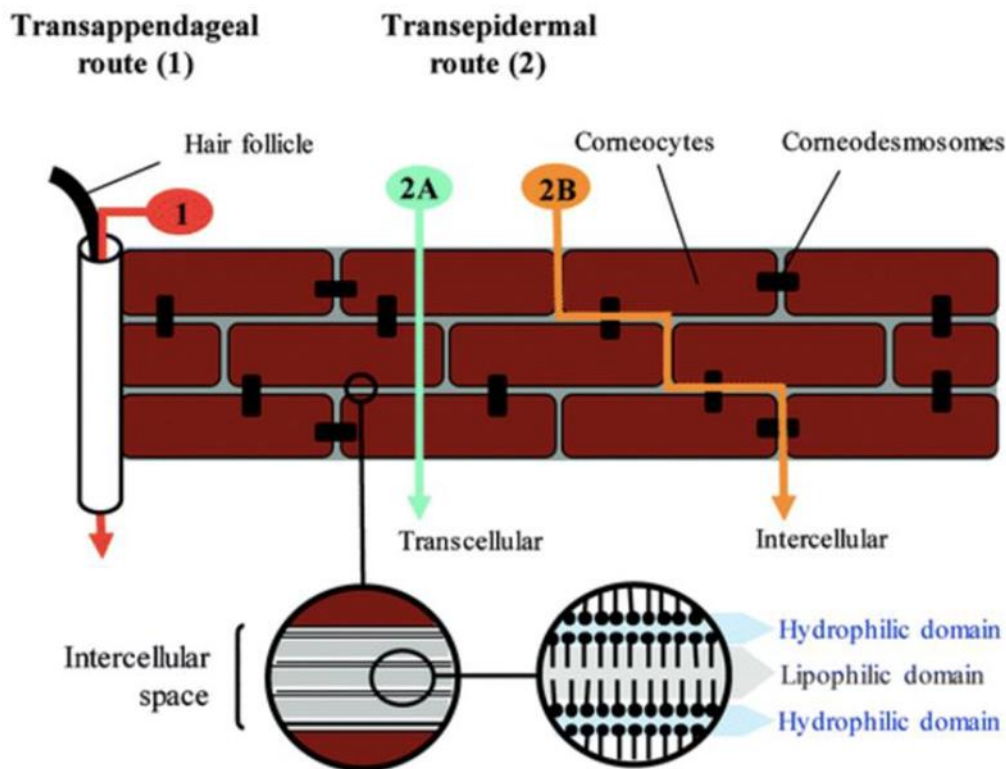


Figure 1.3. 'Brick and mortar' model of the stratum corneum and routes of penetration. Route 1 (highlighted in red) represents the possible transappendageal process; route 2A (highlighted in blue) shows the transcellular way and route 2B (highlighted in orange) illustrates the intercellular route. Adapted from Hadgraft and Lane (2011) (Hadgraft and Lane, 2011)

### 1.2.2 Processes of percutaneous absorption

Percutaneous absorption of a solute involves several steps. Initially, the solute must dissolve. It must be released from the formulation and subsequently partition into the outermost lipid layer of the stratum corneum. The solubility of the drug in both the formulation and the stratum corneum can significantly impact this process (Haque et al., 2018).

Following this, the molecule diffuses through the stratum corneum and enters the viable epidermis. Both solvent-skin and solute-skin interactions influence these processes. Finally, the solute diffuses through the viable epidermis and papillary dermis, where it is absorbed by the capillary plexus and transferred to the circulating blood (Walters, 2002). These processes heavily rely on the solubility and diffusivity of the permeant within each environment. The permeant's release from the dosage form/vehicle and its uptake into the stratum corneum depend on its relative solubility in each environment, and hence the stratum corneum – vehicle partition coefficient.



The diffusion coefficient, or the speed at which the permeant moves within each environment, depends on the permeant properties, including molecular size, solubility, melting point, ionization, and potential for binding within the environment. It also depends on environmental factors such as viscosity and tortuosity or diffusional path length. Although the thickness of the stratum corneum is only 10 – 15µm, the intercellular route is highly tortuous and may be in excess of 150 µm. Given the predominance of the intercellular pathway, factors influencing movement into and within this environment are of considerable importance.

### 1.2.3 Basic physicochemical principles in percutaneous absorption

The permeation of an infinite dose of a molecule applied to the skin surface can be studied as a simple passive diffusion process, which can be represented by Fick's first law of diffusion (Equation 1.1), through a unit area during a unit time (mol/(m<sup>2</sup>·s) or kg/(m<sup>2</sup>·s)):

$$J = \frac{K \times D \times (C_{app} - C_{rec})}{h} \quad \text{Equation 1.1}$$

This equation describes the flux (J) in terms of the partitioning of the diffusing molecule between the skin and the applied formulation (K), the diffusion coefficient (D) of the molecule, the pathlength of the diffusion process (h), the concentration of the molecule in the applied formulation (*C<sub>app</sub>*), and the concentration of the molecule in the receptor medium (*C<sub>rec</sub>*).

Equation 1.1 can be simplified as Equation 1.2, since in most situations, *C<sub>rec</sub>* << *C<sub>app</sub>*.

$$J = k_p \times C_{app} \quad \text{Equation 1.2}$$

In Equation 1.2, *k<sub>p</sub>* is the composite term of K, D, and h, where *k<sub>p</sub>*=KD/h. *k<sub>p</sub>* represents the permeability coefficient of a molecule (Hadgraft & Lane, 2011).

## 1.3 Physicochemical factors affecting permeation across human skin

### 1.3.1 Partition coefficient

A solute must partition into the lipophilic region of the stratum corneum to permeate through it. It should then move into the relatively hydrophilic domain of the viable epidermis before reaching the circulating blood. A highly hydrophilic solute is less likely to partition into the lipophilic stratum corneum, whereas a highly lipophilic solute with a high affinity for the stratum corneum does not readily permeate into the relatively hydrophilic viable epidermis. Therefore, the balanced hydrophilic-lipophilic properties of a drug play an important role in these processes. A drug with a log P of 1 to 3 would be

an ideal choice for transdermal delivery (Lane et al., 2012). This range ensures adequate solubility in both aqueous and lipid environments, facilitating penetration of the drug through the hydrophilic epidermis and into the lipophilic dermal layers of the skin. Drugs outside this range may be either too hydrophilic, resulting in poor skin permeation, or too lipophilic, resulting in inadequate solubility in body fluids after crossing the skin barrier. The logP value is a constant defined in the following manner:  $\log P = \log_{10} (\text{Partition Coefficient})$ ,  $P = [\text{organic}]/[\text{aqueous}]$ .

### 1.3.2 Molecular size

The molecular weight of a drug can have a significant effect on its permeation, as drug permeation requires passive diffusion. There is an inverse relationship between the size of the permeant and skin permeation. In general, a drug suitable for topical and transdermal delivery should have a molecular weight below 500 Daltons (Bos & Meinardi, 2000). Common contact allergens known to penetrate the skin are also less than 500 Daltons. Larger molecules generally do not act as contact sensitizers because they cannot effectively penetrate the skin. Although molecular size is important and is included as a parameter in many mathematical models, other factors such as partition coefficient and ionisation are also important for molecules typically applied to the skin.

### 1.3.3 Melting point or solubility

The solubility of the drug in the intercellular pathway can influence the diffusion coefficient within the stratum corneum. Lipophilic compounds have increased solubility in the intercellular domains, thus increasing flux. However, the skin permeation rate also depends on the concentration of soluble permeant in the applied vehicle. If a lipophilic compound has limited solubility in a topical vehicle, the compound may readily partition into the stratum corneum. Mathematical models relate the drug solubility in lipids to the drug's melting point (MP) (Flynn & Stewart, 1988). Molecular symmetry may underlie this phenomenon, influencing the melting properties and solubility of organic compounds. Generally, symmetrical molecules in crystalline form have higher melting temperatures and exhibit lower solubilities compared with molecules of similar structure but with lower symmetry (Pinal, 2004).

### 1.3.4 Ionization

Drug permeation is also related to the ionization state of the drug. Generally, since hydrophilic ionizable drugs do not readily partition into the *stratum corneum*, the unionized form of a drug (free acid or free base) is preferable for topical and transdermal delivery (Sarveiya et al., 2004). However, the unionized species usually has a low aqueous solubility, which may limit skin permeation of the molecule.

## **1.4 Strategies for passive permeation enhancement**

Passive permeation enhancement has emerged as a dominant strategy for (trans)dermal drug delivery due to its non-invasive nature and ability to maintain stable drug concentrations over extended periods of time (Lane et al., 2012). This methodology encompasses a comprehensive strategy for transdermal drug delivery that systematically addresses the sequential steps essential for effective drug transport through the skin. It begins with the release of the drug from the topical formulation, a critical step in initiating the drug's journey to the deeper layers of the skin. The process then progresses to the penetration phase where the drug actively penetrates the stratum corneum, the outermost barrier of the skin. This is followed by the diffusion phase where the drug traverses the stratum corneum and navigates the complexities of this protective layer. After diffusion, the drug molecules move or diffuse from the stratum corneum into the viable epidermis, as a result of the concentration gradient and the drug's natural tendency to distribute itself evenly throughout the skin layers.

The drug separates into the viable epidermis, the living part of the epidermis, and negotiates its way through this cellular environment. The final stage of this transdermal journey culminates in the drug reaching the capillaries of the dermis for systemic distribution. This sequential approach targets the fundamental mechanisms inherent to the transdermal delivery pathway to ensure efficient and effective drug transport from the surface to the systemic circulation.

### **1.4.1 Enhancing thermodynamic activity of the drug in formulations**

A principal strategy to enhance drug permeation is by increasing drug thermodynamic activity within the formulation. This can be achieved via supersaturation, a state characterized by a drug concentration exceeding its equilibrium solubility limit. This condition facilitates an increased chemical potential gradient across the skin barrier, thus proportionally increasing the flux from the system. To attain a supersaturated state, volatile solvents are employed in solution preparation. Upon the application of these formulations onto the skin, the volatile solvent evaporates from the skin surface, driving the system into a supersaturated state. Supersaturated states can also be achieved by the judicious use of a mixed co-solvent system.

Supersaturated formulations offer an array of advantages for topical and transdermal drug administration, including an increased driving force, facilitating the efficient permeation of molecules across the SC. This allows a potential concentration reduction, as equivalent flux or permeation enhancement can be achieved with lower drug concentrations. However, the increased activity of supersaturated formulations compared to saturated systems presents challenges to their long-term stability, requiring careful formulation strategies and robust stability studies.

### 1.4.2 Utilization of chemical penetration enhancers (CPEs)

Another common strategy involves the use of Chemical Penetration Enhancers (CPEs), which are pharmacologically inert substances designed to interact with skin constituents and promote drug flux. CPEs can partition and diffuse into the skin membrane, particularly the SC, to facilitate the enhanced permeation of drugs. CPEs can influence drug permeation via a multitude of mechanisms, including disrupting and fluidizing the highly ordered structure of the intercellular lipid bilayers in the stratum corneum, acting on intracellular routes (primarily keratin filaments), and modifying the solubility or partitioning behaviour of the drug within the SC (Williams & Barry, 2012). An ideal CPE should exhibit a range of desirable properties. It should be pharmacologically inactive, non-toxic, non-irritating, and non-allergenic. It should significantly enhance drug permeation, and its effects on the SC should be reversible to maintain skin integrity. Furthermore, it should possess characteristics that render it aesthetically acceptable for topical application (Lane, 2013). The interaction of CPEs with the intercellular lipids, which constitute the major resistance to passive drug diffusion through the skin, is crucial. CPEs generally disrupt the highly ordered arrangement of the intercellular lipid bilayers, thereby reducing the diffusional resistance of the SC to most solutes.

CPEs primarily influence permeation by interacting with three main sites within the lipid bilayers (Fig. 1.4):

- Site A: Interaction with the polar head groups of the lipids
- Site B: Interaction within the aqueous domain of the lipid bilayers
- Site C: Interaction with the lipid alkyl chain

These solvents may impact skin permeability by modifying the skin's solubility parameter to match the permeant's solubility parameter, thereby enhancing drug partitioning.

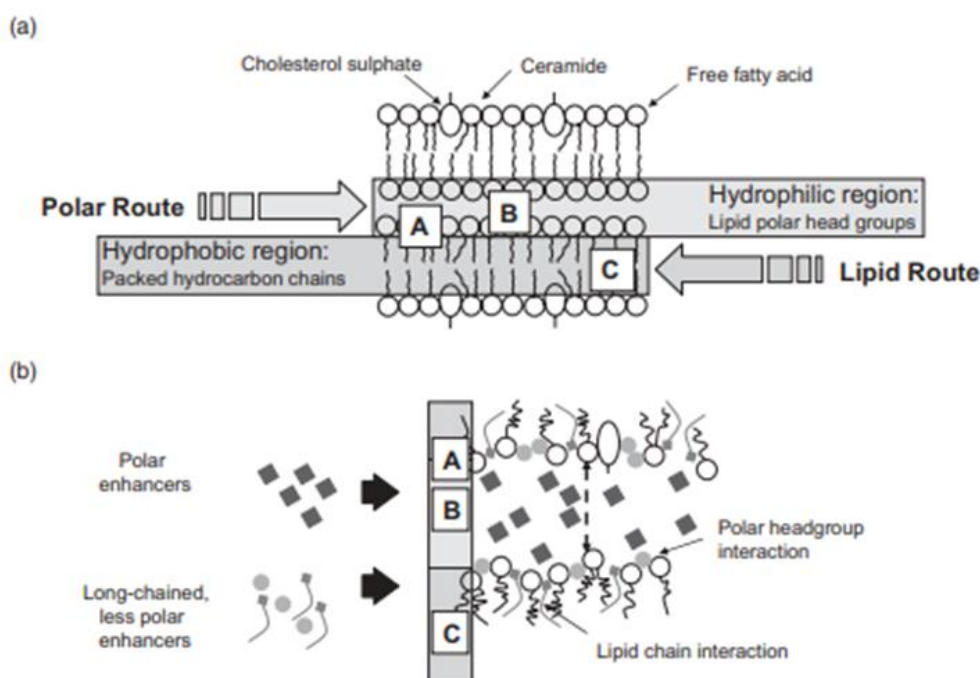


Figure 1.4 Mechanisms of action of CPEs. (a) Schematic representation of the highly ordered and packed lipid bilayers and the hydrophilic and lipophilic routes of drug penetration through SC with proposed sites of action (A, B, and C) for the permeation enhancers. (b) Action of penetration enhancers: long chain enhancers include compounds such as isopropyl myristate (IPM); circles represent small molecules such as water and squares represent solvents such as propylene glycol (PG) and dimethyl sulfoxide (DMSO). Adapted from Barry (Barry, 1991).

The cornified cell envelope and intercellular junctions present additional sites for CPE interaction. Some CPEs can trigger lipid extraction, further disrupting the skin barrier and enhancing drug permeation. Certain CPEs interact with the polar head group of lipids (Site A) through the establishment of hydrogen bonds or ionic forces, which can disrupt the hydration spheres around lipid bilayers. This disruption perturbs the orderly packing within the polar plane of the lipid bilayers, thereby fluidizing the lipid domain and increasing the volume of water between layers. The result is a reduction in diffusional resistance, promoting the flux of both hydrophilic and lipophilic penetrants. The presence of cholesterol sulphate and carboxylic acids can permit the expansion or swelling of the adjacent lipid head groups. This expansion increases the surface area at Site B, facilitating enhanced polar diffusion.

Many CPEs can insert directly between the hydrophobic lipid tails (Site C), disrupting lipid packing, increasing lipid fluidity, and promoting drug permeation. In some cases, this lipid perturbation is accompanied by some perturbation of the polar headgroup region. This further facilitates solute permeation. CPEs can also modify skin permeability by adjusting the skin's solubility parameter to match that of the permeant. The result of this modification is an increase in drug partitioning from the vehicle into the SC. Solubility parameters ( $\delta$ ) are a measure of how materials interact with each other; materials with similar solubility parameters are likely to have a high mutual affinity. Thus, by altering the skin solubility parameter, CPEs can facilitate a more efficient drug partitioning and permeation process, contributing to improved (trans)dermal drug delivery.

In summary, the use of supersaturation and CPEs, together with a thorough understanding of their interaction with skin components, provides a suite of strategies to enhance passive drug permeation through the skin. This multifaceted approach to transdermal drug delivery continues to be the subject of intense research with the aim of improving the therapeutic outcomes of numerous drugs.

### 1.4.3 Ion-pair formation

Ion pairs are neutral entities formed through the electrostatic attraction between oppositely charged ions that possess sufficient lipophilicity to dissolve in a lipid-like medium, such as the SC. Theoretically, ion-pair formation offers several benefits compared to other permeation enhancement strategies, including the enhancement of skin transport of ionic drugs without modifying their structure and without altering the skin barrier function.

As discussed in section 1.3.4, hydrophilic charged molecules struggle to partition through the *stratum corneum*. A lipophilic ion pair, formed by the electrostatic attraction between oppositely charged ions without the formation of a covalent bond, can facilitate

the permeation of ionized drugs. After permeating through the stratum corneum, the lipophilic ion pair complex dissociates into the parent charged drug in the aqueous viable epidermis (Benson, 2005). This strategy provides several advantages over other penetration enhancement methods, such as improved percutaneous absorption, without the need for alterations in skin barrier function. Following the successful enhancement of sodium salicylate permeation using 1-Dodecylazacycloheptan-2-one (Azone) as a counter ion by Hadgraft et al. (1985), ion pair formation has been employed as a strategy to enhance permeation in numerous studies (Green & Hadgraft, 1987; Hadgraft & Valenta, 2000; Sarveiya et al., 2004).

#### **1.4.4 Eutectic mixtures**

The melting point (MP) of a permeant directly impacts its solubility in the skin, and consequently, its skin permeability. The MP of a drug can be manipulated via the formation of a eutectic mixture. In a basic binary eutectic system, the two components interfere with each other's crystallization processes at certain ratios. As previously discussed in section 1.3.3, a drug with a lower melting point should display greater solubility in the intercellular lipids of the stratum corneum compared to a drug with a higher melting point. A simple binary eutectic system with a lower melting point is a mixture of two components that inhibit each other's crystallization processes at certain ratios, without the necessity for the formation of a new chemical entity (Lane et al., 2012). This principle is employed in the anaesthetic cream EMLA (AstraZeneca, Wilmington, DE), which is a mixture of prilocaine and lidocaine and is reported to provide enhanced dermal penetration performance (Stott et al., 2001).

## 1.5 Skin cancer

Skin cancer, consisting of melanoma and non-melanoma skin cancer (NMSC), represents the most common type of malignancy in Caucasian populations, and its incidence is on the rise globally (Leiter et al., 2014). The primary risk factors for skin cancer are associated with fair skin types, exposure to UV radiation, and immunosuppression (Mabruk et al., 2009). Nonmelanoma skin cancer (NMSC) is a group of skin cancers that do not contain the pigment melanin. While NMSC is highly prevalent, malignant melanoma is recognized as the most lethal form of skin cancer (Lin et al., 2009). Notably, the incidence and severity of metastatic melanoma, a particularly aggressive form of the disease, have increased in recent years (Hamm et al., 2008). Melanoma is a tumour that originates from melanocytes, which are the pigment-producing cells of the epidermis. Although NMSC is more common in older individuals, malignant melanoma is comparatively more prevalent in younger people. Data from The National Cancer Intelligence Network (NCIN) indicate that while NMSC is a frequent type of skin cancer, malignant melanoma represents the deadliest form (NCIN, 2022). Indeed, NMSC is the most common group of cancers, accounting for around 20% of all new malignancies and 90% of all skin cancers registered in the UK and Ireland (NCIN, 2022).

### 1.5.1 Nonmelanoma skin cancer (NMSC)

The NMSC category primarily includes basal cell carcinoma (BCC) and squamous cell carcinoma (SCC), which are differentiated based on their respective sites of origin within the skin. Ultraviolet (UV) radiation, primarily from sunlight, is the principal etiological factor in the genesis of non-melanoma skin cancer (NMSC). UV radiation is categorized into three regions based on wavelength: UV-A (320-400 nm), UV-B (280-320 nm), and UV-C (100-280 nm). The earth's atmosphere filters out UV-C rays, rendering them insignificant in terms of terrestrial exposure. UV-B, while constituting a minute proportion of the total UV radiation, is disproportionately potent in its carcinogenicity. It induces a protective tan in the skin, often after initial burning. Chronic UV-B exposure can culminate in photoaging and carcinogenesis. In comparison, UV-A, despite its prevalence, is much less damaging to human skin, almost 10,000 times less damaging than UV-B.

UV radiation instigates distinct mutations in keratinocytes, the predominant cell type in the epidermis, leading to NMSC. UV-B photons are absorbed by cellular DNA, engendering photoproducts. UV-A, on the other hand, indirectly harms DNA by generating reactive oxygen species. Unrepaired DNA damage may precipitate distinct mutations, predominantly C to T (cytosine to thymine) single base substitutions, and to a lesser degree, CC to TT (double base substitutions at pyrimidine sites). The body's defence against UV-induced DNA damage or mutations relies chiefly on two strategies: DNA repair mechanisms and the synthesis of UV-absorbing compounds such as melanin. Nucleotide excision repair (NER) is the predominant mechanism that human cells employ to excise DNA photoproducts. As individuals age, the efficiency of this DNA

repair mechanism diminishes, predisposing older individuals to NMSC. Additionally, certain genetic disorders, such as xeroderma pigmentosum, characterized by defects in the NER gene, impede the removal of DNA photoproducts, thereby elevating the risk of NMSC. Melanocytes synthesize melanin, a pigment that shields surrounding keratinocytes in the basal layer of the epidermis from UV radiation. However, melanin's protective capacity does not extend to the superficial skin layers, as this pigment is sloughed off with keratinocytes from the stratum corneum. Consequently, superficial skin cancers are relatively common. BCCs are the most common type of human cancer in the world, and SCCs are the second most common type of cancer in the United States (Fania et al., 2020; Shreve et al., 2020). In the UK in 2010, approximately 75% of NMSC patients were diagnosed with BCC, with the remainder having SCC (Burns et al., 2022). BCC typically grows slowly, with a local spread and minimal or no metastasis (Jerant et al., 2000). In contrast, SCC is locally invasive and carries a 2 to 6% risk of metastasis (Jerant et al., 2000). Both BCC and SCC can cause significant skin damage if they remain untreated.

BCC and SCC arise from the basal and squamous (spinosum) layers of the epidermis, respectively. The earlier stage of SCC, known as actinic keratosis (AK), represents a crucial biomarker of increased risk for invasive SCC (Zalaudek et al., 2014). Both AK and SCC share genetic tumour markers and the same mutations in the p53 gene, a well-known tumour suppressor gene (Cockerell, 2000). AK begins with DNA damage and mutations induced by UV radiation, leading to the development of a 'hot spot' – an aggregation of small, microscopic, transformed cells. Over time, these aggregates evolve into keratinocytes, exhibiting features of atypia and pleomorphism. Depending on the patient's immune response, these lesions may remain unchanged, grow, or extend into the dermis. Once tumour cells invade the dermis, the condition progresses to SCC. If these tumour cells become metastatic, it could lead to the patient's death (Cockerell, 2000). Treatment strategies for NMSC depend on factors such as lesion type, size, location, and patient age. They often involve radiotherapy and surgery, with additional considerations for lymph node dissection due to the more aggressive nature and higher metastatic tendency of SCC (Telfer et al., 2008).

### **1.5.2 Treatment options for NMSC**

Treatment modalities for non-melanoma skin cancer (NMSC) are multifaceted and depend on a multitude of factors such as the type and size of the lesion, its anatomical location, patient's age, and overall health status.

- **Surgical Intervention:** Surgical removal of the lesion remains the cornerstone of NMSC treatment, offering high cure rates, especially for small, primary, well-defined tumours. Surgical methods include excision, Mohs micrographic surgery (for larger, recurrent, or high-risk tumours), curettage and electrodesiccation, and cryosurgery. The choice of surgical technique depends on tumour characteristics and patient preferences (Elleson et al., 2022).
- **Radiotherapy:** Radiation therapy serves as an alternative for patients who are not suitable for surgery, for instance, due to the location of the tumour or their general health condition. It can be effectively used for both basal cell carcinomas (BCC) and



squamous cell carcinomas (SCC) (Elleson et al., 2022).

- Lymph Node Dissection: For SCCs, which have a higher propensity for metastasis compared to BCCs, lymph node dissection may be considered if there is suspicion or evidence of nodal involvement (Elleson et al., 2022).
- Oral Chemotherapy: Systemic chemotherapy, using agents like retinoids or cisplatin, may be employed in cases of advanced or metastatic NMSC. Retinoids, derived from vitamin A, can interfere with cell growth and proliferation. Cisplatin, a platinum-based drug, disrupts DNA replication in cancer cells (Elleson et al., 2022).
- Photodynamic Therapy (PDT): PDT involves the application of a photosensitizing agent to the lesion, followed by exposure to a specific wavelength of light, which triggers the release of reactive oxygen species to destroy cancer cells. This treatment is often used for superficial BCC and premalignant actinic keratosis (Elleson et al., 2022).
- Topical Chemotherapy: Topical agents such as 5-fluorouracil (5-FU), imiquimod, diclofenac, or tretinoin are applied directly to the skin. 5-FU interferes with DNA synthesis, leading to cell death, while imiquimod stimulates the immune system to attack cancer cells. Diclofenac, a nonsteroidal anti-inflammatory drug, and tretinoin, a retinoid, can also inhibit cancer cell growth (Elleson et al., 2022).
- Laser Surgery: Laser ablation can be employed for certain types of NMSCs. This technique uses focused light to heat and destroy cancer cells (Elleson et al., 2022).

It is noteworthy to mention that the selection of the optimal treatment strategy is individualized, often necessitating multidisciplinary input. Regular follow-up is imperative to monitor treatment response and detect any potential recurrence (Elleson et al., 2022).

### **1.5.3 Melanoma skin cancer**

Melanoma, which originates from melanocytes, the epidermal pigment-producing cells, is more aggressive than NMSC and can metastasize to other organs (Berking & Herlyn, 2001). The primary risk factor for melanoma is UV-B radiation, especially intermittent intense UV exposure. Moles, a family history of melanoma, and genetic mutations like the CDKN2A gene or the BRAF gene are also risk factors (Soura et al., 2016). Melanoma can be classified into four main subtypes based on their growth patterns: superficial spreading melanoma, nodular melanoma, lentigo maligna melanoma, and acral lentiginous melanoma. Early detection is crucial, as the prognosis for melanoma worsens with increased tumour thickness and the presence of metastasis (Scolyer et al., 2020). The main treatment for melanoma is surgical excision with appropriate margins, depending on the tumour's depth. Sentinel lymph node biopsy may be performed to determine if the melanoma has spread to nearby lymph nodes. In the case of advanced or metastatic melanoma, various therapies such as targeted therapies (e.g., BRAF and MEK inhibitors), immunotherapies (e.g., checkpoint inhibitors), chemotherapy, and radiation therapy may be used. However, the efficacy of these treatments in metastatic melanoma remains unsatisfactory, highlighting the need for novel therapeutic approaches (Hamm et al., 2008).

## **1.6 Topical 5- fluorouracil formulation**

5-fluorouracil (5-FU) was developed for a variety of dermatologic and neoplastic disorders in 1957 (Parker & Cheng, 1990). As a known antineoplastic medication, it is a pyrimidine analogue that irreversibly binds and inhibits thymidylate synthetase and thus leads to a reduction in DNA and RNA synthesis (Rahvar et al., 2012). 5-FU's selective cytotoxicity and minimal effect on normal skin cells made it a promising therapeutic option that has evolved over time with demonstrated efficacy in many dermatologic conditions (Yen Moore, 2009). Since 2000, the US Food and Drug Administration (FDA) have approved 5FU in topical dermatologic use for the treatment of multiple actinic or solar keratoses, related to sun exposure, characterized by rough, scaly patches on sun-exposed areas, with a potential risk of developing into squamous cell carcinoma. involving the face and anterior scalp (Gupta et al., 2001).

### **1.6.1 Mechanism of action of 5-FU**

After entering the cells via a facilitated transport mechanism, 5-FU is converted into its active metabolites: fluorodeoxyuridine monophosphate (FdUMP), fluorodeoxyuridine triphosphate (FdUTP), and fluorouridine triphosphate (FUTP). FdUMP complexes with the enzyme thymidylate synthase (TS), inhibiting the production of deoxythymidine monophosphate (dTMP). This inhibition leads to a reduction in thymidine triphosphate (TTP), which is necessary for DNA synthesis and repair. Consequently, the disruption of DNA synthesis triggers apoptosis and inhibits cancer cell proliferation. dTMP is essential for DNA replication and repair, and depletion of this compound results in an imbalance of intracellular nucleotides leading to double-stranded breaks in DNA by the enzyme endonuclease (Zhang et al., 2008). In addition to inhibiting thymidylate synthase, 5-FU also serves as a pyrimidine analogue by mis-incorporating into RNA and DNA in place of uracil or thymine. The overwhelming damage of DNA repair machinery caused by these mechanisms ultimately results in cell death of rapidly proliferating cells (Casale & Patel, 2022). Moreover, a report showed that 5-FU provides a selective cytotoxic effect for actinic skin, leaving normal skin unaffected. The proposed mechanism for this phenomenon is selective inhibition of thymidylate synthase in actinic skin and only partial inhibition in normal skin (Ceilley, 2012). 5-FU exhibits other mechanisms of action that include interference with RNA processing and increasing p53 expression (Prescott et al., 2017). The mechanism by which 5-FU increases p53 expression may be concomitantly responsible for its efficacy in treating dermatologic conditions with altered p53 expression, including actinic keratosis and squamous cell carcinoma (Ceilley, 2012).

### **1.6.2 Indications of topical 5-FU**

Topical 5-FU on the market is used for the topical treatment of superficial pre-malignant and malignant skin lesions; keratoses including senile, actinic and arsenical forms; keratoacanthoma; Bowen's disease and superficial basal-cell carcinoma. Among all

reasons to visit a dermatologist, actinic keratoses (AKs) rank second (Ibrahim & Brown, 2009). After years of exposure to the sun, skin may develop rough, scaly patches, called actinic keratoses (figure 1.5). These lesions develop on the face, lips, ears, back of hands, forearms, scalp or neck. Actinic keratosis is a common intra-epidermal neoplasm and lesions lie on a continuum with squamous cell carcinoma. Highly linked to ultraviolet irradiation, they are more likely to appear in areas of chronic sun exposure, and to prevent their progression to invasive disease, early treatment of these lesions is necessary (Thompson et al., 1993). AKs can be precursor lesions to invasive squamous cell carcinoma (SCC), and low-grade SCC in situ (Ackerman & Mones, 2006). SCC starts in the cells lining the top of the epidermis. Bowen's disease is a precancerous form of SCC sometimes referred to as squamous cell carcinoma in situ. Basal cell carcinoma (BCC), also known as a rodent ulcer, starts in the cells lining the bottom of the epidermis. Overall, treatment with topical 5-FU focuses on epidermal cell lesions without melanoma. In the UK, around 147,000 new cases of non-melanoma skin cancer are diagnosed each year. It affects more men than women and is more common in the elderly. The huge market also indicates the research value in the improvement of topical 5-FU formulations on the market. Currently, topical 5-FU formulations are applied as solutions or creams with strengths varying from 0.5% to 5%. The dosing regimens for actinic keratosis is the solution or 5% cream twice daily for 2 to 4 weeks and for superficial basal cell carcinoma is 5% cream twice daily for 3 to 6 weeks (Del Regno et al., 2022).

### **1.6.3 Side effects and future directions for topical 5-FU Formulation**

While topical 5-FU's efficacy is well-established, its use can be limited by localized adverse effects. These can include skin irritation, inflammation (Prince et al., 2018), erosive dermatitis, pain, pruritus, hypopigmentation, and hyperpigmentation. These side effects, although typically limited to the site of application, can negatively impact patient adherence to treatment. The inflammatory reactions of 5-FU may cause erosive dermatitis, pain, pruritus, hypopigmentation, and hyperpigmentation which result in poor medication compliance. The primary aim of this work is the development of novel and optimized formulations that subsequently should reduce unwanted side-effects. Moreover, based on the aetiology of skin cancer, it is known that its pathogenesis is multifactorial in origin, and hence, a polyvalent drug with a polyvalent approach may offer better therapeutic action as compared to the univalent mechanism of action of a single drug. Therefore, in recent years a combinatorial approach has become a promising strategy where one of the synthetic drugs is combined with a natural bioactive to achieve multifactorial advantages over monotherapy. Combinatorial therapy also may provide a desired therapeutic efficacy with minimum treatment duration and side effects (Dun et al., 2015). In conclusion, topical 5-FU is a cornerstone of treatment for a variety of dermatologic conditions, particularly those characterized by abnormal cell proliferation. While it has proven to be effective, there are opportunities to enhance its clinical utility through the development of novel formulations and combinatorial therapy approaches. Such advancements could substantially improve patient outcomes and quality of life. Moreover, the drug's side effects are typically limited to the site of

application and resolve after discontinuation of treatment and they can lead to poor medication compliance. Therefore, strategies to minimize these side effects without compromising the efficacy of treatment are essential.

## 1.7 Improvement of topical formulations of 5-FU

The existing formulation is a simple cream and is not optimised for targeted delivery of 5-FU to AK lesions. In dermatology, topical 5% 5-FU is approved for actinic keratosis (AK) and superficial basal cell carcinoma (sBCC) (McGillis & Fein, 2004). In non-hyperkeratotic AKs (grade I), complete clearance is described in up to 90% of patients who tolerate twice-daily courses of 2–4 weeks (Dodds et al., 2014). Askew et al. (2009) found that when treating actinic keratoses (AKs) across all grades (I–III), the effectiveness of 5% fluorouracil (5-FU) cream was relatively moderate, achieving a clearance rate of around 50%. Correspondingly, while studies for sBCC report cure rates approaching 93%, 5-FU treatment attempts for nodular BCC describe lacking histological clearance and unsatisfactory recurrence rates (Gross et al., 2007).

As a hydrophilic molecule, lacking treatment efficacy for thick or deeper laying lesions may in part be related to 5-FU's limited penetration through hydrophobic upper skin layers. Also compounded by suboptimal patient compliance due to frequent drug application, lengthy treatment duration and accompanying skin inflammation, 5-FU regimens face persistent therapeutic challenges (Fu & Cockerell, 2003). Enhancing cutaneous drug uptake may thus provide a means to increase potency and reduce duration of 5-FU treatment. This thesis aims to identify formulation components that will deposit the drug in the lesion rather than promote its permeation to the deeper layers of the skin. The presence of a lesion disrupts the skin's surface structure, particularly the integrity and permeability of the stratum corneum, thereby influencing the absorption efficiency of topical formulations. This disruption can lead to increased drug penetration and absorption through the damaged skin, with potential implications for treatment effectiveness and safety. To do this, appropriate solvents and excipients will be selected and their influence on 5-FU deposition in skin will be evaluated. The new topical formulation will be developed for improved patient compliance and topical drug delivery to lesions. According to the data from the electronic medicines compendium (EMC), the topical 5% 5-FU formulation in the UK and EU market is Efudix 5% Cream, which was authorised in 2008. Tables 1.5 and 1.6 detail the composition of Efudix 5% and the physicochemical properties of 5-FU, respectively.

List of excipients	Use
Water	Solvent vehicle
Propyl parahydroxybenzoate	Preservative anti-microbial
Methyl parahydroxybenzoate	Preservative anti-microbial
Propylene glycol	Solvent vehicle

Polysorbate 60	Emulsifier
White soft paraffin	Moisturizer
Stearyl alcohol	Emollient, emulsifier, and thickener

Table 1.5 : The composition of Efudix 5%

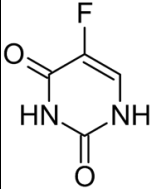
<b>Chemical structure</b>	
<b>Melting point</b>	282-283°C (EPA, 1998)
<b>Water solubility</b>	11.1 mg/mL at 22 °C (Burr and Bundgaard., 1985)
<b>LogP</b>	-0.89 (Hansch et al., 1995)
<b>pK<sub>a</sub></b>	8.02 (Sangster, 1994)
<b>Toxicity</b>	LD <sub>50</sub> =230 mg/kg (orally in mice) (Pfizer, 2012)
<b>Molecular weight</b>	130.08 g/mol
<b>Solubility parameter</b>	16.3 (cal/cm <sup>3</sup> ) <sup>1/2</sup> (van Krevelen and Hoftyzer)

Table 1.6.: Physical and chemical properties of 5-FU

## 1.8 Berberine in topical anti-cancer and anti-inflammatory treatment

Berberine is an isoquinoline alkaloid of the protoberberine subgroup and also known as umbellate, is a quaternary ammonium salt (Dewick, 2002). It has a bright yellow colour and is soluble in water but less soluble in alcohol. It can be found as a purified substance in food supplements in the form of sulphate or hydrochloride in European market. Like Berberol® is the first food supplement containing berberine for controlling blood sugar and blood fat. The genus *Berberis*, encompassing around 500 species, is the foremost natural source of the alkaloid berberine. In traditional Chinese medicine, the stems, bark, roots, and particularly the root bark of *Berberis* plants are utilized. Species such as *Berberis aristata* DC., *Berberis aquifolium* Pursh., and *Berberis vulgaris* L. predominantly grow in Asia and Europe. Additionally, berberine is found in families like Annonaceae, Menispermaceae (e.g., *Coscinium fenestratum* (Goetgh.), *Jateorhiza palmata* (Lam.) Miers, *Tinospora sinensis* (Lour.) Merr.), Papaveraceae (e.g., *Chelidonium majus* L.), Ranunculaceae (e.g., *Hydrastis canadensis* L., *Coptis japonica* (Thunb.) Makino, *Coptis teeta* Wall., *Coptis trifolia* (L.), *Thalictrum flavum* L.), and Rutaceae (e.g., *Phellodendron amurense* Rupr.) (European Food Safety Authority (EFSA), 2023). Berberine concentrations are generally higher in the roots, rhizomes, and bark than in fruits and leaves, with *Berberis* species' roots containing about 1.6-4.3% berberine (Neag et al., 2018). These plants, particularly the *Berberis* species, have been utilized for over 3000 years for external applications in treating inflammatory disorders, skin diseases, wound healing, and bacterial infections (Singh & Sharma, 2018).

Berberine has piqued scientific interest due to its diverse biological and pharmacological activities. Some of its documented properties include anti-inflammatory, anti-bacterial, antioxidant, anti-cancer, anti-diabetic, anti-hyperlipidaemic, and anti-hypertensive effects (Hassani et al., 2016). Traditionally, berberine-containing drugs have been used to treat diarrhoea and other gastrointestinal infections due to its potent antibacterial properties (Chao et al., 2017). Furthermore, as a major component of *Coptis Chinensis*, berberine is frequently employed in Chinese herbal remedies for managing inflammatory reactions and skin conditions (Yoo et al., 2008). Recent research has highlighted the anti-cancer potential of berberine, particularly its pro-apoptotic and anti-inflammatory activity. Berberine has been shown to induce cell cycle arrest, promote apoptosis, inhibit angiogenesis, and suppress metastasis in various cancer cell lines (Tillhon et al., 2012). The molecule exhibits compelling pro-apoptotic activity, marking it as a promising candidate for combination cancer treatments. The sensitization and eradication of drug resistance are emerging areas of berberine research. Studies have demonstrated the synergistic effects of berberine when combined with chemotherapeutic drugs such as 5-FU, doxorubicin, and paclitaxel (Chengwei He et al., 2012; Pandey et al., 2015). These combination therapies have been found to enhance the anti-cancer effects of the drugs, reduce side effects, and potentially overcome drug resistance in different cancer cell lines. Despite its beneficial properties, the oral administration of berberine faces significant challenges due to its poor bioavailability and associated gastrointestinal side effects at higher doses (Chen et

al., 2011). To circumvent these limitations, there is a growing interest in the development of topical berberine formulations, particularly in combination with anti-cancer drugs for skin cancer treatment. The clinical studies evaluating this approach have not yet been conducted in report.

Berberine can inhibit the proliferation, induce apoptosis, and curtail the invasion of human skin squamous cell carcinoma A431 cells (Li et al., 2015). Berberine exhibited cytotoxicity in FaDu head and neck squamous cell carcinoma cells without affecting the viability of primary human normal oral keratinocytes (Seo et al., 2015). More importantly, some *in vitro* studies suggest that berberine could enhance the anti-cancer effects and side effects of topical 5-FU formulations. Combined topical treatment with 5-FU and berberine has not been explored in detail and may offer useful economic and research benefits. Berberine is also reported to improve skin permeation and retention of 5-FU (Namba et al., 1995). Combination therapy for example, can increase therapeutic effects by providing actions on multiple targets and through different mechanisms, while minimizing dose related and other undesired side effects (Fondello et al., 2016). Until now, some researchers focused on other cancer cells such as HEP2 laryngeal cancer, gastric cancer, A549 cells (adenocarcinoma human alveolar basal epithelial cells), which all show combined treatment approaches can enhance the anti-cancer effect of 5-FU (C. He et al., 2012; Palmieri et al., 2018; Pandey et al., 2015). Berberine chloride is the orally bioavailable, hydrochloride salt form of berberine, and will be used in the studies in this work. The use of salt forms, such as Berberine chloride, in berberine research is primarily motivated by three key considerations: enhancing bioavailability through improved solubility and stability, optimizing pharmacokinetic properties for better therapeutic efficacy, and facilitating drug product development while meeting regulatory requirements. The use of salt forms like Berberine chloride in berberine research does not negatively impact its pharmacological applications.

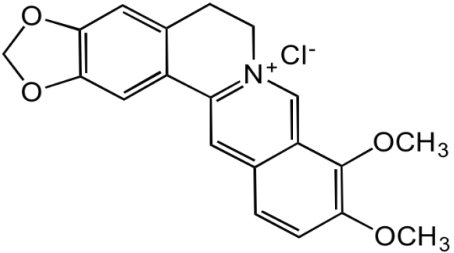
Chemical structure	
Melting point	214 °C (Chemodex)
Solubility	Soluble in DMSO or methanol. Slightly soluble in ethanol or water. (Chemodex)
pK <sub>a</sub>	-4.4 (ChemAxon)
Toxicity	LD <sub>50</sub> = 2,600 mg/kg (orally in mice)(Singh & Sharma, 2018)
Molecular weight	371.8 g/mol (PubChem)

Table 1.7: Physical and chemical properties of berberine chloride

## 1.9 Aims and objectives

The current study aims to combine an anticancer drug and a natural molecule to improve therapeutic efficacy and specificity. It anticipates that the synergy between such molecules will enhance the therapeutic activity, and by confining the systemic therapy to site-specific application, the systemic exposure of the drugs could be minimized, leading to reduced doses. Such a synergistic and site-specific strategy is expected to develop a drug delivery system that contains a combination of a chemotherapeutic agent with a plant metabolite for effective cancer treatment. The primary goal of the cell line experiments is to investigate the potential of combinatorial treatments of human skin squamous carcinoma cells using berberine chloride and 5-FU as active ingredients for topical formulations.

*In vitro* cell experimental strategies

- Evaluation of anti-cancer effects: The cytotoxic activity of berberine chloride and 5-FU against human skin carcinoma cells must be assessed. This will be done by conducting proliferation and viability assays to evaluate the anti-cancer effect of these compounds.
- Evaluation of synergistic effects: The potential synergistic effect of combination treatments on squamous carcinoma cells will be assessed. Additionally, the optimum ratio of the combination of the two compounds will be determined.

Following the evaluation of the combination of berberine chloride and 5-FU, a new topical 5-FU formulation may be developed incorporating berberine chloride. The aims and objectives of this phase of the project are:

- Analytical method development and characterization: Development and validation of analytical methods for the characterization of 5-FU and berberine chloride. This will ensure the accurate measurement and assessment of these compounds in the formulations.
- Formulation: Identification of suitable formulations for the combination of 5-FU and berberine chloride for topical treatment. This will involve exploring a single solvent system and investigating strategies to inhibit penetration for topical formulations.
- Delivery efficacy: Evaluation of the delivery efficacy of the formulations using *in vitro* permeation studies and mass balance studies. These studies will help understand how effectively the formulations deliver the active compounds and will guide the optimization of the formulations.



## Chapter 2. *In vitro* cell culture experiments

### 2.1 Introduction

Both non-melanoma skin cancer and precancerous conditions, such as actinic keratosis (AK), pose significant challenges to healthcare globally. As researchers investigate potential treatments, *in vitro* cell culture experiments are proving to be a key tool. This chapter focuses on the combined effects of berberine chloride and 5-FU on non-melanoma skin cancer and AK cells, rather than solely assessing their efficacies.

Cell culture systems remain an integral part of cancer and precancer research. Using cell lines or primary cells from human or murine origin, these systems provide a controlled setting to unravel the intricacies of disease mechanisms and potential drug actions. While primary cells, directly isolated from donor material, present certain challenges due to their short lifespan and isolation complexities, they notably reflect the *in vivo* genetic features of tumours, thus enabling specific functional experiments (Jacoby & Pasten, 1979). On the other hand, established cell lines, such as those provided by the ECACC, present a more standardized and consistent model for various types of skin conditions, making them invaluable in modern research (Ryan, 2008). Amid the diverse methodologies in cell culture, the Two-Dimensional (2D) model has been of particular focus, and it is the chosen technique for this study focusing on berberine and 5-FU. These cultures, whether in adherent conditions with cells anchored to substrates or in suspensions that might mimic more natural environments, play a critical role in our understanding of these skin conditions (Ryan, 2008). The 2D models, in particular, are appreciated for their economic efficiency, ease of maintenance, and suitability for functional tests. As outlined in this chapter, the methods, results and potential therapeutic implications of the combined effects of berberine and 5-FU on cells associated with skin cancer and AK will be elucidated using the 2D culture model.

In the present work in view of the great interest evoked by the toxicological properties of skin cancer cells, further preclinical investigations were conducted to ascertain the activity of the combination of berberine and 5-FU against the Human malignant melanoma A375 cell line and Human squamous carcinoma A431 cell line. In addition, the main cells in skin tissues, primary cells human dermal fibroblast cells and the aneuploid immortal human skin keratinocyte cell line, HaCaT, were studied to explore the influence of berberine and 5-FU in this chapter. An overview of these primary cells and cell lines is given in Table 2.1.

A375	Human malignant melanoma cell line, A375 is derived from a skin primary melanoma of a 54-year-old female and has an epithelioid morphology carrying two mutant genes, B-RAF and CDKN2. Both mutations are associated with melanoma of sun-damaged skin (Candido et al., 2014). The A375 lines are widely used as cell models to test cancer therapeutics (Granness et al., 2000).
A431	A squamous cell carcinoma (SCC) line, A431 cells were established from an epidermoid carcinoma of the skin (epidermis). A431 cells are used to study cell cycle and cancer-associated cell signalling pathways because they express abnormally high levels of the epidermal growth factor receptor (EGFR). The A431 lines, engineered to express tumour antigens, have been used as cell models to test cancer therapeutics (GRANESS et al., 2000).
HaCaT	HaCaT cells are a spontaneously immortalized, human keratinocyte line that has been widely used for studies of skin biology and differentiation. HaCaT is a spontaneously transformed aneuploid immortal keratinocyte cell line from adult human skin (Schoop et al., 1999). HaCaT cells are utilized for their high capacity to differentiate and proliferate <i>in vitro</i> (Colombo et al., 2017).
Primary dermal Human fibroblasts	Dermal fibroblasts are cells within the dermal layer of the skin that are responsible for producing connective tissue and allowing the skin to recover from injury. They primarily contribute to the secretion of extracellular matrix prophylaxis material to maintain the structural integrity of the connective tissue (Nilforoushadeh et al., 2017). Early passages of these fibroblasts can also be used for cell-based functional assays to study specific disease pathways, mechanisms and subsequent drug screening approaches (Vangipuram et al., 2013).

Table 2.1 Overview of cell models investigated in this chapter.

In recent years, non-melanoma skin cancer (NMSC) and its precursors have emerged as areas of intense research focus, particularly in the field of topical treatments. At present, the repertoire of molecules approved for topical use remains quite limited. One such approved compound is 5-FU, which has been formulated into various topical creams and solutions of different strengths. While its therapeutic efficacy is recognised, as discussed in section 1.6.1, 5-FU is not without its drawbacks. In particular, patients treated with 5-FU often report adverse effects such as pain, pruritus, burning, erythema, erosion and scarring (Sahni & Lerner, 2022). In the search for improved therapeutic modalities, the ancient remedy berberine has attracted considerable interest. Known for its extensive use in traditional medicine for centuries, berberine holds great promise as an adjunct in the treatment of cancer. When combined with 5-FU, it has the potential not only to enhance anti-cancer efficacy, but also to ameliorate some of the

aforementioned side effects associated with 5-FU. The current clinical landscape is characterised by a paucity of innovative drugs for skin cancer. This shortage highlights the need for alternative therapies, particularly for patients whose clinical presentation or genetic profile makes them less amenable to conventional treatments. The proposed approach is to identify and exploit novel agents that act through previously unexplored mechanisms of action, potentially offering improved efficacy or reduced side effects. However, a note of caution is in order: The scientific community has become increasingly vigilant about the reproducibility of results in life science research. This heightened scrutiny stems from past experience, particularly in the context of preclinical *in vivo* studies, where repeated experiments did not always agree with initial observations. This reproducibility challenge underscores the importance of robust experimental designs and methodologies to ensure that our investigations into novel treatments, such as the combination of berberine and 5-FU, stand the test of time and repeated scrutiny.

The A431 cell line, representative of epidermoid carcinoma, has been extensively used in biomedical research. Studies have clearly confirmed the inhibitory effects of berberine on human squamous cell carcinoma (SCC), specifically A431 cells. These include potential suppression of proliferation, induction of apoptosis and inhibition of A431 cell invasiveness (Rauf et al., 2021). In parallel research, berberine was reported to be harmless to the viability of primary human normal oral keratinocytes. Conversely, its cytotoxicity escalated markedly in FaDu cells, a manifestation of hypopharyngeal squamous cell carcinoma, when exposed to berberine chloride for 24 hours. This escalation was largely attributed to the induction of apoptosis and impaired cell migration (Seo et al., 2015). However, there remains a paucity of literature on the enhancement of the anticancer effects of 5-FU in SCC when combined with berberine chloride. This chapter will outline approaches to investigate the combined effects, if any, of 5-FU and berberine on both malignant and healthy skin cell lines.

Cytotoxicity experiments, which are central to oncology research, require a wide range of cellular models for holistic and comprehensive evaluations. Thus, the ensemble of cell lines - A375, A431, HaCaT and primary human dermal fibroblasts - becomes a cornerstone in this research matrix. Each cell line serves as a unique biological microcosm, representing different facets of both malignant and benign skin conditions. Their collective inclusion provides a rich, multi-dimensional canvas on which the effects and potentialities of drug interactions can be vividly painted. Exploring the nuanced cellular responses of these representative cell lines, particularly with regard to cytotoxic effects in pathological and physiological contexts, is at the forefront of unravelling the combinatorial potential of topical 5-FU and berberine formulations. Such meticulous investigations not only demystify the cellular interactions and dynamics under the aegis of these compounds, but also provide a fundamental foundation to further prepare for the translational phase of therapeutic advances.

In the realm of cancer cell biology, the selection of an appropriate cell line model is imperative to ensure rigorous experimental design and the reliability of outcomes. Herein, the A431 and A375 cell lines had been evaluated to determine which stands as a

more fitting model for skin cancer and its precancerous study. The A431 cell line, derived from human epidermoid carcinoma (SCC), predominantly represents non-melanoma skin cancers. Its biological characteristics, notably the overexpression of the Epidermal Growth Factor Receptor (EGFR), render it advantageous for studies on SCC and related precancerous conditions. EGFR plays a pivotal role in the pathogenesis of SCC (Uribe & Gonzalez, 2011), and thus, A431 offers an ideal platform for exploring this pathway. Additionally, the epithelial-like morphology and *in vitro* growth characteristics of A431 facilitate its cultivation and investigation. Conversely, the A375 cell line has its origin in human malignant melanoma. While invaluable for melanoma research, it may not be the optimal choice for studies on epithelial tumours such as SCC and its precursors. In summary, for researchers dedicated to non-melanoma skin cancer and its precursors, the A431 cell line likely provides a more relevant and representative model.

RNA sequencing (RNA-seq) serves as a beacon in this investigative endeavour, providing a panoramic, high-resolution view of the cellular transcriptomic landscape, meticulously chronicling gene expression dynamics in response to therapeutic interventions. Within the scope of this study, a detailed investigation into the transcriptional ecosystem of A431 cells, specifically under the therapeutic influence of both berberine and 5-FU, was orchestrated to identify key pathways, discover potential synergies and provide a molecular rationale for the observed anti-cancer efficacy.

## 2.2 Aims

The overarching objective of this chapter is to delineate the combined anti-cancer effects of berberine and 5-fluorouracil (5-FU) on cell lines pertinent to skin cancer and Actinic Keratosis (AK) by harnessing *in vitro* cell culture techniques. A examination of the potential therapeutic efficacy and interplay of berberine and 5-FU across a diverse array of cell lines, namely A375 (Human malignant melanoma), A431 (Human squamous carcinoma), HaCaT (keratinocyte line of human skin), and Primary dermal Human fibroblasts, is embarked on. Central to our inquiry is an exploration of drug efficacies embodying the vast biological variances of skin cancer and associated conditions, aiming to elucidate the therapeutic merits and potential drawbacks of amalgamating berberine with 5-FU, with a particular emphasis on skin cancer treatment. An in-depth scrutiny of the side effect profile of 5-FU, both as a stand-alone therapy and in conjunction with berberine, is deemed imperative. Pre-clinical cell lab work plays a crucial role in assessing the side effect profile of 5-FU, both as a standalone therapy and in combination with berberine, by providing insights into toxicity, mechanism of action, and dose optimization. It also aids in exploring individualized treatment strategies and evaluating the safety of these therapies in non-target cells. Furthermore, by employing RNA sequencing, we endeavour to unravel the transcriptomic dynamics in A431 cells engendered by berberine, 5-FU, and their combined regimen. This encompasses the identification of key cellular pathways or processes modulated by the treatments, and the discovery of potential synergistic molecular interactions and genes that might be additively or uniquely perturbed by this combination therapy. Through a rigorous pursuit of these aims, this chapter aspires to provide a solid, evidence-based foundation for assessing the potential therapeutic synergy between berberine and 5-FU in tackling skin cancer and associated maladies, aligning with the broader goal of evaluating their combined anti-cancer effects against skin cancer and actinic keratosis (AK) *in vitro*.

## 2.3 Materials and methods

### 2.3.1 Materials

#### Preparation of stock solutions of drugs

5-FU and berberine chloride were separately dissolved in serum-free media solution directly and sterilised by filtration through a 0.23 µm filter unit to make up the stock solution each time before use. Using a 0.23 µm filter unit for sterilization effectively removes bacteria and other microorganisms from solutions by physically retaining them due to the small pore size, which is crucial for preparing sterile solutions such as those containing 5-FU and berberine chloride for cell culture and drug studies. Berberine chloride (Sigma, B3251) was dissolved in DMSO and made up as a stock solution at 10 mM. All prepared stock solutions were stored at -20 °C for no more than four weeks. The prepared stock solution was cold sterilised by using a syringe filter (pore size: 0.2 µm) in a laminar flow cabinet. Cell information is listed in Table 2.3.1.

<b>Squamous cell carcinomas (SCC) lines, A431</b>
The squamous cell carcinoma (SCC) line, A431 (ECACC 85090402) was purchased from Sigma-Aldrich and supplied by the European Collection of Authenticated Cell Cultures (ECACC). These cell lines were used for the cytotoxicity, cell proliferation, and migration assays. The cell lines are classified as Biosafety Level 2. Cell Line A431 was used in the study as a human squamous carcinoma line, which is derived from an epidermal carcinoma of the vulva taken from an 85-year-old female.
<b>Human malignant melanoma cell lines, A375</b>
The human melanoma cell line, A375 (ECACC 88113005) was purchased from Sigma-Aldrich and supplied by the European Collection of Authenticated Cell Cultures (ECACC); This cell line was used for the cytotoxicity, cell proliferation and migration assays. The cell lines are classified as Biosafety Level 2. Cell Line A375 was used as a human malignant melanoma line, which was derived from a 54-year-old female with malignant melanoma.
<b>HaCaT cell lines</b>
HaCaT cell lines were a generous gift from the School of Pharmacy, University College London, London, UK. Under typical culture conditions HaCaT cells have a partially to fully differentiated phenotype due to the high calcium content of both standard media and fetal bovine serum. The cell lines are classified as Biosafety Level 1.
<b>Primary dermal human fibroblasts</b>
Dermal human fibroblasts were a gift from the Zayed Centre, University College London, London, UK (The donor was a 12-year-old healthy female, and cells were taken from the ear lobe). The cell lines are classified as Biosafety Level 1.

Table 2.3.1 Cell lines used for the *in vitro* cell experiments

## **2.3.2 Methods**

### **2.3.2.1 Maintenance of HaCaT cell lines, Human dermal fibroblast cell lines, SCC cells, A431 and melanoma cells, A375**

HaCaT cell lines, Human fibroblast cell lines, A431 and A375 cells were cultured in complete medium which was a combination of modified DMEM (Dulbecco's Modified Eagle's Medium) (Gibco, 10569010) containing GlutaMax™, sodium pyruvate and high glucose, supplemented with 10% of heat-inactivated foetal bovine serum (FBS) (Gibco, 10500-064) and 1% penicillin-streptomycin antibiotic 10,000U/ml (Gibco, 15140-122). The cell types were maintained in a CO<sub>2</sub> incubator at 37°C and 85 ± 5% relative humidity. At 70% confluence, the cells displaying normal morphology and multiplication patterns were obtained for use in further experiments. Both cell lines were grown in cell culture flasks (Nunc), with the surface area from 25 to 125 cm<sup>2</sup>, according to the specific experiment. The prepared media was stored at 4 °C and warmed up to 37°C before use with cells and diluting drugs. Assays were carried out in both lines at the passage range 6 to 25 generations. The passage range of 6 to 25 generations for cell lines in experiments matters because it ensures the cells are in a stable and consistent state for reliable results. Using cells within this range helps minimize potential variations caused by genetic or epigenetic changes that may occur with extensive passaging, allowing for more accurate and reproducible experimental outcomes. All the procedures were performed under aseptic conditions by working in a laminar flow cabinet (Walker Safety cabinet, Class II).

### **2.3.2.2 Cell resuscitation from frozen stock**

In a microbiological safety cabinet, a tissue soaked in 70% ethanol (Fisher, 10680993) was held around the cap of the frozen cryogenic storage vials (Thermo Scientific, 10320013). The cap was turned around a quarter turn to release any residual liquid nitrogen that may be trapped. The cap was retightened. The vials were quickly transferred to a 37 °C water bath until only one or two small ice crystals, if any, remained (1-2 minutes). It was important to thaw rapidly to minimise any damage to the cell membranes. The ampoule was wiped with a tissue soaked in 70% ethanol (Fisher, 10680993) prior to opening. The whole content of the ampoule was pipetted into a sterile tube (e.g., 15 ml capacity (Thermo Scientific™, 11397201)). Slowly 5 ml of pre-warmed medium was added that had already been supplemented with the appropriate constituents. The viable cell density was determined using trypan blue stain (Gibco, 15250-061), a haemocytometer (FORTUNA®, Germany) and an inverted microscope to count the cells or an equivalent cell counting method. The appropriate volume of cell suspension was transferred to achieve the cell seeding density recommended for the cell line data entry. For adherent cell lines the volume of the medium was adjusted and where necessary the flask size, to achieve the cell seeding density recommended for the cell line data sheet. The frozen ampoules were transferred directly to gaseous phase liquid nitrogen without delay.

### 2.3.2.3 Cell subculturing and passaging

Once cell growth reached 70-80% confluence, cells were ready for passage with split ratios 1:3, 1:4 or 1:8. Both cell lines were adherent cells, grown as a monolayer; thus, the detachment process required trypsin to dissociate cells from culture flask surface enzymatically. First, the old media was gently removed and discarded, and the cells were washed with 10 ml of phosphate buffer saline (PBS) pH 7.4 (Gibco, 10010-023), which removed any residual FBS and inhibited the activity of trypsin in the next step. After aspirating PBS, 3-5ml of 0.25% (w/v) trypsin/EDTA (Gibco, 25300-056) was added to cover the entire surface of the cell sheet. Then the culture flask was placed back in the incubator for 4 min at 37°C in 5% CO<sub>2</sub>. Once, cells were sufficiently detached, growth media was added to neutralise the trypsin (1:3 ratio). The flask contents were then transferred to a 15 ml centrifuge tube (Thermo Scientific™, 11397201) and centrifuged for 8 min at 1300 rpm. After aspirating the supernatant, the cell pellet was carefully suspended with 10 ml of growth media. A suitable amount of cell suspension was transferred to a new culture flask containing pre-warmed media. The flask was labelled with the cell name, split ratio, passage number and date, and stored in an incubator at 37°C in 5% CO<sub>2</sub>.

### 2.3.2.4 Cell counting

Trypan blue was used to estimate the proportion of viable cells in a population. Cells were diluted with 0.4% Trypan Blue stain (Gibco, 15250-061) in a 1:1 ratio and dispensed into both sides of a Neubauer haemocytometer. The viable bright cells were counted under the inverted microscope, and the total number of viable cells per ml were estimated as shown figure 2.3.2.

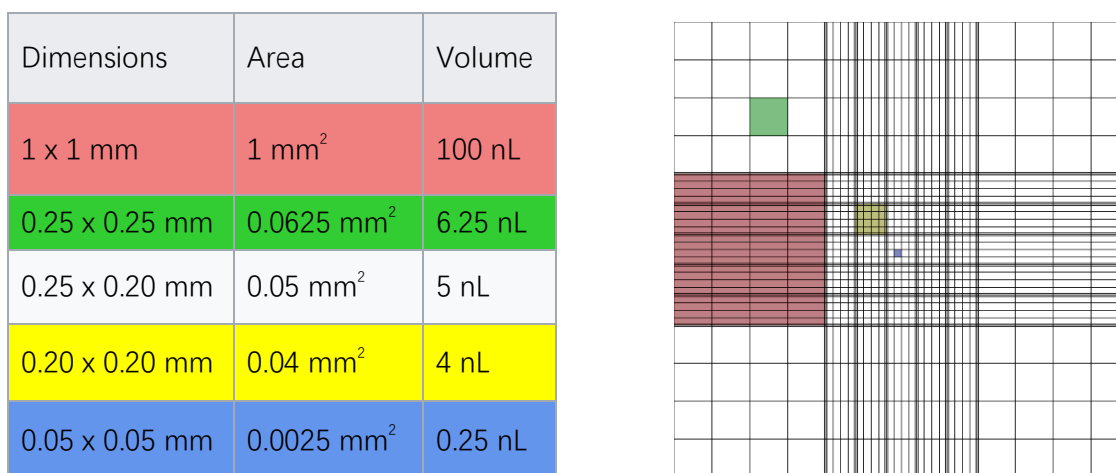


Figure 2.3.2 The calculation principles of the hemacytometer. The grid area of the Improved Neubauer ruled hemacytometer consists of nine 1 x 1 mm (1 mm<sup>2</sup>) squares.



### **2.3.2.5 Preparation of frozen cell stocks**

After subculturing the cells, the cell suspension was centrifuged at 1300 rpm for 8 minutes. After aspiration of supernatant, the pellet was resuspended with pre-prepared medium, 10% (v/v) DMSO in growth media for cell lines, to obtain a desirable cell density between  $1 \times 10^6$  to  $2 \times 10^6$  cells per 1 ml. Cells with freezing media were then aliquoted to sterile cryogenic vials (Nunc), which were labelled with the cell name, passage number and date. The cryovials were stored in a freezing container filled with isopropanol to achieve a  $-1^\circ\text{C}/\text{min}$  cooling rate and stored at  $-70^\circ\text{C}$  overnight before transfer to a liquid nitrogen tank.

### **2.3.2.6 Morphology observation**

Cell morphology was assessed by observing changes in cell proliferation and migration using the EVOS®FL imaging system. Images were captured using IncuCyte™ FLR from Essen Biosciences

### **2.3.2.7 Cell proliferation determination with sulforhodamine B assay**

The sulforhodamine B assay (SRB) is a colorimetric assay developed by the National Cancer Institute (US) in 1990 (Skehan et al., 1990) and is still favoured by this institution for anticancer drug screening (Orellana and Kasinski, 2016). This assay relies on the ability of SRB to bind to protein components of the cell that have been fixed to tissue culture plates by trichloroacetic acid (TCA). Under mildly acidic conditions, the two sulfonic groups of SRB bind to basic amino-acid residues of fixed proteins and dissociate under basic conditions. Therefore, the amount of dye extracted from stained cells can be determined by the optical density, which is directly proportional to the cell mass (Vichai and Kirtikara, 2006). SRB assay results simply and directly refer to the 'cellular viability' or cytotoxicity; however, cell necrosis, apoptosis or the living status of the cells cannot be detected. The reason to choose 72 hours for the cell viability assay was because of the doubling time of the cell line and the exposure time of the treatment. Cell growth undergoes four phases: lag phase, exponential phase, stationary phase and death phase. Cells are most active in the exponential phase and less active in the rest of the phases. The doubling time of A375 and 431 were found at 18 hours. For HaCaT and dermal fibroblasts the times are around 28 hours. Therefore, for 72 hours of incubation with treatment exposure, both cell lines were at their exponential phase of growth. In brief, model cells were plated in a 96-well microplate (no. 3966; Costar, Corning Incorporated, New York, USA) and incubated for 18–24 h. Exponentially growing cells were exposed to a series of concentrations of drug (0.5, 1, 2, 4, and 8  $\mu\text{M}$ ) for specified times (12, 24, 36, and 48 h). The concentration of DMSO in the control well was 0.04% the same as in the well with the highest concentration of drug (8  $\mu\text{M}$ ). After incubation, the culture medium was removed, and the cells were fixed in 10% trichloroacetic acid (TCA; 200  $\mu\text{l}/\text{well}$ ) at  $4^\circ\text{C}$  for 1 h. Then, the TCA solution was removed and 100  $\mu\text{l}/\text{well}$  SRB (0.4%; in 0.1% acetic acid) solution was added. After staining with SRB for 10 min, the cells were washed

with 0.1% acetic acid for five times and then dried overnight at 37°C. Finally, the SRB-labelled cells were dissolved in 10 M Tris and the absorbance was measured by a microplate multi-detection reader (FLUOstar OPTIMA, BMG, Offenburg, Germany) at a wavelength of 540 nm. The percentage of cell proliferation was calculated in comparison with the control group. IC50 is a quantitative measure that indicates how much of a particular inhibitory substance is needed to inhibit, *in vitro*, a given biological process or biological component by 50%. Half-maximal inhibitory concentration (IC50) is the most widely used and informative measure of a drug's efficacy. It indicates how much drug is needed to inhibit a biological process by half, thus providing a measure of potency of an antagonist drug in pharmacological research. In this chapter, IC50 was used as the measure of a drug's efficacy.

### 2.3.2.8 Calcusyn for combination treatment calculation

There are various methods available for assessing the interaction between different drugs and for calculating the effects of combination treatments. (Greco, 1995). This results in the description of three important concepts, which define how effective the combination is, namely, synergism, antagonism and additive effects. Nevertheless, there has not yet been a consensus on any unique definition (Borgert et al., 2005), however, the simplest one would be that synergism is an effect that is more than additive, whereas the definition for antagonism is an effect that is less than additive (Chou and Martin, 2006). This is ascertained by statistical means and several models are proposed. In this project, we chose the median-effect plot based on the multiple drug-effect equation of Chou-Talalay derived from enzymatic models (Chou and Martin, 2006). Combination treatments were performed using the sulforhodamine B assay (SRB) assay. The cells were either treated with the combined compounds using constant ratios or fixed concentrations for 72 hours. Data from combinatorial studies were analysed using the Calcusyn© software (Biosoft, Cambridge, UK) to infer the combination index (CI) values. A combination index (CI) is estimated from dose-effect data of single and combined drug treatments. A value of CI less than 1 indicates synergism; CI = 1 indicates an additive effect; and CI > 1 indicates antagonism. A range of CI values classified by the Calcusyn protocol, are interpreted as shown below in Table 2.3.3:

CI	Combination effect
<0.1	Very strong synergism
0.1-0.3	Strong synergism
0.3-0.7	Synergism
0.7-0.85	Moderate synergism
0.85-0.90	Slight synergism
0.9-1.1	Nearly additive
1.10-1.20	Slight antagonism
1.20-1.45	Moderate antagonism
1.45-3.3	Antagonism
3.3-10	Strong antagonism
>10	Very strong antagonism

Table 2.3.3 Based on the Calcusyn protocol, CI value-Combination effect list

### 2.3.3 Assessment of the Synergistic Effect of Berberine and 5-FU on the A431 Cell Line through RNA-seq Data Analysis

To explore the underlying molecular mechanisms and potential synergistic effects of berberine and 5-FU on A431 cells, a series of in-depth computational analyses were performed, encompassing differential gene expression, gene enrichment, and cellular deconvolution.

#### **Cell Culture and Sample Preparation:**

A431 cells were cultured in a controlled environment at 37°C with 5% CO<sub>2</sub>, using Dulbecco's Modified Eagle Medium (DMEM, Gibco, Thermo Fisher Scientific) supplemented with 10% fetal bovine serum (FBS, Sigma-Aldrich) and 1% penicillin-streptomycin (Thermo Fisher Scientific). Cells were harvested upon reaching 80-90% confluency using 0.25% trypsin-EDTA (Gibco, Thermo Fisher Scientific).

#### **RNA Extraction and Quality Assessment:**

Total RNA was isolated using the RNeasy Mini Kit (Qiagen) according to the manufacturer's instructions. The integrity and concentration of RNA were assessed using the Agilent 2100 Bioanalyzer (Agilent Technologies) and Qubit RNA Assay Kit (Thermo Fisher Scientific), respectively.

#### **Library Preparation and Sequencing:**

RNA-seq libraries were prepared using the NEBNext Ultra II Directional RNA Library Prep Kit (New England Biolabs) following the manufacturer's protocol. The libraries were quantified using the Qubit dsDNA HS Assay Kit (Thermo Fisher Scientific) and validated for size distribution using the Agilent 2100 Bioanalyzer. Sequencing was performed on an Illumina HiSeq 2500 platform (Illumina) to generate 150 bp paired-end reads.

#### **Data Pre-processing:**

Raw readings were subjected to quality control using FastQC (v0.11.9) and trimmed of adapters and low-quality bases using Trimmomatic (v0.39) with a sliding window approach.

#### **Alignment and Read Mapping:**

Clean reads were aligned to the human reference genome (GRCh38) using the STAR aligner (v2.7.3a) with default settings. The resultant BAM files were sorted and indexed using SAMtools (v1.10).

#### **Differential Expression Analysis:**

Read counts were generated using featureCounts (v2.0.1) from the Subread package. Differential expression analysis was conducted using the DESeq2 package (v1.28.1) in R (v4.0.3), specifying the treatment conditions and comparisons of interest.

#### **Functional Enrichment and Pathway Analysis:**

Differentially expressed genes were analysed for functional enrichment using DAVID (v6.8) to elucidate the biological processes and pathways significantly impacted.

#### **Data Visualization:**

Visual representations of the data were generated using ggplot2 (v3.3.2) in R, including MA plots, volcano plots, and heatmaps to exhibit the differential expression and functional insights derived from the analysis.

### 2.3.3.1 Sample Grouping and Differential Gene Expression Analysis

In the process of analysing the differential gene expression, A431 cell samples were meticulously grouped into four distinct categories based on the treatments administered: Control, Berberine, 5-FU, and a combined regimen of Berberine and 5-FU. The detailed methodology encompassed the following steps:

#### **Data Import and Experimental Design:**

Following established guidelines, raw count matrices obtained from RNA-seq were imported into an R computational environment.

The DESeq2 package was utilized to craft the experimental designs, which distinctly specified the treatment conditions: Control, Berberine, 5-FU, and Ber-FU.

#### **DESeq2 Analysis:**

DESeq2 objects were instantiated from the count matrices and the predefined experimental design.

The process of differential gene expression analysis was executed, with the Benjamini-Hochberg method being employed for multiple test corrections.

#### **Residual Optimization:**

Residual optimization, a characteristic feature of DESeq2, was employed to enhance the accuracy of differential gene expression estimations.

This process refined the negative binomial distribution models employed, accommodating both inter and intra-sample variability.

#### **Data Convergence and Visualization:**

To ensure the robustness of the differential gene expression analysis, data convergence was ascertained.

The MA plot function from DESeq2 was employed to visualize the distribution and significance of the differentially expressed genes.

#### **Gene Filtering:**

The results from the differential expression analysis were meticulously sieved, retaining genes based on stringent statistical thresholds.

Particular emphasis was placed on log2FoldChange values and adjusted p-values to filter the genes of interest.

Through the methodical execution of these steps, a comprehensive analysis of differential gene expression across varying treatment conditions was achieved, facilitating a deeper understanding of the molecular interactions and effects induced by Berberine, 5-FU, and their combined regimen on A431 cells.

### 2.3.3.2. Enrichment Analysis of Differential Genes

The biological relevance of identified differential genes was ascertained using enrichment analyses:

**ClusterProfiler Integration:** The ClusterProfiler package, as proposed by Yu et al. (2012), was incorporated for a comprehensive gene ontology enrichment analysis.

**Enrichment Execution and Visualization:** Using the previously derived list of differentially expressed genes, the enrichGO function was deployed. Results were then presented visually, harnessing multiple plotting tools available within the ClusterProfiler package.

#### **2.3.3.3. Gene Set Enrichment Analysis (GSEA)**

Broadening the scope of analysis, GSEA helped discern potential pathways and functional gene sets influenced by the treatments:

GSEA Implementation: Drawing from the methodology outlined by Subramanian et al. (2005), GSEA was undertaken. This involved ranking genes based on expression changes and comparing them to predefined gene sets to discern patterns.

Results Interpretation: The enrichment scores and FDR-adjusted p-values from GSEA facilitated a comprehensive understanding of the relevance of predefined gene sets in the experimental context.

Visualization: GSEA results were rendered graphically, generating enrichment plots and score maps to provide a cohesive representation of gene set enrichment trends.

#### **2.3.3.4. Cellular expression of gene and pathway Analysis using online database**

An online tool, reactome, was used for data analysis. The protein interactions among gene candidates were analysed using String software.

#### **2.3.4 Statistical analysis**

Each assay was performed in duplicate, and the experiments were repeated at least three times (n=6). The statistical analysis results, concentration-effect curves and graphical representations were analysed with GraphPad Prism Program version 8.0. Data were presented as mean  $\pm$  SD. The results were considered to be significant for a value of  $P < 0.05$  by the t-test and one-way analysis of variance (ANOVA).

## 2.4 Results

### 2.4.1 Morphology of cell culture lines

Examining cell morphology is one of the primary ways to determine the health, differentiation status, and potential aberrations in cultured cells. The success of the culturing techniques was evaluated based on cellular morphology. Specific morphological characteristics serve as preliminary indicators of cell health, differentiation status, and potential anomalies. The observations and evaluations for each cell line are reported below. Being immortalized keratinocytes, HaCaT cells usually present with epithelial-like polygonal shapes. They grow in a monolayer and are tightly packed.

Criteria for Successful Culture: Cells that display a uniform shape, tightly packed colonies, minimal cellular debris, and the absence of elongated or spindle-shaped cells, which may indicate cellular stress or senescence (Boukamp et al., 1988).

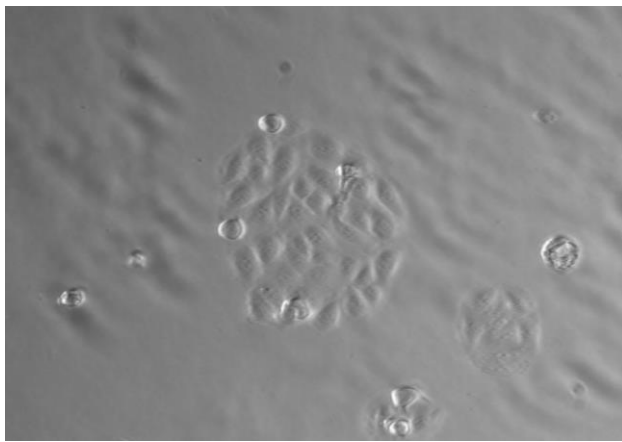


Figure 2.4.1 The cell morphology of HaCaT cell lines. Images were captured in the first passaging and cultured in the flask for 48 hours.

Fibroblasts usually appear elongated, having a spindle-like shape. They grow in a scattered manner, not forming tight colonies. Criteria for Successful Culture: Observation of spindle-shaped cells with elongated processes, devoid of any cell clumping or aggregation (Sorrell et al., 2004).

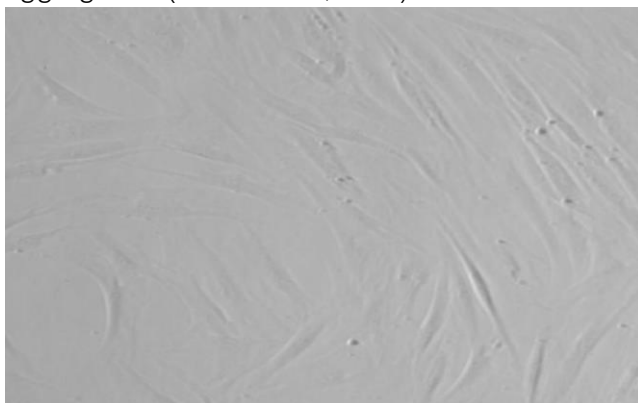


Figure 2.4.2 The cell morphology of Dermal Fibroblast cell lines. Images were captured in the first passaging and cultured in the flask for 48 hours.

A375 cells are usually adherent and can sometimes appear elongated. They may form loose networks or clusters. Criteria for Successful Culture: Cells that have consistent shapes, clear boundaries, absence of excessive cell clumping, and a lack of abundant floating or rounded cells (Fogh et al., 1977).

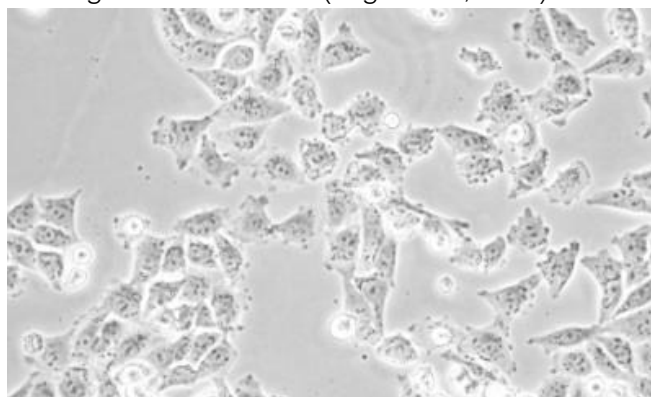


Figure 2.4.3 The cell morphology of A375 cell lines. Images were captured in the first passaging and cultured in the flask for 48 hours.

A431 cells are epithelial-derived and, as such, usually display an epithelial-like morphology. They have a more rounded or polygonal appearance. Successful Culture Indicators: Uniformly polygonal cells with clear boundaries, absence of floating cells (indicative of cell death), and no signs of multi-layering which might indicate loss of contact inhibition and over-confluence.

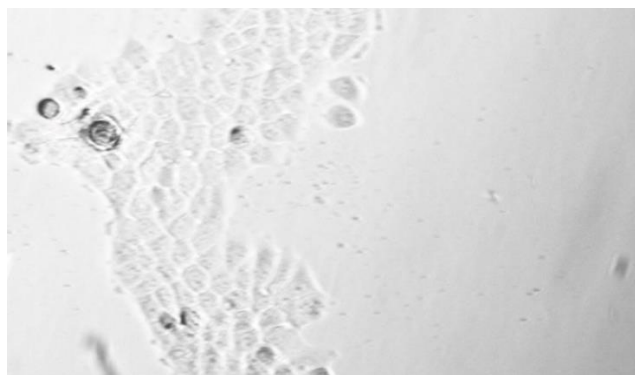


Figure 2.4.3 The cell morphology of A431 cell lines. Images were captured in the first passaging and cultured in the flask for 48 hours.

The examination of cell morphology confirmed the successful establishment of 2D cell culture protocols for A431, HaCaT cell lines, and dermal fibroblasts. Through visual and microscopic assessment, the cultured cells within each line displayed the characteristic morphological traits associated with healthy, proliferative, and morphologically stable *in vitro* cultures. This sets a robust foundation for subsequent experimental manipulations and analyses aimed at elucidating the cellular and molecular mechanisms underpinning the responses to the treatments administered.

## 2.4.2 Effect of single and combinatorial treatments of drugs on proliferation (SRB) assays

Three independent SRB assays were performed. To ensure consistency of results, all procedures involving treatment addition and cell fixation were performed at the same time of day to eliminate both environmental and chronobiological influences (Kiessling et al., 2017). Berberine chloride and 5-FU inhibited proliferation and migration of all cell lines. Based on Table 2.5 below, cytotoxicity screening results and half-maximal inhibitory concentration (IC<sub>50</sub>) of single treatment with 5-FU and berberine chloride were summarised. Berberine chloride and 5-FU inhibited the proliferation and migration of all cell lines to varying degrees. The proliferation assays with primary dermal fibroblasts contribute to the large standard deviation and lack of statistical significance. The results indicated that both berberine chloride and 5-FU exhibited antiproliferative activity against both melanoma and SCC cell lines in SRB assays. Compared to A375 cells, A431 cells are much more sensitive to both compounds in a concentration dependent manner with an IC<sub>50</sub> of 0.5  $\mu$ M for 5-FU and 4  $\mu$ M for berberine over 72 hours.

IC <sub>50</sub>	5-fluorouracil	Berberine chloride
A375 (human melanoma)	35 $\pm$ 2.5 mM	40 $\pm$ 3.5 mM
A431 (epidermoid carcinoma)	0.5 $\pm$ 0.02 mM	4 $\pm$ 0.4 mM
HaCaT cells	42 $\pm$ 1.7 mM	10 $\pm$ 0.1 mM
Primary dermal fibroblasts	N/A	N/A

Table 2.5: IC<sub>50</sub> ( $\mu$ M) of test compounds for both cell lines, A375 and A431, as assessed by the SRB assay at 72 hours. The results were obtained in three independent experiments run in replicate (n=3).

Overall, the results showed that two compounds exhibited anti-proliferative activity against both melanoma and non-melanoma cell lines in SRB assays. In the non-melanoma A431 cell line, both compounds showed higher cytotoxic activities. Furthermore, the IC<sub>50</sub> value of 5-FU was 8 times lower than that of berberine chloride in A431. Based on the results of the cytotoxicity tests on HaCaT cells, it was observed that the inhibitory effect of 5-FU on HaCaT cells was reduced compared to A431. According to the results of the IC<sub>50</sub> tests of single treatments, follow-up experiments were performed to evaluate the anti-proliferative activities of both cell lines, A375 and A431, treated either individually or in combination. As for the combinatorial treatments, at the same concentration of 5FU, berberine can significantly improve the anti-proliferative activity. The software Calcsyn was used to analyse the results of inhibitory activity in order to evaluate the combinatorial effects, additive, antagonism or synergy. As table 2.6 shows, there are three combinational ratio combinations that demonstrate a strong anticancer effect. All combinations of drugs show a synergistic treatment effect which suggests berberine chloride can improve the anticancer effect of 5-FU on the A431 cell line. More tests will be conducted with different ratios of combinations of the drugs to find the optimum ones.



BBR (mM)	5-FU (mM)	CI	Effect
1.0	0.1	0.84208	Moderate synergism
1.0	0.2	0.51013	Synergism
1.0	0.4	0.32746	Synergism
<b>1.0</b>	<b>0.8</b>	<b>0.25015</b>	<b>Strong synergism</b>
<b>1.0</b>	<b>1.6</b>	<b>0.27968</b>	<b>Strong synergism</b>
1.0	3.2	0.34826	Synergism
1.0	6.4	0.49708	Synergism
1.0	12.8	0.58428	Synergism
<b>1.0</b>	<b>25.6</b>	<b>0.26837</b>	<b>Strong synergism</b>
0.5	0.1	0.74854	Moderate synergism
0.5	0.2	0.55079	Synergism
0.5	0.4	0.45902	Synergism
0.5	0.8	0.39906	Synergism
0.5	1.6	0.36371	Synergism
0.5	3.2	0.55659	Synergism
0.5	6.4	0.89242	Slight synergism
0.5	12.8	0.84179	Moderate synergism
0.5	25.6	0.52267	Synergism

Table 2.6: Results for combination index (CI), fraction affected (fa) values and effect of combination treatment with 5FU and berberine chloride on A431.

According to the results reported in Table 2.6, the treatment of A431 with 5-FU and berberine chloride with fixed concentrations (0.5 and 1 mM) inhibited cell proliferation. There was synergy when 5-FU was combined with berberine chloride using a fixed concentration. Three combinations show strong synergistic anti-cancer effects which need to be further investigated in

preclinical trials. The combination of 25.6 mM 5-FU and 1 mM berberine has great potential for application in topical anti-skin cancer formulations primarily composed of 5-FU as the active ingredient. To further investigate the synergistic effect of drug A (berberine) and drug B (5-FU) in the combined treatment on A431 cells, a detailed analysis based on RNA-seq data will be performed. This analysis aims to elucidate the molecular and genetic responses triggered by the combined treatment, which may potentially highlight the synergistic interactions between berberine and 5-FU. By evaluating the gene expression profiles, pathway activation or inhibition, and possibly the involvement of different molecular targets, a comprehensive understanding of the synergistic effects and the underlying mechanisms can be attained. This in-depth analysis will not only contribute to the understanding of the combined drug effects but may also provide valuable insights for optimizing anti-cancer treatment strategies in skin cancer therapeutics. In this analysis of RNA sequences, we utilized the DNBSEQ platform to sequence 12 samples, yielding an average of approximately 6.68 Gb bases per sample. The average mapping ratio against the reference genome was 95.79%, while the average mapping ratio against genes stood at 71.88%; a total of 16,378 genes were identified.

Biological experiments typically involve biological replicates to ensure the reproducibility and robustness of the findings. These replicates are inherent to biological experimentation, and it is customary to categorize multiple samples of biological replicates into a single group for analytical purposes. The subsequent table delineates the grouping of samples employed in the analysis as shown in the table below.

Group Name	Sample Name
<b>Control</b>	P3_Ctrl,P5_Ctrl,P6_Ctrl
<b>Berberine</b>	P3_Ber,P5_Ber,P6_Ber
<b>5FU</b>	P3_Fu,P5_Fu,P6_Fu
<b>Ber-FU</b>	P3_Fu_B,P5_Fu_B,P6_Fu_B

Table 2.7: A total of twelve sets of A431 cell lines were subjected to sequencing analysis, encompassing various passage numbers (denoted as P). These cell lines were categorized into four distinct groups for the investigation: the control group which received no treatment, a group treated with 10 mM Berberine chloride, another group treated with 10 mM 5-Fluorouracil (5-FU), and a final group concurrently treated with 10 mM Berberine chloride and 10 mM 5-FU.

To elucidate the correlation in gene expression across samples, Pearson correlation coefficients were computed for all gene expressions between each pair of samples, and these coefficients were visually represented through a heatmap as Figure 2.8 shown. These correlation coefficients serve as indicators of the overarching similarity in gene expression between each sample. A higher correlation coefficient denotes a higher level of similarity in gene expression levels.

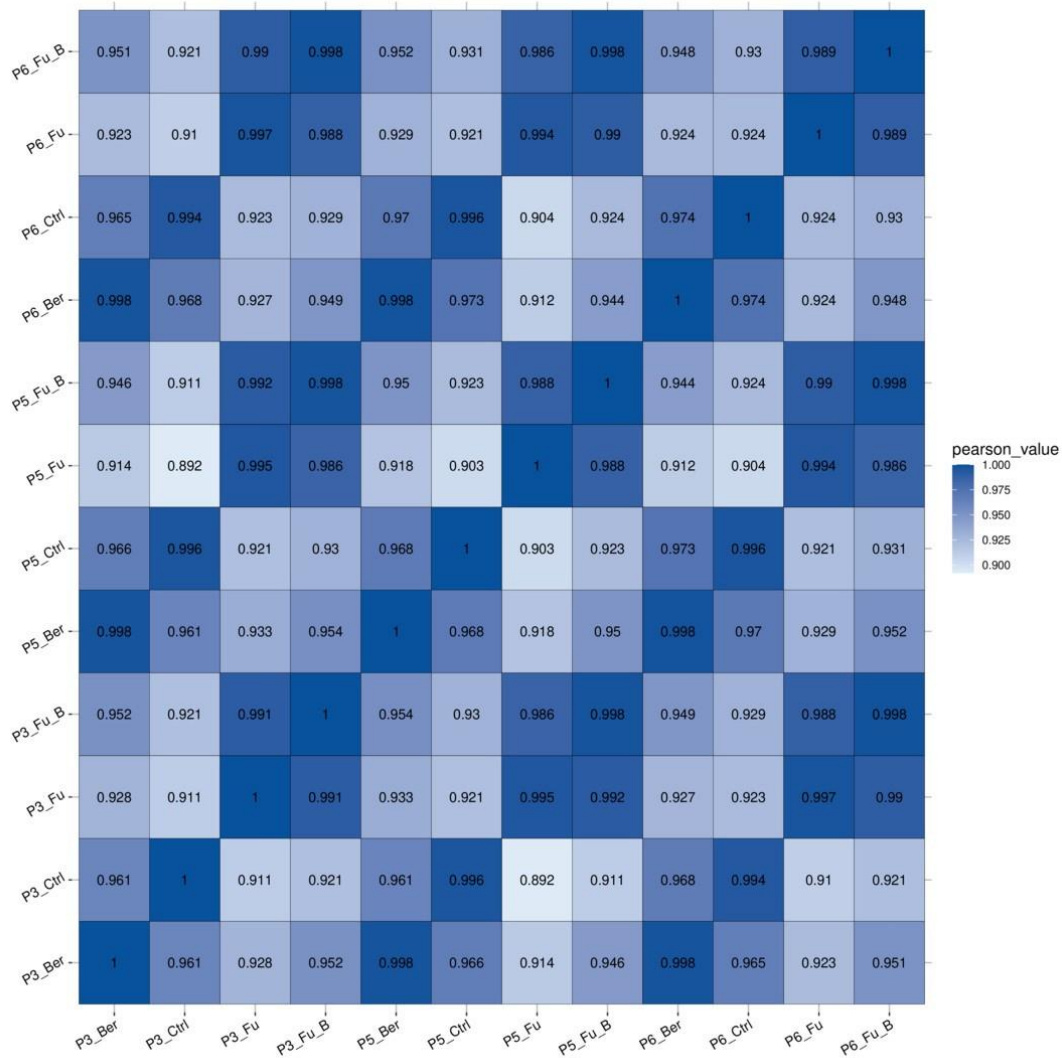


Figure 2.8: Results of the RNA-seq results. Analysis of the degree of correlation between the 12 treated A431 samples using the Pearson correlation coefficient. When  $R^2 > 0.92$ , the two samples were considered correlated.

Under the same treatment conditions, A431 cell lines of different passage numbers exhibited highly similar gene expression profiles. This consistency substantiates that the cell lines remained stable and unaltered during the culturing phase, with no significant variations attributed to differing passage numbers. The overall gene expression demonstrated a high degree of similarity (with Pearson values all exceeding 0.9) across different passage numbers of the A431 cell lines. However, significant disparities were observed in the RNA sequencing (RNA-seq) data among the cell lines subjected to different treatment regimens.

Next, the RNA-seq data was imported into the R environment, and the experimental design was set up using the DESeq2 package for Discovering Differentially Expressed Genes (DEGs). This involved assigning condition or treatment group information for each sample, such as Control, Berberine, 5FU, and Ber-FU. The Figure 2.8 showcases the relationship between the average expression level of each gene and its expression variation under different conditions.

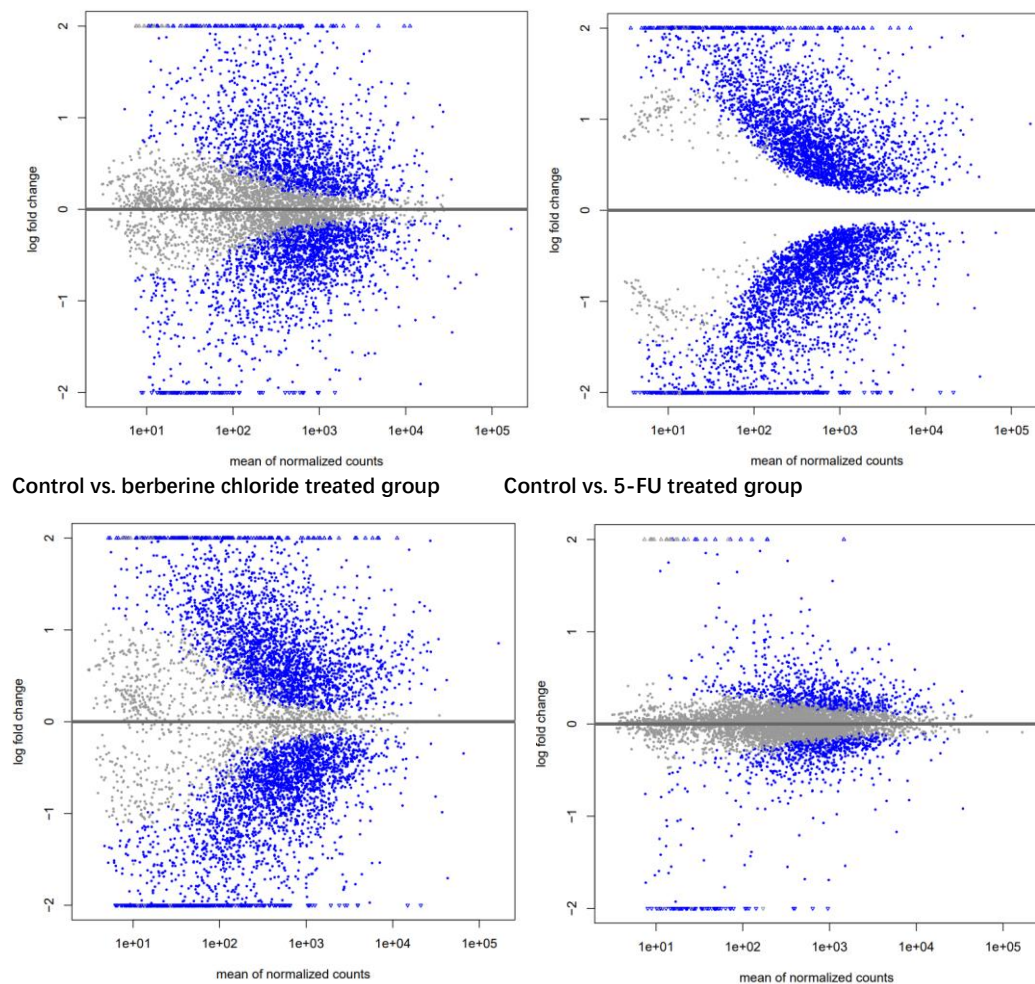
## Differential Expression Analysis

Differential Expression Analysis (DEA) stands as a critical method in the field of genomics, helping to identify genes that undergo significant changes in expression under various biological scenarios, such as the comparison between untreated (control) and treated

groups (Costa-Silva et al., 2017). In this research, MA is used as plots to depict the results from DEA across several comparisons, effectively simplifying the visualization of complex data. "MA plot" (M (log ratio) and A (mean average)) is a type of graphical representation used to visualize the differences between measurements from two conditions in RNA-seq data analysis. Figure 2.9 offers an efficient method to showcase alterations in gene expression, with each gene represented as a point. The horizontal axis illustrates the average expression level of genes after log transformation, and the vertical axis represents the change in gene expression, measured in log2 fold change (log2FC). The further analysis particularly focuses on genes with  $|\log_2FC|$  more than 1, pinpointing genes that have experienced a doubling or more in expression levels as a response to treatment. This selection highlights genes of significant interest due to their substantial role in reacting to the treatments administered. Such genes are crucial for understanding how treatments impact cellular functions and are valuable for uncovering the molecular basis of the treatment effects. By zeroing in on genes within this log2FC window, spotlighting genes that could be central to inducing changes in cellular pathways. This targeted approach enhances the understanding of how treatments work at a molecular level and identifies important genes that could be potential targets for further research or therapeutic development.

Comparison	Total count	Padj<0.05	$ \log_2\text{FoldChange}  \geq 1$
Ctrl vs B	6765	3665	784
Ctrl vs Fu	6765	6494	2632
Ctrl vs Fu_B	6765	5510	2012
Fu vs Fu_B	6765	1574	130

Table 2.9.1: data from a differential gene expression analysis comparing different treatment groups in RNA-seq study. The number of genes with a statistically significant difference in expression (with an adjusted p-value less than 0.05). The number of genes with a log2 fold change of 1 or more, indicating that the gene expression has doubled or more compared to the reference group.



**Control vs. berberine chloride and 5-FU treated group    5-FU vs. berberine chloride and 5-FU treated group**

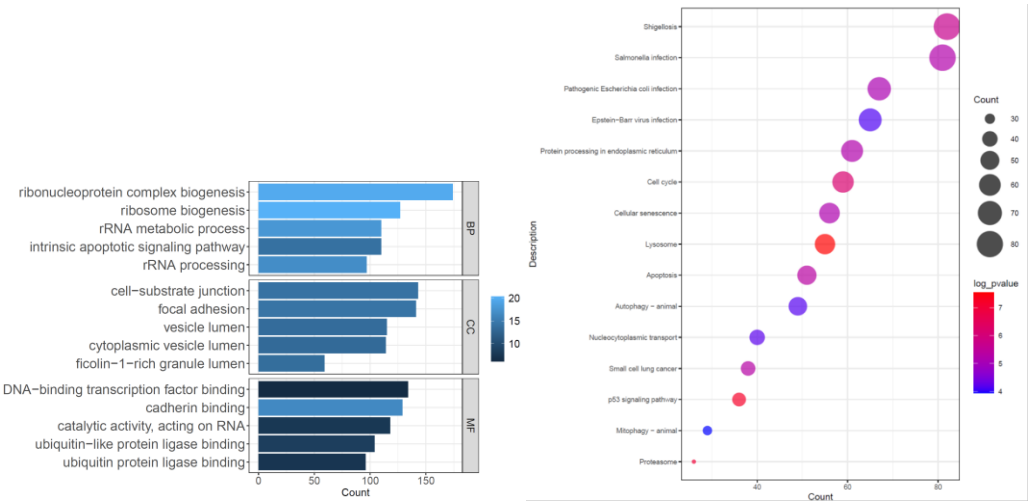
Figure 2.9.2: Differential Expression Analysis between Control group vs Berberine chloride treated group. The y-axis represents the  $\log_2$  Fold Change ( $\log_2FC$ ), indicating the magnitude of changes in gene expression between the two conditions. The x-axis displays the Mean of Normalized Counts, representing the absolute gene expression levels. Genes with significant differential expression are denoted by blue points, whereas those with non-significant differential expression are represented by grey points.

In the comparison between the control group and the group treated with berberine chloride, focusing on genes that exhibit a  $\log_2$  fold change ( $\log_2FC$ ) between 1 and 2 uncovers a smaller, yet significantly upregulated group of genes due to berberine chloride treatment. This specific range underscores the importance of further examining these genes, as they could be key in understanding how berberine chloride affects cells. The comparison between the control group and the group treated with 5-FU reveals a noticeable grouping of genes. This suggests that 5-FU has a strong impact on gene expression, especially for those genes that increase in expression by two-fold or more. This notable change likely mirrors the critical role of 5-FU in hindering nucleotide synthesis, affecting various cellular activities. A treatment with 5-Fluorouracil affects a larger portion of the genome, with 6,494 genes showing significance, and 2,632 with at least a 2-fold change. This implies that 5-FU has a substantial effect on gene expression, likely due to its role in disrupting nucleotide synthesis. In the group receiving combined treatment, genes suggest a more refined and selective effect on gene regulation. When

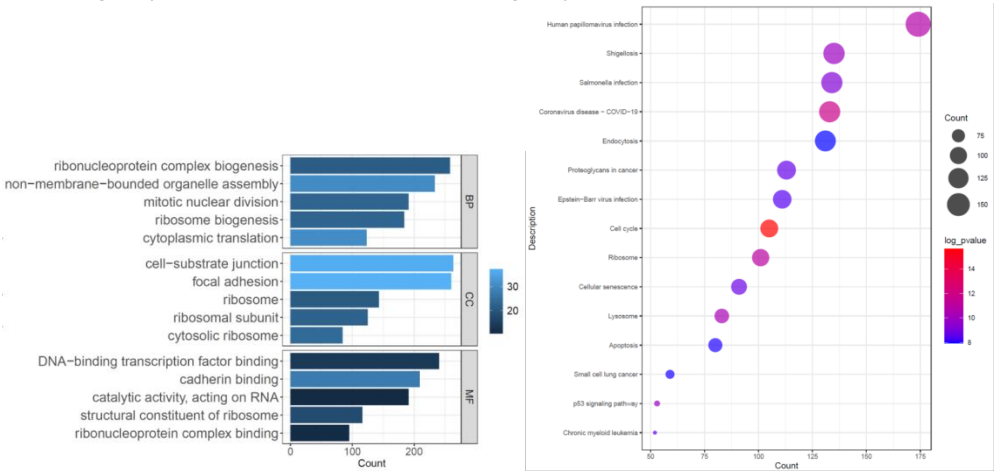
comparing the effects of 5-FU alone to the combined treatment, the presence of genes indicates that berberine chloride might either enhance or diminish the impact of 5-FU on certain genes. This may point to a less measured adjustment of gene expression (130) when both agents are applied together, hinting at the synergy may cause by small amount gene groups. The alterations observed in this range are particularly noteworthy as they could indicate how cells adapt to the combined drug effects.

**The differential gene enrichment analysis**

differential gene enrichment analysis is performed to elucidate the biological implications of treatments with berberine chloride, 5-FU, and their combination on A431 cells to understand the molecular underpinnings of the combined treatments' efficacy. Based on the detailed results of gene enrichment analysis, the study investigates the effects of different treatments on A431 cells. The treatments included berberine chloride, 5-FU and a combination of both. The results are categorised according to Gene Ontology (GO) terms covering Biological Processes (BP), Cellular Components (CC) and Molecular Functions (MF).



Control group vs berberine chloride treated group



Control group vs 5-FU treated group

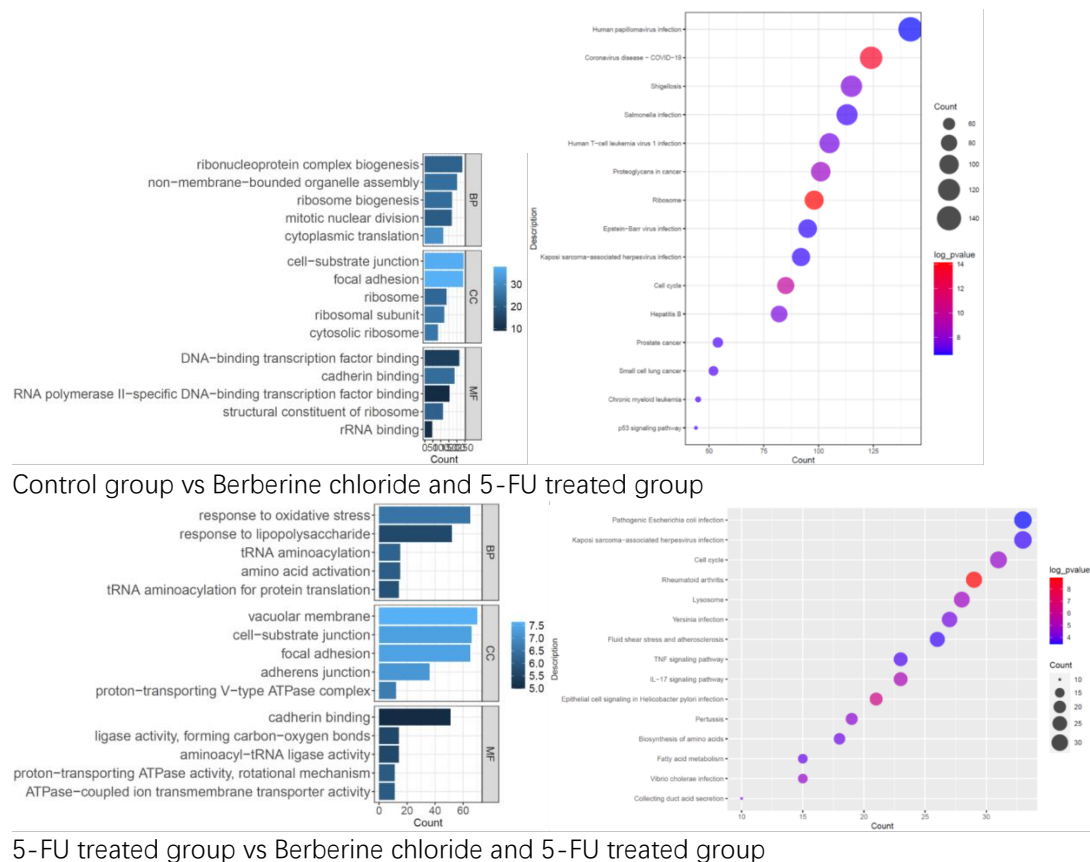


Figure 2.10.1 and Table 2.10.2 from the study present a comprehensive gene enrichment analysis that sheds light on the functions and roles of genes that were significantly altered in expression due to our treatments. These visual aids, including dot plots, help us delve into the specifics of Gene Ontology (GO) terms related to Biological Processes (BP), Cellular Components (CC), and Molecular Functions (MF) that are influenced by the treatments. This visualization makes it easier to understand the complex roles these genes play in biological processes, where they are located within the cell, and the molecular functions they perform. The 'count' value mentioned indicates the number of genes associated with each GO term, showing how represented our genes are within these functional categories. The colour coding, which ranges from lighter to darker shades, acts as a guide to either the quantity of genes tied to each GO term or the significance of their enrichment, with the specific meaning detailed in the figure's legend.

According to the results of the differential gene enrichment analysis, the main pathways that are influenced by 5-FU and berberine chloride can be summarized in table 2.10.3

Ribosome Biogenesis and Function:
This pathway is often highlighted in the presence of changes in genes related to the structure and function of ribosomes, which are essential for protein synthesis. The enrichment analysis indicated that genes involved in ribonucleoprotein complex biogenesis and ribosomal RNA processing were affected, suggesting that both berberine chloride and 5-FU influence protein synthesis machinery.
Cell Cycle Control:
The analysis suggested that pathways related to cell cycle regulation were impacted, especially considering the involvement of genes associated with the cell cycle process and mitotic nuclear division. This aligns with the known mechanism of 5-FU, which disrupts nucleotide synthesis and thereby affects cell division.
Apoptosis and Cell Death:
Enriched GO terms related to intrinsic apoptotic signalling pathways and the p53 signalling pathway were observed. These pathways are crucial for programmed cell death, and their alteration is a common goal in cancer therapy to induce cancer cell death.
Cellular Senescence:
Some pathways related to cellular aging and senescence were enriched, which could imply that the treatments affect not only the proliferation of cancer cells but also their longevity.
DNA Repair and Synthesis:
Enriched pathways may include those involved in DNA binding and repair processes, given the impact on transcription factors and other proteins that interact with DNA. This is particularly relevant for 5-FU, which incorporates into RNA and DNA and disrupts their synthesis.
Amino Acid Metabolism and Transport:
GO terms related to amino acid activation and tRNA aminoacylation for protein translation suggest that these treatments influence the metabolism and transport of amino acids, which are the building blocks of proteins.
Immune Response and Inflammation:
Some analyses indicated changes in genes related to the immune response, such as those involved in the response to lipopolysaccharides and oxidative stress, hinting at the modulation of inflammation and immune surveillance.
Cell Adhesion and Communication:
Pathways associated with focal adhesion, cell-substrate junction, and adherens junction were affected, suggesting changes in how cells interact with their environment and with each other, which could impact cell migration and metastasis.
Protein Degradation:
The ubiquitin-protein ligase binding-related pathways suggest changes in protein degradation processes, which can affect a wide range of cellular functions and may be relevant to the regulation of cancer cell growth.

Table 2.10.3: The pathway summary from differential gene enrichment analysis, treated with 5-FU and berberine chloride.



The colour intensity in the bar graphs serves as an indicator of how much a specific GO term is represented, with the number of associated genes giving a quantitative measure of this representation. Berberine chloride's influence is noted in the formation of ribonucleoprotein complexes and RNA metabolism, hinting at its potential impact on protein synthesis and gene regulation. Observations of changes in cellular components related to cell-substrate interactions and vesicular transport suggest shifts in cell structure and how materials move inside cells. Analysis at the molecular function level points to changes in how transcription factors bind and the activity of protein ligases, indicating adjustments in gene expression and the lifecycle of proteins. Treatment with 5-FU markedly impacts processes associated with ribosomes and cell cycle control, aligning with its known function of disrupting nucleotide synthesis. This leads to interference with the cell's protein-making capabilities and how cells adhere to one another. Enrichments in functions related to RNA processing and the activity of transcription factors indicate widespread effects on how cells communicate and manage gene expression. The use of both treatments together appears to influence genes responsible for assembling organelles and dividing cells, suggesting a reorganization of cell replication and structure. Notable changes in the components of ribosomes and cell adhesion point towards adjustments in protein synthesis and cell interactions. At the molecular level, these changes suggest a sophisticated balancing act in regulating gene expression, cell attachment, and ribosome function, demonstrating the intricate effects of combining these treatments. Comparing the effects of 5-FU alone and in combination with berberine chloride reveals additional impacts on stress response mechanisms and metabolic activities. The observed enrichment in components related to the vascular membrane and cell adhesion indicates structural and interactional changes induced by treatment. Changes in molecular functions like cadherin binding and ligase activity hint at nuanced regulatory shifts brought about by the combined therapy. These treatments modulate genes tied to a variety of diseases, suggesting their relevance across a broad biological spectrum and potential involvement in pathways related to viruses or the immune system. Key pathways affected include those related to infection, cancer, the cell cycle, apoptosis, and p53 signalling, offering a comprehensive overview of the treatments' impacts. Overall, the detailed GO enrichment analysis paints a thorough picture of the cellular and molecular alterations influenced by berberine chloride, 5-FU, and their combined use. It includes the pathways and processes identified through this analysis that are crucial for further investigating how these treatments work, especially regarding their potential applications in cancer therapy. The discovery of 579 unique genes in the comparison between untreated and combined berberine and 5-FU treatments suggests a significant impact of the combination on gene expression in A431 cells. The identification of 141 genes that are differentially expressed specifically when comparing the combined treatment with 5-FU alone hints at berberine's potential to either enhance or reduce the effects of 5-FU on the genetic level. The presence of genes that are consistently differentially expressed across various treatment comparisons (384, 64, 40) points to shared pathways or biological processes that are influenced by these treatments. Particularly, the 42 genes that show differential expression across all examined conditions could be crucial for deciphering the cellular response to these treatments, indicating their central role in mediating the effects of berberine and 5-FU.

These data underscore berberine's significant role in modulating the genetic response of A431 cells to 5-FU, whether by intensifying specific reactions, introducing new effects, or potentially neutralizing some of 5-FU's actions. Conducting further molecular and biological studies on these differentially expressed genes will yield deeper understanding into their specific functions and the cellular processes they influence under the effect of the treatments.

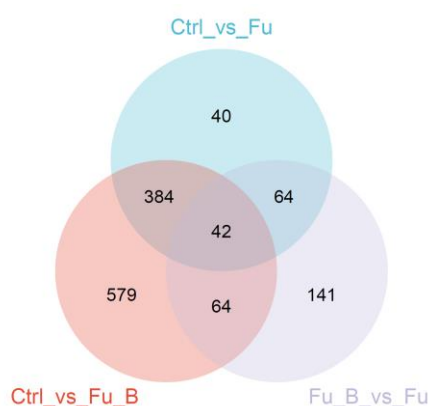


Figure 2.11: Venn diagram depicting differential gene expression across three treatment comparisons in A431 cell lines: Control vs. 5-Fluorouracil (Ctrl\_vs\_Fu), Control vs. combination of Berberine and 5-Fluorouracil (Ctrl\_vs\_Fu\_B), and the combination of berberine and 5-Fluorouracil vs. 5-fluorouracil alone (Fu\_B\_vs\_Fu). The diagram shows that 384 genes are uniquely differentially expressed in the Ctrl\_vs\_Fu\_B comparison, while 40 and 141 genes are uniquely expressed in the Ctrl\_vs\_Fu and Fu\_B\_vs\_Fu comparisons, respectively. Overlaps between the comparisons indicate shared differentially expressed genes, with 42 genes common across all three conditions.

The detailed analyses provided thus far set the stage for a deeper investigation into the interactions between berberine chloride and 5-fluorouracil (5-FU) and their combined effects on the proliferation and gene expression in the A431 cell line. After demonstrating a synergistic impact on cell viability and outlining the transcriptional changes induced by both single and combined drug treatments, we now aim to investigate further the specifics of gene pathway expressions. This next step involves comparing the gene expression profiles of the 5-FU treated group to those of the group treated with both berberine chloride and 5-FU. The Reactome database was utilized to identify the molecular mechanisms driving the observed anticancer synergy by examining the differential activation or suppression of pathways. The data analysis, encompassing read quality testing, mapping, normalization, modelling, and differential expression analysis, was carried out. Statistical analysis aimed to identify differentially expressed genes method applied to adjust P values for multiple testing. A significance threshold of  $P_{adj} < 0.05$  was set for selecting potential gene candidates, and a  $|\log_2 \text{fold change}| > 1$  criterion was used for individual data analysis. Protein interactions among gene candidates were analysed using STRING software. Subsequently, the identified pathways were cross-referenced with the KEGG database to determine the most significantly impacted ones by the treatments.

Table 2.12 lists the most significant pathways, ranked by their p-values to highlight the statistical significance of their association with the treatment conditions. The application of a false discovery rate (FDR) threshold of 0.3 serves to identify pathways with a lower likelihood of being false positives, ensuring a focus on those most relevant to our study. Pathways with an FDR below 0.3 are considered highly likely to be biologically and

directly impacted by the treatment conditions. While pathways above this threshold are not disregarded, they are flagged for further validation due to a higher probability of being false discoveries. This approach underlines the robustness and rigour in the approach to identify the biological processes most affected by the combined treatment of berberine chloride and 5-FU.

Pathway name	Entities				Reactions	
	found	ratio	p-value	FDR*	found	ratio
Response of EIF2AK1 (HRI) to heme deficiency	4 / 29	0.002	2.12e-04	0.061	4 / 20	0.001
Metal sequestration by antimicrobial proteins	3 / 13	8.41e-04	3.10e-04	0.061	3 / 5	3.40e-04
ATF4 activates genes in response to endoplasmic reticulum stress	4 / 34	0.002	3.85e-04	0.061	2 / 7	4.75e-04
PERK regulates gene expression	4 / 42	0.003	8.45e-04	0.101	2 / 11	7.47e-04
TP53 Regulates Transcription of Cell Death Genes	5 / 83	0.005	0.001	0.139	6 / 68	0.005
TP53 regulates transcription of several additional cell death genes whose specific roles in p53-dependent apoptosis remain uncertain	3 / 28	0.002	0.003	0.198	4 / 19	0.001
Epithelial-Mesenchymal Transition (EMT) during gastrulation	2 / 8	5.17e-04	0.003	0.198	5 / 5	3.40e-04
RAB geranylgeranylation	4 / 68	0.004	0.005	0.282	4 / 5	3.40e-04

Table 2.12: The most significant pathways between the 5-FU treated group to those of the group treated with both berberine chloride and 5-FU with the 8 most relevant pathways sorted by p-value.

The pathways that have been uncovered in the research fall into distinct categories based on their biological roles and potential therapeutic implications, especially in the context of anti-cancer and anti-inflammatory strategies:

**Pathways Related to Cellular Stress Response and Apoptosis:**

- Response of EIF2AK1 (HRI) to Heme Deficiency (R-HSA-9648895)
- ATF4's Activation in Response to ER Stress (R-HSA-380994)
- PERK Regulating Gene Expression (R-HSA-381042)

These pathways share a common theme of responding to cellular stress, with EIF2AK1 (HRI) and ATF4 playing pivotal roles in managing protein synthesis and ER stress, respectively. The activation of PERK as part of the unfolded protein response further underscores the cell's effort to maintain homeostasis under stress. These mechanisms are crucial in controlling cell growth, apoptosis, and survival, with direct implications for cancer therapy by targeting cells under chronic stress or manipulating the stress response to favour cancer cell death.(Adema et al., 2022)

**Pathway Related to Host-Pathogen Interaction:**

- Metal Sequestration by Antimicrobial Proteins (R-HSA-6799990)

This pathway highlights the strategic regulation of metal ion availability, a crucial aspect of the host defense against pathogens. The manipulation of metal ions affects microbial growth and survival, illustrating an essential biological battle between host and pathogen. This mechanism's relevance to anti-cancer and anti-inflammatory strategies may be indirect but signifies the complexity of biological systems and their potential exploitation in therapy (Guengerich, 2015).

**Pathways Related to Apoptosis and Cancer Therapy:**

- **TP53 Regulates Transcription of Cell Death Genes (R-HSA-5633008)**
- **TP53 Regulates Transcription of Several Additional Cell Death Genes (R-HSA-6803205)**
- **Epithelial-Mesenchymal Transition (EMT) during Gastrulation (R-HSA-9758919)**

These pathways converge on the regulation of apoptosis and cell death, with TP53 being a central figure in promoting the apoptotic response to damage or stress, highlighting its role as a tumor suppressor. The additional cell death genes regulated by TP53, although with uncertain roles, open new avenues for research into p53-dependent apoptosis mechanisms. The EMT process, critical in development, also draws parallels with cancer progression, particularly in metastasis, suggesting potential targets for anti-cancer strategies (Bieging et al., 2014).

**Pathway Related to Cellular Trafficking:**

- RAB Geranylgeranylation (R-HSA-8873719)

This pathway focuses on the post-translational modification of RAB proteins, crucial for

their function in vesicular trafficking. The implications for cancer and inflammation stem from the role of RAB proteins in regulating membrane traffic, signaling pathways, and potentially influencing tumor growth and the immune response. Targeting this pathway could offer novel approaches to disrupt cancer cell proliferation or modulate the inflammatory response.

Each of these pathways' sheds light on complex biological processes with significant implications for understanding disease mechanisms and developing therapeutic interventions. The EIF2AK1, ATF4, and PERK pathways emphasize the cell's adaptability to stress, offering targets for cancer therapy by exploiting stressed cancer cells' vulnerabilities. The metal sequestration pathway provides insight into host-pathogen dynamics, indirectly relevant to broader therapeutic strategies. TP53's role in apoptosis and the regulation of additional cell death genes underscores its importance in cancer biology and therapy. Lastly, the RAB geranylgeranylation pathway opens new perspectives on targeting cancer and inflammatory diseases through the regulation of cellular trafficking. Analysing individual genes after identifying significant pathways in RNA sequencing studies in the A431 cell lines also is crucial for several reasons. First, it allows researchers to pinpoint the specific genes that contribute most significantly to the observed changes in cell behaviour, offering insights into the mechanisms of drug action or disease progression. By focusing on individual genes with notable expression changes, these findings through targeted experiments, such as qPCR or Western blotting, providing a more detailed understanding of the biological processes at play. The comprehensive analysis of A431 cell lines treated with 5-Fluorouracil (5-FU) alone and in combination with berberine chloride has provided a wealth of RNA sequencing data that underscores the significant expression changes in genes associated with inflammation and anticancer processes. Identifying 130 significant gene sets, based on specific log2FoldChange values, highlights the intricate molecular landscape influenced by these treatments focusing on inflammation and anticancer. This detailed examination not only advances our understanding of the genes directly implicated in inflammation and cancer but also offers a clearer picture of potential therapeutic targets and areas for further research.

Inflammation-Related Genes:	log2FoldChange	Up/Down regulation
CASP1 (Caspase-1): Essential in the inflammatory pathway for processing IL-1 $\beta$ , indicating its pivotal role in mediating inflammatory responses.	-4.23	Down
S100A8/S100A9: Act as central figures in inflammation, promoting chemotaxis and activating neutrophils, highlighting their importance in the body's immune response.	2.25	Up
CXCL8 (Interleukin-8): Serves as a crucial chemotactic factor, recruiting neutrophils and T-cells to inflammation sites, underlining its key position in inflammatory signalling.	1.55	Up
TNFRSF9 (4-1BB): As part of the tumour necrosis factor receptor superfamily, it modulates T-cell activity, linking inflammation to immune responses.	1.12	Up
Anticancer-Related Genes:	log2FoldChange	Up/Down regulation

ADAM10: Influences cell signaling and interactions, affecting tumor progression and metastasis, suggesting its potential as a target in cancer therapy.	1.77	Up
RAF1: Engaged in the RAS-MAPK signaling pathway, it's associated with cell proliferation, differentiation, and anti-apoptotic activities linked to various cancers.	-14.89	Down
SNAI1 (Snail): Regulates epithelial-mesenchymal transition (EMT), facilitating tumor metastasis and invasion, indicating its role in cancer progression.	1.09	Up
DICER1: Involved in miRNA processing, affecting cell proliferation, differentiation, and apoptosis, closely linked to cancer development, underscoring the complexity of gene regulation in oncogenesis.	20.57	Up

Moreover, these potential functional genes were explored in STRING database for comprehensive protein-protein interaction networks and functional enrichment analysis. As the Figure 2.13 showed, a protein interaction network with inflammation function included genes which are obviously influenced with 5-FU and berberine chloride treatment.

The network depicted represents a protein interaction network, not a specific biological pathway. The visual network of these proteins provides insights into potential roles in inflammatory pathways. This network underscores the complexity of interactions that contribute to both inflammatory responses and cancer progression, offering valuable insights into potential targets for therapeutic intervention. The connections among proteins like SPRR1B, S100A7, S100A8/S100A9, CASP1, CXCL8, PLAT, and GBP2 reveal a sophisticated interplay crucial for understanding the molecular mechanisms of inflammation and its relationship with cancer. SPRR1B, a skin-specific protein, might influence barrier function and cellular stress responses. S100 proteins, including S100A7, A8, and A9, are implicated in inflammatory signalling and can modulate immune responses. CASP1 is a key enzyme in inflammasome activation, crucial for pro-inflammatory cytokine processing. CXCL8 (IL-8) is a chemokine involved in leukocyte recruitment and angiogenesis. PLAT (tissue plasminogen activator) has roles in fibrinolysis and tissue remodelling, while GBP2 is involved in the immune response to pathogens. Alterations in these proteins' expression could reflect changes in cell signalling pathways, impacting processes like cell proliferation, apoptosis, and migration, which are vital for both inflammation resolution and cancer progression. These interactions can affect the functional expression of these proteins, potentially altering their roles in inflammation and cancer-related processes, without delineating a linear biochemical route that characterizes a typical pathway.

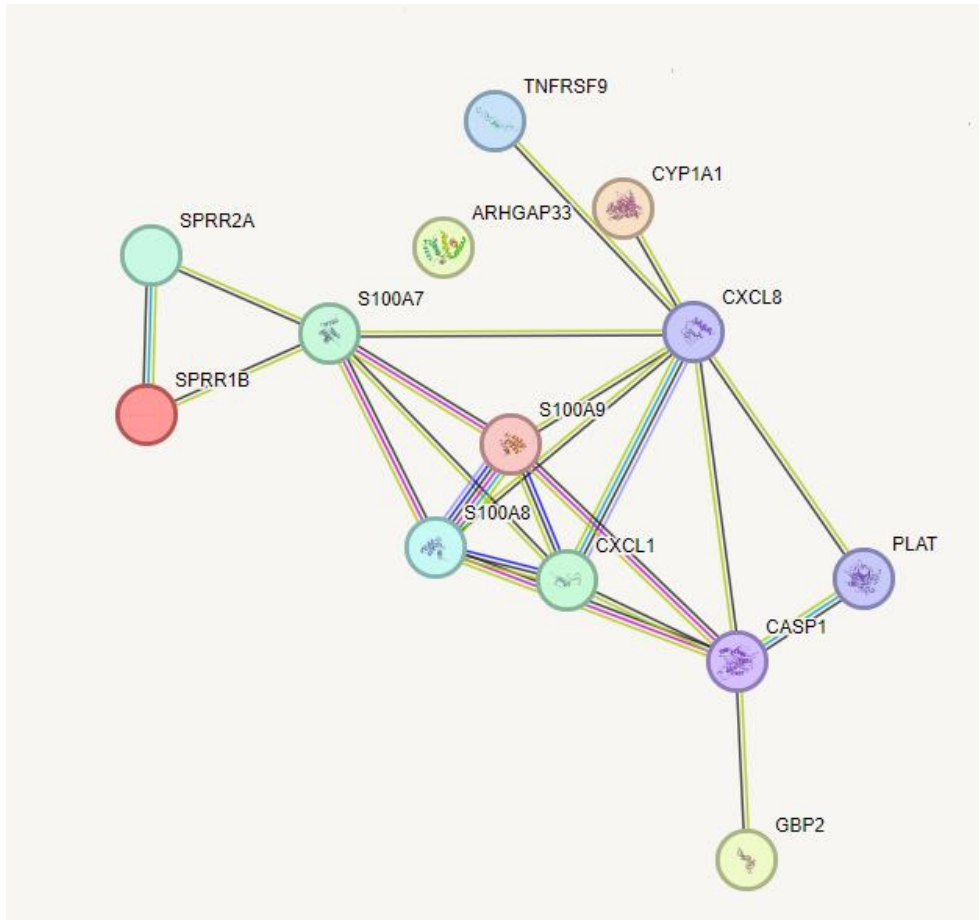


Figure 2.13: This image depicts a protein interaction network centered around SPRR1B, S100A7, S100A8/S100A9, CASP1, CXCL8, PLAT, and GBP2. The proteins directly interacting are represented by coloured nodes, while secondary interactors are shown as white nodes. The edges, the lines connecting the nodes, indicate various types of interactions: solid lines for known interactions from curated STRING databases and dashed lines for predicted interactions based on gene co-occurrence, co-expression, or other criteria.



The utilization of Gene Set Enrichment Analysis (GSEA) via the R programming language, specifically through the cluster Profiler package, has furnished us with a nuanced understanding of the functional consequences of gene expression changes induced by 5-fluorouracil (5-FU) treatment, both alone and in combination with berberine chloride. It can help identify whether the genes that are involved in the specific signalling pathway are differentially expressed when cells are treated with 5-FU and berberine. The interpretation of these analyses revealed critical insights into the molecular mechanisms at play. Notably, the observed suppression of the JAK-STAT signalling pathway post-treatment, especially pronounced with the combined treatment of 5-FU and berberine, highlights the intricate interplay between drug actions and cellular signalling pathways. The Normalized Enrichment Scores (NES) provided quantitative measures of this suppression, offering evidence of the potentiated inhibitory effect on the JAK-STAT pathway by the combined treatment compared to 5-FU alone. This suppression aligns with existing literature on the role of the JAK-STAT pathway in cell survival, proliferation, and immune responses, suggesting that its inhibition could contribute to the anticancer effects observed. Furthermore, the additive or synergistic suppression of this pathway by the combination of berberine and 5-FU opens new avenues for exploring therapeutic strategies that leverage this interaction to enhance anticancer efficacy.

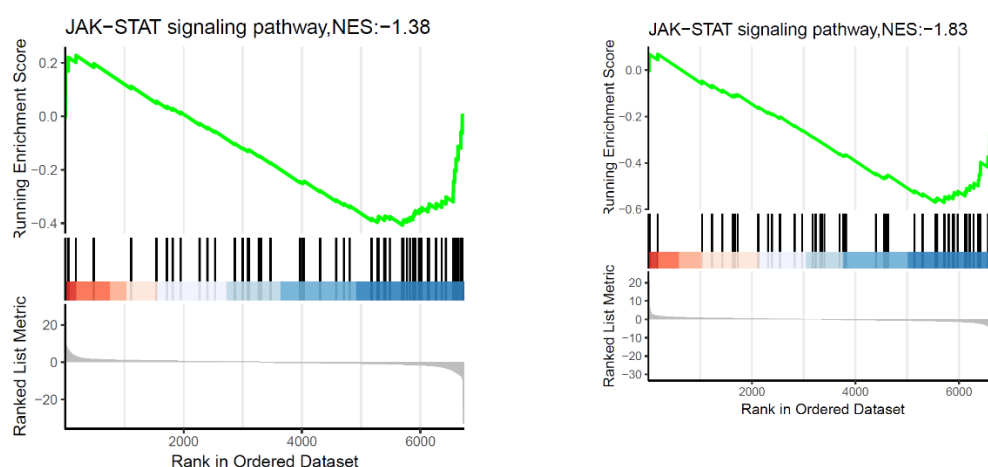


Figure 2.15: Modulation of JAK-STAT Signalling Pathway in A431 Cells Under Different Treatments.

(A) Gene set enrichment analysis (GSEA) plot illustrating the suppression of the JAK-STAT signalling pathway in A431 cells treated with 5-FU alone. The Normalized Enrichment Score (NES) of -1.38 indicates a negative association of the genes in this pathway with the treatment.

(B) GSEA plot showcasing the effect of combined berberine and 5-FU treatment on the JAK-STAT signalling pathway in A431 cells. A more pronounced suppression is evident with an NES of -1.83.

The leading-edge genes from the pathway, which contribute most to the enrichment score, are represented as vertical black lines in the central portion of the plots. The colour gradient (red to blue) below the plots depicts the rank metric score, with genes at the extremes having the highest correlation with the respective phenotype.

## 2.5 Discussion

The combination of 5-FU and berberine chloride significantly inhibited cell proliferation in A431 cells, demonstrating a strong synergistic anticancer effect. This suggests that the combined use of these drugs has greater potential for topical anti-skin cancer formulations than either drug used alone. Next, RNA sequencing revealed significant changes in gene expression profiles following treatment with 5-FU, berberine chloride, and their combination. A total of 16,378 genes were identified, with the analysis highlighting significant differences in gene expression among different treatment groups. The differential expression analysis identified genes with significant changes in expression across treatment comparisons. Notably, the combination of 5-FU and berberine chloride resulted in unique gene expression profiles, suggesting specific molecular mechanisms of action when these drugs are used together. Gene enrichment and pathway analysis revealed that treatments affected several key biological processes, including ribosome biogenesis, cell cycle control, apoptosis, DNA repair, amino acid metabolism, and immune response. This indicates that the drugs impact cancer cells through multiple biological pathways. Identified pathways with potential therapeutic implications in cancer therapy included cellular stress response, apoptosis, host-pathogen interactions, and cellular trafficking. The involvement of TP53 in regulating apoptosis and the impact on RAB geranylgeranylation highlight critical areas for therapeutic targeting. Examination of specific genes related to inflammation and anticancer processes provided insights into the molecular landscape affected by the treatments. This detailed analysis underscores the importance of certain genes in the inflammatory response and cancer progression, offering potential therapeutic targets. Analysis of protein-protein interaction networks revealed complex interactions among proteins involved in inflammatory pathways and cancer progression, highlighting the importance of these networks in understanding the molecular mechanisms underlying the treatments' effects. GSEA indicated suppression of the JAK-STAT signalling pathway, particularly with the combined treatment of 5-FU and berberine. This finding suggests a potential mechanism through which the combination exerts its synergistic anticancer effect, emphasizing the role of this pathway in cell survival and proliferation. In summary, the combined treatment of berberine chloride and 5-FU exhibits a strong synergistic effect on A431 cells by altering gene expression, affecting multiple biological pathways, and demonstrating specific molecular mechanisms of action. These findings provide a comprehensive understanding of the underlying mechanisms driving the observed anticancer synergy, offering valuable insights for optimizing anti-cancer treatment strategies in skin cancer therapeutics.

The findings from the SRB assay underscore the potential synergy between berberine chloride and 5-fluorouracil (5-FU) in inhibiting skin cancer cell proliferation. 5-FU, characterized by its fluorinated pyrimidine analog structure, exhibits a dual mechanism of action. It impedes DNA synthesis and repair by inhibiting thymidylate synthetase, an enzyme fundamental to DNA formation (Micali et al., 2014). Furthermore, 5-FU undergoes RNA incorporation, , thus instigating cell cycle arrest and apoptosis

predominantly in tumour cells due to their elevated proliferation rates and augmented cell membrane permeability (Klein et al., 1966). The anti-proliferative efficacy of berberine chloride and 5-FU across melanoma and non-melanoma cell lines, as delineated in this study, aligns with existing literature which underscores the anticancer potential of these compounds. Berberine chloride's ability to modulate the cell cycle and inhibit cell proliferation across diverse cancer types such as lung and melanoma, has been well documented (Li et al., 2014; Murthy et al., 2012).

Similarly, 5-FU's capability to significantly reduce tumour burden in murine colon and melanoma tumours, contingent on anti-tumour immunity triggered by the activation of cancer-cell-intrinsic stimulator of interferon genes (STING), has been previously demonstrated (Vincent et al., 2010). The heightened sensitivity of A431 cells to both compounds, as observed in this study, hints at potential cellular or molecular discrepancies that may influence the responsiveness to these treatments. The literature elucidates that the anticancer efficacy of 5-FU is predicated on the restoration of T-cell immunity following the elimination of myeloid-derived suppressor cells (MDSCs) (Vincent et al., 2010), whose interactions across varying cellular environments might elucidate the differential responses observed between A375 and A431 cells. The synergistic interaction between berberine chloride and 5-FU, especially manifested in the A431 cell line, highlights the potential of combinatorial treatments in augmenting anticancer efficacy. This synergy, validated through CalcuSyn software analysis, heralds a promising avenue for further exploration towards more efficacious anticancer formulations. The potential of the 25.6 mM 5-FU and 1 mM berberine combination in topical anti-skin cancer formulations underscores the clinical translational relevance of these findings, albeit contingent upon further validation in *in vivo* models and clinical trials. RNA-seq analysis, aimed at evaluating the genetic and molecular responses elicited by the combined treatment on A431 cells, is well-poised to unravel the underlying mechanisms mediating the observed synergy between berberine and 5-FU. Insights gleaned from this analysis could pave the way for optimizing combinatorial treatment strategies, elucidating potential molecular targets, and advancing the understanding of the interactive dynamics between these compounds at both molecular and cellular levels.

In light of the novel observations illuminating the synergistic potential of berberine and 5-FU in mitigating skin cancer, a compelling necessity arose to further investigate. Traditional drug synergy assays largely focus on overt cellular behaviours such as alterations in cell viability or apoptotic tendencies, often overlooking the underlying molecular cascades orchestrating these visible outcomes. Herein, RNA sequencing (RNA-seq) emerges as a seminal tool, offering a panoramic, high-resolution vista of the cellular transcriptomic landscape, meticulously cataloguing the nuanced gene expression dynamics in response to therapeutic interventions (Liu & Trapnell, 2016). Within the ambit of this study, a thorough exploration of the transcriptional ecosystem of A431 cells was undertaken, particularly under the therapeutic auspices of both berberine and 5-FU, with objectives to: Identify Key Pathways: Discern specific cellular circuits and processes distinctly perturbed or modulated by individual or combined

treatments. Discover Potential Synergies: Spotlight specific genes or molecular corridors either uniquely affected or whose responses are accentuated in the combined therapeutic milieu—a phenomenon potentially obscured under mono-therapeutic scenarios. As elucidated in prior research, berberine exhibits remarkable anti-inflammatory, antioxidant, antiapoptotic, and anti-autophagic activity via the regulation of myriad signalling pathways including AMP-activated protein kinase (AMPK), nuclear factor  $\kappa$ B (NF- $\kappa$ B), mitogen-activated protein kinase silent information regulator 1 (SIRT-1), and hypoxia-inducible factor-1 $\alpha$  (HIF-1 $\alpha$ ) (Ai et al., 2021). The synergy between 5-FU and berberine on survivin and STAT3 translates into augmented anticancer activity in gastric cancer cells (Zhang et al., 2008). Berberine may also induce autophagy in human liver carcinoma cell lines, through activation of Beclin-1 and inhibition of mTOR signalling by suppressing the activity of Akt and up-regulating P38 MAPK signalling (Wang et al., 2010).

Moreover, the comprehensive scope of RNA-seq analyses potentially facilitates the anticipation of inadvertent off-target effects, pre-emptive identification of potential resistance mechanisms, and provides empirical insights that could steer the optimization of therapeutic strategies. In the subsequent sections, we traversed the complex thoroughfares of the RNA-seq outcomes, interpreting and contextualizing their revelations within the overarching narrative of berberine and 5-FU's combined therapeutic efficacy. The insights garnered from the RNAseq analysis in this chapter furnish invaluable understanding of the synergistic effects evoked by the confluence of berberine and 5-fluorouracil (5-FU) in A431 cells. The JAK-STAT (Janus Kinase-Signal Transducer and Activator of Transcription) signalling pathway is pivotal for transducing information from chemical signals external to the cell to the cell nucleus, thereby modulating DNA transcription and cell function (Hu et al., 2023). Triggered by the binding of a cytokine or growth factor to its receptor, this pathway activates JAKs, which subsequently phosphorylate STAT proteins. These proteins dimerize, translocate to the nucleus, and modulate gene expression. Dysregulation of this pathway is implicated in an array of diseases, notably cancers, rendering it a significant target for therapeutic interventions (Hu et al., 2021).

The comprehensive analysis of the effects of 5-fluorouracil (5-FU) and berberine chloride on A431 cell proliferation has elucidated a significant synergistic interaction between these two compounds, particularly at specific concentrations. The combination of 25.6 mM 5-FU and 1 mM berberine chloride demonstrated a potent anti-cancer effect, suggesting a promising therapeutic strategy for topical anti-skin cancer formulations. This synergy points towards a novel approach for enhancing the efficacy of 5-FU-based treatments. Further investigations, facilitated by RNA sequencing, aimed to dissect the molecular underpinnings of this observed synergy. Through detailed RNA-seq analysis, a substantial alteration in gene expression profiles was noted, indicating the activation or suppression of specific pathways in response to the combined treatment. Particularly those genes with a log2 fold change ranging from 1 to 2, are crucial for identifying potential molecular targets and understanding how these treatments modulate cellular functions. The combined therapy has demonstrated

potential in three main functions: reducing inflammation, combating cancer, and reducing resistance to the 5-FU drug.

Firstly, the study identified key inflammation-related genes, including CASP1 (Caspase-1), which plays a pivotal role in the inflammatory response by processing pro-inflammatory cytokines such as IL-1 $\beta$  (Kaneko et al., 2019). This highlights its significance in mediating inflammation. Additionally, the importance of S100A8/S100A9 proteins was underscored, known for their role in promoting chemotaxis and activating neutrophils, thus underlining their central role in the body's immune response. Furthermore, CXCL8 (Interleukin-8), identified as a crucial chemotactic factor, recruits neutrophils and T-cells to sites of inflammation, marking its key position in inflammatory signalling (Broderick & Hoffman, 2022). The analysis also emphasized the role of TNFRSF9 (4-1BB), a member of the tumour necrosis factor receptor superfamily, in modulating T-cell activity and linking inflammation to immune responses. Another significant gene, NLRP3, was noted for its involvement in inflammasome function and the regulation of inflammatory responses, highlighting its importance in immune system signalling.

Beyond these specific genes, the study's findings suggest that berberine chloride modulates the expression of genes involved in inflammation. The anti-inflammatory component of this study unveils significant modulation of gene expression related to inflammation by the combined treatment of berberine chloride and 5-FU. These findings enhance our understanding of the molecular basis of the anti-inflammatory effects of these compounds and open up new avenues for research into targeted therapies. Such therapies could leverage these mechanisms for the treatment of inflammatory diseases and cancer, providing a promising direction for future investigations.

Secondly, the research into the anticancer effects of combining berberine chloride and 5-Fluorouracil (5-FU) on A431 cells has yielded profound insights into their molecular interactions and therapeutic potential. Significant findings include the identification of several anticancer-related genes that were differentially expressed following treatment. TP53 is recognized as a fundamental tumour suppressor gene, TP53 is crucial for cell cycle regulation, DNA repair, and apoptosis (Wang et al., 2023). The study's findings underscore its central role in the anticancer mechanisms of the combined treatment, suggesting that the modulation of TP53 expression could be a contributing factor to the observed therapeutic effects. *ADAM10*, this gene influences cell signalling and interactions, affecting tumour progression and metastasis (Cai et al., 2022). Its identification among the differentially expressed genes suggests that the treatment may impact tumor spread and growth, indicating a potential therapeutic target. Involved in the RAS-MAPK signalling pathway, *RAF1* is associated with cell proliferation, differentiation, and anti-apoptotic activities linked to various cancers (Dorard et al., 2023). The modulation of RAF1 expression by the combined treatment highlights its potential in influencing cancer cell behaviours. SNAI1 regulates epithelial-mesenchymal transition (EMT), a process facilitating tumour metastasis and invasion. Its differential expression suggests that the treatment may affect tumour aggressiveness and spread.

As a key player in miRNA processing, DICER1 affects cell proliferation, differentiation, and apoptosis, closely linking it to cancer development. The study points to its role in the molecular basis of the treatment effects. The visual network analysis further elucidated the complex interactions among these proteins, providing insights into the collaborative roles these molecules play in cancer pathways. This network approach helps to understand the comprehensive impact of the combined treatment on cancer-related biological processes, offering valuable directions for future research and therapeutic strategy development.

Moreover, the suppression of the JAK-STAT signalling pathway post-treatment, particularly with the combined use of 5-FU and berberine, highlights the intricate interplay between drug actions and cellular signalling pathways. This observed suppression, along with the identification of key pathways and genes, offers valuable insights into the molecular mechanisms driving the anticancer effects of the combined treatment. Our observations revealed a trend of suppression in the JAK-STAT signalling pathway within the 5-FU treatment group (Figure 2.15.A, NES: -1.38). This aligns with prior studies delineating the inhibitory effects of 5-FU on JAK-STAT signalling. Intriguingly, this inhibition was further augmented in the group subjected to the combined treatment (Figure 2.15.B, NES: -1.83). These findings indicate that the amalgamation of berberine and 5-FU exerts a more pronounced impact on suppressing the JAK-STAT pathway compared to individual treatments, suggesting a potential additive or even multiplicative effect. The leading-edge genes from the pathway, which contribute most to the enrichment score, are represented as vertical black lines in the central portion of the plots. The colour gradient (red to blue) below the plots depicts the rank metric score, with genes at the extremes having the highest correlation with the respective phenotype. To unravel the underlying complexities, a protein-protein interaction network analysis was conducted. Through the identification of functional modules within the genes associated with the JAK-STAT signalling pathway (Figure 2.16), potential therapeutic targets were discerned, and a deeper comprehension of the interaction nature was achieved. Certain proteins may function as hubs or nodes within this network, earmarking them as potential drug targets for more targeted interventions. This analysis facilitated the unveiling of interactions and functional relationships among these genes at the protein level, thus providing insights into the regulatory mechanisms at play.

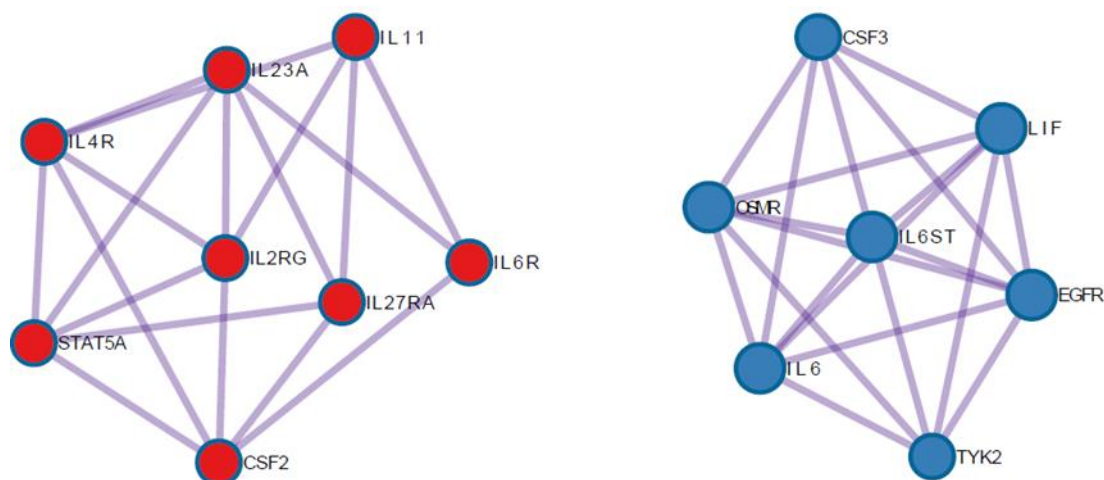


Figure 2.16: illustrates two protein-protein interaction (PPI) networks related to the JAK-STAT signalling pathway. Left Network (Red Nodes): This network includes the following proteins: IL23A, IL11, IL4R, IL6R, IL2RG, IL27RA, STAT5A, and CSF2. The connections between these proteins indicate their interactions, with CSF2 having direct interactions with STAT5A and IL2RG. Right Network (Blue Nodes): This network consists of proteins such as CSF3, LIF, OSMR, IL6ST, IL6, EGFR, and TYK2. Notably, CSF3, which is significant in the context of the study, is seen to interact directly with OSMR, IL6ST, IL6, and TYK2.

A noteworthy finding was the significant suppression of CSF3 (colony-stimulating factor 3) expression upon combined treatment. CSF3 is not merely crucial for haematopoiesis, but is also implicated in tumour microenvironment modulation, potentially fostering tumour angiogenesis and crafting a supportive niche for tumour cells (Beekman & Touw, 2010). Its inhibition may reflect a less conducive environment for tumour progression, appending another layer to the therapeutic potential of the combined treatment. These observations serve as preliminary evidence for the synergistic effect of berberine and 5-FU in retarding tumour growth. Upon deeper exploration, the ramifications of these results on patient outcomes, particularly concerning survival and quality of life, are yet to be fully discerned. Further research is imperative to validate and elucidate the regulatory mechanisms of the JAK-STAT signalling pathway and CSF3 expression in response to the combined treatment of berberine and 5-FU. Moreover, the emergence of resistance mechanisms during therapy, potential off-target effects, and the optimization of drug dosing constitute other significant areas of focus. Additional functional experiments and *in vivo* studies are requisite to affirm the importance of these genes in tumour growth and treatment response, thus paving the way for translational applications. The current study illuminates the potential of amalgamating berberine and 5-FU as a synergistic therapeutic modality for tumour treatment. Our findings not only furnish a scientific rationale for combining these agents but also herald a promising avenue in personalized medicine. The inhibition of the JAK-STAT pathway and suppression of CSF3 expression could serve as potential biomarkers for patient stratification, ensuring that treatment is extended only to those most likely to benefit. Future inquiries should be directed towards elucidating the precise mechanisms underlying these observations and the feasibility of clinical translation, with the paramount objective of amplifying cancer therapy efficacy and precision.

Furthermore, the study's findings suggest that the combined use of berberine and 5-FU may influence the expression of genes and the activation of pathways involved in mediating drug resistance. By potentially modulating the Wnt pathway and affecting the EMT process, the combination treatment may reduce the resistance of cancer cells to 5-FU, thereby enhancing its anticancer efficacy. The exploration into the combined effects of berberine and 5-Fluorouracil (5-FU) on A431 skin cancer cells has shed light on their potential to mitigate 5-FU drug resistance, a significant challenge in cancer chemotherapy. Key insights from the study emphasize the role of the Wnt signalling pathway and the process of epithelial-mesenchymal transition (EMT) in contributing to 5-FU resistance. The Wnt pathway, crucial for cell proliferation, differentiation, and survival, has been implicated in the development of resistance to chemotherapy agents, including 5-FU (Jiménez-Guerrero et al., 2021). Alterations in this pathway can lead to the maintenance of cancer stem cell properties and the promotion of a drug-resistant phenotype. *EMT*, a process vital for embryogenesis and implicated in cancer progression and metastasis, can activate the Wnt signalling pathway (Cai et al., 2024). Activation of this pathway during EMT may contribute to the development of 5-FU resistance, complicating the use of this chemotherapeutic agent. The role of EMT in drug resistance underscores the complexity of the cellular response to chemotherapy and suggests that targeting EMT and the Wnt pathway could be a strategic approach to overcome resistance.

In the context of exploring the synergistic potential of berberine and 5-fluorouracil (5-FU) in combating skin cancer, our investigation extends beyond mere observations of cellular responses to delve into the underlying molecular mechanisms. The pivotal role of the Wnt signalling pathway in mediating 5-FU drug resistance, alongside the process of epithelial-mesenchymal transition (EMT), presents a nuanced landscape for therapeutic intervention. The activation of EMT facilitates a transformation in cancer cells that endows them with migratory and invasive capabilities, contributing to tumour progression and the establishment of distant metastases. Concurrently, EMT has been implicated in the development of drug resistance, a formidable challenge in cancer treatment. The regulatory mechanisms of EMT, influenced by transcription factors such as those within the SNAIL gene family, underscore the suppression of epithelial attributes and the promotion of a mesenchymal phenotype, thereby fostering a cellular environment conducive to drug resistance. The Wnt signalling pathway, a critical mediator of cell proliferation, differentiation, and survival, becomes particularly pertinent in the context of EMT. Its activation during EMT in cancer can perpetuate the properties of cancer stem cells and promote resistance to chemotherapy, including agents like 5-FU. The components of the Wnt pathway, including  $\beta$ -catenin, DVL, Lrp6, and Axin, play instrumental roles in this cascade, affecting not only developmental processes but also the cellular response to cancer therapies (Li et al., 2023). The association between the Wnt pathway and 5-FU resistance, especially in colorectal cancer, has been well-documented, with an overactive Wnt signalling pathway observed in resistant cancer cell lines. This observation suggests a broader implication of Wnt pathway activation in conferring drug resistance across various cancer types, including skin cancers such as squamous cell carcinoma and melanoma. Given the multifaceted roles



of EMT and Wnt signalling in cancer progression and drug resistance, targeting these pathways offers a promising therapeutic strategy. By inhibiting key components of the Wnt pathway or modulating the activity of transcription factors involved in EMT, it may be possible to sensitize cancer cells to 5-FU and other chemotherapeutic agents. Such approaches could potentially reverse drug-resistant phenotypes, enhancing the efficacy of conventional therapies. Further research is necessary to elucidate the specific interactions between EMT, the Wnt signalling pathway, and 5-FU resistance in skin cancer, particularly within the A431 cell line context. Investigating the combined treatment effects of berberine and 5-FU could provide invaluable insights into overcoming drug resistance. Identifying molecular targets within these pathways may pave the way for the development of novel therapeutic strategies, offering hope for improved treatment outcomes in patients facing chemo-resistant cancers.

## 2.6 Conclusion

The chapter details the combination research on berberine chloride and 5-fluorouracil (5-FU) and their collective impact on cancer cells, highlighting the groundbreaking potential for developing innovative anti-nonmelanoma formulations suitable for topical use. The initial phase of cellular studies revealed a notable synergistic effect between these compounds, setting the stage for a deeper investigation. Subsequent RNA-seq analyses provided a clearer point, demonstrating significant alterations in gene expression profiles. These changes spanned a wide array of biological processes and pathways, all of which are crucial for the survival and proliferation of cancer cells, thereby shedding light on the therapeutic potential of the berberine chloride and 5-FU combination. Berberine chloride's anti-inflammatory and anti-drug resistance capabilities significantly contribute to the research, enhancing the value of this combination in the development of topical formulations. The differential gene expression analysis highlighted the treatment's impact on vital pathways, such as the cellular stress response, apoptosis, host-pathogen interactions, and cellular trafficking. One of the standout discoveries was the suppression of the JAK-STAT signalling pathway, suggesting a powerful mechanism through which the combination exerts its anticancer effects. The analysis pinpointed key genes involved in inflammation and cancer-fighting processes, such as CASP1, S100A8/S100A9, CXCL8, TNFRSF9, ADAM10, RAF1, SNAI1, and DICER1, as being significantly modulated by the treatments.

Moreover, the ability of this combination therapy to influence the Wnt pathway and affect the epithelial-mesenchymal transition (EMT) process suggests a novel approach to reducing drug resistance to 5-FU. This could significantly enhance the therapeutic efficacy of the treatment, highlighting the urgent need for further investigation in clinical settings to confirm its effectiveness and safety in human patients. This chapter proceeds to outline the anticipated research directions aimed at elucidating the intricate mechanisms by which this drug combination modulates gene expression and impacts cellular pathways. This future research is critical for refining therapeutic strategies based on the detailed understanding of the molecular and cellular mechanisms at play in the berberine chloride and 5-FU mixture. In conclusion, the future research focusing on elucidating the molecular and cellular mechanisms underlying the berberine chloride and 5-FU mixture is crucial for refining therapeutic strategies. As we prepare for the clinical application of this combination therapy, comprehensive formulation evaluations are imperative. The promising initial findings advocate for the continued exploration of berberine chloride and 5-FU in formulating topical anti-melanoma skin cancer treatments. The anticipation of advancing these therapeutic strategies into clinical trials to validate the efficacy and safety of this innovative combination therapy in real-world settings is palpable. This chapter closes by highlighting the next steps in the research, which will involve meticulous quantitative analyses using high-performance liquid chromatography (HPLC) and mass spectrometry, emphasizing the thorough and careful approach required to bring effective topical cancer treatments to fruition.

## Chapter 3. Development of analytical methods and characterisation of model compounds

### 3.1 Introduction

The venture of pharmaceutical formulation begins with the prudent selection of active pharmaceutical ingredients (APIs) which, when combined with excipients, should exhibit both physicochemical compatibility and stability. Overall, the integrity of the drug must remain intact throughout the manufacturing process and beyond (Allen et al., 2011b). A predominant preference is observed for encapsulating these APIs into tablets and capsules rather than liquid formulations due to the stability concerns associated with the latter (Allen et al., 2011a). The constituents of these formulations, comprise both APIs and excipients, the latter aiding in the manufacturing process while occasionally impacting the stabilization or destabilization of the drug products (Rowe et al., 2009; Ren et al., 2008; Jain et al., 2012; Gu et al., 1990; Stanisiz et al., 2013). However, topical formulations like creams, lotions, ointments, and gels are often used for targeted treatment of skin conditions. Due to desired physical properties, creams, gels and lotions provide a desired mix of physical properties making the product appealing to the patient. Their semi-solid nature ensures they stay on the application site, allowing for sustained release of medication over time (Shelley, 2002).

Upon further substantiation of the prospective synergistic efficacy of berberine chloride and 5-fluorouracil (5-FU) in the therapeutic regimen for non-melanoma skin cancer, the endeavour to develop a novel 5-FU formulation combined with berberine emerged as the subsequent focal point of the investigation. Initially, it is imperative to tackle the challenge of quantitative analysis pertaining to the two active constituents, wherein High-Performance Liquid Chromatography (HPLC) presents itself as an important analytical tool. HPLC has been extensively used over the years as an analytical method owing to its ability to separate and analyse pharmaceutical drugs. It is a key tool for the separation and analysis of active ingredients, facilitating accurate quantification and characterization of these compounds in formulations (Ravi et al., 2019). The development and validation of analytical methods are pivotal components of a drug development program. A robust method for drug analysis is vital for conducting subsequent experiments as it minimizes experimental errors and material and time wastage. Additionally, the quality of the data generated significantly hinges on the development and validation of analytical methods (Singh, 2013). As per the Pharmacopeial Convention (Pharmacopeia, 1985), validation of an analytical method entails laboratory studies to ascertain that the method's performance characteristics align with the requirements for the intended analytical application. In the pharmaceutical realm, organizations like the International Conference on Harmonisation (ICH) and the Food and Drug Administration (FDA) provide method validation guidelines. In high-performance liquid chromatography (HPLC) method development, post-establishment of chromatographic and experimental conditions, the method should undergo validation based on several parameters, including:

- Linearity: Evaluating the relationship between analyte concentration and detector response to establish a linear calibration curve.
- Precision: Assessing the method's repeatability (intra-day) and intermediate precision (inter-day) to ensure consistent results under varying conditions.
- Accuracy: Determining the closeness of measured values to the true values by analysing the recovery of known amounts of analytes in the sample matrix.
- Robustness: Assessing the method's reliability and robustness by studying its sensitivity to deliberate variations in critical parameters, such as pH, temperature, and flow rate.
- Limit of Detection (LOD) and Limit of Quantification (LOQ): Determining the lowest concentration of an analyte that can be reliably detected (LOD) and quantified (LOQ) with acceptable precision and accuracy.
- System Suitability: Verifying that the chromatographic system meets predefined acceptance criteria, which may include parameters such as peak resolution, tailing factor, and plate count.

In the context of drug-skin interactions and the development of topical or transdermal drug delivery systems, the physicochemical properties of the drug substance play a crucial role. Several key properties, such as molecular weight, log P (partition coefficient), melting point, and solubility parameter, influence the drug's ability to interact with the skin and permeate through it. The molecular weight of a drug substance is a determining factor for its diffusion coefficient, with larger molecules generally exhibiting slower diffusion. On the other hand, small molecules with reasonable solubility in both water and oil phases tend to demonstrate optimal permeation results. It is worth noting that compounds with low melting points are particularly important in this context, as thermal analysis is an indispensable step in characterizing candidate compounds for drug delivery systems (Hadgraft, 2004).

Additionally, during the early stage of formulation development, it is crucial to perform solubility studies of candidate compounds in different single solvents. These studies aid in selecting suitable vehicles for drug formulation. The solubility parameters of the candidate compounds and the drug of interest, such as 5-FU, can be obtained using software like Molecular Modelling Pro® to assist in selection of candidate vehicles. Experimental determination of the solubility values of 5-FU in various selected single solvents is necessary. To further guide future permeation studies, the solubility of the compound in water and phosphate-buffered saline (PBS) solution, which is isotonic, meaning it has a similar ion concentration, osmolarity, and pH to that of human body fluids should also be measured. This information is essential in selecting an appropriate receptor medium for permeation studies.

In this approach to designing a topical formulation ready for the market, we selected candidate solvents that could potentially serve as vehicles for our drug delivery system. These candidates were carefully chosen from a list of solvents commonly used in commercially formulated products. This selection was driven by two primary considerations: ensuring the efficacy of drug delivery and meeting the safety and regulatory requirements of commercial products. An overview and introduction of these candidate solvents will be provided, exploring their properties, potential advantages,

and any drawbacks. This includes understanding their solubility, volatility, toxicity, and impact on skin permeability, all critical factors in the design of a topical formulation.

It is worth noting that the selection of an appropriate solvent is a critical step in formulation design. The chosen solvent not only has to ensure the drug is adequately dissolved for efficient delivery but also must be compatible with other formulation components, be safe for use, and comply with regulatory requirements. By utilizing commercially formulated solvents, we aim to leverage the existing knowledge and regulatory approvals these solvents already have. This can potentially accelerate the product development process, reduce associated risks, and increase the likelihood of successful market entry. Table 3.1 provides an overview and introduction of these candidate solvents, which can serve as potential vehicles for the drug delivery system.

#### **Ethyl acetate (EA)**

Ethyl acetate is an organic compound used as a solvent and diluent, being favoured and present in confectionery, perfumes, and fruits (Dutia, 2004).

Solubility: Ethyl acetate is miscible with most organic solvents and is moderately soluble in water.

Volatility: Ethyl acetate has a moderate volatility, which allows for quick evaporation from the skin.

Toxicity: It has low acute toxicity, but prolonged exposure or high concentrations can cause irritation or damage to the skin, eyes, and respiratory system (Agency for Toxic Substances and Disease Registry, 1997).

Impact on Skin Permeability: Ethyl acetate can enhance the permeation of certain drugs by increasing the skin permeability (Cevc et al., 2008).

EA is approved by the FDA as a secondary direct food additive permitted for human consumption (Code of Federal Regulations, Title 21, Section 172.515).

#### **Propylene glycol (PG)**

Propylene glycol, also known as 1,2-propanediol, is a synthetic organic alcohol which absorbs water. It is widely used in food, drugs, and cosmetic and personal care products (Mateus et al., 2013).

Solubility: Propylene glycol is miscible with water and most organic solvents.

Volatility: It has low volatility, leading to slower evaporation from the skin.

Toxicity: PG has low toxicity and is considered safe for topical use. However, some individuals may experience skin irritation or sensitization (Anderson et al., 2017).

Impact on Skin Permeability: Propylene glycol can enhance the permeation of drugs by improving skin hydration and disrupting the stratum corneum barrier (Lodén et al., 2002).

PG is categorized as Generally Recognized as Safe (GRAS) by the FDA for use in food and is permitted in various food categories (Code of Federal Regulations, Title 21, Section 184.1666).

It is also approved by the FDA for use in drugs, cosmetics, and personal care products (Code of Federal Regulations, Title 21, Section 172.810).

**Propylene glycol monolaurate (PGML)**

PGML is a mixture of the propylene glycol mono- and di-esters of lauric acid. It occurs as a colourless or slightly yellow oily liquid at 20°C. It is used as a vehicle and penetration enhancer in transdermal drug delivery systems (Haque et al., 2017).

Solubility: PGML is soluble in both water and oils.

Volatility: The volatility of PGML is relatively low.

Toxicity: PGML is generally recognized as safe for topical use and has low toxicity (Suresh and Venkateswarlu, 2011).

Impact on Skin Permeability: PGML can act as a penetration enhancer by disrupting the lipid structure of the stratum corneum and increasing drug permeation through the skin (Karande et al., 2004).

There is no specific FDA approval for propylene glycol monolaurate. However, its constituent ingredients, propylene glycol and lauric acid, have FDA approval for various applications.

**Glycerol**

Glycerol, which is a trihydroxy sugar alcohol, is an intermediate in lipid and carbohydrate metabolism. Glycerol is widely utilized as a solvent, emollient, and sweetening agent in the pharmaceutical industry. However, one known drawback of the use of glycerol as a solvent is its high viscosity (García et al., 2014).

Solubility: Glycerol is highly soluble in water and moderately soluble in alcohol.

Volatility: Glycerol has low volatility, resulting in slow evaporation from the skin.

Toxicity: Glycerol is non-toxic and considered safe for topical use. However, high concentrations may cause temporary skin irritation (European Medicines Agency, 2017).

Impact on Skin Permeability: Glycerol can increase skin hydration and flexibility, potentially enhancing the permeation of drugs through the skin (Zhou et al., 2018).

Glycerol is generally recognized as safe (GRAS) by the FDA and is approved for use in food, drugs, and cosmetics (Code of Federal Regulations, Title 21, Section 184.1320).

**Dimethyl isosorbide (DMI)**

Dimethyl isosorbide is a water-miscible liquid with a low viscosity. It has been widely used as a pharmaceutical vehicle, absorption enhancer, and viscosity decreasing agent. DMI significantly increases the solubility of water-insoluble ingredients while not affecting ingredient stability (Otto et al., 2008).

Solubility: DMI is miscible with most organic solvents and is soluble in water.

Volatility: DMI has low volatility, allowing for prolonged contact with the skin.

Toxicity: DMI has low toxicity and is considered safe for topical use (National Toxicology Program, 1993).

Impact on Skin Permeability: DMI acts as a penetration enhancer by improving the solubility of hydrophobic drugs and facilitating their transport through the skin (Kim et

al., 2016).

Dimethyl isosorbide does not have specific FDA approval as a solvent. However, it is widely used in the formulation of pharmaceuticals, cosmetics, and food additives.

### **PEG 200, PEG 400 & PEG 600**

Polyethylene glycol (PEG) is a polyether composed of repeated ethylene glycol units. It has an indispensable role in drug delivery systems, acting as a solubilizer, stabilizer, taste-masking agent, bioavailability enhancer, and release-modifier. For hydrophobic compounds, a co-solvent such as PEG increases solubility by decreasing polarity of the solvent system. PEGs in the range of PEG 200 and PEG 400 can be utilized as water-miscible solvents in parenteral and oral liquids (D'souza and Shegokar, 2016).

Solubility: PEGs are highly soluble in water and miscible with most organic solvents.

Volatility: PEGs have low volatility, leading to slow evaporation from the skin.

Toxicity: PEGs have low toxicity and are generally considered safe for topical use (Cosmetic Ingredient Review Expert Panel, 2005).

Polyethylene glycols (PEGs), including PEG 200, PEG 400, and PEG 600, are approved by the FDA for various applications, including as excipients in drugs and as ingredients in food and cosmetic products (Code of Federal Regulations, Title 21, Section 172.820).

### **Hexylene Glycol and Dipropylene Glycol**

Hexylene Glycol and Dipropylene Glycol are used as solvents and viscosity decreasing agents in cosmetics and personal care products (Gesslein, 2020).

Solubility: Hexylene Glycol is soluble in water and is miscible with many organic solvents.

Volatility: It has low volatility, which means it evaporates relatively slowly from the skin.

Toxicity: Hexylene Glycol is considered safe for use in cosmetics and personal care products. It has low acute toxicity and is not known to cause significant skin irritation or sensitization (Cosmetic Ingredient Review Expert Panel, 2014).

Impact on Skin Permeability: Hexylene Glycol can enhance the permeation of certain drugs by increasing the skin permeability through its solvent properties (Montenegro et al., 2015).

Dipropylene Glycol:

Solubility: Dipropylene Glycol is miscible with water and most organic solvents.

Volatility: It has low volatility, resulting in slow evaporation from the skin.

Toxicity: Dipropylene Glycol is generally considered safe for use in cosmetics and personal care products. It has low acute toxicity and is not known to cause significant skin irritation or sensitization (Cosmetic Ingredient Review Expert Panel, 2013).

Impact on Skin Permeability: Dipropylene Glycol can act as a solvent and humectant, helping to increase the skin's moisture content and potentially enhancing the permeation of certain drugs (Montenegro et al., 2015).

Hexylene Glycol is considered safe for use in cosmetics and personal care products within the concentration limits determined by the FDA (Code of Federal Regulations, Title 21, Section 73.1450). Dipropylene Glycol is permitted for use in cosmetics as long as it meets the required specifications and is used within the defined concentration

limits (Code of Federal Regulations, Title 21, Section 73.1460).

#### **Transcutol®**

Transcutol®, also known as diethylene glycol monomethyl ether (DEGEE), is a clear, colourless liquid with a pleasant odour (Sullivan Jr et al., 2014). It is utilized in the formulation and manufacturing process of pharmaceuticals, cosmetics, and food additives worldwide. As an effective solubilizer, it can solubilize actives which are insoluble in common solvents such as propylene glycol and ethanol. It is also used in topical products, and it has been reported to modify the skin penetration properties of active ingredients to achieve enhanced local absorption (Osborne and Musakhanian, 2018).

Solubility: Transcutol® is soluble in water and is miscible with most organic solvents.

Volatility: It has moderate volatility, which allows for relatively rapid evaporation from the skin.

Toxicity: Transcutol® is considered safe for use in pharmaceuticals, cosmetics, and food additives. It has low acute toxicity and is not known to cause significant skin irritation or sensitization when used at appropriate concentrations (Sullivan Jr et al., 2014).

Impact on Skin Permeability: Transcutol® can enhance the permeation of drugs by increasing the solubility of lipophilic compounds and facilitating their transport through the skin (Rhee et al., 2015).

It is considered safe for use in various applications, including topical products, and is included in the FDA Inactive Ingredient Database (FDA Inactive Ingredient Database, DIETHYLENE GLYCOL MONOMETHYL ETHER).

#### **1,5-pentanediol**

1,5-pentanediol is an organic compound used as a plasticizer and it also forms polyesters that are used as emulsifying agents and resin intermediates (Werle et al., 2000).

Solubility: 1,5-pentanediol is miscible with water and many organic solvents.

Volatility: It has moderate volatility, allowing for moderate evaporation from the skin.

Toxicity: 1,5-pentanediol is generally considered safe for use in cosmetics and personal care products. It has low acute toxicity and is not known to cause significant skin irritation or sensitization (Cosmetic Ingredient Review Expert Panel, 2017).

Impact on Skin Permeability: The impact of 1,5-pentanediol on skin permeability is dependent on its specific formulation and concentration. As a solvent, it may enhance the permeation of certain drugs by increasing their solubility and facilitating penetration through the skin.

Pentylene Glycol is listed as an ingredient in a prescription hydrogel wound dressing (medical device classified under 21CFR878.4022), which was approved by the FDA (Section 510(k)). Sources did not specify whether 1,2-Pentanediol or 1,5 Pentanediol was used or the concentration used.

Table 3.1 Candidate solvents considered for the topical formulation development.



When developing an HPLC quantification method for 5-FU and berberine chloride, it is possible that finding a single mobile phase that can be used for both compounds may be challenging. This is because the optimal separation and quantification of different analytes often require specific mobile phase compositions and conditions. However, it is important to note that the mobile phase can be adjusted to accommodate the specific requirements of each compound. There is currently no widely accepted method employing a single mobile phase for the quantification of both compounds. Following the development of the quantitative method, it is crucial to assess the performance of the main active substance, 5-fluorouracil (5FU), in various commonly used solvents. This evaluation aims to determine the solubility and stability of 5-FU in these solvents, providing valuable insights for formulation development and potential applications in the pharmaceutical industry. The compatibility of excipients with drugs is investigated by conducting stability studies under normal and stressed conditions (ICH, 2003). The latter aids in identifying potential degradation products, thereby helping to ascertain the degradation pathways (Reynolds et al., 2002; ICH, 2003). Stability studies can be divided into three steps. Firstly, solutions of the specific drug in pure or mixed solvents are prepared. Secondly, the samples are stored under specified temperature and humidity conditions for a period of time. Lastly, validated stability-indicating analytical methods are employed to determine the concentration of the intact drug. Moreover, the octanol-water partition coefficient is a crucial parameter in pharmaceutical sciences, particularly in the development of topical formulations.

Therefore, the aims and objectives of the work in this chapter are as follows.

1. To develop and validate HPLC analytical methods for the major model active, 5-FU and minor active berberine chloride.
2. To conduct a comprehensive characterization process of these model drugs, including solubility studies, stability studies, miscibility, and octanol/water partition coefficient ( $\log P_{o/w}$ ) determination of 5-FU where applicable.

## **3.2 Materials and methods**

### **3.2.1 Materials**

5-FU was purchased from Cambridge Bioscience, UK. Berberine chloride was purchased from Sigma-Aldrich, UK. Analytically pure propylene glycol (PG), PEG 200 and PEG 400 were purchased from Fisher Scientific, UK. Glycerol was purchased from Sigma-Aldrich, UK. Miglyol 812N® was obtained from Sasol GmbH (Germany). Phosphate buffer saline (PBS) tablets were purchased from Oxoid Limited, England. Dimethyl isosorbide (DMI) was a gift from Croda Limited, UK. Propylene glycol monolaurate (PGML), and Transcutol® were received as gifts from Gattefossé, France. HPLC grade water, acetonitrile (HPLC grade) and Acetonitrile (ACN) (HPLC grade) were purchased from Fisher Scientific (UK).

### **3.2.2 Methods**

#### **3.2.2.1 Analytical method development and validation**

##### **3.2.2.1.1 HPLC method development for analysis**

The HPLC system employed in this study consisted of high-quality instrumentation from Agilent Technologies (U.S.A.) and Hewlett-Packard (U.S.A.). The system included an Agilent Technologies 1100 series degasser, a Hewlett-Packard 1100 series quaternary pump, an Agilent Technologies 1100 series autosampler, a Hewlett-Packard 1100 series system controller, and an Agilent Technologies 1100 series UV detector.

To facilitate data acquisition and analysis, the ChemStation® for LC 3D Rev. A. 09.03 software, provided by Agilent Technologies (U.S.A.), was utilized. This software offered robust capabilities for acquiring and processing the HPLC data, enabling efficient and accurate analysis in the study.

### 3.2.2.1.2 Linearity

Linearity, an essential characteristic of an analytical method, refers to its ability to yield results that are directly proportional or proportionate to the analyte's concentration within a specific range (Ermer and Nethercote, 2014). Demonstrating linearity typically involves preparing standard solutions at five concentration levels, spanning 50% to 150% of the target analyte concentration (Green, 1996). The inclusion of five concentration levels aids in detecting potential non-linear trends in the data, and each standard should undergo preparation and analysis at least three times (Green, 1996). The correlation coefficient is a significant indicator used to assess the acceptability of linearity data, with a value greater than 0.999 generally considered satisfactory (Green, 1996). For this study, a set of eight standards was prepared, covering a concentration range of 0.5 to 100 µg/ml. Each sample underwent three replicates for analysis.

### 3.2.2.1.3 Accuracy

Accuracy, as defined by the Pharmacopeial Convention (1985), refers to the degree of proximity between the results obtained from a method and the true value. Green (1996) outlines four procedures for assessing accuracy, including analysing samples of known concentration, comparing the measured values of a new method with those of an accurate existing method, conducting a recovery study by spiking analyte in bland matrices, and employing standard addition of the analyte. Among these procedures, the recovery study is widely used.

In a recovery study, the analyte is spiked into blank matrices, and the spiked samples are prepared in triplicate at three different levels of the target concentration. For assay methods, accuracy is typically expressed as the percent recovery of the added analyte amount in the sample. To evaluate accuracy, triplicate determinations of three solutions with concentrations of 1, 2, and 20 µg/ml were performed. The mean recovery within the range of  $100 \pm 2\%$  at each concentration, spanning 80-120% of the target concentration, is generally considered acceptable according to FDA guidelines (Shabir, 2004). This criterion ensures that the method is capable of accurately measuring the analyte within the desired concentration range.

$$\% \text{Recovery} = \frac{\text{Measured value}}{\text{Excepted value}} \times 100\% \quad \text{Equation 3.1}$$

### 3.2.2.1.4 Precision

Precision, as defined by the Pharmacopeial Convention (1985), refers to the level of agreement observed among individual test results obtained when applying an analytical method to multiple samplings of a homogeneous batch. To assess precision, the method is typically applied to test a sample a sufficient number of times to obtain valid results. The evaluation of precision involves determining both repeatability (intra-day) and intermediate precision (inter-day). Repeatability is evaluated by conducting twelve repeated analyses of the same working solution under identical experimental conditions on the same day. Intermediate precision is assessed by performing the analysis on three different days by another analyst in the same laboratory (Franz, 1975).

For intra-day assay precision, it is generally acceptable for the relative standard deviation (RSD) to be no more than 1%. This indicates a low level of variation within the same day, ensuring consistent and precise results. On the other hand, inter-day variation accounts for variations that may arise from factors such as different days or equipment within the laboratory. An acceptable inter-day precision would have an RSD no more than 2%.

Precision is commonly expressed as the percent relative standard deviation (RSD), which is calculated using Equation 3.2. The RSD provides a measure of the variability observed in the repeated analyses of the sample.

$$\%RSD = \frac{\text{Standard deviation}}{\text{Mean}} \times 100\% \quad \text{Equation 3.2}$$

The precision of the proposed method was verified through repeatability and intermediate precision by triplicate determinations of three different solutions at low, medium and high concentrations, which were 2, 20 and 80 µg/ml. These experiments were completed within 15 days to verify both intra and inter day variability.

#### **3.2.2.1.5 Robustness**

The robustness of an analytical method refers to its ability to maintain its performance and reliability even when subjected to minor variations in normal test conditions. These variations can include changes in factors such as different analysts, laboratories, instruments, percent organic content and pH of the mobile phase, buffer concentration, temperature, and injection volume. The evaluation of robustness typically involves assessing the method's response to small modifications in these parameters. This can be done by examining each factor individually or by conducting a factorial experiment where multiple factors are varied simultaneously (Virlichie and Ayache, 1995). By evaluating the robustness of an analytical method, its ability to withstand variations in experimental conditions is determined. This assessment ensures that the method remains consistent and reliable even when minor changes occur, thus enhancing its applicability and usefulness in practical analytical settings.

#### **3.2.2.1.6 Limit of detection (LOD) and limit of quantification (LOQ)**

According to the International Conference on Harmonization (ICH) guidelines, there are three methods for determining the detection and quantification limits for an analytical method, namely visual determination, signal-to-noise determination, and standard deviation and slope determination. LOD is the lowest amount of drug which can be detected but not necessarily quantified. However, LOQ is the minimum concentration at which the drug can be quantified (ICH, 2005).

In this validation protocol, the standard deviation and slope determination method was employed. In this method, the limit of detection (LOD) may be expressed as:  $LOD = 3.3 \sigma/S$ , where  $\sigma$  is the standard deviation of the response, and  $S$  is the slope of the calibration curve. The slope  $S$  may be estimated from the calibration curve of the analyte. The estimate of  $\sigma$  may be carried out based on the standard deviation of the blank or based on the calibration curve. A specific calibration curve should be studied using

samples containing an analyte in the range of LOD.

$$LOD = \frac{3.3\sigma}{S} \quad \text{Equation 3.3}$$

The residual standard deviation of a regression line or the standard deviation of the y intercepts of regression lines may be utilized as the standard deviation. To the LOD, the limit of quantification (LOQ) may be expressed as Equation 3.4 Where  $\sigma$  is the standard deviation of the response, and S is the slope of the calibration curve.

$$LOQ = \frac{10\sigma}{S} \quad \text{Equation 3.4}$$

#### 3.2.2.1.7 System suitability

The International Conference on Harmonisation (ICH) has introduced the concept of a system suitability test, which is typically employed after a method has been fully validated and is routinely used for analysing real samples (Krull and Swartz, 1999). The purpose of the system suitability test is to assess the performance of the instrumental system before and after analysing actual batches of samples, demonstrating that the system is functioning properly. In the proposed method, the system suitability was evaluated by conducting six replicate injections of freshly prepared standard solutions at a concentration of 20  $\mu\text{g/ml}$ . A comparison of the obtained chromatogram parameters with a standard trace was then performed. This comparison involved examining peak shape, peak width, and baseline resolution. The standard trace encompasses various parameters, including peak area, retention time, symmetry, number of theoretical plates (N), and tailing factors (T). By comparing these parameters obtained from the system suitability injections with those of the standard trace, the analyst can assess the quality and performance of the instrumental system. This evaluation ensures that the system is operating within acceptable limits and provides confidence in the reliability of the results obtained during routine sample analysis.

#### 3.2.2.2 Thermal analysis

The melting point of berberine chloride was determined using thermogravimetric analysis (TGA) TGA is a suitable method for examining the degradation temperature of a compound and determining the loss of water molecules (Parisi et al., 2015). For the TGA analysis, berberine chloride was accurately weighed and placed in an open aluminium pan. The pan containing the sample was then subjected to controlled heating within the TGA furnace. The analysis started at a temperature of 40  $^{\circ}\text{C}$  and progressed up to a terminal temperature of 550  $^{\circ}\text{C}$ , with a heating ramp rate of 10  $^{\circ}\text{C/min}$ . To create an inert atmosphere around the sample, a nitrogen flow of 25 ml/min was maintained throughout the analysis process.

By monitoring the sample's weight loss and any associated thermal events during heating, TGA provides information about the degradation behaviour, including the

temperature at which the compound undergoes thermal decomposition or loses water molecules. It is worth noting that the determination of the melting point of berberine chloride using DSC may also be performed to further validate the TGA results and obtain additional insights into the compound's thermal properties. However, performing TGA or DSC experiments on 5-FU carries potential risks due to its toxic properties and potential for thermal decomposition into hazardous gases, necessitating strict adherence to safety protocols and personal protective measures. Additionally, careful handling and proper disposal of waste generated from these experiments are crucial to ensure both personnel safety and environmental protection.

### 3.2.2.3 Log $P_{(o/w)}$ determination

To determine the partition coefficient of 5-fluorouracil (5-FU), the shake flask method recommended by the Organisation for Economic Co-operation and Development (OECD) guidelines was employed. The following steps were followed:

Preparation of octanol pre-saturated with water and water pre-saturated with octanol:

- Two stock bottles were prepared, one containing 100 ml of octanol with a sufficient amount of water, and the other containing 100 ml of water with a sufficient amount of octanol.
- The mixtures were stirred for 24 hours at room temperature and then allowed to equilibrate for 48 hours.
- After equilibration, the phases (octanol and water) were separated.

Preparation of Stock Solution:

- A stock solution of 5-FU was prepared in the saturated octanol layer with a concentration of 100 mg/ml.

Variation in Test Substance Concentration and Octanol-Water Ratio:

- Three different concentrations of 5-FU in the octanol phase were studied: 1 mg/ml, 10 mg/ml, and 100 mg/ml.
- Three experiments were conducted using different ratios of octanol to water: 1:1, 1:2, and 2:1.

Test Procedure:

- Test vessels, such as 2 ml centrifuge tubes, were used for the experiment.
- Accurately measured amounts of the stock solution and the two solvents (octanol and water) were added to the test vessels.
- The tubes were rotated through 180° for 5 minutes to ensure thorough mixing of the phases.
- After 48 hours of standing, the two phases (octanol and water) were separated.
- Samples from each phase were diluted and analysed using HPLC.

Calculation of Partition Coefficient:

- The log of the partition coefficient was calculated using the relative concentrations of 5-FU in n-octanol and water phases.

Replicates:

- All measurements were performed in triplicate to ensure accuracy and reproducibility.

By following these steps and conducting the shake flask method, the partition coefficient of 5-FU was determined, providing valuable information about its distribution between octanol and water phases.

### 3.2.2.4 Solubility studies

To select suitable vehicles and receptor phases for *in vitro* permeation studies, various solvents and solvent systems were assessed through solubility studies. The experimental procedure involved the following steps:

Preparation of Solvent Solutions:

- Plastic centrifuge tubes, each containing 2 ml of the chosen solvent or solvent system, were used.
- An excess amount of the active compound was added to each tube.
- A Teflon-coated stirrer was placed in each vial to facilitate mixing.

Sealing and Incubation:

- The tubes were securely sealed using Parafilm® to prevent evaporation or contamination.
- The sealed tubes were placed on a rotator at a controlled temperature of  $32 \pm 1^\circ\text{C}$ . The choice of  $32 \pm 1^\circ\text{C}$  for solubility studies is to mimic the physiological conditions of human skin, ensuring that the experimental results reflect the drug's behaviour under conditions close to those found *in vivo*, and to maintain a stable and controlled temperature environment for enhanced precision and repeatability of the experiments.
- The incubation period lasted for 48 hours, allowing for the production of a saturated solution with a visible excess of the drug.

Preparation of Pipette Tips:

- A sufficient number of pipette tips were placed in an oven set at  $32 \pm 1^\circ\text{C}$ .
- This ensured that the experimental temperature remained consistent during subsequent steps, preventing temperature variations.

Centrifugation and Sample Preparation:

- After the 48-hour incubation, the samples were subjected to centrifugation at 13,200 rpm for 15 minutes, maintaining a temperature of  $32 \pm 1^\circ\text{C}$ .
- The resulting supernatant was carefully collected.
- A known volume of the supernatant was suitably diluted in volumetric flasks to achieve a concentration within the range of the HPLC calibration curve.

HPLC Analysis:

- The concentrations of the compounds in the diluted samples were determined using HPLC.

- HPLC analysis involved injecting the prepared samples into the chromatographic system and quantifying the compounds based on their respective peaks in the chromatogram.

By following this experimental procedure, the solubility of the compounds in various solvents and solvent systems could be determined. The HPLC analysis provided quantitative data on the concentrations of the compounds, aiding in the selection of suitable vehicles and receptor phases for subsequent *in vitro* permeation studies.

#### 3.2.2.5 Solubility parameter studies

The solubility parameter ( $\delta$ ) is a numerical value that indicates the solubility characteristics of a substance. It is useful in predicting the miscibility and solubility of materials in different solvents or with other materials. In the pharmaceutical and cosmetic industries, this parameter is crucial for formulating products with the desired properties. The solubility parameters for 5-FU and various vehicles were calculated using Molecular Modelling Pro® software (version 6.3.3) developed by ChemSW (Fairfield, CA, USA). The software facilitates the determination of the solubility parameter by using the molecular structures of the materials involved. A difference of less than two between the  $\delta$  of two materials usually indicates mutual solubility (Khalil and Martin, 1967; Vaughan, 1985).

#### 3.2.2.6 Miscibility studies

Miscibility refers to the ability of compounds to mix at a molecular level, resulting in the formation of a homogeneous mixture. In the context of polymer blends, the miscibility between the constituents of a polymer mixture is crucial for the development of new polymer blends (Coleman et al., 1995). To investigate the miscibility of binary solvents, studies were conducted using different solvent ratios, such as 1:9, 2:8, 3:7, 4:6, 5:5, 6:4, 7:3, 8:2, and 9:1. Additionally, for ternary miscibility tests, three solvents were combined in varying percentages, with each percentage differing by 10%.

The miscibility studies involved taking the solvents in the predetermined ratios and placing them in pre-marked small sample tubes. The tubes were then manually shaken for approximately 1 minute and placed in a tube stand to observe their miscibility. In some cases, to aid in distinguishing the miscibility of the solvents, two dyes, Sudan III (red colour) obtained from Sigma Aldrich (UK), and methylene blue (blue colour) obtained from Acros Organics (UK), were utilized (Figure 3.4).

By conducting these miscibility studies and visually assessing the homogeneity or phase separation of the solvent mixtures, insights into the compatibility of different solvents and their potential for forming homogeneous blends can be gained. The use of dyes further aids in distinguishing between mixed and phase-separated regions within the solvent mixtures.



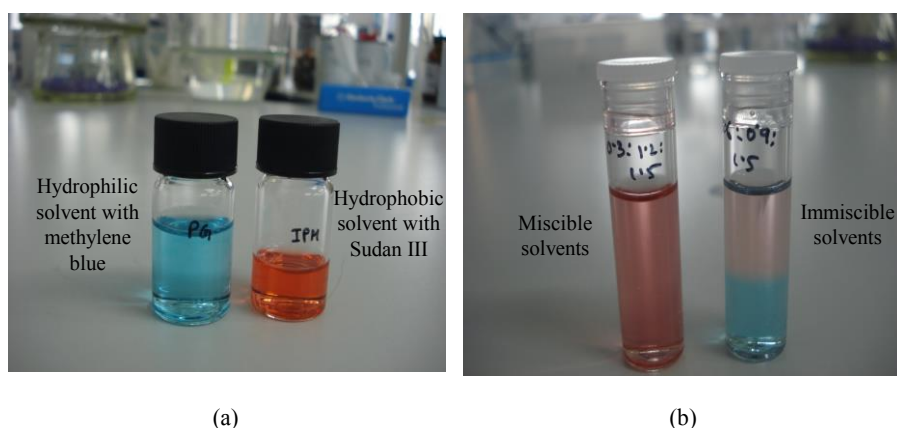


Figure 3.4: Miscibility studies of binary and ternary solvents: (a) methylene blue and Sudan III dyes were added to the hydrophilic and hydrophobic solvents, respectively before starting miscibility studies (b) a clear solution indicated miscible mixture and phase separation or emulsion indicated immiscible mixture.

In cases where the miscibility of the solvents was not readily apparent, the sample tube was left undisturbed for a minimum of 24 hours to allow for further evaluation of phase separation. If the solvents were miscible, a clear solution would be observed, indicating their ability to form a homogeneous mixture. On the other hand, if the solvents were immiscible, an emulsion or phase separation would become evident, with distinct boundaries between the different phases. To visually represent the ternary miscibility system, a ternary phase diagram was constructed. This diagram provides a graphical representation of the solubility and phase behaviour of the ternary solvent system. The construction of the ternary phase diagram was facilitated by using OriginPro® 8.0 software, developed by OriginLab Corporation (USA). This software allows for the accurate plotting and analysis of phase diagrams, aiding in the understanding of the solvents' miscibility and phase behaviour within the ternary system.

### 3.2.2.7 Calculation of solubility parameter values for binary and ternary mixtures

The solubility parameter of 5-FU compounds and solvents was calculated using Molecular ModellingPro® software (version 6.3.3) developed by ChemSW (Fairfield, CA, USA). This software utilizes the van Krevelen Hoftyzer type three-dimensional solubility parameter (denoted as  $\delta$ ) for the calculations. For binary solvents that displayed miscibility with each other, the solubility parameter (denoted as  $\delta_m$ ) was determined using the following equation:

$$\delta_m (\text{binary}) = (\delta_1 \Phi_1 + \delta_2 \Phi_2) / (\Phi_1 + \Phi_2)$$

For ternary solvents, the solubility parameter (denoted as  $\delta_m$ ) was calculated as follows:

$$\delta_m (\text{ternary}) = (\delta_1 \Phi_1 + \delta_2 \Phi_2 + \delta_3 \Phi_3) / (\Phi_1 + \Phi_2 + \Phi_3)$$

Here,  $\Phi_1$ ,  $\Phi_2$ , and  $\Phi_3$  represent the respective volume fractions of the pure solvents 1, 2, and 3, while  $\delta_1$ ,  $\delta_2$ , and  $\delta_3$  are the solubility parameters of the pure solvents 1, 2, and 3, respectively (Braon, 1980). By applying these calculations, the solubility parameter of the compounds and solvents can be determined, aiding in the assessment of their compatibility and potential for forming homogeneous mixtures.

### **3.2.2.8 Stability studies**

The stability of the two model drugs, 5-fluorouracil (5FU) and berberine chloride, in various solvents was investigated over a period of 72 hours at a temperature of  $32 \pm 1$  °C.

To conduct the stability study, solutions of known concentrations of the compounds in the tested solvents were prepared. These solutions were then transferred to glass tubes with screw caps, ensuring proper sealing. The use of screw caps and sealing with Parafilm® helped prevent evaporation or contamination during the study.

The prepared samples were placed in a water bath set at a temperature of  $32 \pm 1$  °C to maintain a controlled environment. The samples remained in the water bath for the entire duration of the stability study. At predetermined time points of 0 hours, 24 hours, 48 hours, and 72 hours, 200  $\mu$ L each solution was withdrawn from the respective glass tubes. These withdrawn samples were subsequently analysed using high-performance liquid chromatography (HPLC). HPLC analysis enables the quantification and detection of the compounds in the samples.

By analysing the samples at different time intervals, the stability of 5-FU and berberine chloride in the tested solvents can be assessed. The HPLC analysis provides valuable information on the degradation or changes in the concentrations of the compounds over the course of the 72-hour study period.

### 3.3 Results

#### 3.3.1 Validation of HPLC analytical method for 5-Fluorouracil

Based on the compound properties provided, a novel HPLC analytical method has been developed for 5-FU (5-fluorouracil) as shown in Table 3.5, validated, and optimized in accordance with recognized standards and guidelines. The British Pharmacopoeia 2013 and the International Conference on Harmonization (ICH) guidelines Q2 (R1) are referenced for the validation of various parameters including linearity, precision, accuracy, specificity, and robustness.

Moreover, a wavelength scan on a 1 mg/ml sample was performed within a range of 200 to 300 nm to ascertain the optimal detection wavelength. The wavelength of 254 nm was chosen, corresponding to the second absorption maximum, likely to ensure adequate sensitivity and specificity in detecting 5-FU.

HPLC method parameters	
Column	C18 250×4.6 mm
Mobile phase(v/v)	98% Water with 0.1% Trifluoroacetic Acid (TFA)
	2% Acetonitrile (ACN)
Temperature (°C)	25
Flow rate (mL/min)	0.7
Run time (min)	10
Retention time (min)	6.5
Wavelength (nm)	254
Injection volume (μL)	5

Table 3.5: HPLC conditions for analysis of 5-Fluorouracil

##### 3.3.1.1 Linearity

The peak areas of 5-FU at different concentrations are shown in Table 3.6 and Figure 3.7. As shown in Figure 1, the representative linear equation was  $y=17.90x + 0.72$  ( $R^2=1.00$ ). In this equation, 17.90 represents the slope and 0.72 is the intercept. In principle, if the coefficient of determination ( $R^2$ ) is  $\geq 0.997$ , it means the method has good linearity (Lam, 2004). Therefore, the value of the determination coefficient of 1.00 confirmed excellent linearity for the calibration curve for the selected method.

Peak areas of 5-FU at different concentrations	
Concentration (µg/ml)	Peak area
0.5	9.023
1	17.579
5	89.907
10	179.854
25	450.409
50	896.726
75	1340.784
100	1790.791

Table 3.6 Peak areas of 5-Fluorouracil at different concentrations

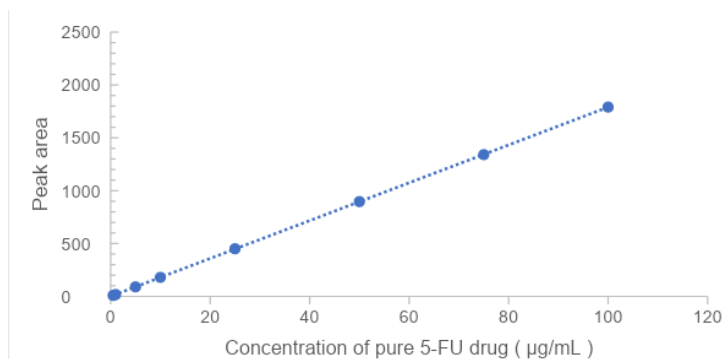


Figure 3.7 Graphical presentation of linearity plots of 5-Fluorouracil (Mean  $\pm$  SD, n=3).

### 3.3.1.2 Accuracy

Table 3.8 showed that the recovery values at the three different concentrations were 102.4, 101.84 and 101.79% with R.S.D values of 0.14, 0.01 and 0.006 %, respectively. The mean value for recovery was 104.7 % and that of the R.S.D was 0.05%. The range for the accuracy limit should be within the linear range. According to Lam et al (2004), the expected accuracy of the recovery of drug substances in a mixture is in the range from 95% to 105%. The result shows that the recovery values for the three selected concentrations, at 5 µg/ml and 25 µg/ml were in the range between 95% and 105%.

Theoretical concentration (µg/ml)	Measured concentration (µg/ml)	Recovery (%)	R.S.D (%)
5	5.12 $\pm$ 0.007	102.4	0.14
25	25.46 $\pm$ 0.003	101.84	0.01
50	50.90 $\pm$ 0.03	101.79	0.006
		mean 101.8	mean 0.05

Table 3.8 Accuracy results for 5-FU, Mean  $\pm$  SD (n=3)

### 3.3.1.3 Precision

Precision is usually verified by the determination of repeatability (intra-day) and intermediate precision (inter-day). The acceptable %RSD value should be less than 10%. TAs can be seen in Table 3.9, the %R.S.D values of the measurements ranged from 0.01 to 1.22% for intra-day variability studies while the results obtained from intermediate precision studies were 3.25, 2.35 and 0.26%, respectively (Table 3.10).

Theoretical concentration (µg/ml)	Intra-day measured concentration (µg/ml)					
	day 1		day 2		day 3	
	Mean±SD	R.S.D%	Mean±SD	R.S.D%	Mean±SD	R.S.D%
5	5.32±0.007	0.14	5.46±0.02	0.3	5.47±0.0005	0.01
25	26.46±0.003	0.01	26.89±0.02	0.08	26.93±0.008	0.03
50	50.90±0.03	0.006	50.9±0.03	0.5	52.04±0.63	1.22

Table 3.9: Summary of intra-day (repeatability) variability data for 5-FU, Mean ± SD (n=3).

Theoretical concentration (µg/ml)	Inter-day measured concentrations(µg/ml)	
	Mean±SD	R.S.D%
5	5.28±0.17	3.25
25	26.17±0.62	2.35
50	50.53±0.13	0.26
mean ± SD (n=3); Inter-day precision was determined from three different runs over a 1-week period.		

Table 3.10: Summary of inter-day (intermediate precision) variability data for 5-FU, Mean ± SD (n=3).

### 3.3.1.4 Robustness

Table 3.11 presents the results and chromatographic conditions selected as variables in each experiment. There were no obvious differences in the chromatograms when specific modifications were made in the given experiments. The correlation coefficients ( $R^2$ ) of the calibration curves were 1.00, 0.99, 0.99 and 0.99, respectively and the recovery ranged between 97.36 and 101.79%. All the data mentioned above illustrate that the selected method is robust for 5-FU. This means the selected method is robust enough for the analysis of 5-FU.

	Wavelength (nm)	Flow rate (ml/min)	Injection volume ( $\mu$ l)	Temperature ( $^{\circ}$ C)	Mobile phase Water: Acetonitrile (ACN) (v/v)	$R^2$	Recovery (%)
1	254	0.9	5	25	98:2	1.00	95.66
2	254	0.7	5	20	98:2	0.99	92.77
3	249	0.7	5	25	98:2	1.00	95.27
4	259	0.7	5	25	98:2	1.00	98.88
5	254	0.7	5	25	96:4	0.99	91.91
6	254	0.7	10	25	98:2	1.00	95.00

Table 3.11 The robustness test for HPLC conditions and obtained responses, \*mean  $\pm$  SD (n=3)

### 3.3.1.5 Limit of detection (LOD) and limit of quantification (LOQ)

Based on the standard deviation and slope determination, the LOD and LOQ of this HPLC method were determined to be 0.13 and 0.39  $\mu$ g/mL, separately.

### 3.3.1.6 System Suitability

A system suitability study was conducted, the results are documented in Table 3.12. The system suitability study is crucial in HPLC method validation to ensure that the system performs adequately for the intended analysis. The parameters evaluated in this study include the percentage relative standard deviation (%R.S.D) for peak area and retention time, which were found to be 0.09 and 0.13, respectively. These values fall within the acceptable limits, indicating the system's performance and suitability for the analysis.

System suitability results for 5-FU 6 times for 10µl/ml		
	Mean ± SD	%R.S.D
peak area	188.36 ±0.34	0.18
retention time(min)	9.15±0.07	0.71
symmetry	0.93±0.007	0.74

Table 3.12 System suitability results, (mean ± SD (n=6), 6 times for 10µl/ml).

In general, according to ICH guidelines the HPLC method validation parameters for 5-FU are summarized in table 3.13.

Values	Estimated values	ICH guidelines
Precision	RSD = 1 ± 0.002 %	RSD < 2%
Linearity	R <sup>2</sup> = 0.9999	R <sup>2</sup> > 0.999
Accuracy	%Recovery = 101.8 ± 0.5	102 > %Recovery > 98
Limit of Detection	0.13 µg/ml	
Limit of Quantitation	0.39 µg/ml	
Robustness	%Recovery = 100 ± 2	102 > %Recovery > 98
System Suitability	Inj. Repeatability RSD = 0.13 %	RSD < 1%

Table 3.13: Experimentally determined values for the 5-FU analytical method in comparison with the ICH guidelines

### 3.3.2 Solubility studies for 5-FU in single solvents

This section shows the results for solubility of 5-fluorouracil (5-FU) in different solvents at a temperature of 32±1°C, as summarized in Table 3.14. Propylene Glycol (PG), glycerol, Polyethylene Glycol (PEG) 200/400, and Transcutol® (TC) are the solvents in which 5-FU exhibits high solubility.

Solvent	Solubility parameter (δ) (cal/cm <sup>3</sup> ) <sup>1/2</sup>	Solubility (mg/ml)
Water	22.97	12.20±2.45
PBS	N/A	14.51±0.55
Ethyl acetate (EA)		0.93±0.09
Propylene glycol (PG)	14.0	17.56±0.38
Propylene glycol monolaurate	9.4	1.32±0.06
Glycerol	17.14	15.6±0.64
Dimethyl sulfoxide	10.26	81.27±3.36
PEG 400	11.67	35.26±1
Hexylene glycol	14.3	3.36±0.06
Dipropylene glycol	12.2	10.23±1.05
Transcutol®	10.6	23.25±0.12
1,5-pentanediol	13.3	6.35±0.36
PEG 200	12.06	36.39±1.04
1,3-butanediol	14.09	7.2±0.15
Isopropyl myristate (IPM)	8.21	0.03±0.001

Table 3.14: The solubility of 5-Fluorouracil in each solvent or solvent system at 32 ± 1°C (n=3, mean ± SD)

### 3.3.3 Stability studies of 5-FU

Figure 3.15 summarizes the results of stability studies for simple formulations of 5-FU. The molecule is stable in the candidate solvents PG, TC and Glycerol and PEG 200, 400. The high percentage recovery values likely reflect loss or evaporation of solvent on manipulation for analytical determinations.

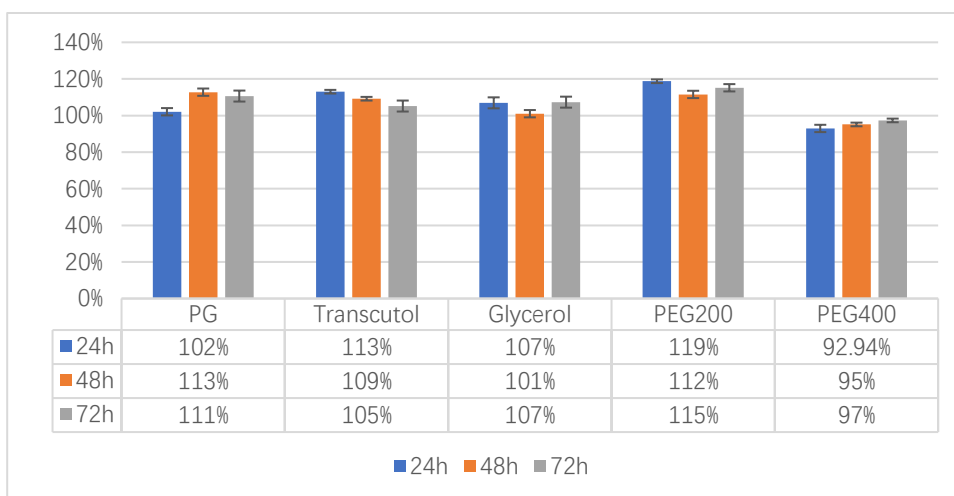


Figure 3.15: Recovery (%) of 1% (w/v) 5-FU in candidate solvents at 32 ±1 °C (n=3; mean ± SD).

### 3.3.4 HPLC method Development for berberine chloride

The UV absorption profile of berberine chloride for the range between 300 and 400 nm was obtained. The wavelength selected for the HPLC analysis was 342 nm, which corresponded to the absorption maximum. Table 3.3 presents the chromatographic conditions developed for the HPLC method for berberine chloride.

HPLC method parameters	
Column	C18 250X4.6 mm
Mobile phase(v/v)	30% Acetonitrile (ACN)
	70% HPLC water with 0.1% (TFA) (v/v)
Temperature (°C)	25±1°C
Flow rate (mL/min)	0.7 ml/min
Run time (min)	10
Retention time (min)	5
Wavelength (nm)	340 nm
Injection volume (μL)	10 μl

Table3.16: HPLC conditions for analysis of berberine chloride



### 3.3.4.1 Validation of HPLC method for berberine chloride

#### 3.3.4.1.1 Linearity

The linear regression data for the calibration curves showed a good linear relationship over the concentration range 10–100 µg/ml for berberine chloride. Samples of concentration 100µg/mL, 75µg/mL, 50µg/mL, 25µg/mL, 20µg/mL, 15µg/mL, 10µg/mL, 5µg/mL, 0µg/mL Berberine chloride dissolved in HPLC grade water were tested and the calibration curve was obtained by charting the concentrations vs their peak area from the chromatograph. With an  $R^2$  value of 0.9974, this was deemed an acceptable curve.

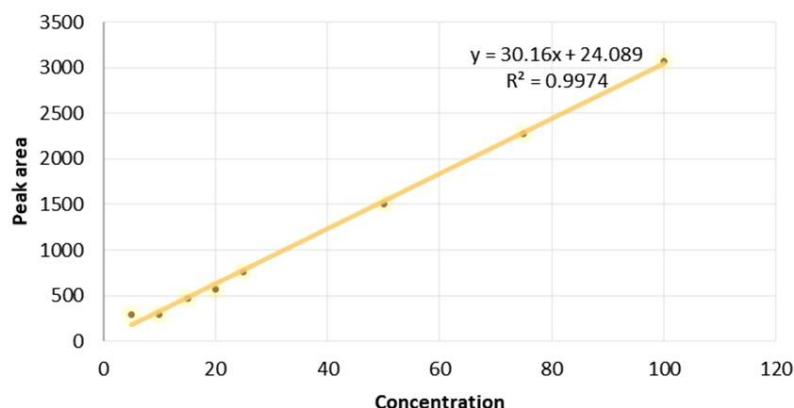


Figure 3.17 Graphical presentation of linearity plots of berberine chloride (Mean  $\pm$  SD,  $n=3$ ).

#### 3.3.4.1.2 Accuracy

The accuracy of the method was evaluated by recovery studies at three different concentrations. The percentage recovery was found to be 99.51, which is within the acceptable range of 98 to 102% according to ICH guidelines. The accuracy was determined by using samples with pure berberine chloride powder dissolved in HPLC grade water to obtain a solution. The accuracy of detection is relatively poorer at lower concentrations of the molecule being tested.

Theoretical concentration (µg/ml)	Measured concentration (µg/ml)	Recovery (%)	R.S.D (%)
5	4.92±0.005	98.4	0.12
25	25.08±0.003	100.34	0.013
50	49.90±0.03	99.79	0.009
		mean 99.51	mean 0.05

Table 3.18 Accuracy results for 5-FU, Mean  $\pm$  SD ( $n=3$ )

#### 3.3.4.1.3 Precision

Precision was assessed in terms of repeatability (intra-day) and intermediate precision (inter-day) with RSD values. The obtained RSD value was  $1 \pm 0.002\%$ , indicating high

precision as per the ICH guideline of RSD < 2%. No significant difference between intra-day and inter-day data.

Concentration	%RSD
10 µg/mL	1.18
25 µg/mL	1.36
50 µg/mL	0.47

Table 3.19 - %RSD values for intra-day testing

Concentration	%RSD
10 µg/mL	1.34
25 µg/mL	1.29
50 µg/mL	0.35

Table 3.20 - %RSD values for inter-day testing

#### 3.3.4.1.4 Robustness

The robustness of the method was evaluated by changing various chromatographic conditions. The % Recovery of  $100 \pm 1$  under altered conditions affirms the method's robustness, aligning with the ICH guideline range of 98 to 102% for recovery.

Wavelength (nm)	Flow rate (ml/min)	Injection volume(µl)	Temperature (°C)	Mobile phase TFA: ACN (v/v)	R <sup>2</sup>	Recovery (%)
340	0.9	10	25	30:70	1.00	98.67
340	0.7	10	20	30:70	0.99	99.97
345	0.7	10	25	30:70	1.00	101.27
345	0.7	10	25	30:70	1.00	98.84
340	0.7	10	25	28:72	0.99	100.93
340	0.7	5	25	30:70	1.00	101.05

Table 3.21 The robustness test for HPLC conditions and obtained responses, \*mean  $\pm$  SD (n=3)

#### 3.3.4.1.5 Limit of Detection (LOD) and Limit of Quantification (LOQ)

The LOD and LOQ for berberine chloride were determined to be 0.993 µg/ml and 3.008 µg/ml, respectively.

### 3.3.4.1.6 System Suitability

A system suitability study was conducted to affirm the system's performance for the intended analysis. The results demonstrated an injection repeatability RSD of 0.2%, well within the ICH guideline of RSD < 1%.

In general, according to ICH guidelines the HPLC method validation parameters for berberine chloride are summarized in Table 3.22.

Values	Estimated values	ICH guidelines
Precision	RSD = $1 \pm 0.002$ %	RSD < 2%
Linearity	$R^2 = 0.9991$	$R^2 > 0.999$
Accuracy	%Recovery = $99.51 \pm 0.38$	$102 > \% \text{Recovery} > 98$
Limit of Detection	0.993 µg/ml	
Limit of Quantitation	3.008 µg/ml	
Robustness	%Recovery = $100 \pm 1$	$102 > \% \text{Recovery} > 98$
System Suitability	Inj. Repeatability RSD = 0.2 %	RSD < 1%

Table 3.22–Experimentally determined HPLC validation parameter values for the berberine chloride analytical method in comparison with the ICH guidelines.

### 3.3.4.2 Berberine chloride TGA analysis

The thermal studies of berberine chloride showed its stability up to 80°C and the degradation of berberine chloride between the temperature range of 80°C to 250°C as shown in figure 3.15.

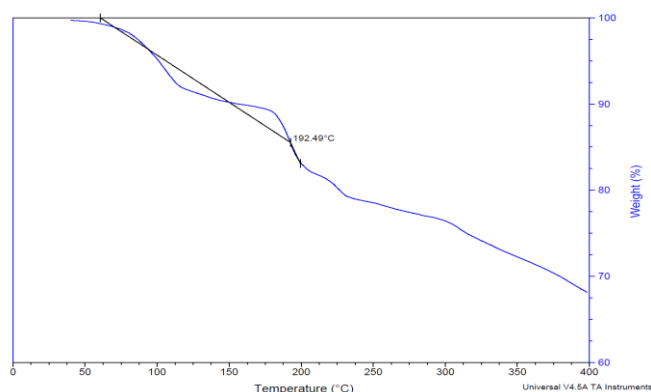


Figure 3.23: Berberine chloride TGA analysis showing the weight loss plotted against temperature from 40°C to 400°C.

### 3.3.4.3 Berberine chloride solubility performance

Berberine chloride was tested in solvents that performed well in solubility tests for 5-Fu but showed poor solubility in both organic and non-polar solvents in table 3.24. of these, Transcutol® showed relatively better performance.

solvent	solubility parameter ( $\delta$ ) (cal/cm <sup>3</sup> ) <sup>1/2</sup>	solubility (mg/ml)
water	22.97	2.13±0.09
pbs	n/a	2.38±0.05
Propylene glycol (PG)	14.0	0.26±0.03
Glycerol	17.14	0.32±0.006
PEG 400	11.67	0.02±0.002
Transcutol®	10.6	1.58±0.03
PEG 200	12.06	0.01±0.008
Isopropyl myristate (IPM)	8.21	N/A

Table 3.24: The solubility of 5-fluorouracil in each solvent or solvent system at 32 ± 1°C (n=3, mean ± SD)

### 3.3.5 Miscibility studies of binary and ternary solvent systems

The miscibility studies of candidate hydrophilic and hydrophobic solvents were conducted. The hydrophilic solvents, PG and TC were miscible with each other in all ratios. The hydrophobic solvent IPM was not miscible with water. IPM showed miscibility with TC in all ratios and immiscibility in PG. In order to prepare ternary formulations of 5-FU, miscibility studies with ternary systems were conducted, as shown in Figure 3.16.

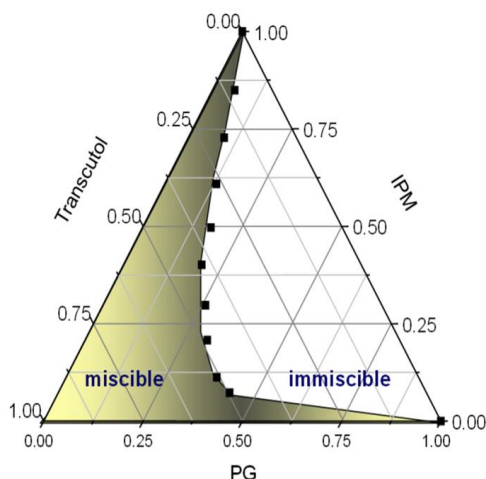


Figure 3.16: Ternary phase diagram of PG-TC-IPM

### 3.3.6 Solubility studies of binary and ternary solvent systems

Based on miscibility studies with PG, TC and IPM (Figure 3.16), the solubility of 5-fluorouracil (5-FU) was investigated in various binary and ternary solvent systems, as summarized in Table 3.17. The solubility studies were conducted at a controlled temperature of  $32 \pm 1$  °C. The binary systems explored included varying ratios of Propylene Glycol (PG) to Transcutol (TC), while the ternary systems encompassed additional variations in the concentration of Isopropyl Myristate (IPM). First, in binary solvent systems, the solubility of 5-FU showed minimal variation with different ratios of PG to TC. Specifically, the solubility values recorded were  $31.20 \pm 0.3$  mg/ml,  $32.01 \pm 3.4$  mg/ml, and  $32.21 \pm 2$  mg/ml for PG:TC ratios of 1:1, 1:2, and 2:1, respectively. In ternary solvent systems, a decreasing trend in 5-FU solubility was observed with the increasing concentration of IPM. The solubility dropped from  $31.68 \pm 1.4$  mg/ml in a PG:TC:IPM ratio of 5:10:1 to  $19.39 \pm 0.7$  mg/ml in a ratio of 2:10:4.

The solubility of 5-FU remained relatively constant when altering the ratios between PG and TC in the ternary solvent systems, showcasing the robustness of 5-FU solubility against changes in PG and TC proportions.

Solvent	$\delta$ Vehicle (cal/cm <sup>3</sup> ) <sup>1/2</sup>	Solubility (mg/ml)
PG: TC =1: 1	12.2	31.20±0.3
PG: TC =1: 2	11.73	32.01±3.4
PG: TC = 2: 1	12.87	32.21±2
PG: TC: IPM= 4: 11: 1	11.3	31.10±0.7
PG: TC: IPM= 3: 12: 1	11.09	30.28±0.1
PG: TC: IPM= 5: 10: 1	11.52	31.68±1.4
PG: TC: IPM= 2: 12: 2	10.73	25.03±0.8
PG: TC: IPM= 4: 10: 2	11.15	24.49±2.6
PG: TC: IPM= 2: 10: 4	10.43	19.39±0.7
PG: TC: IPM= 4: 8: 4	10.85	23.03±0.8

Table 3.17 Summary of the solubility of 5-FU in binary and ternary solvents at 32 ± 1 °C. (mean ± SD; n = 3)

## 3.4 Discussion

### 3.4.1 HPLC method Development for 5-FU and berberine chloride

In this chapter, we developed two novel HPLC analytical methods to accurately quantify 5-FU and berberine hydrochloride, aiming to facilitate subsequent exploration. Through continuous improvement, these new HPLC methods can now be performed on the same columns and with the same inorganic mobile phase. This approach of using the same mobile phase to detect two substances offers several advantages based on chromatographic principles. Chromatography, a widely employed analytical technique for separating and detecting components in mixtures, involves injecting the mixture into a mobile phase and separating it on a stationary phase, with different components moving at different rates based on their affinity for the stationary phase.

The use of 0.1% trifluoroacetic acid (TFA) in water as a mobile phase for high-performance liquid chromatography (HPLC) offers numerous advantages. TFA, being a highly polar organic acid, enhances the polarity of the mobile phase, facilitating efficient separation of a broad range of organic compounds, particularly polar analytes. Furthermore, its incorporation in the mobile phase allows for fine-tuning the polarity and ionization of compounds, leading to improved separation efficiency and resolution. The versatility of the 0.1% TFA water solution extends to various compounds, not limited to polar analytes but also including neutral and some non-polar compounds, making it suitable for a wide spectrum of analytes. Additionally, the controlled acidity of the low TFA concentration ensures the stability and reliability of the mobile phase during prolonged chromatographic runs, while also reducing environmental pollution and potential hazards to laboratory personnel. However, careful consideration is required to avoid adverse reactions with sensitive detectors or column materials, emphasizing the need for prior validation and optimization experiments to ensure the selected mobile phase meets specific analytical requirements. In conclusion, the use of 0.1% TFA in water as a mobile phase in HPLC provides an effective and versatile approach for achieving efficient and reliable chromatographic separations, enabling accurate quantification and identification of organic compounds in complex mixtures. Acetonitrile is favoured in HPLC due to its solvent properties, compatibility with UV detection, suitable polarity and volatility for the elution of analytes, and its role in affecting chromatographic selectivity. Firstly, acetonitrile is highly soluble and can effectively dissolve a wide range of ions and non-polar compounds. This property is critical for the mobile phase in HPLC, which must dissolve analytes for separation and detection. Secondly, acetonitrile has an exceptionally low UV absorbance at short wavelengths, making it suitable for highly sensitive analysis using UV detection. It helps maintain a stable and noise-free baseline, which promotes more accurate detection and quantification. Thirdly, acetonitrile is a highly volatile, non-proton polar organic solvent, acetonitrile is used as both a solvent and a mobile phase in analytical chemistry. Its volatility facilitates analysis after rapid evaporation, and its polarity affects the elution strength of analytes during chromatography.

The use of a single mobile phase has significant benefits, such as saving time and reducing the cost of chemical reagents, as there is no need to create different mobile phases for each substance (Altria, 2016). Furthermore, utilizing the same mobile phase ensures that both substances are detected under identical conditions, ensuring comparability and consistency of results, which facilitates data comparison and analysis (Zhao et al., 2018). Moreover, optimizing the same mobile phase provides a better understanding of its properties and effects, enabling easier adjustments and improvements to the analytical method (Wang et al., 2019). Additionally, employing a uniform mobile phase can decrease errors and uncertainties arising from variations in different mobile phases, thus enhancing the reliability and accuracy of the chromatographic results (Altria, 2016). Furthermore, certain substances may exhibit higher sensitivity to specific mobile phases, making the use of the same mobile phase more suitable for such substances (Zhao et al., 2018). While the advantages of using the same mobile phase are evident, it is essential to acknowledge potential limitations. For instance, in cases where substances significantly differ in their properties, a single mobile phase may not be sufficient to satisfy the separation requirements for both substances. In such instances, different mobile phases or alternative analytical methods may be necessary to better meet the specific analysis needs (Wang et al., 2019). Therefore, when choosing analytical methods and mobile phases, researchers must carefully consider the characteristics of the samples and the experimental objectives to ensure optimal chromatographic analysis.

Overall, the development of these two new HPLC methods with a uniform mobile phase marks a significant step forward in the accurate quantification of 5-FU and berberine chloride, providing valuable insights for subsequent explorations and research in this field.

### **3.4.2 Solubility studies for 5-FU in single solvents**

The solubility of 5-fluorouracil (5-FU) across varying solvents is significantly impacted by an array of factors encompassing the intrinsic chemical structure and attributes of both the solute and the solvent, alongside the intermolecular interactions brewing between them. The reported solubility of 5-FU in water is 12.2 mg/ml, closely mirroring the value of 12.5 mg/ml delineated in prior literature (Troy, 2006). A slight elevation in solubility is observed with PBS (Phosphate Buffered Saline) where 5-FU achieves a solubility of 14.5 mg/ml. This subtle rise in solubility can be rationalized by the marginally elevated pH of PBS compared to water, which could potentially foster the generation of salts, thereby boosting 5-FU dissolution. Considering the higher solubility solvents as illustrated in the table, it becomes apparent that the polarity and hydrogen bonding capability of the solvents emerge as prime factors modulating the solubility dynamics. The molecular architecture of 5-FU, adorned with functional groups like fluorine atom and carbonyl groups, bestows it with a polar character and the ability to partake in hydrogen bonding. Therefore, these solvents like Propylene Glycol (PG), Glycerol, and Polyethylene Glycols (PEG200 and PEG400), are polar and can form hydrogen bonds. These solvent attributes promote favourable intermolecular interactions with 5-FU, propelling its solubility.



Furthermore, the renowned solvation credentials of PG, Glycerol, and PEGs, especially for polar and hydrogen-bonding susceptible molecules, provide a favourable solubility milieu for 5-FU. Their solvation spectrum encapsulates a broad range of substances, transcending the solubility limitations posed by water or other conventional solvents. Transcutol®, with its noted solubilizing capacity, often finds its way into pharmaceutical formulations aimed at solubility enhancement. The efficacy of Transcutol® as a solubilizer may be rooted in its molecular design that fosters favourable interactions with polar entities like 5-FU. Additionally, literature reports elucidating the formulation synergy between PG, PEG, and 5-FU in anticancer efficacy further corroborate the solubility findings, underscoring the pivotal role solvents play in pharmaceutical formulation and delivery. The recurring emphasis on PG and PEG as facilitators of 5-FU delivery across diverse studies lends credence to the solubility data and suggests potential avenues for optimizing 5-FU formulations and delivery systems through judicious solvent selection (Yi et al., 2010, Paek et al., 2006, Thakur et al., 2019). Transcutol® and Propylene Glycol (PG) were chosen among solvents that already have relatively good solubility performance because of their advantage of enhancing drug penetration into the skin, making them promising choices for 5-FU formulations. Firstly, Transcutol® is a high purity diethylene glycol monomethyl ether (DEGEE) recognized for its solubilizing and enhancing effects on a wide range of drug actives. It has been used in combination with other permeation enhancers such as nitron, oleic acid and ethanol to study the permeation of drug saturated solutions (Osborne and Musakhanian, 2018). Its effectiveness as a penetration enhancer lies in its ability to promote the accumulation of topically applied drugs in the lipid layer of the skin without disturbing its structure, which is essential for maintaining skin integrity while enhancing drug delivery (Carrer et al., 2020). On the other hand, propylene glycol is used as a co-solvent in formulations and enhances drug penetration of topical formulations through the skin (Haq and Michniak, 2018). When used in combination with other penetration enhancers, it has a significant impact, showing a synergistic effect that can increase the efficacy of the drug delivery system (Strusovskaya et al., 2019). The unique properties of Transcutol® and PG that contribute to their effectiveness as permeation enhancers include their ability to solubilize a variety of drug actives, which increases the availability of drugs for absorption at the skin surface. In addition, their interaction with lipid components of the skin can temporarily alter skin barrier function, thereby increasing drug penetration. Therefore, Transcutol® and propylene glycol (PG) were used as the two base solvents in the miscibility experiments for further studies.

### **3.4.3 Solubility studies of binary and ternary solvent systems**

The miscibility of solvents is a fundamental aspect that can significantly influence the solubility of drugs like 5-FU. In this study, it was observed that hydrophilic solvents PG and TC were miscible in all ratios, indicating a favourable interaction between these solvents. Conversely, the hydrophobic solvent IPM exhibited immiscibility with water but was miscible with TC in all ratios, which might be attributed to the contrasting polarities of these solvents. The ternary phase diagram of PG-TC-IPM provided valuable insights into the miscibility behaviour in a three-component system. Such ternary systems are

complex, and their behaviour can be dictated by the interplay of molecular interactions among the components. The observed miscibility can lead to an enhanced solvent effect, which is critical for achieving higher solubility of 5-FU. The solubility studies in binary and ternary solvent systems further elucidated the impact of solvent composition on the solubility of 5-FU. It was interesting to note that the solubility of 5-FU did not significantly change with varying ratios of PG and TC, suggesting that these solvents have a comparable solvation capability for 5-FU. However, an increase in IPM concentration in the ternary systems led to a decrease in 5-FU solubility, which could be due to the hydrophobic nature of IPM diminishing the solvation of 5-FU. One study discussed the dissolution behaviour of 5-FU in various solvents, highlighting the importance of solvent effects, and providing insights on the Hansen solubility parameter, molecular simulation, and thermodynamic aspects affecting the solubility of 5-FU (Liu 2022). Another report discussed the exploitation of ternary solubility phase diagrams for the resolution of chiral molecules, shedding light on the interpretation and application of such diagrams for designing separation processes of chiral molecules (Cascella et al., 2019). Isopropyl myristate (IPM) is often added to binary systems with propylene glycol (PG) and Transcutol to enhance drug penetration through the skin (Karande and Mitragotri, 2009). IPM is a lipid-based compound that can disrupt the lipid structure of the stratum corneum, the outermost layer of the skin, which can increase drug permeability (Zhao et al., 2016). When used in combination with PG and Transcutol, which are also penetration enhancers, IPM may contribute to a synergistic effect, resulting in increased solubility and permeability of the drug through the skin (Osborne and Musakhanian, 2018). This makes IPM a valuable component in transdermal delivery systems, especially when a higher degree of skin penetration is desired. Furthermore, the findings in this study corroborate with a previously mentioned research study where a formulation comprising Poloxamer 188, propylene glycol, and 5-FU enhanced the anticancer effect of 5-FU, suggesting a potential benefit in using polar solvents like propylene glycol in 5-FU formulations. These observations underscore the importance of understanding the miscibility and solubility behaviour of candidate solvents in optimizing systems for drug formulation and delivery. The insights gained from these studies provide a solid foundation for the development of effective 5-FU formulations, paving the way for further exploration in the realm of drug solubility and delivery systems.

### 3.5 Conclusions

Studies on the solubility, and HPLC method development for 5-FU and berberine chloride have provided valuable insights into the analysis and formulation of these compounds. The new HPLC method developed for 5-FU and berberine chloride utilizes a single mobile phase of water and acetonitrile containing 0.1% trifluoroacetic acid (TFA), providing a simplified, economical, and consistent method for the quantitative analysis of these two compounds. Advantages of this method include improved comparability and consistency of results, time savings and reduced consumption of chemical reagents. Solubility studies have clarified the effect of various solvents on the solubility of 5-FU, highlighting the role of solvent polarity and hydrogen bonding ability in improving

solubility. Solvents such as PG and glycerol show the highest solubility of 5-FU due to the fact that their polarity and ability to form hydrogen bonds matches the chemical structure of 5-FU. In the field of formulation science, Transcutol® and PG have emerged as excellent penetration enhancers due to their unique properties of solubilizing a wide range of drug actives and temporarily altering skin barrier function to facilitate drug penetration. The use of Transcutol® and PG as the base solvents for the miscibility experiments in this study highlights their potential for the development of topical formulations of 5-FU.

In addition, the results of the binary and ternary solvent systems provide a nuanced understanding of miscibility and solubility behaviour, which is critical for optimizing drug formulations. These insights can guide the development of more efficient drug delivery systems, especially for 5-FU. The subsequent chapters will investigate permeation studies of topical formulations, building upon the groundwork laid by the solubility and analytical method development reported here.

## Chapter 4. Development of topical formulations containing 5-FU

### 4.1 Introduction

A successful topical formulation must be (i) physically and chemically stable (Allen et al., 2011b), (ii) effectively release the active pharmaceutical ingredient (API), which in this case is 5-FU, from the formulation and deliver it efficiently to the skin (Lane et al., 2012), and (iii) be easy to apply and well-received by patients. Therefore, pre-formulation studies were conducted at an early stage. The stability and solubility of the API, 5-FU, in a range of solvents were assessed, and compatibility studies with solvent combinations and excipients were carried out. In the previous chapter, the stability of 5-FU in a range of commonly used commercial carriers was assessed. Table 4.1 provides the outlines of key stages in the process and the factors considered at each stage for drug development, particularly for transdermal delivery systems where skin permeation is a critical step. In this chapter, the objective is to measure the amount of drug penetration through pig and human skin by performing *in vitro* permeation studies to (i) ensure that the drug is released from the formulation and (ii) to measure the rate and extent of drug penetration across the skin. This will aid in the identification of promising formulations. Moreover, non-melanoma skin cancers, particularly basal cell carcinoma and squamous cell carcinoma, are primarily concentrated in the epidermis, the outermost layer of the skin. Table 4.1 provide the outlines of key stages in the process and the factors considered at each stage for drug development, particularly for topical delivery systems where skin permeation is a critical step. As mentioned in Chapter 1, the main factors affecting the transdermal absorption of a compound are its physicochemical properties, such as molecular weight, solubility, lipophilicity, ionization, and melting point (Lane et al., 2012). These factors allow formulators to make an informed judgment about the likelihood of a given compound traversing the SC (stratum corneum).

Topical 5-FU delivery aims to circumvent systemic side effects and enhance drug efficacy against skin cancer and pre-cancer, a condition with a growing global incidence (Pandey et al., 2021). This makes the development of effective topical treatments increasingly critical. Despite having potent anticancer properties, 5-FU belongs to the Biopharmaceutics Classification System (BCS) class III, and thus possesses pharmaceutical limitations of poor solubility and bioavailability that restrict its therapeutic potential, particularly when deeper skin penetration is required (Oliveira et al., 2020). Additionally, the stratum corneum of the skin may allow those drugs to cross the membrane that have a lipophilicity between 1 and 3, melting point (MP) under 200 °C, and a molecular weight under 500 Da. In this case, 5-FU as a free drug poorly crosses the stratum corneum due to its negative LogP value, indicating challenges in penetrating the lipophilic barrier of the skin effectively (Safwat et al., 2018). Similarly, berberine chloride faces challenges in skin penetration owing to its high hydrophilicity, presenting a barrier to effective topical administration (Rathod et al., 2023). There are creams and solution formulations of 5-FU currently available on the market in a range of strengths. Existing formulations have not been consistently assessed for absorption rates, necessitating a detailed investigation to enhance the delivery of 5-FU to skin tissues

effectively. The systemic absorption of topical 5-FU is minimal, with most patients having undetectable drug levels, making detailed absorption data less critical in regulatory submissions. Regulatory focus remains on its local efficacy and safety for dermatological conditions. Therefore, the aim of the present work was to conduct pre-formulation and permeation studies with 5-FU in order to identify vehicles that would preferentially deliver 5-FU to the skin rather than through the skin.

	Step	Considerations
1	Drug selection based on its physicochemical properties	<ul style="list-style-type: none"> <li>- Partition coefficient (Log P)</li> <li>- Molecular size</li> <li>- Solubility/melting point</li> <li>- Ionization (<math>pK_a</math>)</li> </ul>
2	Compatibility and stability studies	<ul style="list-style-type: none"> <li>- Drug-excipients</li> <li>- Excipient-excipient</li> </ul>
3	Solubility of drug in the selected excipients	
4	Selection of solvent systems	- Single- Binary- Ternary
5	Development of different formulations	
6	<i>In vitro</i> skin permeation studies	To screen the formulations to ensure the drug is released from the formulation & reaches the target tissues.
7	Selection of the lead formulation based on the stability and permeation studies for clinical testing	
8	Approval & manufacturing of commercial product	

Table4.1 Topical formulation development flowchart

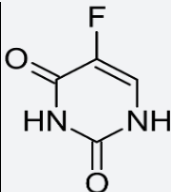
Chemical structure	
Melting point	283°C (Ashwanikumar et al., 2014)
Water solubility	11.1 mg/mL at 22 °C (Burr and Bundgaard, 1985)
Log P	-0.89 (Hansch et al., 1995)
$pK_a$	8.02 (Sangster, 1994)
Toxicity	LD <sub>50</sub> =230 mg/kg (orally in mice) (Pfizer, 2012)
Molecular weight	130.08 g/mol

Table 4.2 The physical and chemical properties of 5-FU. The solubility parameter of 5-FU is calculated using Molecular Modelling Pro® software (version 6.3.3) developed by ChemSW (Fairfield, CA, USA)..

The assessment of percutaneous permeation of molecules is an important step in the development of any dermal or transdermal drug delivery system, especially in the initial design or in the later evaluation. Skin absorption can be studied in living humans or animals or *in vitro* by using excised skin in diffusion cells (Bronaugh et al., 1982). Generally, the most reliable skin permeation data are collected in human studies, although such studies are less feasible during the initial development of a new formulation or consideration of a new candidate compound (Godin and Touitou, 2007). Meanwhile, a good agreement between the *in vivo* absorption studies and the *in vitro* studies has been observed by previous studies (Mateus et al., 2014). Moreover, the *in vitro* method has unique advantages over the *in vivo* methods. For example, for *in vitro* permeation studies, the sample is measured directly below the skin surface rather than measured in the systemic circulation. Thus, *in vitro* methods to assess permeant skin profiles are used extensively in industry and academia (Walters, 2002). Diffusion cells are the most common apparatus to conduct *in vitro* permeation studies. Basically, a diffusion cell consists of a donor chamber and a receptor chamber between which the isolated skin is placed (OECD, 2004). The epidermal side of the skin in the donor chamber, also is exposed to ambient laboratory conditions, while the dermal side of the skin is in contact with the receptor chamber which is full of receptor fluid representing the body fluid (OECD, 2004). Buffered isotonic saline is the most common choice of the receptor medium, and its temperature is controlled by thermostatically controlled water circulating through a jacket surrounding the chamber to maintain the skin surface at 32 °C. For cells designed without a jacket, a water bath or a heating block can be applied for temperature control (Finnin et al., 2012). The amount of tested compound permeating from the donor to the receptor side is determined as a function of time. To mimic the real *in vivo* environment, the receptor medium should have adequate solubility for the tested compound so that sink conditions are sustained throughout the length of study (Finnin et al., 2012). Different designs of diffusion cells have been developed, ranging from a simple two-compartment static diffusion cell to multi-jacketed flow-through cells (Walters and Brain, 2002). Static and flow-through types are both acceptable. Figure 4.3 shows an example of a typical design, which is also the same diffusion cell used in this study.



Figure 4.3 Image of the Franz diffusion cells used in following assays. A is the donor chamber; B is the receptor chamber; C is the membrane which would be mounted between the donor chamber and the receptor chamber during permeation; D is the clamp used to fix the diffusion cells.

Skin from both human and animal sources can be utilized in *in vitro* permeation studies (OECD, 2004). Human skin is considered the gold standard for *in vitro* drug permeation studies due to its physiological relevance. However, due to ethical considerations and the practical challenges associated with obtaining human tissue, animal skin models such as those from rats, rabbits, guinea pigs, pigs, and snakes have been used as alternatives. Notably, domestic pig skin is often regarded as the closest approximation to human skin in terms of its permeability and anatomical characteristics (Simon & Maibach, 2000). Moreover, synthetic membranes like silicone have emerged as cost-effective and ethically neutral substitutes for biological skin in certain experimental setups (Finnin et al., 2012). The synthetic skin models have limitations in terms of physiological relevance, permeability differences, inability to mimic skin diseases, regulatory acceptance, and limited customization make them less than ideal for many *in vitro* permeation studies. The use of human and porcine skin models, while more challenging to obtain and use, provides a more accurate and relevant representation of skin for these types of studies. In this chapter, we aim to refine our topical formulation using these assessment methods, focusing on human and porcine skin models. The targeted delivery facilitated by these models is expected to minimise side effects and amplify the anticancer efficacy, contributing to the development of more effective treatments for skin-related conditions. The targeted delivery of such agents should result in reduced side effects and improved anticancer effect to develop effective medicines for the management of the condition.

## 4.2 Aims

Firstly, an unlimited (infinite) dose permeation and mass balance study of 5-FU will be conducted to evaluate the permeation and retention properties of candidate solvents in both porcine and human skin models. This investigation will determine the efficiency of the solvent system in facilitating the delivery of the API across the skin barrier. Secondly, finite dose permeation and mass balance studies of 5-FU on human skin will be conducted. These studies aim to understand the permeation dynamics of 5-FU when applied in doses that reflect its intended clinical application, thereby informing the development of an optimally effective dosage form for therapeutic use.

## 4.3 Materials and methods

### 4.3.1 Materials

5-FU was purchased from Cambridge Bioscience, UK. Berberine chloride was purchased from Sigma (UK), B3251. Analytically pure propylene glycol (PG), t-butyl alcohol (T-BA), poly (ethylene glycol) 200 (PEG 200) and PEG 400 were purchased from Fisher Scientific, UK. Glycerol was purchased from Sigma-Aldrich, UK. Phosphate buffer saline (PBS) tablets were purchased from Oxoid Limited, England. Propylene glycol monolaurate (PGML), and Transcutol® were received as gifts from Gattefossé, France. HPLC grade water, acetonitrile (HPLC grade) and methanol (HPLC grade) were purchased from Fisher Scientific (UK). Phosphate buffer saline (PBS) tablets were purchased from Oxoid Limited, England. HPLC grade water, acetonitrile (HPLC grade) and methanol (HPLC grade) were purchased from Fisher Scientific (UK). Porcine tissues were obtained from a local abattoir. The 250 µm silicone membrane was obtained from Samco (Nuneaton, UK).

### 4.3.2 Methods

#### 4.3.2.1 Franz cell diffusion experiments

The permeation studies were conducted using Franz-type diffusion cells, consisting of two compartments, a donor, and a receptor, with a membrane clamped between them. The membrane was either porcine/human skin or synthetic membrane cut with a cork borer to an appropriate size. The diameters of both the donor and the receptor compartments of each Franz cell were measured using an electronic digital micrometre (Fisher Scientific, U.K.). Before placing the membrane in the cells, a thin layer of high vacuum grease (Dow Corning, U.S.A.) was applied on the compartments. The donor was held tightly on the receptor compartment with a metallic clamp so that a leak proof seal was created. For the preparation of the receptor fluid, PBS solutions were prepared and degassed for at least 30 mins in a Hilsonic ultra sonicator (Hilbre Ultrasonics LTD, England) prior to use in the permeation studies. The exact amount of PBS that was used to fill the receptor of each Franz cell was measured gravimetrically. A small Teflon coated magnetic bar was added in the receptor chamber to keep the liquid in motion throughout the experiment. Finally, the assembled Franz cells were placed in a SUB 28 (Grant Instruments, U.K.) thermostatically controlled water bath equipped with a Telesystem HP 15 (Variomag®, U.S.A.) submersible magnetic stirrer. The membrane temperature was checked with a TM-22 (Digitron, U.S.A.) digital thermometer and the permeation experiment was not started until it was equilibrated to the experimental temperature ( $32 \pm 1^\circ\text{C}$ ).

#### 4.3.2.2 Permeation studies

The protocol for permeation studies is detailed methodically to ensure precise and reproducible results: Setup of Diffusion Cells: Glass Franz-type diffusion cells with a



surface area of approximately 1 cm<sup>2</sup> and a receptor volume of around 2.3 ml were utilized. Human epidermis or porcine ear skin was sectioned into circular pieces roughly 2.5 cm in diameter and mounted onto the cells. The stratum corneum faced the donor compartment to simulate physiological conditions. Ensuring Integrity: To prevent leakage, silicone grease was applied at the juncture of the skin and cell chambers, which were then firmly clamped together. The integrity of the skin was verified by measuring electrical resistance, with higher conductivity indicating compromised barrier function. Receptor Medium Preparation: The receptor compartment was filled with a phosphate buffer saline (PBS) solution at pH 7.4, with sodium azide (0.01% w/v) added as a preservative against microbial contamination. This solution was degassed and constantly stirred to maintain homogeneity. Equilibration and Temperature Control: Cells were placed in a water bath at 34°C, allowing the stratum corneum to reach a stable temperature of 32°C. Parafilm® was used to cover the side arm to prevent evaporation. Sample Collection and Analysis: Formulations were applied in either infinite or finite dose conditions. Samples were withdrawn at predetermined intervals from the receptor compartment and analysed using HPLC without dilution. The procedure was replicated a minimum of five times per vehicle. Documentation: The stages of the permeation study, including the setup and sample collection, are depicted in Figure 4.4 for clarity and reference.

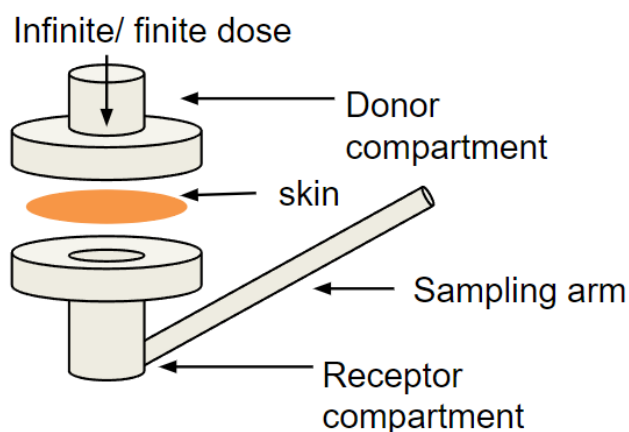


Figure 4.4: Franz cell structure schematic

#### 4.3.2.3 Porcine skin *in vitro* permeation study

Porcine tissue was obtained from a local abattoir and prepared on the day of slaughter. The porcine ear skin was separated from the cartilage at room temperature. The skin was then separated carefully with the help of a scalpel and tweezers. Prior to dissection, the ears were gently cleansed with distilled water to remove extraneous matter, and excess hairs were trimmed with precision. An incision was carefully made circumferentially, maintaining a 5 mm margin from the ear's edge, to separate the skin from the cartilage without compromising the integrity of the dermal layer. Secondly, the dissected skin was promptly arranged on sterile aluminium foil, encased in polyethylene bags, and stored at a temperature of -20°C to prevent degradation. This step ensures

the preservation of the tissue's histological and biochemical characteristics, which are crucial for accurate permeation studies. Thirdly, once the porcine skin was required for experimentation, it was thawed and tailored into circular sections congruent with the dimensions of the Franz diffusion cells. This procedure was executed with care to avoid any deformation of the tissue's structure. Finally, with the aid of a scalpel, the epidermis was carefully separated from the cartilage by making gentle incisions through the connective tissue. Both sides of the epidermis were then subjected to a thorough wash under deionized water. Post-cleaning, the skin was floated onto an aluminium foil substrate, where it was immediately utilized for permeation assays. The detailed steps undertaken in the preparation of the porcine ear skin for drug permeation studies are graphically depicted in Figure 4.5.

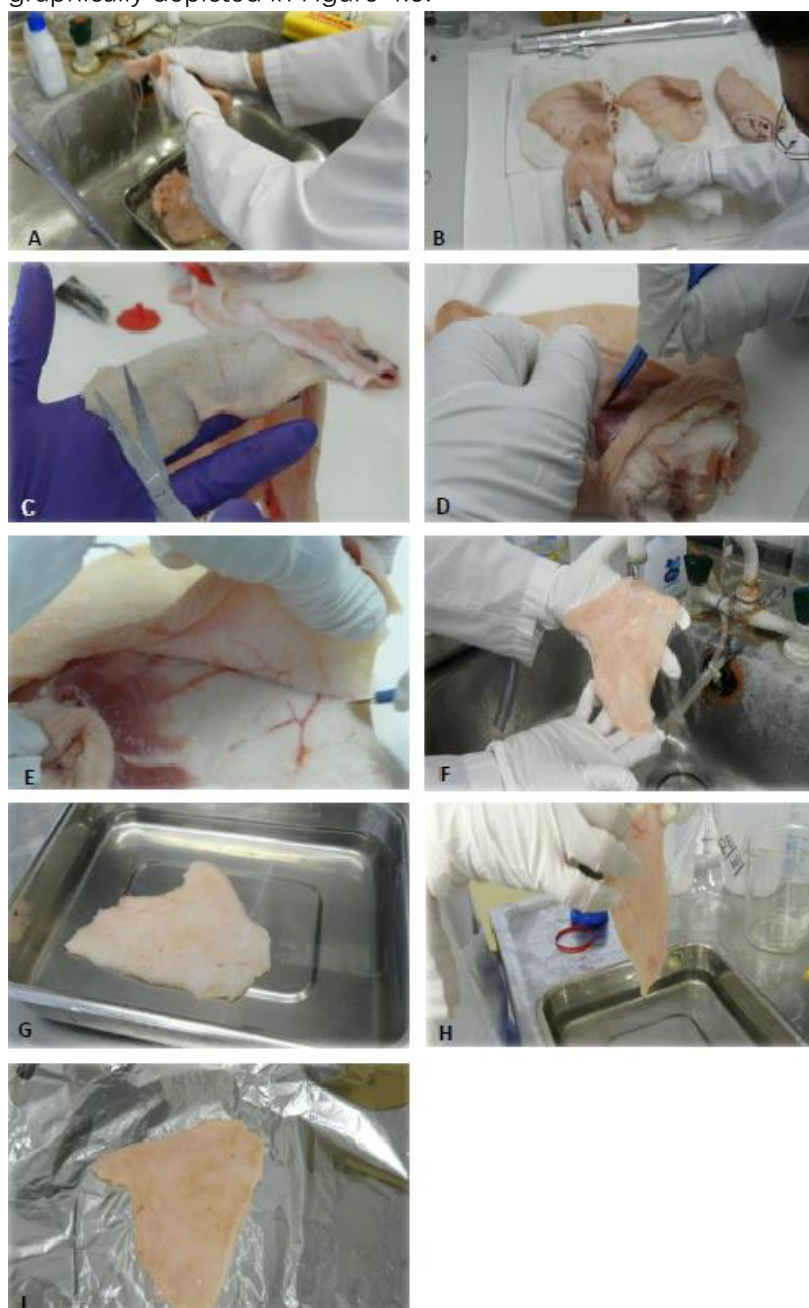


Figure 4.5: The preparation stages of porcine ear skin. A: cleaning; B: drying; C: cutting hair; D&E: separating; F: washing; G: floating in deionized water; H: removing from water; I: spreading the prepared skin on aluminium foil.

#### 4.3.2.4 Human skin *in vitro* permeation study

Abdominal human skin from a Caucasian female donor following plastic surgery was obtained from a tissue bank with institutional ethical approval (Research Ethics Committee reference 07/H1306/98). The preparation of the human epidermis for permeation studies was conducted using the heat separation technique, as delineated by Kligman and Christophers (1963). The following protocol was adhered to ensure the reproducibility and integrity of the epidermal samples: Initial Preparation: Human skin, was placed dermis-side down on a cork plate. Any excess subcutaneous tissue was carefully removed using a scalpel to facilitate uniform heat transfer during the separation process. Heat Separation Technique: Distilled water was preheated to approximately 65°C. Constant stirring was employed to ensure a uniform temperature distribution until the water attained a stable temperature of 60°C. Using forceps, the skin was then submerged in the heated water and gently agitated for precisely 45 seconds. Epidermal Layer Separation: Following the heat treatment, the skin was repositioned on the cork plate, with the dermis facing downwards. The edges of the skin were gripped using forceps, and the epidermis was carefully detached by rubbing and peeling from the edges towards the centre, ensuring the skin remained taut to prevent tearing. Cleansing and Storage: The separated epidermis was floated epidermal side up in a basin filled with deionized water to remove any remaining debris. To facilitate handling, a filter paper (Whatman grade No.1, UK) was placed beneath the epidermis, which was then lifted and transferred onto a fresh piece of filter paper to dry. The prepared epidermis was covered with an additional filter paper, wrapped in aluminium foil, and stored at -20°C (Swarbrick et al., 1982; Harrison et al., 1984). Mounting for Permeation Studies: On the day of the permeation experiments, the frozen epidermis was thawed and excised into circular sections using a stainless-steel punch. The epidermal disks were then carefully mounted between the donor and receptor chambers of the Franz diffusion cells, ensuring proper orientation and fit.

#### 4.3.2.4 Mass balance studies

After finite or infinite dose permeation experiments a mass balance study was conducted to account for the applied dose as shown in Figure 4.6. When the final sample of receptor fluid was removed, the remaining receptor fluid was discarded. Using 50 % (v/v) methanol in water the surface of the membrane was washed with three consecutive 1 ml volumes. Each wash was transferred to a 2 ml centrifuge tube. After the washing procedure the Franz cells were disassembled, and each membrane was placed into a centrifuge tube. 1 ml of methanol 50 % (v/v) was added to serve as the extraction solvent. Tubes for extraction were sealed with Parafilm™ and placed in a shaking incubator for 12 h at 32 ± 1°C. Samples obtained from washes and extractions were centrifuged at 13,200 rpm for 15 min at 32°C. 200 µl aliquots of the supernatant were analysed for drug content using HPLC.

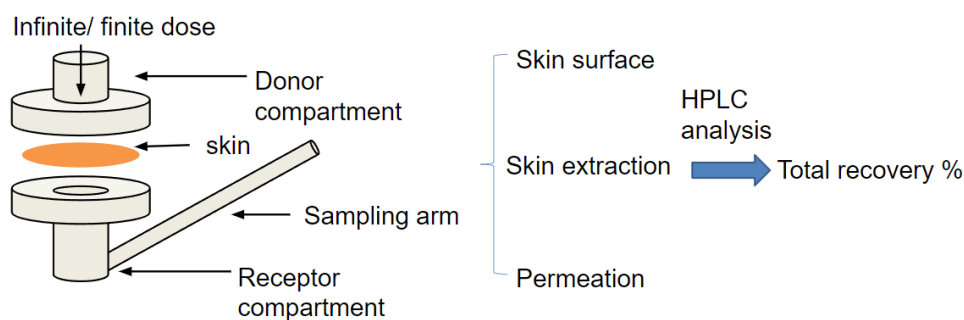


Figure 4.6 Schematic diagram showing mass balance study stages.

#### 4.3.2.5 Preparation of gel

In the preparation phase of the gel formulation, the process commences with the dissolution of active ingredients within a candidate multi-solvent, subsequently introducing this solution into the mixing vessel. Carbopol ETD 2020 is chosen for gel formulation due to its exceptional thickening and gel-forming capabilities, allowing for the creation of stable and homogeneous gel products. Its biocompatibility, stability, and ability to control release rates of active ingredients make it ideal for pharmaceutical and cosmetic applications. Furthermore, Carbopol ETD 2020 is easy to process and can be dispersed and mixed into various solvents, facilitating the production of high-quality gel formulations. Following this, a 1% w/w concentration of Carbopol ETD 2020 was dispersed into the base fluid. Utilizing a magnetic stirrer, a significant vortex was generated to amalgamate the powder and liquid efficiently, ensuring rapid and homogeneous mixing. Following the initial amalgamation, the mixture was propelled through the slots of the mixer's work head, facilitating its re-entry into the main body of the mixture. This mechanism is instrumental in disintegrating any potential agglomerates, thereby enhancing the dispersion quality. The process is characterized by a vigorous circulation within the mixing vessel, orchestrated by the mixer. This dynamic movement ensures the continuous passage of the material through the work head. Such action is pivotal for gradually diminishing the particle size while augmenting the surface area exposed to the liquid medium, culminating in the efficient hydration of Carbopol. This step is crucial for achieving the desired gel consistency and homogeneity.

#### 4.3.2.6 Statistical analysis

IBM SPSS Statistics software (version 24) was used for statistical evaluation. For comparing results among varied groups, one way analysis of variance (ANOVA) was conducted as a parametric test. If the sample sizes of each compared group were the same, multiple comparisons between each individual group were performed by a post hoc Tukey test. If the sample sizes of each compared group were varied, the Scheffe test was used.

## 4.4 Results and Discussion

### 4.4.1 *In vitro* infinite dose permeation studies of 5-FU in porcine skin

To evaluate the efficacy of optimized formulations, 1% w/v 5-FU solutions were subjected to infinite dose conditions in permeation studies using porcine skin. Conventionally 5-FU is available in several strengths, including 1%, 2% and 5% solutions and 0.5%, 1% and 5% creams for topical use (Khan et al., 2014). Unfortunately, there is not as yet a precise target dose available that specifies the exact amount of 5-FU that needs to penetrate the skin to effectively treat skin cancer. Treatment protocols can vary based on factors such as the formulation, concentration of the drug, type and stage of skin cancer, and individual patient response. The selection of a 1% w/v concentration for the 5-FU formulations strikes a balance between solubility considerations and experimental practicality. Furthermore, at this concentration, the risk of potential adverse effects may be minimized during experimental trials. This concentration also facilitates a relevant comparison between different solvents in terms of their permeation enhancement potential. Pre-formulation solubility studies were conducted in various candidate solvents (detailed in Table 4.7), leading to the selection of five candidates, notably Propylene glycol (PG), Glycerol, PEG400, PEG200, and Transcutol® (TC) for *in vitro* infinite dose (50  $\mu$ L) permeation studies using Franz diffusion cells with porcine skin. These studies aimed to simulate the maximum saturation of the drug within the skin, a critical condition for assessing the upper limit of the formulation's delivery capability. The results of the mass balance studies conducted after permeation are shown in Figure 4.8.

Solvent	Solubility Parameter [(cal/cm <sup>3</sup> ) <sup>1/2</sup> ]	LogP	Solubility (mg/ml)
PG	14.07	-0.47	17.56 $\pm$ 0.38
Glycerol	17.14	-2.32	15.6 $\pm$ 0.64
PEG400	11.67	-4.8	35.26 $\pm$ 1
TC	10.62	-0.25	23.25 $\pm$ 0.12
PEG200	12.06	-1.18	36.39 $\pm$ 1.04

Table 4.7: Solubility of 5-FU in single solvent system at 32  $\pm$  1  $^{\circ}$ C (mean  $\pm$  SD; n = 3).

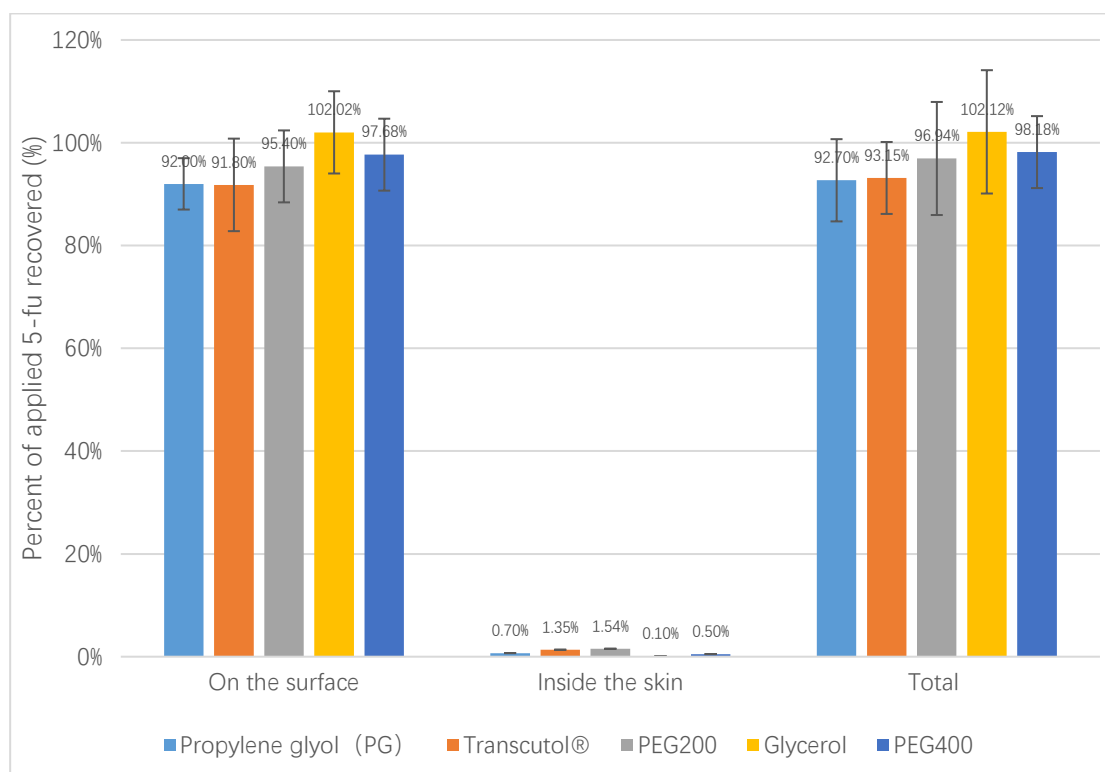


Figure 4.8 Infinite dose (50  $\mu$ l) mass balance studies of five tested formulations of 5-FU in Franz cells with porcine skin. Each data point represents the mean  $\pm$  SD, n=5.

The total recovery values of all five tested formulations were acceptable, with over 90% of the active ingredient remaining on the skin surface for all formulations. This further substantiates the stability of the drug within the solvents and affirms the suitability of the experimental design. After 24 hours, for the five tested systems, the drug did not permeate through porcine skin. None of the single-solvent formulations allowed more than 2% of 5-FU to penetrate the inner layers of the skin. Among the solvents tested, Propylene glycol (PG), Transcutol® (TC), and PEG200 showed a slightly higher internal skin drug concentration. These findings may reflect the stratum corneum's (SC) pronounced barrier effect against hydrophilic molecules like 5-FU, impeding their partitioning into this layer.

The SC is a heterogeneous membrane consisting of a mosaic of cornified cells containing crosslinked keratin filaments and intercellular lipid-containing regions. The aqueous protein bricks" refers to the protein-rich, water-retentive components of the stratum corneum, specifically the corneocytes. Corneocytes are the "bricks" in the "brick and mortar" model of the stratum corneum. These cells are filled with keratin, a type of protein, and retain water, giving them an aqueous characteristic. The intercellular lipids act as the "mortar," creating a barrier that regulates permeability and maintains skin hydration. In this context, 5-FU (5-fluorouracil) diffuses into these protein-filled corneocytes through transcellular pathways. However, for it to completely traverse the skin, it must move across the lipophilic mortar substance to another region of aqueous proteins (Phillips and Michniak, 1995). Hydrophilic molecules such as 5-FU have very low partitioning into lipophilic environments on the basis of thermodynamics, resulting in

the expected low permeation seen for 5-FU (Lee et al., 1999). Consequently, the permeation of 5-FU observed is low, suggesting that single solvent systems may not be ideal for the formulation of 5-FU. While porcine ear skin does share anatomical and physiological similarities with human skin, such as stratum corneum thickness, there are inherent differences. These differences underscore why human skin data is often more reliable for permeation studies in formulation development. After confirming the feasibility of permeation experiments in porcine ear skin, the next stage was *in vitro* infinite dose permeation studies of 5-FU on human skin (SC).

#### 4.4.2 *In vitro* infinite dose permeation studies of 5-FU in human skin (SC)

In this section, 1% w/v 5-fluorouracil solutions were applied on skin under infinite dose conditions in human skin permeation studies. Based on the results of infinite dose permeation studies of porcine skin, the PG, TC and PEG 200 vehicles were chosen to evaluate the effect of 5-FU concentration and the correlation between applied dose and permeation. Besides, based on the previous studies, the binary solvent system of PG and TC has been reported to significantly enhance the skin permeation of methadone compared to neat solvents. Specifically, the PG:TC (50:50) formulation showed a remarkably higher permeation of methadone through porcine skin (Kung et al., 2020). The binary system (PG+TC) also was tested in permeation studies with human skin. After 24 hours, the results of the mass balance studies conducted after permeation are shown in Figure 4.9.

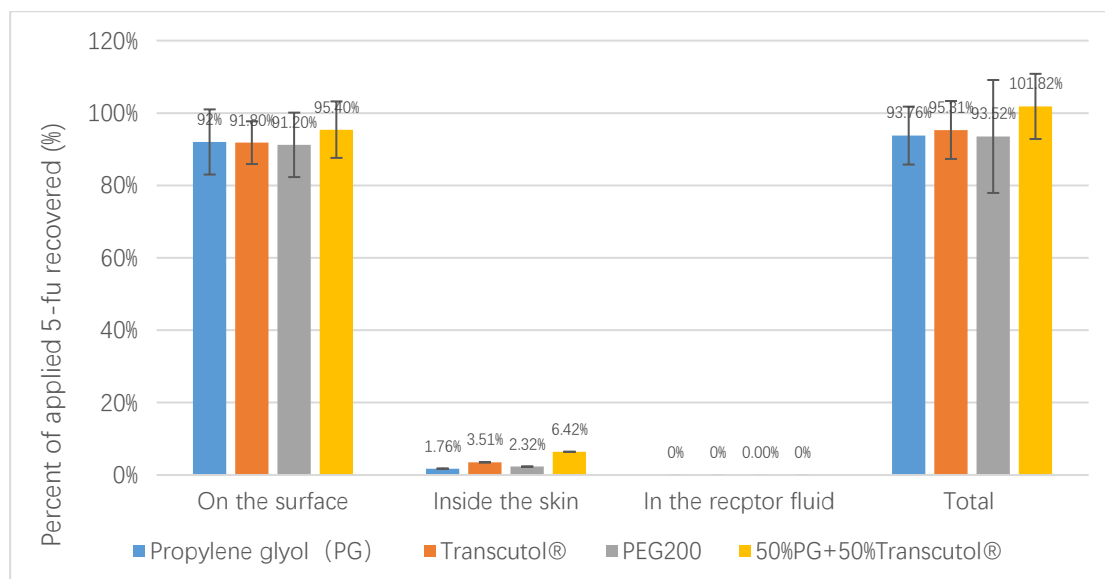


Figure 4.9. Mass balance results for 5-FU after 24 h infinite dose (50  $\mu$ l) permeation studies for 1% (w/v) 5-FU in PG, PEG200 and 50:50 v/v PG/TC with human skin (SC) at  $32 \pm 1^\circ\text{C}$  (mean  $\pm$  SD; n = 5).

The four tested systems did not promote permeation of the drug through human skin, which is the same as the result for porcine skin. The drug values inside the skin are higher than porcine skin which may be caused by the variations in lipid composition and

metabolic activities between human and porcine skin (Khial et al., 2019). Moreover, there is a significant increase inside the skin of the amount of 5-FU for binary systems (50%PG+50%TC) ( $p < 0.01$ ) with no permeation for the infinite dose (50  $\mu$ L) experiment with human skin. There was no significant difference in the results among these tested single formulations ( $p > 0.05$ ). Concerning the single solvents, some authors reported that pre-treatment of skin membranes with PG *in vitro* for 12 hours prior to the application of a solvent deposited dry drug film (100  $\mu$ L of a 0.3% solution in acetone: ethanol 1:1 v/v), has been shown to increase the penetration of 5-FU by 12-fold, compared with untreated skin (Goodman and Barry, 1989). With the finite dose technique, PG pre-treatment increased drug penetration. Additionally, PG may aid more drug to partition into the skin. The authors also suggested that the vehicles themselves, which are likely to disrupt lipid bilayers, were more effective with PG than with water vehicles. However, as a single vehicle, PG, is not a suitable vehicle for 5-FU.

Transcutol® is known to enhance drug solubilization, absorption rates, and retention within the skin by interacting with the hydrophilic head groups of stratum corneum structures, influencing the drug's partitioning and diffusion into the skin without disrupting the barrier physically. The principal mode of action of Transcutol® enhancement activity was attributed to the facilitation of drug partitioning and diffusion into skin (Harrison et al., 1996). Based on the previous researcher, the dependence of Transcutol® permeation on dilution with water or PBS can be explained in part by the high affinity of Transcutol® for water (Strusovskaya et al., 2019). In the absence of water, neat Transcutol® is likely attracted to the aqueous regions of the bilayers in the stratum corneum, becoming immobilized (retained), and in certain instances increasing the stratum corneum rigidity and reducing its permeability (Osborne and Musakhanian, 2018). It may help keep 5-FU in skin Instead of entering the circulatory system.

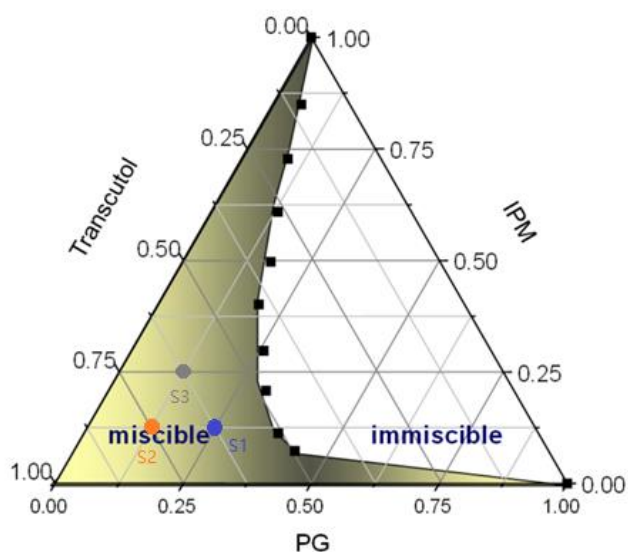
The solvents PG and Transcutol ® may both affect the aqueous domain by increasing the solubility for the permeant. The increased skin uptake of TC in the presence of PG reported previously suggests potential mechanisms behind this enhanced permeation. The study hypothesized that PG could interact with skin lipids, modifying their properties and thereby enhancing the permeability of both TC and IPA (Kung et al., 2020). Transcutol® can readily penetrate the stratum corneum and strongly interact with the water of the intercellular path to modify the skin permeation of the active pharmaceutical ingredient (Goodman and Barry, 1989, Osborne and Musakhanian, 2018, Hadgraft, 1999). However, in a study by Moghadam et al., PG did not influence the lamellar spacing of the SC membrane (Moghadam et al., 2013). Meanwhile, TC caused a reduced intensity of SAXS and WAXS peak patterns of SC lipid organisation. The authors suggested that PG influenced drug permeation by changing the drug solubility or partitioning in the SC and that TC increased membrane fluidity and caused slight disorder in the lamellar structure. If this is the case, TC may permeate through the skin in higher quantities than PG. The permeation of Transcutol® facilitates also the co-administration of other penetration enhancers known to disrupt (fluidize) epidermal lipid structure, i.e., decrease the skin barrier (Osborne and Musakhanian, 2018).



The combination of multiple solvents may also have potential for synergistic effects on skin delivery, especially when combining solvents with different mechanisms of penetration enhancement. The work of Kung and co-authors showed that the presence of PG in binary formulations increased not only the permeation of actives but also the skin uptake of TC in solvent uptake studies (Kung et al., 2020). Synergistic actions between propylene glycol and Transcutol® on the penetration enhancement of 5-FU were also observed in this experiment. The synergy between propylene glycol and Transcutol enhances 5-FU penetration through skin by disrupting the stratum corneum barrier, increasing drug solubility and thermodynamic activity, and promoting lipid fluidity, thereby facilitating deeper drug diffusion. Ternary systems need also to be considered in further experiments. Finite-dose studies reported that permeation enhancement was achieved by combining PG with lipophilic solvents such as isopropyl myristate (IPM). Moreover, neat IPM was found to be present in higher quantities in the skin and therefore, aided higher retention of the drug of interested anthramycin in the skin rather than permeation (Haque et al., 2017).

Considering the related references and miscibility study in chapter 3, IPM is added to ternary systems in future work. Three ternary solvents were selected from the miscibility studies of PG, TC and IPM, as shown in Figure 4.10. The results of the mass balance studies conducted after permeation for *in vitro* infinite dose permeation studies of 5-FU in human skin (SC) are shown in Figure 4.11.

- Solvent 1 (S1) = 25% PG+62.5% TC+12.5% IPM
- Solvent 2 (S2) = 12.5% PG+75% TC+12.5% IPM
- Solvent 3 (S3) = 12.5% PG+62.5% TC+25% IPM



Figur4.10: Ternary phase diagram of PG-TC-IPM. Three ratios of ternary solvents were selected as S1, S2 and S3.

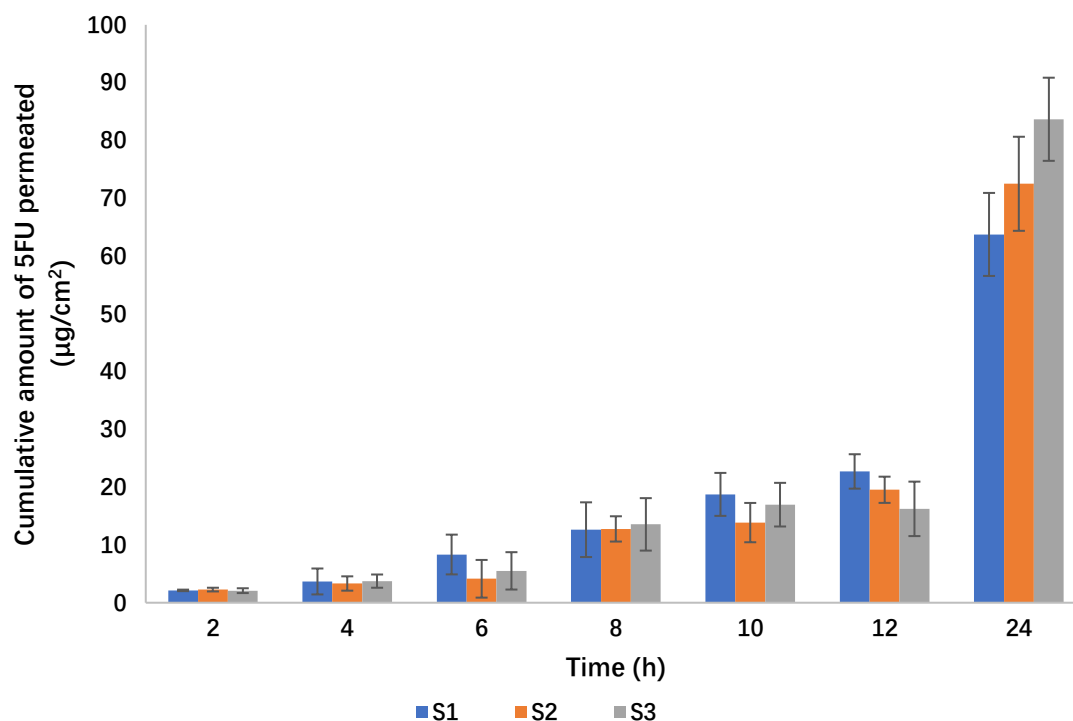


Figure 4.11: Comparison of permeation profiles of 5-FU through human skin after application of 1% (w/v) 5FU in S1, S2 and S3 for infinite dose (50 µl) at  $32 \pm 1^\circ\text{C}$ . Each data point represents the mean  $\pm$  SD (n = 5).

Considering the results shown in Figure 4.11, permeation was enhanced with increasing percent of IPM from PG/TC binary systems to PG/TC/IPM ternary systems ( $p < 0.01$ ). For the three solvents drug started to permeate at 2 hours. This suggests that the thermodynamic activity of 5-FU in the residual phase of the formulation and the effect of IPM play an important role in enhancing permeation. Moreover, the amount of drug inside the skin also was enhanced with increasing percent of IPM ( $p < 0.01$ ). One of the reasons could be isopropyl myristate (IPM) as a lipophilic penetration enhancer can induce disordering effects to the rigid SC lipid membranes (Eichner et al., 2017). This experiment was conducted as an infinite dose; therefore, the results cannot be related to *in-vivo* situations as the application dose was unrealistically large. Finite dose experiments are closer to clinical use wherein depletion of dose, evaporation of excipients, and gradual change in vehicle composition may occur (Arce Jr et al., 2020). Table 4.12 presents a summary comparison of the infinite dose mass balance profiles of 5-Fluorouracil (5-FU) through human skin using various solvent systems. The ternary solvents demonstrate potential for further development since the target for drug API delivery is within the epidermis, thus showing an ability to potentially breach the stratum corneum. In the case of infinite dosing, mono-solvent and binary solvent systems fail to facilitate drug delivery through the stratum corneum, and the same is true for finite dosing. The study demonstrates the potential benefits of using a combination of solvents, particularly with the inclusion of IPM, for topical drug delivery. The enhanced permeation seen with ternary systems, especially S3, indicates a promising direction for the formulation of topical agents where deep skin penetration is desired. These findings should be interpreted cautiously as infinite dosing does not reflect real-life application;

hence, the finite dosing results are more clinically relevant. Therefore, *in vitro* finite dose permeation studies of 5-FU in human skin (stratum corneum) will be explored.

Solvent	Receptor fluid	Inside the skin	Recovery
100% Propylene glycol (PG)	0	1.76%	93.76%
100% PEG200	0	2.32%	95.31%
100% Transcutol®	0	3.51%	93.52%
50%PG+50%TC	0	6.42%	101.82%
S1: 25%PG+62.5%TC+12.5%IPM	13%	4.79%	97.08%
S2: 12.5%PG+75%TC+12.5%IPM	14.49%	5.74%	99.49%
S3: 12.5%PG+62.5%TC+25%IPM	16.73%	7.62%	95.51%

Table 4.12 Mass balance studies of formulations in Franz cells with human skin (SC) with infinite dose(50µl). Each data point represents the mean  $\pm$  SD, n=5.

#### 4.4.3 *In vitro* finite dose permeation studies of 5-FU in human skin

Based on the same method, finite dose (10 µl) 1% 5-FU (V/W) ternary solutions were applied on human skin (SC) for permeation studies. The results of the finite dose ternary systems mass balance studies are shown in Figure 4.10. The comparison of permeation profiles is shown in Figure 4.13.

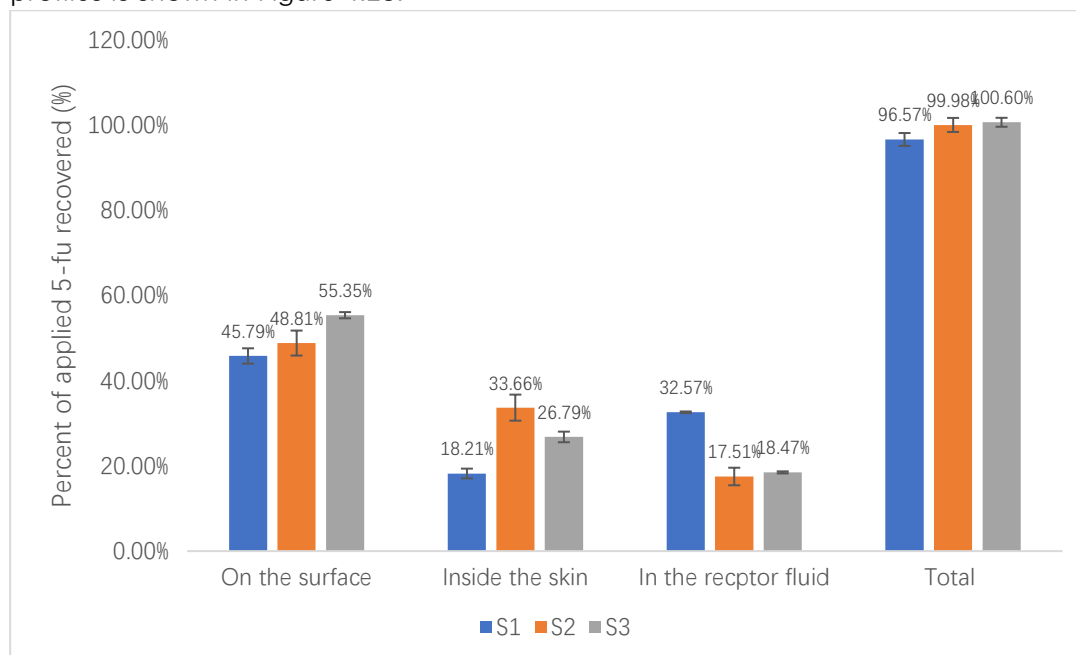


Figure 4.13. Mass balance results after 24 h finite dose (10 µl) permeation studies for 1% (w/v) 5-FU in ternary solvents S1, S2, S3 at 32  $\pm$  1°C (mean  $\pm$  SD; n = 5).

There is a significant portion of 5-FU remaining on the skin surface across all three solvent systems (S1, S2, and S3). S1 resulted in the highest amount remaining on the surface, while S3 deposited the lowest amount. The observation that S3 has the lowest amount of 5-FU remaining on the skin surface compared to S1 and S2 suggests that it may improve the penetration efficiency of the drug. This conclusion is supported by

considering the physicochemical properties of the solvents used in these ternary systems. Solvents with better solubility for 5-FU and optimised evaporation rates may facilitate more effective drug delivery across the stratum corneum, suggesting that the composition of S3 may be more conducive to 5-FU penetration, whereas S1 and S2 may either not solubilise 5-FU as effectively or evaporate more rapidly, leaving more drug on the skin surface. Secondly, the amount of 5-FU that penetrated inside the skin is considerably lower than on the surface for all solvents, with S2 showing the highest penetration, followed by S3, and then S1. This indicates that S2 might have the most suitable properties for facilitating 5-FU transport into the skin, possibly due to a balance between lipophilicity and solubility. As for the receptor fluid represents the amount of 5-FU that has successfully permeated through the skin. Here, S3 shows a significantly higher percentage, indicating that this solvent system might provide the best permeation for 5-FU. The low values for S1 and S2 suggest limited permeation through the skin barrier.

The total recovery of 5-FU is acceptable (>90%) that indicates the overall feasibility of the solvent system in delivering 5-FU through the skin. In a permeation study, if the formulation S1 results in around 30 µg of 5-FU being detected in the receptor medium, this indicates a significant penetration of 5-FU through the stratum corneum and into the dermal layer beneath. This further suggests that a considerable amount of 5-FU has successfully traversed the primary barrier of the skin and has the potential to enter the body's systemic circulation, which is not the experimental objective. S3 appears to be the most effective solvent system for the delivery of 5-FU through the skin in a finite dose model. S2, while not as effective as S3 in terms of total permeation, does show potential given its higher retention within the skin which may be beneficial for localized treatment. So, for the next stage of the work the development of S2 and S3 ternary solvent systems was prioritised.

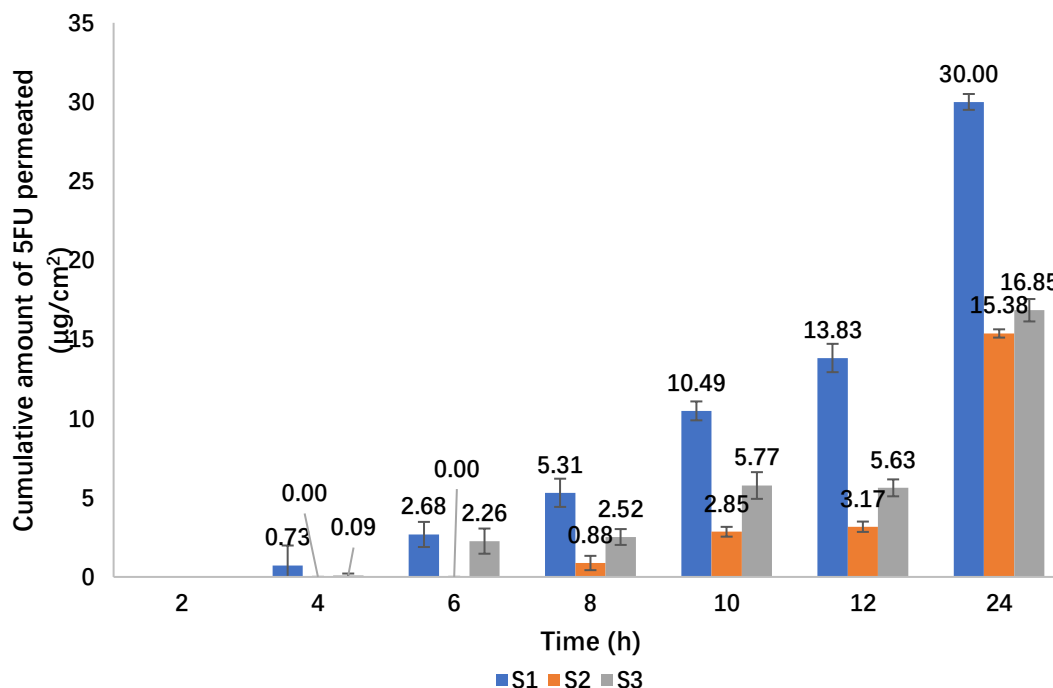


Figure 4.14. Comparison of permeation profiles of 5-FU through human skin (SC) after application of 1% (w/v) 5-FU in S1, S2 and S3 for finite dose (10 µl) at 32 ± 1°C. Each data point represents the mean ± SD (n = 5).

Figure 4.14 shows the cumulative amount of 5-FU that permeated through human skin over time, measured at 2, 4, 6, 8, 10, 12, and 24 hours after application. The study compares three different solvent systems labelled as S1, S2, and S3, with the application of a finite dose. All formulations start with no permeation at the 2-hour mark. By the 4-hour and 6-hour marks, there is a noticeable increase in permeation for all formulations. S3 continues to lead, suggesting it begins to act faster than S1 and S2. As time progresses, the cumulative amount of 5-FU permeated continued to increase for all solvent systems. S3 consistently showed a higher amount of drug permeation than S1 and S2 at each time point, which could indicate a more efficient penetration enhancement or a more favourable drug release profile. A substantial increase in permeation is observed at the 24-hour mark, particularly for S3 ( $p < 0.01$ ), which shows the highest cumulative permeation by a significant margin. S3 outperforms S1 and S2 at every measured time point, indicating it is the most effective of the three at facilitating the permeation of 5-FU. The trend suggests that the formulation of S3 may be more conducive to maintaining a sustained release of the drug, which is desirable for therapeutic effectiveness. The permeation profile of S3 suggests it could be a promising vehicle for transdermal delivery, possibly due to a higher concentration of penetration enhancers like IPM, or a more optimal balance of solvent components. The data also suggest that S3 could provide a more consistent and prolonged drug exposure, which is often necessary to maintain therapeutic levels of a medication.

In conclusion, the finite dose permeation study illustrates that S2 and S3 exhibit enhanced performance in the skin delivery of 5-FU, potentially offering a more effective and patient-centric therapeutic system. Further research is warranted, including the design of appropriate dosage forms. The formulation of Efudix 5% Cream, a prevalent product in the market, is summarized in Table 4.15. As discussed in Chapter 1, the excipients in Efudix 5% Cream play pivotal roles in its pharmaceutical attributes: Stearyl alcohol acts as an emulsion stabilizer, fragrance ingredient, surfactant/emulsifying agent, foam booster, and viscosity-increasing agent. White soft paraffin, also known as white petrolatum, functions as an occlusive moisturizer in topical applications, forming a protective barrier on the skin to impede moisture loss. Polysorbate 80, a non-ionic surfactant and emulsifier, is incorporated for its ability to stabilize emulsions. Propylene glycol is recognized for its solvent properties, serving as a humectant and enhancing the absorption of active ingredients into the skin. It is instrumental in dissolving other constituents in a formulation and facilitating the transdermal delivery of active drugs. Given these considerations, if S2 and S3 solvent systems are to be developed into a pharmaceutical form, they could potentially surpass the pharmaceutical performance of Efudix 5% Cream.

<b>Product Name</b>	Efudix 5% Cream
<b>Active Ingredient</b>	5% w/w fluorouracil
<b>Pharmaceutical Form</b>	White opaque cream
<b>Therapeutic Indications</b>	Topical treatment of superficial pre-malignant and malignant skin lesions
<b>Application Frequency</b>	Once or twice daily; occlusive dressing optional unless for malignant conditions
<b>Contraindications</b>	Hypersensitivity to fluorouracil or excipients; coadministration with certain antivirals
<b>Special Warnings</b>	Risk of severe inflammatory response; avoid use on impaired skin barriers
<b>Drug Interactions</b>	Possible interactions due to metabolism by DPD enzyme
<b>Pregnancy and Lactation</b>	Contraindicated during pregnancy and breastfeeding
<b>Side Effects</b>	Erythema, skin erosion, pain, blistering, systemic drug toxicity (rare)
<b>Pharmacokinetics</b>	Minimal systemic absorption through intact skin; increased with damaged skin or occlusion
<b>Preclinical Safety Data</b>	Genotoxic, embryotoxic, and teratogenic in animal studies
<b>Excipients</b>	Stearyl alcohol, white soft paraffin, polysorbate 60, propylene glycol, etc.
<b>Shelf Life</b>	60 months; 90 days after opening
<b>Storage</b>	Store below 30°C; do not dilute
<b>Packaging</b>	40g aluminium tubes
<b>Disposal</b>	Dispose of in accordance with local requirements
<b>Authorisation Holder</b>	Mylan Products Ltd.
<b>Authorisation Number</b>	PL 46302/0128
<b>First Authorisation Date</b>	22/07/2008
<b>Date of Revision</b>	April 2023

Table 4.15: This summarizes the key characteristics of Efudix 5% Cream

In the development of topical formulations for the delivery of 5-FU, the choice of an appropriate vehicle is pivotal in determining the efficacy, stability, and patient compliance. 5-FU is commonly used in cream form for the treatment of actinic keratosis,

with varying concentrations affecting both efficacy and the rate of adverse events (Kaur et al., 2010). Tolerability rates between formulations warrant further examination given the possible enhanced systemic absorption. Creams are generally preferred for their moisturizing effect, which can be beneficial for dry and scaly lesions. They may also provide a barrier that can enhance the absorption of the active ingredient. However, gels and lotions have their own advantages. Gels, being aqueous based, can be cooling upon application and may be preferred for their lighter texture and ease of application over larger areas. They can be absorbed quickly and typically do not leave residue on the skin. Lotions, on the other hand, are often preferred for treating large or hairy areas because they spread easily and can be less occlusive than creams, which some patients may find more comfortable.

Gel formulations, particularly those employing Carbopol® ETD 2020 as a gelling agent, have garnered attention as a potent delivery vehicle. This discussion delineates the rationale for selecting Carbopol ETD 2020 in the 5-FU ternary formulation, juxtaposed with conventional cream and lotion bases. First, Carbopol ETD 2020, a readily dispersible cross-linked polyacrylic acid copolymer, offers notable advantages in the formulation process due to its low dispersion viscosity prior to neutralization, which enables a lump-free gel preparation. This characteristic ensures the homogeneous distribution of 5-FU within the gel matrix—essential for uniform drug delivery. Second, post-neutralization, Carbopol ETD 2020 polymers demonstrate exceptional thickening properties, integral for attaining the requisite rheology for topical application. The gel thus formed can sustain a stable suspension of 5-FU, obviating drug sedimentation, which is vital for consistent application and dosage. Moreover, Carbopol ETD 2020 stability across various environmental stressors, including thermal and freeze-thaw cycles, underlines its appropriateness for 5-FU formulations. Maintaining the formulation's stability is crucial for preserving the chemical integrity and therapeutic efficacy of 5-FU during storage and application. The polymer's compatibility with electrolytic systems and various surfactants enhances its versatility as a gelling agent for 5-FU, which may encompass diverse ionic components due to the nature of the active pharmaceutical ingredient (API) or other formulation constituents. Gels, predominantly aqueous, enhance the penetration of hydrophilic drugs like 5-FU compared to the occlusive nature of creams and lotions. This penetration is critical for 5-FU to effectively reach its target within the skin. Gels, being non-greasy, do not occlude the skin. This attribute is beneficial for treating lesions where occlusion may aggravate the condition. The absence of post-application residue can also foster patient compliance, a pivotal factor in the efficacy of topical treatments. The alcohol content in gels can impart a drying effect, advantageous for lesions necessitating desiccation. Additionally, the evaporative quality of gels provides a cooling sensation upon application, which can alleviate symptoms for inflamed or irritated skin conditions often associated with 5-FU treatment. Gels are favoured for their aesthetic qualities, offering a transparent and clean application. This contrasts with creams and lotions that may leave a noticeable film on the skin, potentially discouraging regular use, especially during the day or on visible skin areas.

In conclusion, incorporating Carbopol® ETD 2020 polymer into a 5-FU gel formulation should potentially result in numerous benefits, including enhanced drug penetration, patient compliance owing to the cosmetic elegance of gels, and the polymer's contribution to chemical stability. Carbopol® ETD 2020's composition as a cross-linked polyacrylic acid polymer, combined with its easy dispersibility, makes it a valuable ingredient for creating a wide range of products with improved texture, stability and ease of processing. Future research should endeavour to quantify these advantages in clinical scenarios, contrasting the therapeutic efficacy of gel-based 5-FU formulations with traditional cream and lotion vehicles. The ultimate objective is to optimize the therapeutic effectiveness of 5-FU and improve the quality of life for patients undergoing treatment for skin conditions susceptible to 5-FU therapy.

Formulation	Drug concentration (w/v)	Amount of formulation applied (μL)	Amount of 5-FU in the skin (μg)
S2- Carbopol® ETD 2020	1%	10	20.59
S3- Carbopol® ETD 2020	1%	10	12.28
Efudix 5% Cream	5%	10	13.94

Table 4.16: Formulation composition.

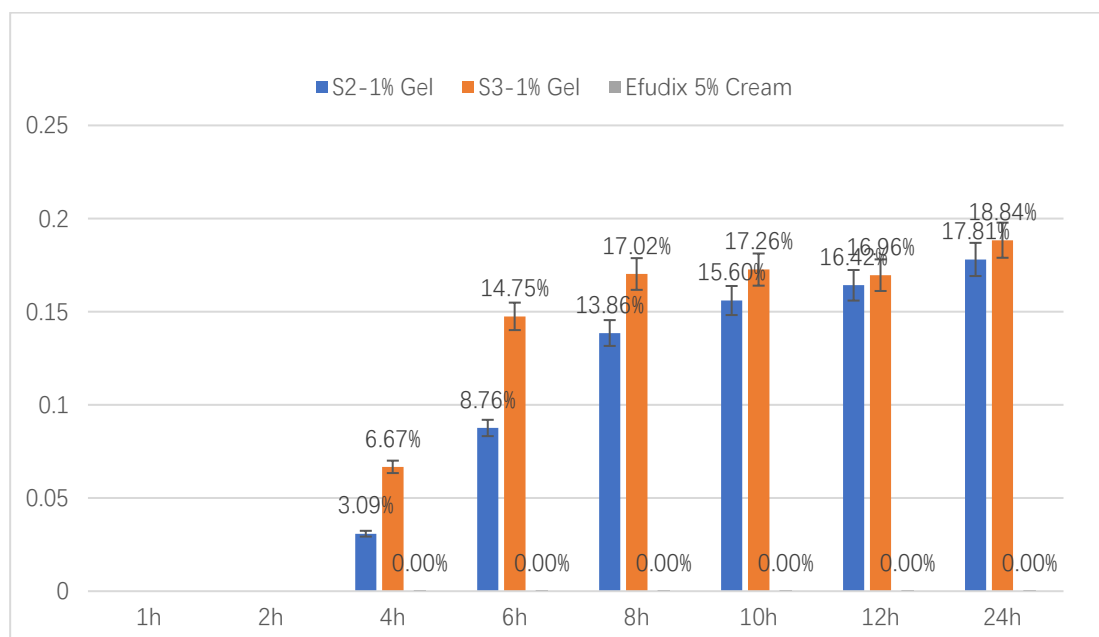


Figure 4.17. Comparison of permeation profiles of 5-FU through human skin (SC) after application of 1% (w/v) 5-FU in S2 and S3 Carbopol® ETD 2020 gels and Efudix 5% Cream for finite dose (10 μL) at 32 ± 1°C. The y-axis represents the percentage of total drug quantity of different formulations. Each data point represents the mean ± SD (n = 5).



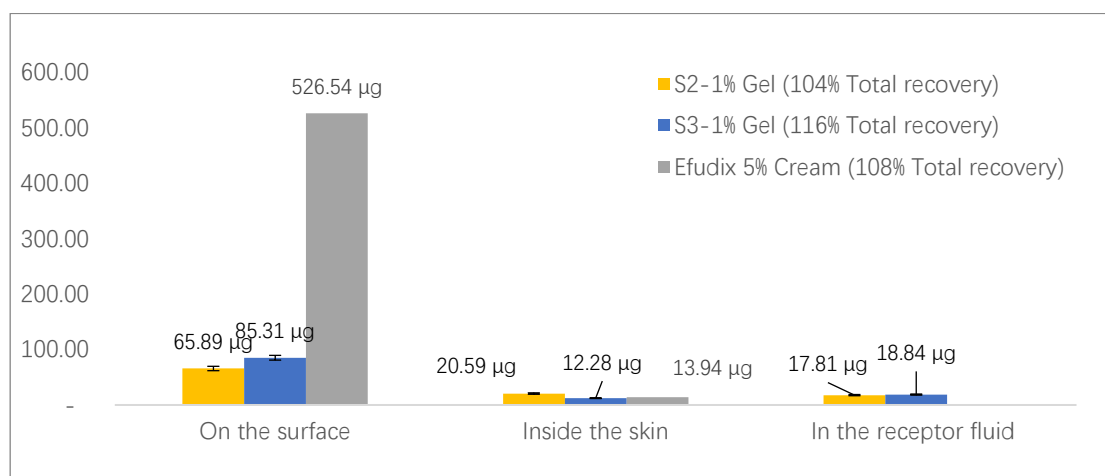


Figure 4.18. Mass balance results after 24 h finite dose (10 µl) permeation studies for 1% (w/v) 5-FU in ternary solvents S2 and S3 Carbopol® ETD 2020 gels and Efudix 5% Cream at 32 ± 1°C (mean ± SD; n = 5).

The experimental investigation into the transdermal delivery efficiency of the gel formulations of S2 and S3, compared to the market available Efudix 5% Cream, revealed significant findings. Despite the lower concentration of 5-FU in S2 and S3 (1% w/v) compared to Efudix Cream (5% w/v), S2 demonstrated superior cutaneous drug retention, with 20.59 µg of 5-FU remaining on the skin. This retention was notably higher than that observed with S3 (12.28 µg) and Efudix Cream (13.94 µg), suggesting an enhanced potential for S2 in facilitating localized treatment effectiveness with reduced systemic exposure risk. Efudix Cream's lack of significant skin penetration, despite its higher 5-FU concentration, might be attributed to its occlusive base or other factors in its formulation. In contrast, S2's formulation not only retained a greater quantity of the drug on the skin but also exhibited reduced transdermal permeation. This characteristic may prove beneficial in clinical scenarios that necessitate high local drug concentrations without substantial systemic absorption. The comparative analysis emphasizes that a higher drug concentration does not necessarily equate to better skin penetration and retention, as exemplified by the performance of S2 over Efudix Cream. The implication is that S2 could offer a more precise and localized drug delivery mechanism, minimizing systemic toxicity—a critical consideration for drugs like 5-FU, which are associated with systemic side effects. These outcomes position S2 as a promising candidate for further development in topical drug application. Future research should concentrate on refining S2's formulation to optimize drug release and retention. The total recovery of applied 5-FU is highest for the S2-1% Gel (116.43%), indicating that not only is the formulation effective at retaining the drug on and inside the skin, but it may also exhibit some degree of accumulation or less evaporation. The S3-1% Gel shows a lower total recovery (104.29%) than S2, which could be due to different release dynamics or a higher degree of drug absorption into the skin that was not accounted for in the "inside the skin" measurement. Additionally, clinical trials are imperative to evaluate the therapeutic efficacy and safety of the S2 gel formulation relative to conventional treatments, such as Efudix Cream. In conclusion, the gel-based S2 formulation demonstrates potential as an advantageous alternative for topical 5-FU delivery, warranting extensive research to substantiate its clinical benefits over traditional cream-based therapies.

## 4.5 Conclusion

This chapter has reported a thorough comparative analysis of the skin delivery profiles of two innovative Carbopol® ETD 2020 gel formulations, S2 and S3, the established Efudix 5% Cream. The data show that the ternary solvent systems, particularly those incorporating Isopropyl Myristate (IPM), markedly improve the permeation of 5-FU through human skin relative to mono-solvent and binary solvent systems. The escalating permeation concomitant with increasing IPM concentrations indicates that IPM, owing to its lipophilic nature, substantially disrupts the lipid membranes of the stratum corneum (SC), thereby enhancing drug penetration. The incorporation of IPM amplifies the thermodynamic activity of 5-FU in the formulation's residual phase, which is pivotal in augmenting both permeation and retention of the drug within the skin. Additionally, IPM's capacity to induce disorder in the SC's lipid structure is critical for deeper drug penetration. The roles of Propylene Glycol (PG) and Transcutol (TC) within the ternary solvent system are significant. PG, serving as a humectant and solvent, bolsters the solubility of 5-FU, potentially aiding in its stabilization and bioavailability at the SC. Conversely, Transcutol acts as a solubilizer and penetration enhancer, potentiating the permeation of 5-FU by modulating the skin's barrier properties. Permeation and mass balance studies reveal that the gel formulations, S2 in particular, exhibit enhanced drug retention and permeation when compared to conventional cream formulations. S2's superior retention of 5-FU in the skin suggests a potential increase in localized therapeutic efficacy and a reduction in systemic exposure.

The promising characteristics of S2, delineated by its controlled release and increased drug availability, emphasize the critical role of the formulation matrix in the drug's delivery efficiency. These insights suggest the advancement and fine-tuning of the S2 gel formulation. Subsequent research should concentrate on the kinetic profiles of drug release and skin absorption, with a focus on potential clinical applications. The overarching aim is to optimise the efficacy of topical treatments, thereby improving patient adherence and enhancing the quality of life for those requiring localized drug administration.

## Chapter 5 Conclusions and future work

### 5.1 Conclusions

To improve the efficacy and drug delivery performance of topical anticancer drugs, it is essential to understand the structure and function of the skin. The skin acts as a defence against various external threats, and its layers (epidermis, dermis, and subcutaneous tissue) each have specific roles in this protective function. Skin penetration mechanisms are crucial for effective topical therapies, involving routes of transdermal absorption and governed by physicochemical principles. Passive penetration enhancement strategies, along with factors like partition coefficients, molecular size, and drug ionization, significantly influence drug permeation. The current global incidence of skin cancer, including melanoma and non-melanoma, highlights the need for effective treatments. Among these, 5-fluorouracil (5-FU) is a primary focus due to its history, mechanism of action, indications, and side effects. Improved formulations of 5-FU are necessary to increase efficacy and minimize adverse effects. Berberine's potential in topical anticancer and anti-inflammatory therapy, as well as its synergy with 5-FU, is promising. Studies show that combining berberine with chemotherapeutic agents can enhance therapeutic outcomes. This thesis underscores the role of the skin in drug delivery, the challenges of localized cancer therapy, and the potential for combining 5-FU with natural compounds like berberine to enhance treatment efficacy. The comprehensive study as described below confirms the synergistic effect of berberine chloride and 5-fluorouracil (5-FU) against non-melanoma skin cancer cells. Using the commonly employed A431 and A375 cell lines, representing squamous cell carcinoma and malignant melanoma respectively, cell proliferation and migration were inhibited following treatment with berberine chloride and 5-FU. The  $IC_{50}$  values indicated that A431 cells were highly sensitive to these two compounds, with 0.5  $\mu$ M for 5-FU and 4  $\mu$ M for berberine at 72 h. The combination of berberine and 5-FU had a strong anticancer effect, especially on the A431 cell line. Calcsyn software analysis showed that combination of the two actives showed synergistic effects, suggesting that berberine chloride could enhance the anticancer effect of 5-FU and facilitate investigation of the optimal ratio of drug combinations. Subsequent RNA-seq analysis further elucidated this effect, revealing that a number of gene ontologies were significantly regulated under the combination regimen. The molecular and genetic response to the combination therapy was studied in detail. This included the sequencing of 12 samples with high average mapping ratios to the reference genome and the identification of a large number of genes.

The analysis aimed to identify the activation or inhibition of pathways and the involvement of different molecular targets to provide a comprehensive understanding of the synergistic effects and their underlying mechanisms. The JAK-STAT pathway showed a trend towards inhibition in the 5-FU-treated group, which was further enhanced in the combination-treated group. Combined treatment with berberine and 5-FU had a greater effect on inhibiting the JAK-STAT pathway than treatment alone. In addition, the expression of CSF3 (colony stimulating factor 3) was significantly suppressed by the combination treatment. CSF3 plays a critical role in tumour growth and metastasis, and

inhibition of CSF3 may help suppress tumour proliferation and spread. These results provide preliminary evidence for the synergistic effect of berberine and 5-FU in inhibiting tumour growth.

Following studies of the stability and solubility of berberine chloride and 5-FU, a solid basis for formulation design was developed. Preliminary results suggest that this is a promising avenue for advancing therapeutic strategies for non-melanoma skin cancer. To further explore the possibility of applying this approach to topical formulations, quantitative analysis using high performance liquid chromatography (HPLC) was developed and conducted. These analytical techniques are essential for the accurate and synergistic identification of the concentration of the compounds, allowing a more precise elucidation of their efficacy and the development of novel anti-melanoma formulations for topical application.

Therefore, two new HPLC analytical methods have been developed for the accurate quantification of 5-FU and berberine hydrochloride to facilitate subsequent studies. The solubility and stability of 5-Fluorouracil (5-FU) as the main drug was investigated in several commonly used commercial solvents. Solubility is significantly influenced by a number of factors, including the intrinsic chemical structures and properties of solutes and solvents, as well as the intermolecular interactions between them. Solubility in different solvents at a temperature of  $32 \pm 1^\circ\text{C}$  was conducted for Propylene glycol (PG), glycerol, polyethylene glycol (PEG) 200/400 and Transcutol® (TC) and are the solvents in which 5-FU has a high solubility and all solvents show a high degree of stability for the drug.

A detailed study of the high solubility solvents listed indicates that the polarity and hydrogen bonding ability of the solvent are the main factors regulating the solubility dynamics. 5-FU has a molecular structure that contains functional groups such as fluorine atoms and carbonyl groups, which give it its polarity and hydrogen bonding ability. This molecular structure is harmoniously matched in solvents such as propylene glycol (PG), glycerol and polyethylene glycol 200 (PEG200) and polyethylene glycol 400 (PEG400), which are polar and capable of hydrogen bonding. The properties of these solvents create favourable intermolecular interactions with 5-FU and enhance its solubility. Transcutol® and propylene glycol (PG) were selected for use in 5-FU formulations because of the advantages they offered in previous literature for enhancing drug penetration in the skin. Further solubility studies were carried out in binary and ternary solvent systems. Solubility studies in binary and ternary solvent systems further elucidated the effect of solvent composition on 5-FU solubility. Interestingly, the solubility of 5-FU did not change significantly with the ratio of PG to TC, suggesting that these solvents have comparable solubility for 5-FU. However, an increase in the concentration of IPM in the ternary system resulted in a decrease in the solubility of 5-FU, which could be attributed to the hydrophobicity of IPM reducing the solubility of 5-FU.

These studies provide a number of directions to take forward for the development of effective and reliable 5-FU formulations and pave the way for further exploration of drug solubility and delivery systems. Building on the foundation laid by the development of

solubility and analytical methods, subsequent chapters addressed permeation studies of topical formulations to advance pharmaceutical science and therapeutic applications, including appropriate dosage forms such as creams, lotions or gels.

The development of topical formulations containing 5-fluorouracil (5-FU) and the evaluation of their permeation and retention properties were conducted using *in vitro* infinite and finite dose permeation studies of 1 (w/v) % 5-FU in porcine and human skin. After confirming the feasibility of the porcine ear skin permeation experiments, the next step was the *in vitro* infinite dose permeation study of 5-FU in human skin (SC), and the finite dose study was initiated after the infinite dose (50 µl) permeation study. The *in vitro* permeation study was performed using Franz diffusion cells for five candidate solvents, propylene glycol (PG), glycerol, PEG400, PEG200 and Transcutol® (TC). The overall recovery values of all five solution formulations tested were satisfactory, confirming the stability of the drugs in the solvents and confirming the appropriateness of the experimental design. After 24 hours, none of the drugs from the five systems tested permeated through porcine skin. Slightly higher intradermal drug concentrations were found for propylene glycol (PG), Transcutol® (TC) and PEG200. These findings may reflect a more pronounced barrier effect of the stratum corneum (SC) to hydrophilic molecules such as 5-FU, preventing their entry into the stratum corneum.

Subsequently, the binary system (PG+TC) was also tested in human skin permeation studies, which showed a significant increase in the amount of 5-FU in the skin. The synergistic effect of propylene glycol and Transcutol® to enhance 5-FU penetration was demonstrated. Based on the previous studies in the literature where the combination of propylene glycol with isopropyl myristate (IPM) resulted in enhanced penetration, three ternary solvents with different concentration ratios were selected from the miscibility studies of PG, TC and IPM, from the binary system of PG/TC to the ternary system of PG/TC/IPM (S1,S2,S3), which showed enhanced drug penetration with increasing percentage of IPM. Drug penetration started after 2 hours for all three solvents.

The ternary solvents showed potential for further development. In an *in vitro* finite dose penetration study, a significant amount of 5-FU was left on the skin surface for all three solvent systems (S1, S2 and S3). S1 showed the highest amount of residue on the skin surface while S3 showed the lowest amount of residue. This may indicate that S3 has better drug penetration or that S1 and S2 have higher evaporation rates or lower solubility of 5-FU. Since S1 would allow an excessive amount of 5-FU to penetrate the receptor, it would increase the risk of 5-FU entering the human circulation, which is not desirable. In the finite dose model, S3 appears to be the most effective solvent system for delivery of 5-FU through the skin. S2, although not as effective as S3 in terms of overall penetration, shows potential due to higher drug retention within the skin, which may be beneficial for localized treatment. Therefore, the next phase of the work focused on the development of the ternary solvent systems S2 and S3. In addition, comparative experiments were carried out with popular topical formulations of 5-FU available on the market.

Analyses of commonly used formulations available on the market indicate that there are currently no topical formulation components designed to address the properties of

5-FU. If the S2 and S3 solvent systems are developed into pharmaceutical forms, they have the potential to exceed the pharmaceutical properties of the 5% Efudix cream in terms of medicinal properties. New solvent systems like S2 and S3 hold the promise of substantially enhancing 5-fluorouracil's (5-FU) solubility and stability, enabling higher drug concentrations to be achieved at the application site. Additionally, these systems can potentially facilitate targeted delivery of 5-FU to the epidermis, minimizing systemic absorption and ensuring that the drug's effects are concentrated locally. In addition, a gel formulation using Carbopol® ETD 2020 as a gelling agent was assessed as a potential delivery vehicle for the development of a topical formulation for the administration of 5-FU.

The results showed that the transdermal delivery efficiency of the S2 and S3 gel formulations showed a significant advantage over the commercially available 5% ETD cream. Although the concentration of 5-FU in S2 and S3 (1% w/v) was lower than that of Efudix cream (5% w/v), the drug retention in the skin was higher with S2, with 20.59 µg of 5-FU remaining in the skin. This retention amount was significantly higher than that of S3 (12.28 µg) and Efudix cream (13.94 µg), suggesting that S2 has greater potential to promote topical therapeutic efficacy and reduce the risk of systemic exposure ( $p < 0.05$ ). This means that S2 may provide a more precise, localized delivery mechanism that minimizes systemic toxicity - an important consideration for drugs with systemic side effects such as 5-FU. These results suggest the S2 gel as a promising candidate for further development in local drug delivery. Future studies should focus on improving the formulation of S2 to optimize drug release and retention. Overall, this is a comprehensive analysis of different formulations for the transdermal delivery of 5-FU, highlighting the potential of multi-solvent systems in enhancing drug permeation and retention.

## 5.2 Limitations of this work

First, 5-FU as a chemotherapeutic agents is a challenge for the testing of formulations in clinical trials. Although, the preliminary *in vitro* cell modelling experiments are promising, differences between *in vitro* experiments and *in vivo* studies significantly limit the broad applicability of the findings, especially in studies using human skin cancer cell lines. Due to the specific characteristics of A431 cells, such as their high sensitivity to mitogenic stimuli and their unusual response to different concentrations of EGF (promoting cell growth at low concentrations and inhibiting growth by inducing terminal differentiation at higher concentrations), results obtained from studies using these cells may not be fully representative of other types of non-melanoma skin cancer.

Primary cells are generally considered superior to cell lines like A431 for certain types of research due to their closer resemblance to *in vivo* conditions. However, issues such as misidentification, contamination, and genetic and phenotypic differences from their tissue origin complicate interpretation of data derived solely from them.

*In vivo* human studies are considered the 'gold standard' for studying the transdermal delivery of active ingredients, due to the fact that data from these studies provide the most accurate and reliable insights into how a drug or active ingredient is absorbed through the skin in real-life conditions. *In vivo* dermal absorption studies in human subjects allow for a comprehensive evaluation of topical and transdermal delivery systems, ensuring that the results are directly applicable to human health and treatment outcomes. But there are challenges in assessing the skin permeability of active ingredients and formulation components especially considering the safety of chemotherapeutic drugs. Specifically, challenges are likely to be encountered with participant recruitment, ethical approval and measurement sensitivity.

In cancer treatment, combination therapy is a common strategy involving the simultaneous or sequential use of different treatments to attack cancer cells. This approach can improve treatment efficacy, reduce the risk of drug resistance and potentially reduce side effects. However, this approach is still in the early stages of research, especially in certain types of cancer such as non-melanoma skin cancer. As for research into other forms of berberine salts as potential complementary ingredients, studies have mainly focused on berberine chloride and have not been able to fully explore its potential in cancer treatment. Due to resource and time constraints in the present work studies have been limited to the chloride salt. However, berberine has demonstrated a wide range of anticancer molecular targets, including p-53 activation, inhibition of invasion and metastasis, and modulation of reactive oxygen species. This limitation i.e. only use of the chloride salt, may have limited the exploration of berberine's full potential in cancer therapy.

For example, other researchers prepared four berberine salts by modifying berberine hydrochloride with the sodium salts of butyric, capric, octanoic and decanoic acids. The researchers tested the cytotoxicity of these salts against various cancer cell lines (B16-F10, A549, HepG2, U373) and investigated their mechanism of apoptosis induction by mitochondrial assay and Western blotting. These four berberine fatty acid salts

enhanced the inhibitory effects on the tested cancer cell lines, especially on B16-F10 cells. These salts also effectively inhibited cell migration and induced apoptosis via the mitochondrial pathway. Importantly, they inhibited tumour growth in an *in vivo* melanoma model without significant side effects (Xu et al., 2022).

In addition, in previous cellular experiments of this research, the ability of drugs to kill cancer cells was assessed using cytotoxicity as a means of evaluating anti-cancer effects. However, this method has limitations. Firstly, it is usually performed *in vitro* and may not fully reflect what happens *in vivo*. Secondly, cytotoxicity tests usually do not take into account the effects of the drug on normal cells. Therefore, relying solely on cytotoxicity to assess anticancer effects may not be sufficient to provide a complete picture of the true effects of treatment. In particular, the cytotoxicity results of primary keratinocytes are so variable that they are not statistically significant, demonstrating the inadequacy of single-cell modelling experiments (Finnegan et al., 2019).

Challenges to conducting clinical trials with 5-FU for novel topical uses include both regulatory and efficacy barriers. Common side effects of topical use in the clinic include mouth sores, loss of appetite, low blood counts, hair loss, skin irritation and sometimes direct irritation at the application site. Regulatory challenges revolve around the approval process and safety standards that novel chemotherapeutic agents such as 5-FU must meet. These include rigorous testing and demonstration of efficacy and safety in different patient populations, adherence to ethical guidelines and compliance with evolving regulatory policies. In addition, the efficacy of 5-FU varies widely in different tumour types. Non-coding RNAs can significantly influence patient response to 5-FU by interfering with oncogenic pathways, apoptosis, and autophagy. Regulation of microRNAs or long non-coding RNAs can affect a variety of biological signalling pathways, thereby increasing the sensitivity of tumour cells to 5-FU. In addition, the cytotoxic effects of 5-FU are mainly induced by inhibition of cellular thymidylate synthase, which leads to blockage of DNA replication and inhibition of RNA synthesis and integration of its metabolites into RNA (Ghafouri-Fard et al., 2021). Therefore, there is a need for targeted design of clinical trials in patients with non-melanoma skin cancer. There is also a need for an in-depth understanding of the drug's mechanism of action and safety, as well as an in-depth understanding of patient-specific response and the underlying molecular biology of 5-FU's interaction with cancer cells. There is also considerable evidence that 5-FU can harness the host immune system to prevent cancer progression, adding to the complexity of clinical trial design (Vincent et al., 2010). Currently, it is difficult to move reagents from the laboratory trial stage to further clinical validation.

Due to the difficulty of clinical trials, Raman spectroscopy, a commonly used tool to check the penetration of topical reagents, is not suitable for further use in 5-FU formulation development trials. Long-term studies on skin cancer treatment outcomes face recruitment and retention challenges, and skin biopsies complicate trials due to their invasiveness. Due to limited skin penetration depth, ethical concerns in testing on healthy volunteers, interference from biological tissues, and the complexity of skin composition. Raman spectroscopy, a type of vibrational spectroscopy, is an analytical



technique used for chemical analysis and material identification. It consists of shining a monochromatic light on a sample and analysing the scattered light. Most of the scattered light remains at the same wavelength (Rayleigh scattering), but a small proportion changes wavelength due to the Raman effect. This wavelength change is caused by the light interacting with molecular vibrations, rotations, and other low frequency modes in the system. The resulting Raman spectrum is like a molecular fingerprint, and molecules or materials can be identified by comparing the spectrum to a reference library. It can analyse samples for chemical composition and properties including crystallinity, polymorphism, impurities, and physical state. This makes it a versatile tool for qualitative and quantitative analysis in pharmaceutical formulation and quality control (Fu et al., 2021), including the analysis of skin penetration of topical drugs. This non-destructive, non-invasive optical detection technique shows great potential for real-time visualization and analysis of drug permeation dynamics. Raman spectroscopy allows real-time monitoring of drug distribution in the skin, even at high resolution down to 100 microns below the skin surface. It provides valuable information for understanding the chemical and structural properties of the skin and the physical distribution of its constituents. A further important area is differentiation of closely related chemical species. One of the key challenges is the ability to distinguish between closely related chemical species, such as a prodrug and its active form. Raman spectroscopy provides molecular fingerprints for substances, but accurately identifying and differentiating these in complex biological matrices like skin can be challenging. Confocal Raman microscopy allows for the non-destructive analysis of skin layers. However, accurately determining the concentration and distribution of the prodrug and drug at different skin depths involves intricate spectral analysis and comparisons. The presence of other substances in the skin, such as proteins, lipids, and water, can interfere with the Raman signals of the prodrug and drug. Minimizing and interpreting this interference requires careful spectral analysis. Distinguishing between the solution and crystalline states of 5FU in the skin using Raman spectroscopy adds another challenge. While Raman spectroscopy allows for *in situ* analysis without the need for external labels, it is limited by the depth of penetration and the resolution possible within the skin layers. These limitations might affect the utility of the data obtained. The results obtained from Raman spectroscopy often need to be validated by other standard methods such as histopathology or PCR, which can add complexity to the overall analysis in a clinical trial setting.

Rheological properties of pharmaceutical products in the context of drug formulations such as 5-fluorouracil (5-FU) topical formulations need to be understood. Most pharmaceutical products exhibit non-Newtonian properties, with viscosity varying with shear rate. Understanding and interpreting the rheological profiles of different types of materials is essential for the development of efficient topical formulations. Rheological testing methods can vary in robustness, sensitivity and specificity, and there may be no inherent linearity in the acquisition of rheological profiles, posing a challenge for method validation. This is an integral part of the microstructure equivalence documentation for topically applied semi-solid gel formulations.

However, the gel formulations discussed in this thesis may have stability and

homogeneity issues in the future after large-scale production, which may require higher standards for checking the formulations and create technical challenges for the development of gel formulations in advance. Confocal Raman spectroscopy measurements use specific wavelengths and require careful calibration. This demonstrates the complexity of the technology and the potential limitations in depth and accuracy of skin composition analysis. In terms of the penetration enhancement mechanism of formulations, compounds such as PG have been investigated, but the specific interactions between ingredients such as PG and TC in enhancing skin penetration still require more experimental investigations into the more specific nature of the principles underlying their mechanism of action.

In addition, tape stripping and trans-epidermal water loss (TEWL) measurements, which are commonly used in formulation development were not explored in this study. The tape stripping technique, although useful for investigating the distribution of 5-FU in the stratum corneum (SC), may be somewhat harmful to skin cancer patients who are already suffering from localized symptoms, and the experiment is labour intensive and operator dependent. This method requires sequential peeling of the outer layers of the skin, which can lead to inconsistent results during application and peeling.

The development and manufacture of topical formulations such as 5-FU presents particular challenges. Ultimately, comparisons with commercially available drugs, the differences in formulation and cost between the 5-FU formulations in this study and commercially available products limit the possibility of direct comparisons as also shown in this study, longer shelf-life stability testing, preservation of formulations that have been exposed to varying temperatures and light conditions still require further research and experimentation. In addition, there is a need to move from small-scale development to large-scale production of novel medicines. This scale-up is becoming increasingly challenging due to the need for larger batches for Good Laboratory Practice (GLP), animal studies and the rapid transition from small to medium or large-scale production.

### 5.3 Future work

In the field of academic research, the search for effective treatments for skin cancer, particularly with 5-fluorouracil (5-FU) and natural compounds such as berberine, represents a significant endeavour in modern pharmacology. Despite progress, there remains considerable scope for improvement and innovation, particularly in understanding the synergy between these compounds. A critical area of future research is to elucidate the regulatory mechanisms of JAK-STAT and CSF3 expression following combined treatment with berberine and 5-FU, as these pathways are central to tumour growth and metastasis. Understanding how combined therapy approaches may modulate these pathways could lead to more effective cancer treatments. In addition, functional experiments and *in vivo* studies are essential to validate the efficacy of combined berberine and 5-FU therapy. These studies should focus on the drugs' effects on tumour growth, apoptosis and metastasis in animal models, providing insights beyond the capabilities of *in vitro* studies. At the same time, protein validation experiments have the potential to provide deeper insights into the cellular mechanisms affected by cancer treatments. Detailed studies of how berberine and 5-FU affect protein expression in cancer cells are critical to understanding their therapeutic mechanisms, potentially including proteomic profiling and pathway analysis.

Given the variability in patient response to 5-FU, personalized medicine approaches are also a critical area for future research. Tailoring treatments based on individual immune responses and skin characteristics could significantly improve outcomes while minimizing side effects. In addition, technological advances, particularly in tools such as confocal Raman spectroscopy, are essential for molecular analysis. Future research efforts should focus on refining these technologies to increase their depth and accuracy, particularly in analysing skin composition and drug penetration. Exploring the combination of 5-FU with other natural compounds and different formulations of berberine offers promising treatment avenues. Investigating how these combinations can improve treatment efficacy while minimizing side effects could be groundbreaking. In addition, optimization of drug formulations and delivery systems is essential to improve local treatment strategies and reduce systemic side effects. Future studies should explore innovative formulation techniques and drug delivery systems, such as microencapsulation or nanoparticle-based delivery, to improve the efficacy of topical treatments.

The development of more advanced, less invasive techniques for skin permeation studies is essential to accurately assess drug delivery and efficacy. Techniques that offer greater precision and less discomfort will be integral to future research. Bridging the gap between *in vitro* studies and real-world applications remains a major challenge. The development of more representative *in vitro* models that closely mimic human skin conditions is an essential step towards this goal. These future research directions have the potential to significantly advance the field of skin pharmacology and transdermal drug delivery, particularly in cancer treatment. Addressing these areas promises considerable progress in improving patient outcomes and advancing therapeutic strategies against skin cancer.

## References:

1. Ackerman, A., & Mones, J. (2006). Solar (actinic) keratosis is squamous cell carcinoma. *British journal of Dermatology*, 155(1), 9-22.
2. Ai, X., Yu, P., Peng, L., Luo, L., Liu, J., Li, S., Lai, X., Luan, F., & Meng, X. (2021). Berberine: A review of its pharmacokinetics properties and therapeutic potentials in diverse vascular diseases. *Frontiers in pharmacology*, 12, 762654.
3. Albery, W. J., & Hadgraft, J. (1979). Percutaneous absorption: in vivo experiments. *Journal of Pharmacy and Pharmacology*, 31(1), 140-147.
4. Alexander, A., Dwivedi, S., Ajazuddin, Giri, T. K., Saraf, S., Saraf, S., & Tripathi, D. K. (2012). Approaches for breaking the barriers of drug permeation through transdermal drug delivery. *J Control Release*, 164(1), 26-40. <https://doi.org/10.1016/j.jconrel.2012.09.017>
5. Authority, E. F. S. (2023). *Protocol for the Scientific Opinion on the evaluation of the safety in use of plant preparations containing berberine* (2397-8325).
6. Beekman, R., & Touw, I. P. (2010). G-CSF and its receptor in myeloid malignancy. *Blood, The Journal of the American Society of Hematology*, 115(25), 5131-5136.
7. Benson, H. A. (2005). Transdermal drug delivery: penetration enhancement techniques. *Current drug delivery*, 2(1), 23-33.
8. Benson, H. A. E. (2011). Skin Structure, Function, and Permeation. In *Topical and Transdermal Drug Delivery* (pp. 1-22). <https://doi.org/https://doi.org/10.1002/9781118140505.ch1>
9. Berking, C., & Herlyn, M. (2001). Human skin reconstruct models: a new application for studies of melanocyte and melanoma biology. *Histol Histopathol*, 16(2), 669-674. <https://doi.org/10.14670/HH-16.669>
10. Bos, J. D., & Meinardi, M. M. (2000). The 500 Dalton rule for the skin penetration of chemical compounds and drugs. *Experimental Dermatology: Viewpoint*, 9(3), 165-169.
11. Boukamp, P., Petrussevska, R. T., Breitkreutz, D., Hornung, J., Markham, A., & Fusenig, N. E. (1988). Normal keratinization in a spontaneously immortalized aneuploid human keratinocyte cell line. *The Journal of cell biology*, 106(3), 761-771.
12. Burns, C., Kubicki, S., Nguyen, Q.-B., Aboul-Fettouh, N., Wilmas, K., Chen, O., Doan, H. Q., Silapunt, S., & Migden, M. (2022). Advances in Cutaneous Squamous Cell Carcinoma Management. *Cancers*, 14(15), 3653.
13. Candido, S., Rapisarda, V., Marconi, A., Malaponte, G., Bevelacqua, V., Gangemi, P., Scalisi, A., McCubrey, J. A., Maestro, R., & Spandidos, D. A. (2014). Analysis of the B-RafV600E mutation in cutaneous melanoma patients with occupational sun exposure. *Oncology reports*, 31(3), 1079-1082.
14. Casale, J., & Patel, P. (2022). Fluorouracil. In *StatPearls*. <https://www.ncbi.nlm.nih.gov/pubmed/31747215>
15. Ceilley, R. I. (2012). Mechanisms of action of topical 5-fluorouracil: review and implications for the treatment of dermatological disorders. *J Dermatolog Treat*, 23(2), 83-89. <https://doi.org/10.3109/09546634.2010.507704>
16. Chao, J., Dai, Y., Verpoorte, R., Lam, W., Cheng, Y.-C., Pao, L.-H., Zhang, W., & Chen, S. (2017). Major achievements of evidence-based traditional Chinese medicine in treating major diseases. *Biochemical pharmacology*, 139, 94-104.
17. Chen, W., Miao, Y.-Q., Fan, D.-J., Yang, S.-S., Lin, X., Meng, L.-K., & Tang, X. (2011). Bioavailability study of berberine and the enhancing effects of TPGS on intestinal absorption in rats. *Aaps Pharmscitech*, 12, 705-711.
18. Cichorek, M., Wachulska, M., Stasiewicz, A., & Tyminska, A. (2013). Skin melanocytes: biology and development. *Postepy Dermatol Alergol*, 30(1), 30-41.

<https://doi.org/10.5114/pdia.2013.33376>

19. Cockerell, C. J. (2000). Histopathology of incipient intraepidermal squamous cell carcinoma ("actinic keratosis"). *J Am Acad Dermatol*, 42(1 Pt 2), 11-17. <https://doi.org/10.1067/mjd.2000.103344>
20. Colombo, I., Sangiovanni, E., Maggio, R., Mattozzi, C., Zava, S., Corbett, Y., Fumagalli, M., Carlino, C., Corsetto, P. A., & Scaccabarozzi, D. (2017). HaCaT cells as a reliable in vitro differentiation model to dissect the inflammatory/repair response of human keratinocytes. *Mediators of inflammation*, 2017.
21. Crowther, J., Sieg, A., Blenkiron, P., Marcott, C., Matts, P., Kaczvinsky, J., & Rawlings, A. (2008). Measuring the effects of topical moisturizers on changes in stratum corneum thickness, water gradients and hydration in vivo. *British journal of Dermatology*, 159(3), 567-577.
22. Del Regno, L., Catapano, S., Di Stefani, A., Cappilli, S., & Peris, K. (2022). A review of existing therapies for actinic keratosis: current status and future directions. *American Journal of Clinical Dermatology*, 23(3), 339-352.
23. Dewick, P. M. (2002). *Medicinal natural products: a biosynthetic approach*. John Wiley & Sons.
24. Dodds, A., Chia, A., & Shumack, S. (2014). Actinic keratosis: rationale and management. *Dermatology and therapy*, 4(1), 11-31.
25. Dun, J., Chen, X., Gao, H., Zhang, Y., Zhang, H., & Zhang, Y. (2015). Resveratrol synergistically augments anti-tumor effect of 5-FU in vitro and in vivo by increasing S-phase arrest and tumor apoptosis. *Experimental Biology and Medicine*, 240(12), 1672-1681.
26. Elleson, K. M., DePalo, D. K., & Zager, J. S. (2022). An update on local and systemic therapies for nonmelanoma skin cancer. *Expert Review of Anticancer Therapy*, 22(5), 479-489.
27. Fania, L., Didona, D., Morese, R., Campana, I., Coco, V., Di Pietro, F. R., Ricci, F., Pallotta, S., Candi, E., & Abeni, D. (2020). Basal cell carcinoma: from pathophysiology to novel therapeutic approaches. *Biomedicines*, 8(11), 449.
28. Filingeri, D., & Havenith, G. (2015). Human skin wetness perception: psychophysical and neurophysiological bases. *Temperature (Austin)*, 2(1), 86-104. <https://doi.org/10.1080/23328940.2015.1008878>
29. Finnegan, A., Cho, R. J., Luu, A., Harirchian, P., Lee, J., Cheng, J. B., & Song, J. S. (2019). Single-cell transcriptomics reveals spatial and temporal turnover of keratinocyte differentiation regulators. *Frontiers in genetics*, 10, 775.
30. Flynn, G. L., & Stewart, B. (1988). Percutaneous drug penetration: choosing candidates for transdermal development. *Drug Development Research*, 13(2-3), 169-185.
31. Fondello, C., Agnetti, L., Villaverde, M. S., Simian, M., Glikin, G. C., & Finocchiaro, L. M. (2016). The combination of bleomycin with suicide or interferon- $\beta$  gene transfer is able to efficiently eliminate human melanoma tumor initiating cells. *Biomedicine & Pharmacotherapy*, 83, 290-301.
32. Fu, W., & Cockerell, C. J. (2003). The actinic (solar) keratosis: a 21st-century perspective. *Archives of dermatology*, 139(1), 66-70.
33. Fu, X., Zhong, L.-m., Cao, Y.-b., Chen, H., & Lu, F. (2021). Quantitative analysis of excipient dominated drug formulations by Raman spectroscopy combined with deep learning. *Analytical Methods*, 13(1), 64-68.
34. Ghafouri-Fard, S., Abak, A., Tondro Anamag, F., Shoorei, H., Fattahi, F., Javadinia, S. A., Basiri, A., & Taheri, M. (2021). 5-Fluorouracil: a narrative review on the role of regulatory mechanisms in driving resistance to this chemotherapeutic agent. *Frontiers in Oncology*, 1210.
35. GRANESS, A., HANKE, S., BOEHMER, F. D., PRESEK, P., & LIEBMANN, C. (2000). Protein-tyrosine-phosphatase-mediated epidermal growth factor (EGF) receptor transinactivation and EGF receptor-independent stimulation of mitogen-activated protein

- kinase by bradykinin in A431 cells. *Biochemical Journal*, 347(2), 441-447.
36. Green, P. G., & Hadgraft, J. (1987). Facilitated transfer of cationic drugs across a lipoidal membrane by oleic acid and lauric acid. *International journal of pharmaceuticals*, 37(3), 251-255.
  37. Gross, K., Kircik, L., & Kricorian, G. (2007). 5% 5-Fluorouracil cream for the treatment of small superficial Basal cell carcinoma: efficacy, tolerability, cosmetic outcome, and patient satisfaction. *Dermatologic surgery*, 33(4), 433-440.
  38. Gupta, A. K., Weiss, J. S., & Jorizzo, J. L. (2001). 5-fluorouracil 0.5% cream for multiple actinic or solar keratoses of the face and anterior scalp. *Skin Therapy Lett*, 6(9), 1-4. <https://www.ncbi.nlm.nih.gov/pubmed/11550079>
  39. Hadgraft, J., & Lane, M. E. (2005). Skin permeation: the years of enlightenment. *International journal of pharmaceuticals*, 305(1-2), 2-12.
  40. Hadgraft, J., & Lane, M. E. (2011). Skin: the ultimate interface. *Physical Chemistry Chemical Physics*, 13(12), 5215-5222.
  41. Hadgraft, J., & Valenta, C. (2000). pH, pKa and dermal delivery. *International journal of pharmaceuticals*, 200(2), 243-247.
  42. Haeberle, H., & Lumpkin, E. A. (2008). Merkel Cells in Somatosensation. *Chemosens Percept*, 1(2), 110-118. <https://doi.org/10.1007/s12078-008-9012-6>
  43. Hamm, C., Verma, S., Petrella, T., Bak, K., Charette, M., & Melanoma Disease Site Group of Cancer Care Ontario's Program in Evidence-based, C. (2008). Biochemotherapy for the treatment of metastatic malignant melanoma: a systematic review. *Cancer Treat Rev*, 34(2), 145-156. <https://doi.org/10.1016/j.ctrv.2007.10.003>
  44. Haque, T., Rahman, K. M., Thurston, D. E., Hadgraft, J., & Lane, M. E. (2018). Topical delivery of anthracycline II. Influence of binary and ternary solvent systems. *European Journal of Pharmaceutical Sciences*, 121, 59-64.
  45. Hassani, F. V., Hashemzaei, M., Akbari, E., Imenshahidi, M., & Hosseinzadeh, H. (2016). Effects of berberine on acquisition and reinstatement of morphine-induced conditioned place preference in mice. *Avicenna journal of phytomedicine*, 6(2), 198.
  46. He, C., Rong, R., Liu, J., Wan, J., Zhou, K., & Kang, J. X. (2012). Effects of Coptis extract combined with chemotherapeutic agents on ROS production, multidrug resistance, and cell growth in A549 human lung cancer cells. *Chin Med*, 7(1), 11. <https://doi.org/10.1186/1749-8546-7-11>
  47. He, C., Rong, R., Liu, J., Wan, J., Zhou, K., & Kang, J. X. (2012). Effects of Coptis extract combined with chemotherapeutic agents on ROS production, multidrug resistance, and cell growth in A549 human lung cancer cells. *Chinese Medicine*, 7(1), 1-6.
  48. Hu, Q., Bian, Q., Rong, D., Wang, L., Song, J., Huang, H.-S., Zeng, J., Mei, J., & Wang, P.-Y. (2023). JAK/STAT pathway: Extracellular signals, diseases, immunity, and therapeutic regimens. *Frontiers in Bioengineering and Biotechnology*, 11, 1110765.
  49. Ibrahim, S. F., & Brown, M. D. (2009). Actinic keratoses: a comprehensive update. *The Journal of clinical and aesthetic dermatology*, 2(7), 43.
  50. Jacoby, W., & Pasten, I. (1979). Methods in Enzymology: Cell Culture. Vol. 58. In: Academic Press, New York.
  51. James, W. D. B., Timothy G. Elston, Dirk M. Odom, Richard B. (2006). *Andrews' diseases of the skin : clinical dermatology*. Saunders Elsevier.
  52. Jerant, A. F., Johnson, J. T., Sheridan, C. D., & Caffrey, T. J. (2000). Early detection and treatment of skin cancer. *Am Fam Physician*, 62(2), 357-368, 375-356, 381-352. <https://www.ncbi.nlm.nih.gov/pubmed/10929700>
  53. Johnson, R. S., Titze, J., & Weller, R. (2016). Cutaneous control of blood pressure. *Curr Opin Nephrol Hypertens*, 25(1), 11-15. <https://doi.org/10.1097/MNH.000000000000188>
  54. Kiessling, S., Beaulieu-Laroche, L., Blum, I. D., Landgraf, D., Welsh, D. K., Storch, K.-F.,

- Labrecque, N., & Cermakian, N. (2017). Enhancing circadian clock function in cancer cells inhibits tumor growth. *BMC biology*, 15(1), 1-18.
55. Klein, E., Stoll Jr, H. L., Milgrom, H., Traenkle, H. L., Graham, S., & Helm, F. (1966). Tumors of the skin: VI. Study on effects of local administration of 5-fluorouracil in basal cell carcinoma. *Journal of investigative dermatology*, 47(1), 22-26.
  56. Kubo, A., Nagao, K., & Amagai, M. (2012). Epidermal barrier dysfunction and cutaneous sensitization in atopic diseases. *J Clin Invest*, 122(2), 440-447. <https://doi.org/10.1172/JCI57416>
  57. Lancerotto, L., Stecco, C., Macchi, V., Porzionato, A., Stecco, A., & De Caro, R. (2011). Layers of the abdominal wall: anatomical investigation of subcutaneous tissue and superficial fascia. *Surgical and radiologic anatomy*, 33(10), 835-842.
  58. Lane, M. E. (2013). Skin penetration enhancers. *International journal of pharmaceuticals*, 447(1-2), 12-21.
  59. Lane, M. E., Santos, P., Watkinson, A. C., & Hadgraft, J. (2012). Passive skin permeation enhancement. *Topical and transdermal drug delivery*. Wiley, Hoboken, 23-42.
  60. Leiter, U., Eigentler, T., & Garbe, C. (2014). Epidemiology of skin cancer. *Adv Exp Med Biol*, 810, 120-140. [https://doi.org/10.1007/978-1-4939-0437-2\\_7](https://doi.org/10.1007/978-1-4939-0437-2_7)
  61. Li, D., Zhang, J., Zhang, Y., Zhao, P., & Yang, L. (2015). Inhibitory effect of berberine on human skin squamous cell carcinoma A431 cells. *Genet Mol Res*, 14(3), 10553-10568.
  62. Li, M.-H., Zhang, Y.-J., Yu, Y.-H., Yang, S.-H., Iqbal, J., Mi, Q.-Y., Li, B., Wang, Z.-M., Mao, W.-X., & Xie, H.-G. (2014). Berberine improves pressure overload-induced cardiac hypertrophy and dysfunction through enhanced autophagy. *European journal of pharmacology*, 728, 67-76.
  63. Linos, E., Swetter, S. M., Cockburn, M. G., Colditz, G. A., & Clarke, C. A. (2009). Increasing burden of melanoma in the United States. *J Invest Dermatol*, 129(7), 1666-1674. <https://doi.org/10.1038/jid.2008.423>
  64. Liu, S., & Trapnell, C. (2016). Single-cell transcriptome sequencing: recent advances and remaining challenges. *F1000Research*, 5.
  65. Mabruk, M. J., Toh, L. K., Murphy, M., Leader, M., Kay, E., & Murphy, G. M. (2009). Investigation of the effect of UV irradiation on DNA damage: comparison between skin cancer patients and normal volunteers. *Journal of cutaneous pathology*, 36(7), 760-765.
  66. McGillis, S. T., & Fein, H. (2004). Topical treatment strategies for non-melanoma skin cancer and precursor lesions. *Seminars in cutaneous medicine and surgery*,
  67. Micali, G., Lacarrubba, F., & Nasca, M. (2014). Topical pharmacotherapy for skin cancer: Part I. Pharmacology.([quiz 977-978]). *J Am Acad Dermatol*, 70(965), e1-965.
  68. Murthy, K. N. C., Jayaprakasha, G. K., & Patil, B. S. (2012). The natural alkaloid berberine targets multiple pathways to induce cell death in cultured human colon cancer cells. *European journal of pharmacology*, 688(1-3), 14-21.
  69. Namba, T., Sekiya, K., Toshinal, A., Kadota, S., Hatanaka, T., Katayama, K., & Koizumi, T. (1995). Study on baths with crude drug. II: the effects of coptidis rhizoma extracts as skin permeation enhancer. *Yakugaku Zasshi: Journal of the Pharmaceutical Society of Japan*, 115(8), 618-625.
  70. NCIN. (2022). *The Importance of Skin Cancer Registration - NCIN Data Briefing*. Retrieved 08/17 from [http://www.ncin.org.uk/publications/data\\_briefings/skin\\_cancer\\_registration](http://www.ncin.org.uk/publications/data_briefings/skin_cancer_registration)
  71. Neag, M. A., Mocan, A., Echeverría, J., Pop, R. M., Bocsan, C. I., Crişan, G., & Buzoianu, A. D. (2018). Berberine: Botanical occurrence, traditional uses, extraction methods, and relevance in cardiovascular, metabolic, hepatic, and renal disorders. *Frontiers in pharmacology*, 9, 557.
  72. Nemes, Z., & Steinert, P. M. (1999). Bricks and mortar of the epidermal barrier. *Exp Mol Med*, 31(1), 5-19. <https://doi.org/10.1038/emmm.1999.2>
  73. Nilforoushadeh, M. A., Ashtiani, H. R. A., Jaffary, F., Jahangiri, F., Nikkhah, N., Mahmoudbeyk,



- M., Fard, M., Ansari, Z., & Zare, S. (2017). Dermal fibroblast cells: biology and function in skin regeneration. *Journal of Skin and Stem Cell*, 4(2).
74. Palmieri, A., Iapichino, A., Cura, F., Scapoli, L., Carinci, F., Mandrone, M., & Martinelli, M. (2018). Pre-treatment with berberine enhances effect of 5-fluorouracil and cisplatin in HEP2 laryngeal cancer cell line. *J Biol Regul Homeost Agents*, 32(2 Suppl. 1), 167-177. <https://www.ncbi.nlm.nih.gov/pubmed/29460537>
  75. Pandey, A., Vishnoi, K., Mahata, S., Tripathi, S. C., Misra, S. P., Misra, V., Mehrotra, R., Dwivedi, M., & Bharti, A. C. (2015). Berberine and curcumin target survivin and STAT3 in gastric cancer cells and synergize actions of standard chemotherapeutic 5-fluorouracil. *Nutrition and cancer*, 67(8), 1295-1306.
  76. Parker, W. B., & Cheng, Y. C. (1990). Metabolism and mechanism of action of 5-fluorouracil. *Pharmacol Ther*, 48(3), 381-395. [https://doi.org/10.1016/0163-7258\(90\)90056-8](https://doi.org/10.1016/0163-7258(90)90056-8)
  77. Pinal, R. (2004). Effect of molecular symmetry on melting temperature and solubility. *Organic & biomolecular chemistry*, 2(18), 2692-2699.
  78. Potts, R. O., & Francoeur, M. L. (1991). The influence of stratum corneum morphology on water permeability. *J Invest Dermatol*, 96(4), 495-499. <https://doi.org/10.1111/1523-1747.ep12470197>
  79. Powell, J. (2006). Skin physiology. *Women's Health Medicine*, 3(3), 130-133.
  80. Prescott, S. L., Larcombe, D. L., Logan, A. C., West, C., Burks, W., Caraballo, L., Levin, M., Etten, E. V., Horwitz, P., Kozyrskyj, A., & Campbell, D. E. (2017). The skin microbiome: impact of modern environments on skin ecology, barrier integrity, and systemic immune programming. *World Allergy Organ J*, 10(1), 29. <https://doi.org/10.1186/s40413-017-0160-5>
  81. Prince, G. T., Cameron, M. C., Fathi, R., & Alkousakis, T. (2018). Topical 5-fluorouracil in dermatologic disease. *Int J Dermatol*, 57(10), 1259-1264. <https://doi.org/10.1111/ijd.14106>
  82. Rahvar, M., Lamel, S. A., & Maibach, H. I. (2012). Randomized, vehicle-controlled trials of topical 5-fluorouracil therapy for actinic keratosis treatment: an overview. *Immunotherapy*, 4(9), 939-945.
  83. Rauf, A., Abu-Izneid, T., Khalil, A. A., Imran, M., Shah, Z. A., Emran, T. B., Mitra, S., Khan, Z., Alhumaydhi, F. A., & Aljohani, A. S. (2021). Berberine as a potential anticancer agent: A comprehensive review. *Molecules*, 26(23), 7368.
  84. Ryan, J. A. (2008). Introduction to animal cell culture. *Technical Bulletin*.
  85. Sahni, D., & Lerner, A. (2022). *Advanced Skin Cancer: A Case-based Approach*. CRC Press.
  86. Sarveiya, V., Risk, S., & Benson, H. A. (2004). Liquid chromatographic assay for common sunscreen agents: application to in vivo assessment of skin penetration and systemic absorption in human volunteers. *Journal of Chromatography B*, 803(2), 225-231.
  87. Schaefer, H., & Redelmeier, T. E. (1996). *Skin barrier*. Karger Publishers.
  88. Schaefer, H., Zesch, A., & Stüttgen, G. (1977). Penetration, permeation, and absorption of triamcinolone acetonide in normal and psoriatic skin. *Arch Dermatol Res*, 258(3), 241-249. <https://doi.org/10.1007/BF00561126>
  89. Schoop, V. M., Fusenig, N. E., & Mirancea, N. (1999). Epidermal organization and differentiation of HaCaT keratinocytes in organotypic coculture with human dermal fibroblasts. *Journal of investigative dermatology*, 112(3), 343-353.
  90. Scolyer, R. A., Prieto, V. G., Elder, D. E., Cochran, A. J., & Mihm, M. C. (2020). Classification and histopathology of melanoma. *Cutaneous Melanoma*, 317-379.
  91. Senel, S., Kremer, M., Katalin, N., & Squier, C. (2001). Delivery of bioactive peptides and proteins across oral (buccal) mucosa. *Current Pharmaceutical Biotechnology*, 2(2), 175-186.
  92. Seo, Y.-S., Yim, M.-J., Kim, B.-H., Kang, K.-R., Lee, S.-Y., Oh, J.-S., You, J.-S., Kim, S.-G., Yu, S.-J., & Lee, G.-J. (2015). Berberine-induced anticancer activities in FaDu head and neck squamous cell carcinoma cells. *Oncology reports*, 34(6), 3025-3034.



93. Shreve, C., Shropshire, C., & Cotter, D. G. (2020). Metastatic squamous cell carcinoma: A cautionary tale. *Cureus*, 12(10).
94. Simon, G. A., & Maibach, H. I. (2000). The pig as an experimental animal model of percutaneous permeation in man: qualitative and quantitative observations—an overview. *Skin pharmacology and physiology*, 13(5), 229-234.
95. Singh, N., & Sharma, B. (2018). Toxicological effects of berberine and sanguinarine. *Frontiers in molecular biosciences*, 5, 21.
96. Sorrell, J. M., Baber, M., & Caplan, A. (2004). Site-matched papillary and reticular human dermal fibroblasts differ in their release of specific growth factors/cytokines and in their interaction with keratinocytes. *Journal of cellular physiology*, 200(1), 134-145.
97. Soura, E., Eliades, P. J., Shannon, K., Stratigos, A. J., & Tsao, H. (2016). Hereditary melanoma: Update on syndromes and management: Genetics of familial atypical multiple mole melanoma syndrome. *Journal of the American Academy of Dermatology*, 74(3), 395-407.
98. Stott, P. W., Williams, A. C., & Barry, B. W. (2001). Mechanistic study into the enhanced transdermal permeation of a model  $\beta$ -blocker, propranolol, by fatty acids: a melting point depression effect. *International journal of pharmaceutics*, 219(1-2), 161-176.
99. Supe, S., & Takudage, P. (2021). Methods for evaluating penetration of drug into the skin: A review. *Skin Research and Technology*, 27(3), 299-308.
100. Taylor, K. L., Lister, J. A., Zeng, Z., Ishizaki, H., Anderson, C., Kelsh, R. N., Jackson, I. J., & Patton, E. E. (2011). Differentiated melanocyte cell division occurs in vivo and is promoted by mutations in Mitf. *Development*, 138(16), 3579-3589. <https://doi.org/10.1242/dev.064014>
101. Telfer, N. R., Colver, G. B., Morton, C. A., & British Association of, D. (2008). Guidelines for the management of basal cell carcinoma. *Br J Dermatol*, 159(1), 35-48. <https://doi.org/10.1111/j.1365-2133.2008.08666.x>
102. Thompson, S. C., Jolley, D., & Marks, R. (1993). Reduction of solar keratoses by regular sunscreen use. *New England Journal of Medicine*, 329(16), 1147-1151.
103. Tillhon, M., Ortiz, L. M. G., Lombardi, P., & Scovassi, A. I. (2012). Berberine: new perspectives for old remedies. *Biochemical pharmacology*, 84(10), 1260-1267.
104. Uribe, P., & Gonzalez, S. (2011). Epidermal growth factor receptor (EGFR) and squamous cell carcinoma of the skin: molecular bases for EGFR-targeted therapy. *Pathology-Research and Practice*, 207(6), 337-342.
105. Vangipuram, M., Ting, D., Kim, S., Diaz, R., & Schüle, B. (2013). Skin punch biopsy explant culture for derivation of primary human fibroblasts. *JoVE (Journal of Visualized Experiments)*(77), e3779.
106. Vincent, J., Mignot, G., Chalmin, F., Ladoire, S., Bruchard, M., Chevriaux, A., Martin, F., Apetoh, L., Rébé, C., & Ghiringhelli, F. (2010). 5-Fluorouracil selectively kills tumor-associated myeloid-derived suppressor cells resulting in enhanced T cell-dependent antitumor immunity. *Cancer research*, 70(8), 3052-3061.
107. Walters, K. A. (2002). *Dermatological and transdermal formulations* (Vol. 119). CRC Press.
108. Walters, K. A., & Brain, K. R. (2002). Dermatological formulation and transdermal systems. In *Dermatological and transdermal formulations* (pp. 337-418). CRC Press.
109. Wang, N., Feng, Y., Zhu, M., Tsang, C. M., Man, K., Tong, Y., & Tsao, S. W. (2010). Berberine induces autophagic cell death and mitochondrial apoptosis in liver cancer cells: the cellular mechanism. *Journal of cellular biochemistry*, 111(6), 1426-1436.
110. Wertz, P. W., Swartzendruber, D. C., Madison, K. C., & Downing, D. T. (1987). Composition and morphology of epidermal cyst lipids. *J Invest Dermatol*, 89(4), 419-425. <https://doi.org/10.1111/1523-1747.ep12471781>
111. Williams, A. C., & Barry, B. W. (2012). Penetration enhancers. *Advanced drug delivery reviews*, 64, 128-137.
112. Xu, F., Liu, M., Liao, Y., Zhou, Y., Zhang, P., Zeng, Y., & Liu, Z. (2022). Improvement of

- anticancer effect of berberine by salt formation modifications. *Phytomedicine*, 104, 154314.
113. Yen Moore, A. (2009). Clinical applications for topical 5-fluorouracil in the treatment of dermatological disorders. *Journal of dermatological treatment*, 20(6), 328-335.
  114. Yoo, K. Y., Hwang, I. K., Kim, J. D., Kang, I. J., Park, J., Yi, J. S., Kim, J. K., Bae, Y. S., & Won, M. H. (2008). Antiinflammatory effect of the ethanol extract of *Berberis koreana* in a gerbil model of cerebral ischemia/reperfusion. *Phytotherapy Research: An International Journal Devoted to Pharmacological and Toxicological Evaluation of Natural Product Derivatives*, 22(11), 1527-1532.
  115. Yousef, H., Alhajj, M., & Sharma, S. (2017). Anatomy, skin (integument), epidermis.
  116. Yousef, H., Alhajj, M., & Sharma, S. (2022). Anatomy, Skin (Integument), Epidermis. In *StatPearls*. <https://www.ncbi.nlm.nih.gov/pubmed/29262154>
  117. Zalaudek, I., Piana, S., Moscarella, E., Longo, C., Zendri, E., Castagnetti, F., Pellacani, G., Lallas, A., & Argenziano, G. (2014). Morphologic grading and treatment of facial actinic keratosis. *Clin Dermatol*, 32(1), 80-87. <https://doi.org/10.1016/j.clindermatol.2013.05.028>
  118. Zhang, N., Yin, Y., Xu, S. J., & Chen, W. S. (2008). 5-Fluorouracil: mechanisms of resistance and reversal strategies. *Molecules*, 13(8), 1551-1569. <https://doi.org/10.3390/molecules13081551>

## Appendix

Gene_id	baseMean	log2FoldChange	lfcSE	pvalue	padj
HERC2	94.7505987	23.2698402	3.58278828	1.8574E-11	6.7374E-11
ASH1L	92.8827057	21.5577158	4.3478368	4.4778E-08	1.1431E-07
RFWD3	27.5536535	21.2395399	4.38753626	6.6753E-08	1.6731E-07
MATN2	124.366451	11.0747684	1.25104645	8.7013E-22	7.0077E-21
WARS1	122.404892	11.0230822	1.2894526	1.3799E-20	1.0124E-19
TPRA1	92.8186885	9.78673242	1.2412529	1.7179E-17	1.0276E-16
ANO9	72.1606188	9.06478333	1.91312785	2.6357E-08	6.8633E-08
ACIN1	35.0691564	8.95701983	1.41502888	4.2557E-12	1.6508E-11
UCKL1	37.3119761	8.35132028	1.52610125	1.4325E-09	4.2559E-09
CREB1	37.5667114	8.32799422	1.53492384	1.8847E-09	5.5385E-09
ERF	33.7009896	8.09789436	1.89678903	3.7618E-07	8.6588E-07
LOC102724788	21.1834402	7.94217436	1.38736298	5.4209E-10	1.683E-09
ATOH8	32.50547	7.92125066	1.29275064	5.1718E-11	1.7942E-10
ZNF800	37.4245489	7.85778492	1.3574304	4.0873E-10	1.2879E-09
KMT2C	20.4834305	7.70097646	1.84573251	6.4505E-07	1.4459E-06
PCNP	15.0755294	6.96084659	1.61048198	5.098E-07	1.1558E-06
PIGR	618.895365	6.88114004	1.17021332	4.92E-10	1.5331E-09
MLXIPL	12.9311187	6.57589477	1.60351773	1.0547E-06	2.3076E-06
PTGIS	133.655363	6.30361037	0.46587354	2.6486E-42	6.4453E-41
CHID1	22.3768272	5.89828966	2.96730718	0.00014981	0.00025223

PSMG4	7.8653562 3	5.70255497	2.0386970 7	2.7979E-0 5	5.1673E-0 5
JAK1	22.543443 6	5.64901786	2.6695955 7	0.0001245	0.0002118 3
MMP13	41.944805 6	5.51834044	0.6659046 7	3.1642E-1 7	1.8453E-1 6
ZC3H3	19.830045 1	5.23666154	2.9625265 5	0.0002749 8	0.0004469 6
HCFC1R1	69.607495 1	5.1399502	0.8840801 5	4.1433E-1 0	1.3033E-0 9
ZC3H6	36.795746 9	4.53077765	0.5978281 4	1.9647E-1 5	1.0099E-1 4
ZNF302	12.054228 1	4.5126919	3.0833896 7	0.0006273 7	0.0009705 3
LOXL4	302.33516 6	4.30602395	0.2778548 6	4.2899E-5 5	1.7696E-5 3
LYPD2	61.264532 2	4.28766163	0.5323688 2	2.3701E-1 7	1.3954E-1 6
ATP6V1B1	112.10260 2	4.19079654	0.3491706 8	1.7906E-3 4	3.0435E-3 3
ALPG	493.34591	4.10748988	0.4342389 7	6.3594E-2 3	5.4944E-2 2
CD74	168.38423 5	4.08829918	0.4189480 3	3.3885E-2 4	3.1749E-2 3
H1-2	194.46403 4	4.05952849	0.2215833 8	2.5487E-7 6	2.0526E-7 4
RARB	34.774442 3	3.99302778	1.1701495 3	1.6314E-0 6	3.5014E-0 6
CEP170	11.119217 3	3.94683327	3.0032094 4	0.0010527 8	0.0015837 3
NEMP2	11.124160 6	3.92915995	2.9583630 2	0.0010338 2	0.0015566
ACOT11	10.971683 3	3.90879908	1.3575416 4	1.0598E-0 5	2.0704E-0 5
FOS	4834.0238 5	3.88252245	0.2368361 2	2.7297E-6 2	1.4773E-6 0
CARD14	13.009076 9	3.87808751	3.1971896 4	0.0012959 7	0.0019226 4
KRT4	916.89166 6	3.50711572	0.3431636 7	9.3138E-2 8	1.0915E-2 6
METTL7A	62.642634 1	3.48538856	0.3831893 4	4.8695E-2 3	4.2342E-2 2
RARRES1	142.52073 7	3.48255575	0.3442371 2	2.3303E-2 7	2.6629E-2 6

ATF3	379.69475 5	3.42313112	0.6249315 5	2.7477E-1 1	9.8248E-1 1
CCDC14	31.391243 6	3.41186045	3.4341130 4	0.0022837	0.0032766 2
SREBF1	14.726714 7	3.30520009	2.7847725 5	0.0018512 4	0.0026967 3
ADAM10	328.80871 3	3.28793292	0.3369712 4	3.5843E-2 6	3.8066E-2 5
MXRA5	405.81277 3	3.2395776	0.2031676 3	3.5826E-6 1	1.8361E-5 9
TNFRSF13C	17.258044 2	3.23325541	0.8801327	2.7564E-0 7	6.4233E-0 7
APCDD1	33.718798 7	3.18569066	0.4764779 6	6.9579E-1 5	3.3961E-1 4
FUZ	6.7733163 7	3.12939717	2.5701257	0.0019169 9	0.0027817 3
ANK3	123.45338 1	3.07916265	0.3887666 6	4.9859E-1 9	3.3264E-1 8
DENND1A	37.187657 7	3.06853847	1.2090415 1	3.0584E-0 5	5.6147E-0 5
SYTL1	403.19446 7	3.04086638	0.1716133 3	2.4111E-7 4	1.8327E-7 2
ITLN1	17.665932 3	3.01191354	0.8392869 6	4.212E-07	9.6395E-0 7
CAMK2A	8.8204276 7	3.00867481	2.8363778 6	0.0027761 3	0.003943
EXD3	8.2548709	2.97658327	2.0720095 9	0.0011997 9	0.0017881 8
SLC10A7	36.449701 1	2.96528959	0.5915966	3.2478E-1 0	1.0315E-0 9
TRAPPC9	111.26542 3	2.92680256	0.4351508 8	6.0632E-1 5	2.9745E-1 4
FXD3	16.447113 9	2.91082931	1.1224321	2.7078E-0 5	5.0119E-0 5
TSTD1	120.75232 6	2.87182038	0.2910593 2	1.3051E-2 6	1.4333E-2 5
AOC1	1896.4606 3	2.86531527	0.3918029 7	9.1866E-1 7	5.1919E-1 6
CDADC1	7.5972146 2	2.81472716	2.6102054	0.0030824 7	0.0043525 1
VWA2	5.4283650 9	2.80408257	2.5645929 9	0.0030201 7	0.0042734 7
TBC1D8B	52.504080 1	2.80321102	1.6185024	0.0005526 8	0.0008618 9

UBA2	127.69023 7	2.80045024	0.3469180 7	2.669E-19	1.8183E-1 8
MAP2K6	23.378745 5	2.72864699	1.7280025 4	0.0009190 1	0.0013917 9
TRIM31	176.32995 6	2.7215967	0.3170918 1	4.8911E-2 1	3.7262E-2 0
ID4	28.403097	2.70577184	0.653889	5.2022E-0 8	1.3206E-0 7
SCEL	95.1537	2.66475527	0.8721791 7	6.1998E-0 6	1.2483E-0 5
ASH2L	376.63720 9	2.65531746	0.7265443 4	5.3339E-0 7	1.2056E-0 6
FBP1	18.563610 3	2.65399002	1.3758338 6	0.0003348 3	0.0005377 8
ALDH3A1	215.40705 1	2.65289772	0.3765360 2	1.6712E-1 5	8.6636E-1 5
ID1	1619.9266 7	2.64734887	0.1605570 9	2.8252E-6 4	1.6765E-6 2
STK39	94.964526 4	2.63418657	0.7527958 5	1.0906E-0 6	2.3838E-0 6
PBX1	247.59351 6	2.62759338	0.2474562 9	2.0216E-2 9	2.62E-28
ST6GALNAC2	286.68147	2.62571871	0.1440320 5	2.2119E-7 7	1.8248E-7 5
RNASE4	23.095822 2	2.61201921	0.8828506 5	9.9262E-0 6	1.947E-05
DCLRE1C	11.116202 5	2.6115726	2.6883335 3	0.0042767 8	0.0059417 3
BTN3A3	134.83933 2	2.59110795	0.2577485 5	9.6309E-2 7	1.0698E-2 5
RASA4	134.19646	2.57687086	0.2455787	1.0946E-2 8	1.3563E-2 7
ALDOA	39.928981	2.57253705	0.5263217	1.871E-09	5.5007E-0 9
DBP	199.65011 8	2.5588945	0.2247658 1	6.5663E-3 3	1.0096E-3 1
HSD17B8	12.507064 7	2.55814329	0.8044205 3	4.7538E-0 6	9.6663E-0 6
HEXD	77.915280 1	2.55228904	0.3644012 5	3.9112E-1 5	1.947E-14
PHYKPL	45.997197 9	2.54854109	0.6713669 4	3.8666E-0 7	8.8941E-0 7
LDHD	51.771513	2.53828077	1.0524569 3	7.9901E-0 5	0.0001396 7

METTL27	55.740333 2	2.53483298	0.3317334 8	3.6338E-1 7	2.1119E-1 6
ACKR3	1206.5377 9	2.53293412	0.1309215 1	3.3604E-8 6	3.6666E-8 4
TMCO6	42.292582 8	2.49105913	0.8978257 5	2.4974E-0 5	4.6543E-0 5
IL17RD	11.131237 4	2.48458439	2.8744346 2	0.0053749 5	0.0073830 5
SNRPD1	18.130262 7	2.46453242	0.6561822 1	6.0368E-0 7	1.3572E-0 6
INHBB	267.18882 2	2.46339503	0.1638468 7	1.1556E-5 3	4.467E-52
UGT1A10	867.33513	2.43129672	0.1217356 2	3.3122E-9 1	4.0012E-8 9
KIF20A	1038.8293 9	2.40842385	0.0776782 7	1.9E-213	2.143E-21 0
ITGB4	42.053477 3	2.40515159	1.0584823 5	0.0001580 9	0.0002650 5
TCEA2	109.09790 4	2.40084507	0.1850815 9	7.3325E-4 1	1.6872E-3 9
PCDHGB2	30.203920 4	2.40021321	0.9201954 1	5.4022E-0 5	9.6223E-0 5
KEL	13.853791 1	2.39411156	1.0035902 9	0.0001129 3	0.0001932 2
GBP2	468.74851 9	2.38155715	0.1470240 9	2.5141E-6 1	1.3184E-5 9
SH2D2A	20.729254 6	2.38115021	1.5197905 5	0.0012893 6	0.0019132 6
ASPM	113.33218	2.3811302	0.3187291	3.5056E-1 6	1.9079E-1 5
UNK	165.44718 9	2.37906232	0.2464134 8	2.174E-24	2.0685E-2 3
PROM2	3811.3275 6	2.37180296	0.1259726 8	2.3498E-8 1	2.2078E-7 9
H1-0	2386.7010 9	2.36297738	0.1212343 4	7.3576E-8 7	8.1597E-8 5
IDI1	40.884426	2.35870661	0.5023778 1	1.2948E-0 8	3.4925E-0 8
PIP5K1C	18.948866 7	2.35635202	2.7962846 2	0.0061884 9	0.0084303 5
SMAD6	29.243298 8	2.35298526	0.4707914 5	2.8846E-0 9	8.2934E-0 9
ALDH3B1	385.60894 2	2.34312142	0.2049728 5	1.7638E-3 2	2.6457E-3 1

SRSF11	118.27206 3	2.3424865	0.5082809 8	2.1295E-0 8	5.599E-08
SH2B3	8.2706324 9	2.33758652	2.6014413 4	0.0059912 3	0.0081847 1
PRKAG3	5.1988404 3	2.32818236	2.4549618 1	0.0056670 5	0.0077575 1
AZI2	20.632665 6	2.3255958	0.6178305 4	9.7531E-0 7	2.1443E-0 6
ZNF276	210.35578	2.30893031	0.2844051 5	3.2999E-1 8	2.0613E-1 7
PAQR8	194.45564 5	2.30279356	0.1570943	9.7088E-5 1	3.3172E-4 9
HPS3	87.356913 2	2.30038461	0.5145661 4	4.9972E-0 8	1.2704E-0 7
FOSB	1077.0224 5	2.29021722	0.3459799 3	2.6548E-1 3	1.1389E-1 2
TMEM143	51.026534 5	2.28941529	0.3746969 3	7.1948E-1 2	2.7192E-1 1
KCP	129.77159 7	2.28054669	0.3697378 3	5.2653E-1 2	2.0215E-1 1
SYT8	25.332145 4	2.27768559	0.5534675 3	2.7337E-0 7	6.3749E-0 7
SRGAP1	18.075646 9	2.27550314	2.7463141	0.0067869 1	0.0091863 7
ACSL1	300.56825 3	2.25588234	0.2818459 5	1.1534E-1 7	6.967E-17
NBEAL2	334.81744 1	2.24765519	0.2484486 8	1.5369E-2 1	1.2175E-2 0
BRI3	75.261589 2	2.24397613	0.2646754 6	2.3913E-1 9	1.6357E-1 8
CORO2A	27.546465 8	2.24080831	2.0453659 2	0.0047105 2	0.0065193 7
ALPP	1449.9480 8	2.23803994	0.3238321 4	4.8466E-1 4	2.2094E-1 3
TRAPPC6A	61.695994 8	2.23518829	0.2810324 9	1.9544E-1 7	1.1639E-1 6
SPTLC3	54.069590 6	2.23275027	0.4743129 9	2.2496E-0 8	5.8987E-0 8
MAML3	67.847097	2.23225574	0.2691581 3	1.2227E-1 8	7.9536E-1 8
PIF1	138.41527 1	2.22688992	0.2420115 4	4.1774E-2 2	3.4548E-2 1
H1-10	1863.1743 8	2.21757093	0.0763574 2	2.831E-18 7	2.394E-18 4



GPRC5C	42.611304 7	2.21259115	0.4715558 1	2.6733E-0 8	6.9558E-0 8
TRIP10	108.80699 3	2.20436656	0.2519816 4	2.8779E-2 0	2.0756E-1 9
SCNN1A	1445.4305 3	2.20127388	0.1358423 6	7.174E-61	3.5685E-5 9
HES4	69.141422 5	2.19575492	0.3023132	4.9234E-1 5	2.4329E-1 4
INTS11	57.807006 9	2.1840419	0.3788485	1.0236E-1 0	3.4313E-1 0
IFT140	15.793390 6	2.17751417	2.0550737	0.0053869 4	0.0073965 2
RFT1	39.104546 3	2.17506649	0.4202293 2	2.8262E-0 9	8.1427E-0 9
ACTR1B	482.75733 3	2.17135643	0.1375633	7.185E-58	3.3066E-5 6
CDK7	37.090601 9	2.1647077	0.3525780 3	1.1826E-1 1	4.3576E-1 1
ZNF862	16.680102	2.16103927	0.8967809 2	0.0001817 1	0.0003016 7
LAMA5	6652.7941	2.158006	0.1228513 3	8.7962E-7 1	6.2638E-6 9
ISOC2	269.96130 2	2.15544928	0.1435611 5	1.1577E-5 2	4.3269E-5 1
ERMARD	48.724572 1	2.14734749	0.549753	1.1682E-0 6	2.5444E-0 6
KMT5C	108.86590 9	2.14420512	0.3928952 7	7.2371E-1 0	2.2204E-0 9
TNFSF10	1364.2909 3	2.13988943	0.1650217 8	3.8845E-4 0	8.7015E-3 9
CCDC61	109.48791 2	2.13986685	0.2833187 1	7.6105E-1 6	4.0797E-1 5
EMC10	87.933753 1	2.13117176	0.4236007 3	7.4636E-0 9	2.0542E-0 8
DNAJB1	38.858111	2.12857636	0.3803268	3.5916E-1 0	1.1375E-0 9
ABHD14B	230.85615 5	2.12273009	0.2544711	1.4844E-1 8	9.5638E-1 8
EGR1	6897.4258	2.12135621	0.1382941 6	9.7241E-5 5	3.9157E-5 3
PSRC1	101.47441 2	2.12061628	0.5257188 1	7.8225E-0 7	1.7385E-0 6
SLC29A3	397.67872 5	2.1166049	0.1839643 9	2.825E-32	4.191E-31

PLAT	474.91607 1	2.11623442	0.1432420 5	5.1486E-5 1	1.7862E-4 9
ISYNA1	114.65121 1	2.10942803	1.2684544 2	0.0014666 7	0.0021630 8
CALHM2	33.826063 8	2.09654017	0.4462894 3	4.5794E-0 8	1.1673E-0 7
ACCS	128.59006 6	2.09065129	0.3773074	5.9431E-1 0	1.8384E-0 9
ARFRP1	10.803598 2	2.08696394	2.6899075 7	0.0085817 2	0.0114530 2
COMTD1	142.83015 2	2.08526166	0.1848672 6	4.3837E-3 1	6.1526E-3 0
DALRD3	125.30055 7	2.08215312	0.3725185 5	4.7173E-1 0	1.4726E-0 9
UGT1A6	298.03792 3	2.07903033	0.1196953 5	4.0903E-6 9	2.795E-67
WNT10A	593.93288 5	2.06783155	0.1426374 7	3.7938E-4 9	1.2339E-4 7
KRT15	3680.0309 3	2.06435926	0.1967149 1	2.6529E-2 7	3.0214E-2 6
IGFBP3	11227.590 9	2.06262964	0.1475440 2	6.3431E-4 6	1.7955E-4 4
TMEM129	89.275744 3	2.04749455	0.5287267 4	2.0778E-0 6	4.394E-06
LEMD1	6.4375327	2.04376547	1.6821187 7	0.0045257 1	0.0062733 2
NOTCH3	368.85473 5	2.04277755	0.2185691 7	2.8201E-2 2	2.3612E-2 1
ATG16L2	63.920421 8	2.03230576	0.2725176	2.6658E-1 5	1.3549E-1 4
SKIV2L	67.413416 2	2.02878662	0.3995409 2	9.6253E-0 9	2.6203E-0 8
EEFSEC	46.099274 8	2.02474323	0.6097111 8	1.7276E-0 5	3.2885E-0 5
RASSF1	35.008353 2	2.01566173	0.3945533 8	8.7231E-0 9	2.3862E-0 8
PRKRA	22.604559 8	2.0114062	0.5457827 8	4.9832E-0 6	1.0114E-0 5
KCTD18	94.546145 2	2.00701302	0.5572542 2	6.9179E-0 6	1.3834E-0 5
PTPRU	1234.3815 1	2.00483602	0.1444047	3.1547E-4 5	8.6054E-4 4
AR	619.7539	2.00274317	0.1766540 7	3.3266E-3 1	4.6982E-3 0

LY6D	5852.0817 3	2.00126602	0.2183839 6	1.8594E-2 1	1.4627E-2 0
KCNAB2	187.73324 6	1.99824298	0.3882515 7	7.7557E-0 9	2.1302E-0 8
FAM149B1	46.621642 5	1.99671079	0.8277152 1	0.0002917 1	0.0004723 4
SATB1	69.104916 6	1.99135657	0.2597173 4	6.4492E-1 6	3.4654E-1 5
IFITM10	61.034215 2	1.9808299	0.2851023 4	1.3746E-1 3	6.0739E-1 3
GAA	523.21469 8	1.97654445	0.2132226 5	7.7269E-2 2	6.2452E-2 1
LUM	106.88413 6	1.97365501	0.2956274 4	9.2175E-1 3	3.7723E-1 2
SCD	27164.193 7	1.97062985	0.0576725 4	3.306E-25 7	5.591E-25 4
LEPR	19.576999 5	1.96502765	0.8433876 9	0.0003983	0.0006322 1
PEX11G	19.314158 8	1.96173097	0.529049	5.6652E-0 6	1.1454E-0 5
RNF152	208.36359 4	1.960739	0.2089304	2.8034E-2 2	2.3501E-2 1
SLC1A3	893.69749 9	1.96034705	0.1612852 9	2.5338E-3 5	4.5109E-3 4
FAM181B	103.24301 8	1.95833171	0.2175333 8	9.801E-21	7.2862E-2 0
SEMA4B	781.21553 6	1.95509166	0.1372174 1	2.2389E-4 7	6.7316E-4 6
CRELD1	16.39838	1.95403386	1.5963721 4	0.0049991 5	0.0068948 5
ARAP1	441.56643 7	1.94950878	0.1572861 3	1.3655E-3 6	2.6317E-3 5
PRR15L	49.115523 5	1.9361219	0.3848697 7	1.8567E-0 8	4.92E-08
JADE2	744.24059 4	1.93478094	0.2139698 2	7.5021E-2 1	5.6454E-2 0
ANXA9	128.98134 3	1.92102682	0.2810203 9	3.8602E-1 3	1.627E-12
SESN1	77.510173 8	1.91914663	0.3488287 5	1.6202E-0 9	4.7821E-0 9
ZNF488	400.19177 5	1.91265024	0.1153115 5	5.0322E-6 3	2.8369E-6 1
MSI2	255.55497 2	1.91063993	0.2695793 4	6.8386E-1 4	3.0842E-1 3

PSCA	457.78789 6	1.90072348	0.2244408 6	1.3644E-1 8	8.8327E-1 8
SPNS1	80.081438 1	1.89381584	0.8608869 9	0.0006810 5	0.0010483
HMGN1	11.062392	1.88871582	2.5323364 6	0.0110483 6	0.0145667 8
OSBPL5	54.701153 1	1.8819149	0.3474538	3.0276E-0 9	8.686E-09
CLK2	158.86930 9	1.87838455	0.2616984 4	4.0461E-1 4	1.857E-13
THEM6	1374.8722 7	1.87691043	0.1212816 8	3.3261E-5 5	1.3804E-5 3
NEBL	559.86678 5	1.87576376	0.1231643 3	1.477E-53	5.6774E-5 2
RPL3	15464.607 3	1.87341702	0.0390239 4	0	0
HMGN3	51.746945 8	1.87143841	0.2982927 7	1.9622E-1 1	7.1101E-1 1
SLC27A1	118.07915 1	1.86265382	0.2711319 5	3.8333E-1 3	1.6167E-1 2
TRIM22	396.51767	1.85710166	0.2188626 6	1.3942E-1 8	9.0162E-1 8
CRACDL	78.336471	1.8547705	0.3913369 1	1.0967E-0 7	2.6716E-0 7
FAM178B	77.336119 9	1.85280815	0.4395690 4	1.1858E-0 6	2.5819E-0 6
KLRC2	5.5651733 6	1.84632606	1.8273327 7	0.0086137 9	0.0114935 5
BMF	143.32897 5	1.84550081	0.2925908 2	1.7486E-1 1	6.3495E-1 1
MAGED1	469.14150 9	1.84352025	0.1267780 4	4.8631E-4 9	1.5592E-4 7
FAM20C	239.80735 1	1.84256103	0.1457668 9	9.178E-38	1.859E-36
NCOA2	520.95414 4	1.84253693	0.5222501	1.7859E-0 5	3.389E-05
PRPF40A	171.88734 5	1.83973653	0.2747849 9	1.3875E-1 2	5.597E-12
FOXO3	512.16867 3	1.83388069	0.1714507 7	7.7743E-2 8	9.1626E-2 7
TRIOBP	811.80614 1	1.83372614	0.0858500 3	2.455E-10 2	3.863E-10 0
RPL14	124.39371 8	1.83319284	0.3212974 3	7.1659E-1 0	2.1998E-0 9

LRSAM1	120.64403 6	1.82797817	0.4966350 2	1.0924E-0 5	2.1303E-0 5
TOR2A	67.709406 5	1.82526513	0.4077226 1	4.1981E-0 7	9.6174E-0 7
UNG	251.57079 3	1.8206782	0.1757417 4	2.8806E-2 6	3.0737E-2 5
PPOX	37.090400 7	1.81809385	0.5835117 7	7.6872E-0 5	0.0001346 2
PUM2	87.755877 9	1.81137722	0.3847696 9	1.5141E-0 7	3.6246E-0 7
PRRT1	17.334075 6	1.81062512	0.7366577 2	0.0004837 8	0.0007607 6
LNP1	18.853389 1	1.80981014	0.6079321 5	0.0001205 8	0.0002056 8
RALGPS2	632.99819 9	1.808694	0.2191219 9	1.1668E-1 7	7.0354E-1 7
DUSP6	87.779513	1.80737714	0.2980042 8	9.2182E-1 1	3.1134E-1 0
CDCA8	248.12599 9	1.80507407	0.3527696 5	2.0194E-0 8	5.324E-08
FAM189B	241.33014 4	1.79748998	0.1370712 3	2.3333E-4 0	5.2616E-3 9
DNHD1	218.62913 2	1.79617443	0.1623727 3	1.6026E-2 9	2.097E-28
MIF4GD	23.780624 5	1.79585167	1.1064859 2	0.0030221 3	0.0042753 5
ACOT13	126.90607 3	1.79564011	0.1682955	1.178E-27	1.3692E-2 6
SLC2A10	50.313275 2	1.79451678	0.3195054 6	1.3792E-0 9	4.1047E-0 9
ACBD4	22.212603	1.79160085	0.8510910 5	0.0011559 3	0.0017281 4
FOXQ1	1000.7818 8	1.78747228	0.0744341 1	1.783E-12 8	5.245E-12 6
H2AC6	60.787462 2	1.7795724	0.2761566 7	9.1648E-1 2	3.4198E-1 1
FFAR2	80.385495 1	1.77691111	0.4621094 4	7.1782E-0 6	1.4325E-0 5
MACROD1	314.10145 3	1.77611559	0.1364713	9.1651E-4 0	2.0262E-3 8
SYTL4	73.375445 3	1.77411276	0.4329099 6	2.6376E-0 6	5.5004E-0 6
CIITA	8.3261361 4	1.77362163	1.7511436 4	0.0094727 2	0.0125825 6

KAT14	117.19990 6	1.77289539	0.3510807 6	3.2131E-0 8	8.3156E-0 8
ADCK5	91.784098 7	1.76807571	0.2107564 9	4.296E-18	2.6736E-1 7
C17orf113	52.925257 2	1.76791218	0.3711696 4	1.3655E-0 7	3.292E-07
NAT14	205.59150 1	1.76497219	0.1298664 7	4.2846E-4 3	1.0856E-4 1
PSAPL1	68.541705 1	1.76486003	0.2867155 2	6.1068E-1 1	2.1046E-1 0
RAPGEFL1	402.20832 3	1.7618062	0.1933336 5	7.2995E-2 1	5.499E-20
TLR3	171.56387 3	1.76135516	0.1631071 2	3.252E-28	3.9355E-2 7
SCRIB	227.26326 2	1.75918162	0.2174415	5.3342E-1 7	3.0711E-1 6
RBM43	77.310853	1.75908724	0.2534603 7	3.3818E-1 3	1.4388E-1 2
PLK2	2916.0928 4	1.75786537	0.0929072 5	7.5557E-8 1	7.002E-79
ACADS	80.909087 1	1.7561588	0.2386630 4	1.6505E-1 4	7.8468E-1 4
ABI1	173.07091 4	1.75535325	0.4069981 4	1.135E-06	2.4762E-0 6
NTN4	916.89749 5	1.75331849	0.1169365 1	7.925E-52	2.8517E-5 0
MAMDC4	25.962895 1	1.75312914	0.4251868 5	2.5718E-0 6	5.3732E-0 6
FOXO4	204.44287 8	1.75197945	0.1415722 4	3.4658E-3 6	6.4768E-3 5
C4orf19	97.977656 1	1.74806682	0.2029049 2	6.567E-19	4.3342E-1 8
FAM72D	116.92091 3	1.74782701	0.2163718	6.1274E-1 7	3.5099E-1 6
ACP5	95.296173	1.72732403	0.2850964 5	1.2622E-1 0	4.1899E-1 0
ATG9A	471.24303 4	1.72658198	0.2373164 9	3.357E-14	1.548E-13
C10orf95	26.179136 8	1.72340248	0.5145517 3	5.2453E-0 5	9.3602E-0 5
CDK11B	66.163348 6	1.72069221	0.6527951	0.0004302 8	0.0006813 8
LTBP3	662.3141	1.71745472	0.1944089 7	1.0471E-1 9	7.2725E-1 9

SLC44A2	199.22612 9	1.7155561	1.4792991 5	0.0081406	0.0109116 6
RCC1	1018.4781 6	1.70655287	0.1145065 7	3.528E-51	1.2303E-4 9
AFMID	12.518230 3	1.704513	1.4188204 1	0.0077473 3	0.0103989 4
CEP63	43.79383	1.69832831	0.5370813 2	0.0001054 4	0.0001811 3
MOSPD3	31.283901 6	1.69411773	0.4295280 8	6.6151E-0 6	1.3275E-0 5
MUC1	579.69755 3	1.69188947	0.2156740 1	4.7742E-1 6	2.5857E-1 5
CDH23	49.601784 5	1.69187002	0.500462	5.3116E-0 5	9.4661E-0 5
SORBS2	53.956444 7	1.68797934	0.2575124 9	5.9469E-1 2	2.2614E-1 1
AQP3	5206.8376 2	1.68750829	0.1077124 1	3.0484E-5 6	1.3305E-5 4
DNAH1	27.728309 7	1.68512028	0.5956163 4	0.0002944 1	0.0004762 6
ITGBL1	216.52489 1	1.68394108	0.2128969 6	2.9113E-1 6	1.5935E-1 5
NOP53	2572.5497 8	1.6818218	0.0877112 9	7.3927E-8 3	7.1445E-8 1
JOSD2	93.980613 2	1.68176183	0.2571404 1	6.6845E-1 2	2.5319E-1 1
FAM72C	94.238473 5	1.67968247	0.2476641 2	1.3095E-1 2	5.2856E-1 2
PYROXD2	54.046604	1.67705596	0.42221	6.2801E-0 6	1.264E-05
CDRT1	75.613620 2	1.67521008	0.2289668 5	2.9044E-1 4	1.3476E-1 3
LOC10537398 9	11.026056 1	1.67518035	0.6482750 6	0.0005791 4	0.0009010 8
ELMO3	740.36928	1.67371117	0.0805346 9	7.8189E-9 7	1.1499E-9 4
DLK2	55.772964 2	1.6714569	0.3897871 7	1.7016E-0 6	3.6393E-0 6
D2HGDH	41.288902 4	1.66753911	0.7612973 3	0.0014518 2	0.0021421 1
RNF135	87.741615 8	1.66741994	0.2787432 6	2.4445E-1 0	7.8898E-1 0
TNFAIP8L1	303.39350 6	1.66604767	0.1518804 2	6.6448E-2 9	8.3709E-2 8

VAV3	295.55887 4	1.66524515	0.1183557 4	7.3633E-4 6	2.0669E-4 4
FAM72B	156.44029 7	1.66501111	0.1783780 4	1.2443E-2 1	9.9145E-2 1
BICRAL	547.68284 4	1.66302468	0.2681382 4	6.3267E-1 1	2.1781E-1 0
BCAS3	7.2959341 4	1.6628378	2.3424129 8	0.0152021 6	0.0197016 5
TNS3	764.81697 7	1.65670106	0.1536176 3	5.1748E-2 8	6.207E-27
FAM135A	8.4872688 1	1.65578649	2.4039239 1	0.0153584 6	0.0198927 8
TCF25	97.590063 4	1.64691629	0.2564088 3	1.6076E-1 1	5.8534E-1 1
LANCL1	201.84396 3	1.64688339	0.2465792 6	2.9246E-1 2	1.1523E-1 1
FOXO6	29.163345 3	1.63990161	0.4009080 6	4.3903E-0 6	8.9622E-0 6
AKR1A1	217.62818 3	1.6391723	0.2739266 6	2.6296E-1 0	8.4469E-1 0
MR1	15.842863 9	1.63822998	1.3320929 6	0.0083909 8	0.0112272 5
FAM114A1	185.68665 7	1.6381892	0.3874545 4	2.4659E-0 6	5.1647E-0 6
DHFR2	145.0802	1.63546475	0.1607906 3	3.5675E-2 5	3.5702E-2 4
SUN2	326.13210 2	1.63418538	0.2947479 5	3.5313E-0 9	1.0042E-0 8
GTPBP6	14.710135 3	1.63345275	1.4583281 9	0.0100087 6	0.0132477 5
TCIRG1	562.65609 3	1.63191257	0.1655844 3	8.7609E-2 4	7.9023E-2 3
SLCO3A1	131.92823 5	1.63050404	0.2869260 3	1.6178E-0 9	4.7771E-0 9
ABCA2	928.41210 1	1.62908155	0.1553459 2	1.3593E-2 6	1.4856E-2 5
GBP4	601.69728	1.62370285	0.1165505	5.7858E-4 5	1.5656E-4 3
RIN1	12.305560 4	1.62346928	2.4080061 8	0.0160935 5	0.0207971 1
MBOAT1	238.36362 6	1.62314538	0.1463643 7	1.9654E-2 9	2.552E-28
TRANK1	374.83112 1	1.62273789	0.2495061 4	1.0144E-1 1	3.7685E-1 1



NRBP2	250.26914 8	1.62145993	0.2742084 9	4.254E-10	1.3348E-0 9
COASY	429.69340 9	1.61701003	0.1826441 8	1.1798E-1 9	8.186E-19
ATF6B	395.03856	1.61371528	0.1323711 2	5.018E-35	8.7944E-3 4
STS	289.81484 7	1.61283205	0.1777219 3	1.6013E-2 0	1.1711E-1 9
RGS3	33.870157 1	1.61263462	0.3793259 6	2.4223E-0 6	5.078E-06
SLC29A2	236.82379 6	1.61150918	0.153291	1.0831E-2 6	1.2012E-2 5
MAG	45.648611 3	1.61021716	0.3500806 3	5.0607E-0 7	1.1481E-0 6
ZMYM3	516.21444 9	1.60801282	0.2414496 3	3.7231E-1 2	1.4525E-1 1
TARBP2	105.30963 8	1.60788214	0.2097228 6	2.4623E-1 5	1.2571E-1 4
DGKH	188.24862 8	1.60350835	0.3801956 7	2.8845E-0 6	5.9969E-0 6
SF3B1	179.95642 9	1.60180383	0.1773015 5	2.3938E-2 0	1.7394E-1 9
ACER2	156.52692 1	1.59932178	0.2597594 3	1.0135E-1 0	3.4009E-1 0
FANK1	22.889201 4	1.59825123	0.4877328	0.0001045 9	0.0001799 1
EFCAB11	70.800942 8	1.5978177	0.3375499 6	2.7743E-0 7	6.4628E-0 7
ERBB2	42.216488 3	1.59357462	1.0747431 8	0.0063132 9	0.0085917 2
CDK19	159.74409 8	1.5921911	0.2539980 5	5.1044E-1 1	1.7727E-1 0
SLC37A4	30.298092 6	1.59150508	0.7187302	0.0017976 6	0.0026209 5
CAT	1113.4546 1	1.59028442	0.0594476 2	1.888E-15 8	9.124E-15 6
DDIT4	3867.9577 3	1.58815629	0.0873098 3	9.7361E-7 5	7.5707E-7 3
PAN2	20.150787 2	1.5880841	0.6719596 7	0.0013271 7	0.0019650 4
MPP7	59.568915 1	1.58679145	1.0790588 6	0.0065428 2	0.0088844 2
CAVIN2	52.393707 7	1.58235192	0.3078076 1	3.7209E-0 8	9.571E-08

DYNC211	152.08643 4	1.58221409	0.3193656 5	9.7438E-0 8	2.39E-07
H6PD	593.08151 6	1.57728999	0.1584022 6	3.6564E-2 4	3.3931E-2 3
MED25	401.28931 7	1.57372992	0.1474603	2.1788E-2 7	2.4982E-2 6
RPL10A	5447.7199 8	1.57236949	0.059606	3.884E-15 4	1.752E-15 1
R3HDM2	39.406026 2	1.57199604	0.6725827 6	0.0014873 7	0.0021902 5
OSBPL7	229.77281 7	1.57179424	0.2573871 8	1.4978E-1 0	4.9307E-1 0
HMMR	224.57436 9	1.57139487	0.3192107 8	1.179E-07	2.8629E-0 7
FRS2	11.187998 2	1.57107251	2.3607081 9	0.0174371 6	0.0224092 7
IGBP1	449.03142 3	1.56950886	0.1560456 6	1.3522E-2 4	1.3143E-2 3
SCARA3	36.908489 5	1.56800619	0.6684299 2	0.0014807 5	0.0021819 4
H2BC12	257.46114 3	1.56721212	0.1690728 2	2.9824E-2 1	2.3058E-2 0
MRPL43	35.933933 8	1.56705414	0.5316885 4	0.0003227	0.0005194 1
CTSF	81.306062 8	1.56618221	0.2845026 6	5.3733E-0 9	1.4953E-0 8
CROCC	219.68006 4	1.56479211	0.2158111	6.4391E-1 4	2.9177E-1 3
ATF4	308.23977 5	1.56448378	0.1470378 4	3.1537E-2 7	3.5857E-2 6
SEMA3F	311.53639	1.56157931	0.1062263 1	1.0662E-4 9	3.5184E-4 8
C19orf54	50.946826 3	1.56103838	0.9505763 3	0.0054205 3	0.0074411 2
PSMB10	957.76985 9	1.56074555	0.0932323 7	1.1163E-6 3	6.51E-62
AMOTL1	281.88563 5	1.55926295	0.2820391 3	4.7973E-0 9	1.3438E-0 8
TRPV6	1070.2510 8	1.55896325	0.1067862 3	4.7843E-4 9	1.5412E-4 7
PARVB	82.380489 6	1.55400783	0.3047285 3	5.0036E-0 8	1.2716E-0 7
REV1	31.998989 7	1.54578707	0.5619391	0.0006007 6	0.0009325 8

GALNT12	338.73329 8	1.54565041	0.1685908 3	8.1044E-2 1	6.0783E-2 0
DAPK2	104.28148 3	1.54462155	0.4448472 7	6.4303E-0 5	0.0001134 5
PNRC1	232.00476 8	1.53980792	0.1274080 1	2.1924E-3 4	3.6894E-3 3
CITED4	433.26683	1.53739869	0.1128958 4	5.532E-43	1.3912E-4 1
CNGA1	27.200157 8	1.53419334	1.3386437 7	0.0116771 5	0.0153419 9
AURKA	380.11162 9	1.53200459	0.1535820 7	3.4353E-2 4	3.2099E-2 3
CREB3L2	469.47920 1	1.53170691	0.2209357 8	6.9382E-1 3	2.8655E-1 2
KNTC1	707.79335 1	1.53049095	0.1746606 7	3.3192E-1 9	2.2477E-1 8
PCYT2	257.40823 3	1.53000692	0.1973954 9	1.5663E-1 5	8.1447E-1 5
TMEM187	52.301837 9	1.52822629	0.3032564 1	7.35E-08	1.8334E-0 7
GALK1	72.988975 8	1.52470882	0.2771797 7	6.1644E-0 9	1.7035E-0 8
TDP1	82.733427 5	1.5158631	0.3302426 9	6.9804E-0 7	1.5595E-0 6
CENPF	1066.6816 5	1.51567431	0.1687025 5	4.7141E-2 0	3.3428E-1 9
FUBP1	69.781797 8	1.51526712	0.3943425 9	1.7706E-0 5	3.3628E-0 5
UBA7	699.45792 7	1.51372865	0.1260336 9	5.8118E-3 4	9.4285E-3 3
CD22	350.45219 8	1.51172563	0.4274623 4	5.6686E-0 5	0.0001006 3
NKTR	168.39126 2	1.51164015	0.2616648 9	1.2993E-0 9	3.8705E-0 9
ZNF236	38.769909 5	1.51044312	0.5474690 3	0.0006633 1	0.0010230 9
MOV10	696.24302	1.50763507	0.2122104 6	2.1691E-1 3	9.4125E-1 3
PAIP2B	42.067445 1	1.50577445	0.3339005 6	1.0453E-0 6	2.2886E-0 6
CYP26A1	27.018973 4	1.50162154	0.6397730 6	0.0018639 4	0.0027123 1
DEPP1	174.86605 9	1.50042944	0.1669183 8	4.6891E-2 0	3.3286E-1 9

H2AW	72.356482 1	1.49905187	0.2429583 2	1.2228E-1 0	4.0628E-1 0
WNK2	98.628018 6	1.49325324	0.3127562 6	3.0636E-0 7	7.1099E-0 7
HADH	614.61937 7	1.49245586	0.0895702 2	4.864E-63	2.7885E-6 1
MFSD3	173.33587 5	1.49077193	0.1645777 7	2.5543E-2 0	1.8481E-1 9
HSPG2	1209.7791 7	1.49066007	0.3685453 5	8.3977E-0 6	1.6602E-0 5
SIAE	104.51856 2	1.49029375	0.1832465 8	8.0054E-1 7	4.5548E-1 6
TBC1D14	135.26527 4	1.49014469	0.3345342 3	1.4073E-0 6	3.0417E-0 6
VWF	43.510797	1.48587887	0.3754447 9	1.2171E-0 5	2.3626E-0 5
WDR27	27.524588	1.48580435	0.6617731 5	0.0024411 7	0.0034921 8
PEG10	628.93605 8	1.48497905	0.1052616 5	6.8385E-4 6	1.9276E-4 4
ORAI3	73.274222 9	1.48418211	0.2282413 6	1.481E-11	5.4184E-1 1
FGD3	62.493721 1	1.4782069	0.4138070 1	5.5063E-0 5	9.7949E-0 5
NUDT18	48.954577 5	1.47647344	0.2955214	1.0546E-0 7	2.5737E-0 7
TSHZ1	78.172475 2	1.47482487	0.3630822 8	8.1712E-0 6	1.6187E-0 5
RALGPS1	6.1988348 2	1.47472668	2.1354918 2	0.0204758 9	0.0260717 9
LAS1L	160.68757 2	1.47472161	0.1864801 7	5.1559E-1 6	2.7837E-1 5
FUCA1	218.26764 3	1.47436677	0.1582181 4	2.3668E-2 1	1.8489E-2 0
ADD3	139.06975 5	1.47282826	0.2417464 1	2.1219E-1 0	6.9011E-1 0
SVIL	189.89571 3	1.47211632	0.2854244 2	4.6021E-0 8	1.1726E-0 7
ZSCAN2	15.751000 8	1.47197063	1.3974459 9	0.0149000 2	0.0193471 5
FDFT1	347.55232 9	1.47174357	0.2323126 9	4.5685E-1 1	1.5923E-1 0
DNAJC4	104.99354 7	1.46963395	0.2126754 1	9.5058E-1 3	3.8739E-1 2

ZBED9	19.745676	1.46835047	0.4841558 3	0.0003464 4	0.0005552 3
FZD3	543.20298 2	1.46802339	0.1789443 8	4.6912E-1 7	2.7102E-1 6
MUC16	924.32971 5	1.46612493	0.2030391 9	1.0295E-1 3	4.5789E-1 3
MARCKS	2774.5830 3	1.46520737	0.0844173 6	3.7012E-6 8	2.431E-66
PLXNB2	816.48787 4	1.46388746	0.2225540 3	9.4481E-1 2	3.5158E-1 1
ADIRF	2314.0060 2	1.46382376	0.1217352 9	5.5118E-3 4	8.9633E-3 3
SSH3	1053.1668 8	1.46307781	0.0752871 3	8.5707E-8 5	8.9202E-8 3
DCAF11	185.14253	1.46161491	0.1961746 3	1.8801E-1 4	8.8821E-1 4
GSTO2	181.44582 2	1.45969814	0.2292298 3	3.809E-11	1.3386E-1 0
ADGRF1	3856.4939 6	1.45961508	0.0875797 7	4.9319E-6 3	2.8037E-6 1
H2BC21	89.144372 5	1.45875753	0.2938191 2	1.2959E-0 7	3.1322E-0 7
HR	140.41109 3	1.45704096	1.1517634	0.0119553 6	0.0156846 4
ANAPC16	327.07744 3	1.45467457	0.1324810 3	1.0106E-2 8	1.2567E-2 7
HPS4	49.753526 9	1.4482965	0.3666611 7	1.3943E-0 5	2.6843E-0 5
ZMIZ1	1121.1703 6	1.44688785	0.1284653 1	4.335E-30	5.8419E-2 9
BPTF	140.59167 9	1.44567274	0.2865328 7	8.857E-08	2.1836E-0 7
H2AJ	419.02829 7	1.44535225	0.1019058	2.5537E-4 6	7.3515E-4 5
MFSD11	22.493860 4	1.44493994	1.3206689 4	0.0150295 6	0.0195041 3
TRPC4AP	64.687993 6	1.44431352	0.4382888 4	0.0001606 1	0.0002690 1
MID1IP1	984.42505 3	1.44145238	0.1345537 8	1.938E-27	2.2334E-2 6
PRELID2	67.521148 1	1.44144491	0.4214787 9	0.0001056 2	0.0001813 9
FBXO46	89.732984 3	1.439882	0.3066639 4	5.1793E-0 7	1.1734E-0 6

MMAA	28.363763 3	1.4388046	0.6056922 6	0.0021720 3	0.0031263 4
C3	9625.6440 9	1.43860131	0.0899761 6	3.4249E-5 8	1.6316E-5 6
DPP7	348.95155 6	1.43772257	0.1372042 6	2.3841E-2 6	2.5682E-2 5
GIT1	74.273782 8	1.43599015	1.3818804 4	0.0163013 7	0.0210375 4
CCNG2	119.56324 8	1.4348093	0.2466272 4	1.2387E-0 9	3.7096E-0 9
PDK1	99.342534 9	1.43455933	0.2689843	1.968E-08	5.1924E-0 8
ANKMY1	18.389249 7	1.43310931	0.5858449 9	0.0018846	0.0027394 4
ALPK1	104.3843	1.4307113	0.3208793 4	1.6153E-0 6	3.4703E-0 6
RTN3	43.454116	1.43004166	0.4777225 9	0.0004391 9	0.0006946 7
MUC4	7966.4695	1.42991501	0.2416422 5	6.8905E-1 0	2.1198E-0 9
VPS28	433.44808 7	1.42936623	0.1038740 8	9.999E-44	2.6017E-4 2
LRATD1	420.89297 2	1.42679313	0.1238702 5	2.417E-31	3.4279E-3 0
CCDC146	45.916225 4	1.42605262	0.3141947	1.1285E-0 6	2.4642E-0 6
TLR5	39.548626	1.4259245	0.5811980 6	0.0018979	0.0027564
RIPK4	690.10273	1.42350655	0.0860722 4	4.4826E-6 2	2.3878E-6 0
GGA3	157.74691 1	1.42249034	0.3247643 8	2.3597E-0 6	4.953E-06
PLK1	1646.4624 9	1.42101076	0.0836459 3	2.3294E-6 5	1.4197E-6 3
HAUS4	476.05469 5	1.41940256	0.1041815 1	6.6662E-4 3	1.6641E-4 1
KLHDC2	233.65578 4	1.41937862	0.1859644 2	5.1558E-1 5	2.5404E-1 4
HEG1	944.78250 3	1.4179888	0.1472384 1	1.3612E-2 2	1.1511E-2 1
MPND	68.517894 4	1.41616056	0.2545227 3	5.6765E-0 9	1.5751E-0 8
DCAF6	215.85265 6	1.41604978	0.2101385 9	3.5545E-1 2	1.3899E-1 1

GAS6	1102.4748 8	1.4144527	0.0700350 6	2.4966E-9 1	3.0708E-8 9
SLC44A5	196.42319 6	1.41433869	0.1576264 6	6.6497E-2 0	4.6665E-1 9
KHDRBS1	169.45884 2	1.4143255	0.2929142 6	2.8776E-0 7	6.6943E-0 7
HIBCH	159.24616 2	1.41245166	0.1454794 3	6.4109E-2 3	5.5319E-2 2
ABTB1	309.23480 4	1.41175755	0.1291567 8	1.927E-28	2.3616E-2 7
RAB26	24.992454 3	1.41131273	0.8018163 2	0.0072915	0.0098221 8
MFSD10	774.23891 3	1.40719945	0.0898356 1	6.3678E-5 6	2.7265E-5 4
FBXL4	94.433437 4	1.40645202	0.6202892	0.0030576 6	0.0043219 9
MXRA7	73.097968 2	1.40595449	0.2651985 3	2.5079E-0 8	6.5429E-0 8
SLC44A1	389.98080 6	1.40505081	0.2044320 6	1.4379E-1 2	5.7867E-1 2
KRT13	173.30891 3	1.40219219	0.3245424 2	3.2448E-0 6	6.7046E-0 6
DUT	236.57465 8	1.40154754	0.1589882 4	2.8169E-1 9	1.9152E-1 8
FURIN	876.17623 4	1.40084378	0.1997766 5	5.435E-13	2.2668E-1 2
CBX7	209.42668 2	1.4005195	0.2553545 8	9.2325E-0 9	2.5205E-0 8
PHPT1	33.154176 8	1.4000271	0.4158654 8	0.0001429 6	0.0002414 1
RTP4	221.01474 9	1.39890696	0.1262181	3.6449E-2 9	4.6357E-2 8
ZNF580	109.86507 9	1.39834096	0.2061601 6	2.7322E-1 2	1.0784E-1 1
SYNPO	328.82011 7	1.39738362	0.2249935 6	1.2096E-1 0	4.0231E-1 0
ZNF775	20.444894 6	1.39605383	0.4662533 7	0.0004848	0.0007616 5
PLAC8	131.80094	1.39489162	0.2151003 2	2.0626E-1 1	7.4537E-1 1
COLCA2	20.543787 6	1.39339432	0.7640165 9	0.0070558 9	0.0095294 7
AMBRA1	219.44486 9	1.39249608	0.3753055 7	4.1687E-0 5	7.5465E-0 5

SPTBN2	85.989620 1	1.39195069	0.3482105 6	1.3321E-0 5	2.5704E-0 5
TYMP	188.18790 2	1.39149644	0.2014927	1.1767E-1 2	4.7638E-1 2
CAMK2N1	2123.4667 5	1.38713603	0.0888006 2	1.314E-55	5.5559E-5 4
INCENP	514.32728 5	1.38585465	0.2375615	1.2645E-0 9	3.7752E-0 9
FAM72A	126.54055 5	1.38415119	0.2580835 3	1.8846E-0 8	4.9841E-0 8
ARHGEF39	111.09514 8	1.381505	0.2987979 5	8.4472E-0 7	1.8693E-0 6
SSPN	103.71484 7	1.3809992	0.2549817 1	1.4174E-0 8	3.8095E-0 8
CRYBG1	143.62630 6	1.38028634	1.2548076 3	0.0172601 7	0.0221986 8
IFT80	354.50718 5	1.38025644	0.2144313 8	2.9257E-1 1	1.0422E-1 0
DLGAP5	323.34730 1	1.38021042	0.1192696 6	1.4333E-3 1	2.0587E-3 0
NMNAT3	14.438258	1.37910197	1.2630847 9	0.0174517 8	0.0224237 9
SOX4	404.60441 9	1.37867102	0.1171594 6	1.4493E-3 2	2.1982E-3 1
HMBOX1	6.3122625 3	1.37814925	2.0362985	0.0242183	0.0304926 1
TRPT1	17.805244 7	1.37790258	0.7591481 1	0.0075304	0.0101238 5
HDAC10	287.85763 7	1.37699921	0.1494512 4	7.8802E-2 1	5.9233E-2 0
ADGRG1	23.159476 6	1.37626286	1.5016452 1	0.0208837 2	0.0265311 5
IER5L	261.43097 9	1.37596288	0.1304765 2	1.3437E-2 6	1.4733E-2 5
USP21	89.267213 8	1.37530573	0.4802968 1	0.000759	0.0011598 5
SORL1	1021.7144 7	1.3735367	0.0745349 2	2.0189E-7 6	1.6455E-7 4
C1RL	220.37162 9	1.37310229	0.1575325 6	7.222E-19	4.748E-18
TRIM5	240.56884 6	1.37221735	0.1859511 6	3.9441E-1 4	1.8114E-1 3
LRRC20	98.754632 6	1.37023168	0.2539844 6	1.6337E-0 8	4.3545E-0 8



CACNG4	155.12534 5	1.36947773	0.2159909 9	5.6172E-1 1	1.9438E-1 0
KLK13	542.24581 3	1.36947106	0.2133008 2	3.3387E-1 1	1.1813E-1 0
ID3	362.20200 6	1.36933263	0.1702954 3	2.2445E-1 6	1.2395E-1 5
BEX3	644.50896 5	1.36370396	0.1304512	3.6511E-2 6	3.8715E-2 5
BMP8B	120.11525 8	1.36349569	0.2420239 4	4.3026E-0 9	1.2108E-0 8
ARHGAP19	434.68236 1	1.36328259	0.1917213 7	2.9094E-1 3	1.2441E-1 2
ARRDC3	418.61103 7	1.36304495	0.1426663 3	3.2211E-2 2	2.6803E-2 1
TBC1D22A	254.68239 1	1.36080165	0.3454679 6	1.8309E-0 5	3.4702E-0 5
MYLIP	164.48330 4	1.35930244	0.1382656 7	2.1575E-2 3	1.9104E-2 2
ENGASE	210.94062	1.35781384	0.1305243 5	6.3204E-2 6	6.6291E-2 5
AUH	80.576630 7	1.35502093	0.4399680 2	0.0004177 3	0.0006619 7
SIRT3	46.577271 1	1.35291813	0.3503920 1	2.5562E-0 5	4.7533E-0 5
USP47	8.5469434 9	1.35103868	2.2036303 7	0.0249277 4	0.0313275 4
YPEL1	16.884451 6	1.35046758	0.4753879 4	0.0008706 5	0.0013220 9
SLC25A6	2724.4165	1.35007739	0.0592646 2	1.946E-11 5	4.247E-11 3
SMIM19	96.850942 1	1.34717321	0.2791584 3	3.422E-07	7.8983E-0 7
KLF4	247.88475 6	1.3452705	0.1790615 5	1.5243E-1 4	7.267E-14
TOP2A	5341.3747 9	1.34421908	0.0485314 6	2.04E-169	1.15E-166
ANOS1	402.55863 2	1.34375139	0.1345891 5	4.8263E-2 4	4.4362E-2 3
C17orf49	140.39230 4	1.34346567	0.1713920 9	1.2104E-1 5	6.3675E-1 5
NUBP2	339.95392 8	1.34293962	0.1136060 6	8.2746E-3 3	1.2665E-3 1
HACE1	194.98482 1	1.34253175	0.2359100 5	3.2376E-0 9	9.2612E-0 9

PCED1A	314.73618 2	1.34160174	0.1093855 4	3.8212E-3 5	6.7671E-3 4
PXYLP1	82.842718 5	1.3415393	0.2936736 4	1.2074E-0 6	2.6256E-0 6
DMPK	92.051806 7	1.34022757	1.4224638 9	0.0219535 8	0.0278067 7
PHF3	43.930561 1	1.33951335	0.3379350 4	1.743E-05	3.3149E-0 5
NUDCD3	20.532898	1.33787397	0.5991779 9	0.0041172 3	0.0057346 3
ATF1	22.881815 5	1.33674657	0.5350622 4	0.0022619 6	0.0032474 9
ANKRD23	44.844855	1.33667516	0.2780667 1	3.8482E-0 7	8.8548E-0 7
KLK10	1497.3581 5	1.33618052	0.1522697 3	4.6447E-1 9	3.1049E-1 8
MEGF8	1223.2209 9	1.33570165	0.1135880 6	1.7502E-3 2	2.6312E-3 1
NBAS	378.06839 1	1.33492044	0.1969448 6	3.2462E-1 2	1.2738E-1 1
ZMYM2	76.753989 8	1.33456541	0.2471900 7	1.7321E-0 8	4.6096E-0 8
RABL2B	73.409074 2	1.33314368	0.4544489 2	0.0006958 8	0.0010689 4
ECT2	432.63693 3	1.3314282	0.3739808 9	8.5721E-0 5	0.0001491 9
NFIA	133.09890 3	1.33110711	0.4222851 3	0.0003534 3	0.0005656 4
PRICKLE4	250.96554 5	1.32831126	0.2000475 7	8.4658E-1 2	3.1764E-1 1
DENND6B	46.195915 8	1.32612095	0.5126528 6	0.0018688 6	0.0027188 9
ALDH5A1	102.44217	1.32500043	0.4171606 6	0.0003320 1	0.0005333 8
PEX7	69.346433 5	1.32481724	0.2344159 7	4.2296E-0 9	1.1922E-0 8
BTN3A1	75.575123 2	1.3246192	0.3965948 7	0.0001914 9	0.0003170 4
SLC25A26	51.558384 9	1.32454625	0.3321700 9	1.6385E-0 5	3.1276E-0 5
NCAPD2	3541.0356	1.32405345	0.0406352 6	1.996E-23 3	2.7E-230
JMJD8	451.09182 6	1.32200188	0.1085663 1	1.1739E-3 4	2.0259E-3 3

PDE5A	122.28080 9	1.31994646	0.1857180 9	3.2748E-1 3	1.3969E-1 2
TMEM135	91.703308 1	1.31923428	0.3406554 9	2.6499E-0 5	4.9127E-0 5
PAM	67.373925 5	1.31864681	0.3240910 7	1.184E-05	2.3002E-0 5
SPG11	550.60263 6	1.31830231	0.2492644 6	3.2861E-0 8	8.4978E-0 8
ACY1	299.64299 8	1.3175773	0.0998739 2	2.7923E-4 0	6.2757E-3 9
CDKN2C	235.18292 9	1.31639764	0.1580905 8	2.3445E-1 7	1.3816E-1 6
TBX19	64.444898 2	1.31615449	0.2688551 6	2.5914E-0 7	6.0576E-0 7
MED16	391.57166 8	1.31401628	0.1195945 4	1.2677E-2 8	1.5621E-2 7
BHLHE41	522.09093 5	1.31385945	0.1095037 7	1.0484E-3 3	1.6648E-3 2
EDAR	99.635682	1.31142437	0.3873308 7	0.0001687 8	0.0002815
RNPEPL1	639.68412 9	1.30638295	0.1128832 5	1.6578E-3 1	2.371E-30
PTPN13	376.71535	1.30580432	0.2904163	1.8335E-0 6	3.8969E-0 6
TMEM47	426.35262 6	1.30580103	0.1143604 8	9.9384E-3 1	1.3777E-2 9
KICS2	45.166323 7	1.30577772	0.3219110 7	1.2855E-0 5	2.489E-05
GLUL	1015.1950 6	1.30275949	0.1052326	9.9465E-3 6	1.7944E-3 4
CRIP2	737.59756 9	1.30099177	0.1316398 9	1.4528E-2 3	1.2983E-2 2
TMSB4X	20451.652 8	1.30062399	0.0665976 2	1.8454E-8 5	1.9507E-8 3
ZNF235	43.787370 7	1.29873166	0.2914608 7	2.2455E-0 6	4.7235E-0 6
INAVA	143.03185	1.29697722	0.9734095 1	0.0172469 9	0.0221859 5
FRMD4B	51.736920 5	1.29695935	0.4600854 8	0.0010757 8	0.0016161 8
TFAP2A	304.79867 3	1.29503294	0.1510155 5	2.9165E-1 8	1.8353E-1 7
RBM4	95.309467 1	1.29449581	0.2373193 4	1.3857E-0 8	3.7288E-0 8

BICRA	179.39097 3	1.29396877	0.3634310 6	9.3861E-0 5	0.0001624 4
CLDN7	137.40696 8	1.29245031	0.2042137 2	7.1458E-1 1	2.4427E-1 0
GSTA4	79.974936 8	1.29244417	0.2822233 7	1.2788E-0 6	2.7754E-0 6
SNCG	108.44975 9	1.29067786	0.2534731 3	9.9726E-0 8	2.4417E-0 7
UNKL	59.579249 4	1.29007315	0.6112524	0.0061330 5	0.0083582
TECPR2	210.22444 7	1.28997573	0.1430254 6	5.6749E-2 0	4.0032E-1 9
FRMD3	41.922661 8	1.28968468	0.9236883 5	0.0166148 6	0.0214175 9
OSER1	339.84985 5	1.28847162	0.1641466 9	1.2435E-1 5	6.5313E-1 5
ARID5B	237.87810 2	1.28724768	0.1802753 6	2.7551E-1 3	1.1796E-1 2
BIRC5	280.0517	1.28666485	0.1588667 6	1.6593E-1 6	9.2543E-1 6
SLC25A23	512.57689 6	1.27940041	0.1404552 5	2.546E-20	1.8441E-1 9
SECTM1	589.64911 5	1.27705984	0.2364777 6	1.9459E-0 8	5.1382E-0 8
TBC1D8	680.36890 1	1.27684594	0.1103927 9	1.8957E-3 1	2.6998E-3 0
RPL12	10654.694 2	1.2755946	0.0458319 6	5.621E-17 1	3.802E-16 8
ALG6	152.95312 1	1.27447231	0.1417415 6	7.5311E-2 0	5.2523E-1 9
DOC2A	35.331357 9	1.27298734	0.4817817 8	0.0018776 5	0.0027305
SSH1	11.260809 8	1.27284016	0.6711029	0.009467	0.0125774 2
DYNLT2B	69.878335 3	1.27226351	0.2374078 2	2.4702E-0 8	6.4521E-0 8
LRRC37A2	64.250433 9	1.27194657	0.3391510 4	4.8019E-0 5	8.6098E-0 5
TAF1C	268.61217 3	1.27156242	0.1853277	2.0808E-1 2	8.2802E-1 2
DPYD	142.67149 3	1.27086852	0.2189373 5	1.9305E-0 9	5.6659E-0 9
CCP110	117.97655 3	1.26992763	0.4280679 9	0.0007440 4	0.0011387 9

DET1	38.252184 9	1.26989356	0.7564378 9	0.0130479 3	0.0170667 6
ARHGAP27	19.685555 7	1.26905195	1.3739311 8	0.02602	0.0326456 4
MPST	122.11818 6	1.26762037	0.2371541 5	2.6915E-0 8	7.0005E-0 8
LLGL2	465.80597 4	1.26711417	0.2407222 9	4.1979E-0 8	1.0757E-0 7
GABRE	1365.2918 5	1.26660277	0.0996638 1	1.6809E-3 7	3.3445E-3 6
ID2	67.947204 4	1.26608672	0.3318004 5	3.762E-05	6.8432E-0 5
MPPED2	24.297182	1.265128	2.3834278 7	0.0270207 5	0.0338698 2
PRDM2	51.921844	1.26380527	0.4581095 6	0.0013957 8	0.0020634 7
HFE	105.65676 7	1.26340606	0.2012050 5	1.0445E-1 0	3.4979E-1 0
JARID2	140.29748 2	1.26106497	0.8720978 2	0.0173541 1	0.0223110 2
CLMN	637.15166 1	1.2609293	0.1080804 4	6.0554E-3 2	8.9054E-3 1
DTX4	787.20771 1	1.26040087	0.2056145	2.7074E-1 0	8.6805E-1 0
RTN4	100.41011 9	1.25993169	0.3803711 3	0.0002470 5	0.0004041 8
RPL13A	23334.011 2	1.2594211	0.0551253 1	5.149E-11 6	1.161E-11 3
ZBTB45	185.84610 4	1.25888262	0.1758388 5	2.5433E-1 3	1.0945E-1 2
IFT122	47.860057 6	1.25566089	0.6621198 4	0.0100213	0.0132617 5
ATP5F1D	533.38648 4	1.25411581	0.1297391 2	1.3505E-2 2	1.1449E-2 1
MAN2C1	271.49061	1.25405245	0.1994628 6	1.0114E-1 0	3.3955E-1 0
FKTN	32.806559 6	1.25327046	0.9062066 5	0.0188585 2	0.0241076 9
SORBS3	95.348668 2	1.25204226	0.2151515 1	1.8387E-0 9	5.4151E-0 9
AIG1	53.777507	1.24954313	0.3485642 4	9.5093E-0 5	0.0001643 6
EDEM2	318.33516	1.24911922	0.1233606 7	1.3859E-2 4	1.3432E-2 3

GEMIN8	126.35234 2	1.24736082	0.2130279	1.4963E-0 9	4.434E-09
LRP1	4237.0946 6	1.24480736	0.1443182 9	2.0849E-1 8	1.3231E-1 7
RACGAP1	388.03216	1.23996525	0.1916714 3	3.1778E-1 1	1.1273E-1 0
RAB34	105.30291 1	1.23877695	0.3142224 3	2.3986E-0 5	4.4812E-0 5
P4HTM	174.56670 2	1.23769825	0.1493636	3.8525E-1 7	2.2352E-1 6
KRTCAP3	141.61306 4	1.23658058	0.1857608 7	9.1102E-1 2	3.4031E-1 1
NFIB	25.780089 9	1.23613417	1.2070034 9	0.0261642 5	0.0328205 4
ERMP1	4901.2276 9	1.23602048	0.1042219 7	6.4623E-3 3	9.9584E-3 2
CASK	256.74365 3	1.23489674	0.1948931 8	7.6536E-1 1	2.6044E-1 0
LAT	65.474202 8	1.23484624	0.2767121 5	2.5005E-0 6	5.2307E-0 6
ABHD12	55.735383 8	1.23434026	0.3109546 1	2.1656E-0 5	4.0707E-0 5
CHMP2A	663.90714 9	1.23416488	0.0896789 4	1.4609E-4 3	3.7721E-4 2
EOLA1	6.8984768 9	1.23401508	1.9702123 5	0.0315727 4	0.0393061 5
TKFC	121.31971 1	1.23360294	0.2647909 7	9.9313E-0 7	2.1799E-0 6
PTBP2	5.9521041 4	1.23233682	1.9643690 5	0.0316936 2	0.0394493 8
ANKH	60.867292 8	1.23189832	0.3079703	1.9182E-0 5	3.6257E-0 5
CEP70	74.247775 8	1.23124921	0.3905417 2	0.0004527 8	0.0007148 3
NDRG2	200.14898 5	1.23109356	0.1848015 5	8.909E-12	3.3298E-1 1
TECPR1	99.662271 3	1.22974523	0.3493936 9	0.0001266	0.0002152 3
SCRN2	61.493005 7	1.22945028	0.2371616 4	6.9621E-0 8	1.7405E-0 7
PRR15	28.302902 3	1.22825981	0.4860342 5	0.0028665 3	0.0040662 7
RAB11FIP4	470.04249 2	1.22804153	0.1379235 1	1.8228E-1 9	1.2557E-1 8

ZNF286A	8.3654394 4	1.22799055	2.1532736 3	0.0306924 2	0.0382383 5
TUBB6	168.04647 2	1.22563402	0.1774013	1.6308E-1 2	6.5356E-1 2
LMBR1L	104.80314	1.22496568	0.3140171	2.9263E-0 5	5.3941E-0 5
DCP1B	53.021868 9	1.22444842	0.2562185 1	5.6327E-0 7	1.271E-06
ETHE1	558.34882 3	1.2231622	0.0992261	2.235E-35	3.9999E-3 4
PHLPP1	583.29179 1	1.22195613	0.1145893 5	5.1749E-2 7	5.8347E-2 6
JAG2	785.18694 4	1.2209145	0.1754787 7	1.166E-12	4.7263E-1 2
ARSA	67.835913 8	1.2199594	0.2427245 2	1.6279E-0 7	3.8832E-0 7
MKS1	155.28405 5	1.2196235	0.4471750 9	0.0017085 2	0.0024985 2
TCTN1	66.546110 9	1.219101	0.2327424 6	5.3217E-0 8	1.3484E-0 7
DPH6	57.744367 5	1.2184083	0.2602195 6	9.1483E-0 7	2.0179E-0 6
SRGAP3	259.98524 3	1.21837629	0.1210893 8	2.8179E-2 4	2.6514E-2 3
EFEMP1	574.20439 2	1.21787907	0.1108381	1.5168E-2 8	1.8657E-2 7
NR2F2	393.98428 8	1.2123953	0.1604253 4	1.417E-14	6.7648E-1 4
DNPH1	684.1045	1.21176165	0.1082875 9	1.5995E-2 9	2.097E-28
METTL25B	113.27378 2	1.21167137	0.2611926 4	1.1423E-0 6	2.4904E-0 6
KRT5	26940.180 1	1.20884998	0.0783275 9	3.4793E-5 4	1.3606E-5 2
ARHGEF10L	107.00943	1.20794239	0.5525190 4	0.0067559 3	0.0091499 2
CENPX	110.39315	1.20654221	0.1964507 9	2.7958E-1 0	8.947E-10
TBCK	79.812147	1.2054759	0.2614612	1.3254E-0 6	2.8701E-0 6
MUC20	1097.4010 9	1.20317447	0.2465492 2	3.55E-07	8.1852E-0 7
ACP6	128.86750 5	1.20106709	0.1898692 1	8.745E-11	2.9565E-1 0

CHEK2	14.339848 4	1.20082983	0.9507344 8	0.0244904 6	0.0308066 1
PLAAT4	738.56514 3	1.20074335	0.1548099 8	3.0858E-1 5	1.5544E-1 4
GCNT4	56.754146 5	1.19995472	0.2766847 4	4.7662E-0 6	9.6855E-0 6
PLA2G4A	64.368595 2	1.19994189	0.2853991 1	8.5774E-0 6	1.6922E-0 5
QARS1	2385.8974 6	1.19822123	0.0437458 7	1.298E-16 5	6.753E-16 3
ZNF516	70.238691 3	1.19813588	0.2920901 6	1.3403E-0 5	2.5855E-0 5
SGSM3	24.480336 1	1.19742315	1.3603394 2	0.0315600 7	0.0392976
FASN	17425.661 5	1.19734494	0.1030880 7	1.2518E-3 1	1.8134E-3 0
PPP6R2	40.133436 5	1.19725975	0.3930397 3	0.0006917 9	0.0010633 9
PPP3CB	221.79370 3	1.19613384	0.2668747 9	2.4735E-0 6	5.1774E-0 6
NDE1	110.22847 4	1.19593423	0.1840005 8	2.8286E-1 1	1.0103E-1 0
CREG2	43.810889 2	1.1942025	0.2967821 9	1.8801E-0 5	3.5567E-0 5
GALM	62.694212 1	1.1925941	0.2588125 9	1.3768E-0 6	2.9777E-0 6
EXTL3	1393.9467 5	1.19245633	0.4325124 4	0.0016791 2	0.0024581 8
BAG1	168.08471 1	1.19235717	0.1396303 4	4.86E-18	3.0163E-1 7
SLX1A	994.81571 1	1.19226638	0.0607573 9	3.5885E-8 6	3.8534E-8 4
ABRAXAS1	48.324741 2	1.19202459	0.3186711 6	5.9452E-0 5	0.0001053 4
ROGDI	323.8451	1.19081356	0.1319805 5	6.6487E-2 0	4.6665E-1 9
PIR	594.61573 1	1.19071977	0.0924466 3	2.135E-38	4.4994E-3 7
SPATA20	134.89887 1	1.19049484	0.3690181 3	0.0003890 6	0.0006188 6
NUMB	42.735261 7	1.18954768	0.7276682 8	0.0180400 5	0.0231269 5
KLHL13	107.14887 1	1.18906191	0.2674889	2.9735E-0 6	6.1742E-0 6



RPP25L	266.54623 9	1.18872082	0.1375467 9	1.9986E-1 8	1.2719E-1 7
FAM120C	105.63491 7	1.18868472	0.2726852 3	4.4092E-0 6	8.9979E-0 6
VMP1	269.93083 3	1.187556	0.3620823	0.0003261 3	0.0005246 7
MON2	83.585408 1	1.18695909	0.3962207 4	0.0008308	0.0012638 5
MTR	368.94263 6	1.18644126	0.4424372 7	0.0021085 5	0.0030427 3
DHRS3	339.77434 9	1.18582386	0.1740898 3	3.4695E-1 2	1.3575E-1 1
RNF165	100.31340 2	1.1832043	0.3401095 5	0.0001627	0.0002721 6
GSTZ1	83.302386 5	1.18292276	0.2137171	1.1024E-0 8	2.9902E-0 8
OMA1	245.58093	1.1823858	0.1197954 2	2.0718E-2 3	1.8394E-2 2
ST6GALNAC6	97.557300 8	1.18230714	0.5020900 9	0.0049611 7	0.0068452 7
WBP1	226.56610 4	1.18220537	0.1426716 3	4.2834E-1 7	2.4809E-1 6
RCCD1	259.85143 3	1.18202088	0.1652738 2	3.1086E-1 3	1.3276E-1 2
CBX6	236.95725 4	1.18121417	0.2847697 5	1.1385E-0 5	2.2184E-0 5
TAPBP	164.12824 8	1.1803828	0.9778093 7	0.0271049 8	0.0339628
SH3BGRL	135.83281 4	1.18020174	0.1639494 5	2.2184E-1 3	9.6115E-1 3
CELSR1	1078.2599 6	1.18001237	0.1454041 1	1.7789E-1 6	9.8964E-1 6
GPC1	4110.0674	1.17993854	0.0483811 2	8.544E-13 2	2.752E-12 9
MARK2	284.08862 7	1.17787131	0.8970901 3	0.0254177 2	0.0319314 6
CUTC	198.83911 8	1.17658066	0.1428454 8	6.5474E-1 7	3.7442E-1 6
PML	493.17627 5	1.17600778	0.1369312 4	3.2755E-1 8	2.048E-17
ZFP62	55.993913 7	1.17514069	0.3259268 1	0.0001034 6	0.0001781
EIF4A2	4380.8647 6	1.17501692	0.0538588 6	6.124E-10 6	1.12E-103

FBXO4	42.196789 1	1.17445848	0.3542274 9	0.0002965 4	0.0004793 5
C2CD5	58.346228	1.17371541	0.5059968 2	0.0055144 1	0.0075592 7
TBCD	353.49349 5	1.17331717	0.1736754 2	5.2204E-1 2	2.0066E-1 1
ZNF337	255.49115 8	1.17324186	0.1400944 6	2.0634E-1 7	1.2255E-1 6
U2SURP	596.08971 4	1.17129037	0.1482882 3	1.05E-15	5.5536E-1 5
SDHAF4	25.814446 5	1.170674	0.4329119	0.0020558 9	0.0029699
IKBKE	355.97458	1.1706737	0.1478427 6	8.9796E-1 6	4.7794E-1 5
G6PC3	370.75285	1.17037121	0.1216669	2.4927E-2 2	2.0922E-2 1
FBXW4	225.00201 2	1.16888648	0.1188643 9	3.0443E-2 3	2.6781E-2 2
SCX	71.933448 9	1.16766986	0.2346552 4	2.3333E-0 7	5.4826E-0 7
ALDH3A2	1011.0038 5	1.16753148	0.0703426	2.7719E-6 2	1.4882E-6 0
DUOX2	235.35079 5	1.16728772	0.1554890 5	2.2607E-1 4	1.0599E-1 3
PPP1CB	452.44970 1	1.16657838	0.2700794 3	5.511E-06	1.1152E-0 5
FDXR	353.75725 6	1.16524883	0.1076564 7	1.0137E-2 7	1.1824E-2 6
SLC24A1	35.393798 1	1.16430216	0.4256687	0.0019110 5	0.0027743 1
AGRN	10374.590 5	1.16184816	0.0623722 3	7.4336E-7 8	6.286E-76
FOXA1	324.60777 3	1.15852301	0.1257433 8	1.2135E-2 0	8.9624E-2 0
SBF2	567.48645 1	1.15744141	0.1817100 9	7.1308E-1 1	2.4388E-1 0
PLD1	8.1372535 6	1.1534889	2.0979213	0.0352422 5	0.0435936 7
RNF207	191.70991 6	1.15322076	0.2630352	4.2177E-0 6	8.6281E-0 6
GRAMD1C	72.122492 9	1.15319224	0.3651882 5	0.0005305 6	0.0008296 9
GLB1	165.09287 7	1.15287438	0.4336635 7	0.0024366 8	0.0034865

BCKDHB	79.640484 8	1.15253399	0.2880316 2	2.2454E-0 5	4.2124E-0 5
IRX3	475.93569	1.14889559	0.1596211 3	2.3634E-1 3	1.0203E-1 2
ADAMTS16	58.584745 4	1.14866916	0.2880379 8	2.3935E-0 5	4.4742E-0 5
SORCS2	463.65282 5	1.147181	0.1590561 3	2.1271E-1 3	9.2538E-1 3
DMAC2	283.51871 9	1.14694898	0.1935155	1.1771E-0 9	3.5298E-0 9
CNOT6L	396.40740 2	1.14675779	0.2233302 7	1.0608E-0 7	2.5869E-0 7
CCDC103	36.545824 7	1.14628786	0.4613154 2	0.0039383 6	0.0055002 1
H2AC18	93.090377 5	1.14514568	0.2414457 1	7.8532E-0 7	1.7447E-0 6
MAGEA4	561.50114 3	1.14229366	0.1917304 5	9.8354E-1 0	2.9757E-0 9
APOL1	1606.3426 7	1.14105052	0.1295433 4	5.0241E-1 9	3.3486E-1 8
ZNF225	42.242369 5	1.13981876	0.5091064 4	0.0072576	0.0097784 7
WDFY3	84.132803 6	1.13838118	0.4717524 7	0.0048146 6	0.0066553 3
ZFP36L2	2863.6761 6	1.13779339	0.0592535 6	1.4358E-8 2	1.3681E-8 0
BOLA1	102.02516 3	1.13762822	0.1883502 7	5.9879E-1 0	1.8514E-0 9
FIGN	220.80712 5	1.13701314	0.1773353 5	5.6255E-1 1	1.9456E-1 0
PRSS21	46.676963 7	1.13637424	0.6130363 2	0.0156619 9	0.0202587 7
NECTIN1	2956.9461 1	1.13591653	0.0770315 5	1.3169E-4 9	4.3246E-4 8
PIK3C2B	349.64712 4	1.13579164	0.2834291 8	2.2633E-0 5	4.2436E-0 5
C8orf82	357.88644 6	1.13563215	0.1355542 7	2.1488E-1 7	1.2707E-1 6
TSC22D3	766.70345 9	1.13471505	0.1217922 2	4.8014E-2 1	3.6619E-2 0
SIN3A	63.464879	1.13389017	0.8644928 2	0.0294010 6	0.0366835 5
DOCK7	168.54386 7	1.13247315	0.2525312 4	2.7657E-0 6	5.7534E-0 6

TRAPPC1	108.46051	1.13108585	0.1824515 9	2.2327E-1 0	7.2512E-1 0
MZT2A	43.792160 8	1.13088084	0.3364404 3	0.0002766 8	0.0004496 2
BABAM2	289.66100 8	1.12943358	0.1338375 1	1.2901E-1 7	7.7715E-1 7
THBS3	236.77291 3	1.12845299	0.2143950 7	5.5073E-0 8	1.3928E-0 7
YPEL3	288.48721 7	1.12627631	0.1427654 4	1.2289E-1 5	6.4599E-1 5
VPS13A	252.13423 8	1.12518319	0.1082477 7	1.0728E-2 5	1.108E-24
GPCPD1	480.01465 5	1.12364421	0.0925744 4	2.7401E-3 4	4.577E-33
DEAF1	183.15914 9	1.12275682	0.2682235 6	1.082E-05	2.1112E-0 5
FDPS	800.15153 8	1.12198587	0.1222248 6	1.7686E-2 0	1.2907E-1 9
SLC35E2B	720.30501	1.12091806	0.1030769	6.2766E-2 8	7.4888E-2 7
CKAP2	119.81320 5	1.12019774	0.3221616 8	0.0001864	0.0003092 9
ZNF658	41.482085 8	1.11972651	0.3564193 5	0.0006006 6	0.0009325 8
NR6A1	130.69898 9	1.11947228	0.7815101 7	0.0281475 5	0.0352169 7
PAQR4	523.21762 9	1.11858688	0.1536469 8	1.3564E-1 3	6.0051E-1 3
TMEM106B	61.567411 8	1.11725158	0.2701397 6	1.3583E-0 5	2.6187E-0 5
AASDH	96.037682 2	1.11695357	0.9017044 3	0.0325486 1	0.0404614 7
JRK	1067.6529 8	1.11519976	0.0763034	9.3817E-4 9	2.9937E-4 7
KDM3A	435.52037 2	1.11438112	0.2989963 7	7.3268E-0 5	0.0001285 8
PAX9	509.58564 2	1.11352692	0.1043058 7	5.5204E-2 7	6.2139E-2 6
MYOF	4125.7218 9	1.11262506	0.0894246 3	6.4738E-3 6	1.1901E-3 4
ARNT	155.11450 2	1.11196291	0.3163028 3	0.0001645 3	0.0002750 9
RNF167	63.446763 8	1.11103671	0.3100390 4	0.0001278 8	0.0002172

GPR108	348.71287 3	1.11086709	0.1607383 1	1.9784E-1 2	7.8914E-1 2
CILK1	468.15353 5	1.11051246	0.1276147 1	1.3564E-1 8	8.7978E-1 8
DDHD2	35.592045 3	1.10962652	0.6695567	0.0228008 4	0.0288044 2
KIFC1	419.86379 6	1.10918831	0.1024347 2	1.0627E-2 7	1.2373E-2 6
BPHL	134.30809 2	1.10823746	0.1576914 1	8.6695E-1 3	3.5567E-1 2
JADE1	84.087582 8	1.10786288	0.1896315 5	2.103E-09	6.148E-09
CCNB2	1013.4649 9	1.10765659	0.0763813 9	5.0092E-4 8	1.5333E-4 6
PRKAB2	510.67542 7	1.10473087	0.1191827 1	7.8992E-2 1	5.931E-20
SERPINB6	99.493809 7	1.10416414	0.2473909 6	3.2159E-0 6	6.649E-06
IQGAP3	1241.9911	1.10299127	0.1429682 8	5.0751E-1 5	2.5042E-1 4
S100P	1931.8943 2	1.10276703	0.1311757 4	1.7744E-1 7	1.0576E-1 6
CDC25B	901.99813 4	1.10237139	0.2184948 8	1.8389E-0 7	4.3649E-0 7
GOLGB1	609.52059 2	1.10217061	0.4354376 5	0.0038696 6	0.0054076 1
KAT5	173.50642 5	1.10124369	0.4254088 6	0.0033222 6	0.0046754 9
ZNF652	261.06993 1	1.10119859	0.2936325 9	6.8605E-0 5	0.0001207 7
LRBA	855.91123 8	1.10095569	0.0707908 1	6.5854E-5 5	2.6677E-5 3
PECR	71.214702 4	1.10067446	0.2227631	3.1579E-0 7	7.3211E-0 7
LPCAT4	437.71621 7	1.09760679	0.1449143 8	1.5277E-1 4	7.2782E-1 4
TRIM6	179.72259	1.09669372	0.1891164 5	2.7737E-0 9	8.0086E-0 9
TMEM107	123.44273 8	1.09605447	0.2107748 4	8.2055E-0 8	2.0304E-0 7
PTPN18	183.80517 3	1.09567937	0.3416301 1	0.0005061 9	0.0007935 9
DAPK1	391.35980 4	1.08971442	0.2415746 7	2.6433E-0 6	5.5089E-0 6

TEF	635.56426 7	1.08914751	0.1459506 5	3.6386E-1 4	1.6756E-1 3
HBP1	169.86944 6	1.08810102	0.2874362 1	6.1161E-0 5	0.0001081 7
NIPSNAP2	1877.6118 1	1.08801421	0.0713551 1	7.4424E-5 3	2.7971E-5 1
CCDC191	67.959871 5	1.08786494	0.2424153 9	2.9567E-0 6	6.1431E-0 6
TSNARE1	28.803504 6	1.08652261	0.7068617 5	0.0283988 9	0.0355051 7
EPS8L1	271.55624 8	1.08633447	0.2087487 8	8.172E-08	2.0228E-0 7
IKBKB	366.12608 6	1.08597608	0.2910725 1	7.6147E-0 5	0.0001334 2
SLC50A1	180.46112 4	1.08464006	0.1447829	2.9396E-1 4	1.3621E-1 3
CKS2	706.95978 1	1.08442705	0.1048861 7	2.0496E-2 5	2.0695E-2 4
ZBTB12	48.456450 3	1.08319746	0.3758036 5	0.0014777 4	0.0021779 7
ATXN10	1730.7119 4	1.083067	0.0529072 9	1.7261E-9 3	2.1625E-9 1
PPP1R3E	59.35376	1.08214665	0.2540688 2	8.4403E-0 6	1.6676E-0 5
SLC22A23	178.13337 5	1.08201573	0.1987314 8	2.2016E-0 8	5.7841E-0 8
BTBD2	1286.4438 7	1.0818958	0.1245367 3	1.6189E-1 8	1.0361E-1 7
EDIL3	223.3917	1.08096092	0.1904900 6	5.9264E-0 9	1.6411E-0 8
ZNF524	110.76882 6	1.08090084	0.1832834 5	1.5795E-0 9	4.6722E-0 9
CLDN11	400.23767 6	1.08000239	0.0969787 8	3.6753E-2 9	4.6648E-2 8
OSBPL9	189.95078 6	1.07977416	0.2938749 3	9.6017E-0 5	0.0001657 4
TJP3	73.856733 6	1.07923162	0.4488848 4	0.0056614 6	0.0077514 2
NF1	1692.4569 3	1.07860659	0.0752320 8	5.6994E-4 7	1.6691E-4 5
SSBP4	91.834348 6	1.07839963	0.3715165 2	0.0014020 8	0.0020718 8
PRKD2	330.34196 6	1.07752857	0.1450302 9	4.7528E-1 4	2.1696E-1 3

CAV1	3460.047	1.07719774	0.0687754 6	1.2152E-5 5	5.1703E-5 4
MTIF3	56.444043 1	1.07644128	0.3025899 5	0.0001506 5	0.0002533 9
SEMA4F	55.752574 1	1.07600871	0.2672475	2.3366E-0 5	4.3714E-0 5
CLIC1	14.277183 2	1.07568335	2.1042030 1	0.0399775 8	0.0491238 4
TLE3	408.58226 3	1.07319811	0.1525731 1	8.7999E-1 3	3.608E-12
SH3YL1	74.770885 2	1.06982477	0.5044293 7	0.0112506 1	0.0148218 8
TMEM179B	320.42885 5	1.06879581	0.0959524 7	3.6455E-2 9	4.6357E-2 8
GTF2I	3518.1745 1	1.06830268	0.0721061 8	5.2366E-5 0	1.7682E-4 8
NECAB3	259.01821 4	1.06644803	0.1594180 8	9.8901E-1 2	3.6782E-1 1
IFT172	160.83196 2	1.06640835	0.2966645 1	0.0001334	0.0002261 8
MITD1	117.09981	1.06635936	0.2726406 6	3.8331E-0 5	6.9595E-0 5
RPS9	426.15502 2	1.06592259	0.1558925 2	3.5688E-1 2	1.3947E-1 1
SDC1	591.86840 9	1.06543556	0.1761478 6	6.4293E-1 0	1.9833E-0 9
ITGB1	155.75305 1	1.06519249	0.2771870 1	5.0708E-0 5	9.0655E-0 5
PIGZ	164.84848 7	1.06508221	0.1715747 8	2.3708E-1 0	7.6703E-1 0
SET	88.995590 6	1.06476093	0.4574343 7	0.0070735 1	0.0095513 6
ARHGAP12	246.62674 3	1.06439627	0.1901854	9.5713E-0 9	2.6088E-0 8
TSPAN1	2298.8971 3	1.06312891	0.0588283 2	2.4275E-7 3	1.8246E-7 1
PIP5KL1	64.770694 1	1.06263364	0.2301854 9	1.681E-06	3.5977E-0 6
HMGCS1	92.185145 4	1.06216295	0.4564167 7	0.0071241 8	0.0096121
STK25	285.10487 9	1.06204469	0.1916469 2	1.316E-08	3.5469E-0 8
NUMA1	1260.2516 9	1.06067715	0.1117926 8	1.0678E-2 1	8.5788E-2 1

FAM193B	63.253414	1.06017216	0.3778769 5	0.0019519 5	0.0028276
THSD4	472.84414 5	1.0601588	0.1742348	5.1818E-1 0	1.6117E-0 9
PHKB	753.08748 4	1.06014001	0.1436021 8	6.9758E-1 4	3.144E-13
CDK16	186.09611 3	1.05863272	0.1515628 5	1.2805E-1 2	5.1716E-1 2
TXNRD3	110.27600 8	1.05834234	0.3061237 2	0.0002255 9	0.0003704 2
SMARCA2	251.34187 4	1.05831026	0.2763980 7	5.4295E-0 5	9.666E-05
SHFL	13.772904 1	1.05779746	0.6980841 6	0.0319446 3	0.0397471 9
AGAP5	213.15168 5	1.05710313	0.1107667 2	6.2905E-2 2	5.1333E-2 1
PTK2B	124.01720 1	1.0550913	0.2961961 6	0.0001539 4	0.0002585 4
G2E3	74.490326	1.05430825	0.7211908 3	0.0341261 1	0.0423291 4
ASIC1	117.91784 2	1.05269678	0.2387869 8	4.5317E-0 6	9.2368E-0 6
XXYLT1	287.90581 4	1.05163466	0.2202703 5	7.9433E-0 7	1.763E-06
PLEKHA2	692.02077 4	1.0508577	0.2120516	3.1919E-0 7	7.3898E-0 7
RFX7	112.26638 8	1.04867459	0.2291712 9	2.0882E-0 6	4.4146E-0 6
PEX2	270.95316 7	1.04675668	0.2182687 2	7.2015E-0 7	1.6068E-0 6
EGFL8	37.824887 5	1.0458883	0.3101458 3	0.0003135 8	0.0005054 6
RPS29	1958.8692 1	1.04571705	0.1269376	8.0801E-1 7	4.5896E-1 6
HMGB1	143.51136 2	1.0446176	0.2454529	9.1488E-0 6	1.8007E-0 5
PBX2	582.00037 4	1.04439809	0.2043879 5	1.4473E-0 7	3.4811E-0 7
FZD4	186.93047 4	1.04396726	0.1404407 8	4.8741E-1 4	2.2204E-1 3
CDPF1	77.973334	1.04231115	0.2131515 7	4.5228E-0 7	1.0326E-0 6
RNF145	520.51036	1.04194378	0.2023823 7	1.1852E-0 7	2.8769E-0 7



PER3	188.04058 8	1.04185941	0.2301766	2.6703E-0 6	5.5619E-0 6
PATJ	739.02670 6	1.04046301	0.1048133 1	1.4897E-2 3	1.3295E-2 2
HID1	153.77785 9	1.03934271	0.2121340 6	4.3325E-0 7	9.9051E-0 7
PDLIM1	4365.0593 7	1.038666	0.0719296 3	1.3691E-4 7	4.1534E-4 6
C16orf54	551.03139 3	1.03856761	0.1064761 9	8.3227E-2 3	7.127E-22
PC	866.32756 2	1.03804552	0.1530493 6	5.4727E-1 2	2.0976E-1 1
CMTM4	1511.6327 5	1.03785102	0.2239386 1	1.6071E-0 6	3.4535E-0 6
PPARA	80.314007 7	1.0374749	0.5415456 1	0.0185086 8	0.0236962 9
ALKBH7	105.04143 9	1.03639662	0.2449333 5	1.0342E-0 5	2.0238E-0 5
NAAA	75.267264 7	1.03584318	0.3465872 6	0.0011647 3	0.0017409 2
PLCD1	266.59517 8	1.03498329	0.1683541 3	3.638E-10	1.1511E-0 9
EEF2K	174.81719 9	1.03410141	0.2508512 2	1.6698E-0 5	3.1839E-0 5
ZNF224	202.78580 7	1.03373837	0.1825167 8	6.8238E-0 9	1.8796E-0 8
MDK	133.53531 1	1.03367358	0.2144396 1	6.5104E-0 7	1.4579E-0 6
MVP	1137.9755 6	1.03357685	0.1275982 6	2.5786E-1 6	1.4194E-1 5
AK4	134.68769 4	1.03252491	0.2499526 1	1.614E-05	3.0843E-0 5
NDST2	251.75401 9	1.03127536	0.1416431 2	1.5587E-1 3	6.8561E-1 3
RPS27	7985.7446 1	1.03039949	0.0689301 5	7.6311E-5 1	2.6205E-4 9
PTMA	1990.2611 1	1.03001279	0.1417173 6	1.716E-13	7.5249E-1 3
MAB21L4	193.30542 9	1.02973769	0.2513603 9	1.8787E-0 5	3.555E-05
TTC30A	238.40153 4	1.02931385	0.1221299 2	1.666E-17	9.9742E-1 7
UPK3BL1	1132.0332 8	1.02884294	0.1189595 1	2.4729E-1 8	1.5635E-1 7

TPP1	1641.6242 3	1.02605309	0.0635492 7	5.8637E-5 9	2.8538E-5 7
CHD6	591.37617 5	1.02603584	0.3607331 2	0.0018581 3	0.0027044 5
CENPH	394.94284 7	1.02467086	0.1027096 8	9.276E-24	8.3447E-2 3
DSC3	1357.6033 4	1.02445449	0.1299850 8	1.5429E-1 5	8.029E-15
ALDH6A1	173.49762	1.02384882	0.1416202 7	2.3022E-1 3	9.9515E-1 3
DGAT1	396.49907 2	1.02256134	0.1335161 5	8.9615E-1 5	4.3303E-1 4
COG8	170.49772 1	1.01887067	0.2064642 2	3.7417E-0 7	8.6155E-0 7
TTC39B	170.50454 4	1.01877738	0.1497423 1	4.8729E-1 2	1.8762E-1 1
DENND11	308.10063 7	1.01762387	0.1072099	1.0986E-2 1	8.8058E-2 1
SREBF2	4342.4625	1.01717662	0.0397084 3	4.943E-14 5	2.09E-142
FAT2	3789.9497	1.01712274	0.1017544 8	7.7103E-2 4	6.9826E-2 3
STX16	1236.2310 4	1.0163201	0.1588386 8	7.4967E-1 1	2.5562E-1 0
ARL6IP4	594.06743 6	1.01594922	0.1307761 3	3.827E-15	1.9078E-1 4
FIG4	204.90458 9	1.0149849	0.1401217 8	2.1043E-1 3	9.1667E-1 3
IQCA1	135.64480 9	1.01463606	0.2465656 6	1.7804E-0 5	3.38E-05
ZBTB5	435.52178 1	1.01440111	0.0786085 4	2.0791E-3 8	4.4092E-3 7
UNC93B1	1201.1452 9	1.01434218	0.0713952 5	4.0392E-4 6	1.153E-44
NDUFAF3	303.07981 2	1.01407623	0.1001145 2	1.9997E-2 4	1.9081E-2 3
EFHC1	457.21350 2	1.0140014	0.0897138 5	6.2246E-3 0	8.3056E-2 9
TRIM34	126.64385 8	1.01390969	0.2366329 6	8.4706E-0 6	1.6723E-0 5
PIGN	91.951986 4	1.01344441	0.2721611 5	8.9135E-0 5	0.0001546 5
MBOAT2	124.16513 2	1.01279936	0.2847875 5	0.0001695 6	0.0002826

OBSL1	673.05378 9	1.01220652	0.1016442 2	1.1335E-2 3	1.0184E-2 2
MYO18A	1020.8492 6	1.0112154	0.1285343 3	1.7615E-1 5	9.1105E-1 5
HYAL2	159.78399 7	1.01099597	0.2063459 5	4.5354E-0 7	1.0341E-0 6
ASS1	271.05574 5	1.01077342	0.1663516 2	5.9126E-1 0	1.8306E-0 9
RNASE10	256.29177 7	1.01020176	0.1359249 1	5.1928E-1 4	2.3608E-1 3
OARD1	143.36372 8	1.01007572	0.1531474	2.0479E-1 1	7.4085E-1 1
CDC42	353.92104 2	1.00933946	0.1932335 3	8.3618E-0 8	2.0675E-0 7
RPGRIP1L	16.766424 3	1.00922491	0.5878655 3	0.0282352	0.0353201 1
VSIR	3078.0787	1.00903164	0.1228681 8	1.0596E-1 6	5.9489E-1 6
ETAA1	51.539338 9	1.00878102	0.3263515	0.0008792 5	0.0013342 6
THBD	3012.8155 7	1.00860035	0.0612391 7	2.9909E-6 1	1.5446E-5 9
LMO4	37.207169	1.00851682	0.6532081	0.0361190 1	0.0446129 5
KLC4	406.77233 2	1.00801082	0.1759093 4	4.8169E-0 9	1.3488E-0 8
LAMTOR2	324.85039 7	1.00744087	0.1285812 8	2.2904E-1 5	1.173E-14
LTBP2	266.30993 8	1.00740087	0.2278135 5	4.5925E-0 6	9.3524E-0 6
SLC6A6	511.47343 9	1.00700201	0.1725642 7	2.5835E-0 9	7.4817E-0 9
NUCKS1	5285.2637 8	1.00655859	0.0629739 5	8.2365E-5 8	3.7649E-5 6
PLXNA1	7883.5291 8	1.0049018	0.0441532	5.772E-11 5	1.22E-112
MIPEP	273.57590 1	1.00456143	0.1555329 7	5.134E-11	1.782E-10
ZBTB34	181.24811 5	1.00269479	0.2905708 5	0.0002550 2	0.0004163 2
PABPC4	1771.0982 9	1.00050158	0.0585366 6	8.5488E-6 6	5.3057E-6 4
EXOC6B	813.36531 7	1.00034449	0.0744342 6	1.779E-41	4.1934E-4 0

TSPAN17	47.000054 7	-1.00008831	0.4195859 9	0.0070772 8	0.0095545 4
TXNDC17	508.86501 3	-1.00044744	0.0997351 5	5.5386E-2 4	5.0497E-2 3
SLC25A20	115.81779 6	-1.00128316	0.1996594 9	2.5485E-0 7	5.9636E-0 7
MIX23	383.45833 8	-1.00145329	0.1478656 7	6.1937E-1 2	2.354E-11
TMX2	564.34639 9	-1.00153126	0.1625785	3.5399E-1 0	1.1217E-0 9
ZFAND3	59.976103 7	-1.0019825	0.3658169 2	0.0026622 2	0.0037915 7
WWC1	530.24121 5	-1.00250168	0.1262441 7	9.8819E-1 6	5.2432E-1 5
TUBA1A	67.164120 6	-1.00303718	0.2244497 4	3.7241E-0 6	7.653E-06
MRPS2	176.75845 5	-1.00307387	0.3308290 7	0.0010771	0.0016178 1
ARL13B	195.38973 4	-1.00455751	0.1734188 3	3.3487E-0 9	9.5505E-0 9
BIK	585.42792 8	-1.00463984	0.1128963 8	2.7829E-1 9	1.894E-18
MX1	416.33130 5	-1.00553645	0.2196177	2.2142E-0 6	4.6664E-0 6
PIP4K2C	1061.7079 3	-1.00591725	0.0907173 8	7.0563E-2 9	8.8728E-2 8
RABIF	349.10730 6	-1.00883274	0.0919518 9	2.5845E-2 8	3.156E-27
LOC10042137 2	665.70119 1	-1.00928816	0.0755779 9	5.5199E-4 1	1.2745E-3 9
RRS1	920.80986 3	-1.00950404	0.0952224 4	1.4404E-2 6	1.5717E-2 5
ARMC6	175.59545 9	-1.01070967	0.1788752 4	7.6523E-0 9	2.1036E-0 8
CPSF7	1411.2784 4	-1.01074838	0.1080254 1	4.0278E-2 1	3.0928E-2 0
CDK2AP1	1624.3484 8	-1.01101846	0.1120486 7	8.9349E-2 0	6.2186E-1 9
ZNF114	235.38901	-1.01151688	0.1893461 4	4.3654E-0 8	1.1178E-0 7
SCAMP3	182.30850 7	-1.01201718	0.1878559 5	3.401E-08	8.7783E-0 8
KAT2B	85.806795 5	-1.01411161	0.2462699 5	1.7605E-0 5	3.3445E-0 5

OGDH	223.24751 8	-1.01431327	0.2255034 3	3.1924E-0 6	6.6024E-0 6
SLC25A29	197.85375 4	-1.01458462	0.1823978 4	1.262E-08	3.4081E-0 8
HTRA3	53.462803 1	-1.01493307	0.3238257 7	0.0007538 8	0.0011525 5
FNIP2	180.53173 8	-1.01535757	0.1916682 1	5.543E-08	1.3997E-0 7
ELOVL7	303.58376 5	-1.01657248	0.1807421 8	8.8107E-0 9	2.4083E-0 8
SLPI	1305.4579 3	-1.0170273	0.1179362 6	3.1374E-1 8	1.9652E-1 7
FAM177A1	298.76768 1	-1.01745856	0.1756259 1	3.2691E-0 9	9.3392E-0 9
TMEM199	568.00263 9	-1.02016491	0.0749659 1	1.734E-42	4.2501E-4 1
AKT1S1	171.22248	-1.02049213	0.2698327 4	6.9982E-0 5	0.0001230 7
ARNT2	58.258231 6	-1.02393801	0.3213740 7	0.0006230 2	0.0009644 7
VPS18	497.47840 8	-1.02424859	0.1211914 8	1.3738E-1 7	8.2685E-1 7
EPB41L5	513.87049 5	-1.02432529	0.0907701	7.5035E-3 0	9.9531E-2 9
RTTN	206.50301 3	-1.02561518	0.1977379 4	9.9207E-0 8	2.4304E-0 7
CCDC69	791.78260 1	-1.02572534	0.0622729 2	2.8398E-6 1	1.4778E-5 9
RNF40	589.11100 5	-1.02604149	0.1673498 7	4.0941E-1 0	1.2894E-0 9
EIF3C	125.00604 8	-1.02616446	0.3967854 3	0.0039225 4	0.0054792 4
AIF1L	164.38637 5	-1.02670635	0.1880805	2.2271E-0 8	5.8441E-0 8
SLC20A1	2818.8212 3	-1.0267149	0.1167737 3	6.979E-19	4.5971E-1 8
DUSP3	1063.5780 8	-1.02739073	0.0598363 4	2.1445E-6 6	1.3687E-6 4
CHST11	828.15852 2	-1.02740823	0.1679792 5	4.4835E-1 0	1.4048E-0 9
BRMS1	1161.8239 4	-1.02903291	0.0909646 1	5.4399E-3 0	7.2873E-2 9
TUBA4A	1729.6194 9	-1.02960374	0.0745071 1	9.3926E-4 4	2.4533E-4 2

UFC1	126.89768 7	-1.03024244	0.2224127 5	1.6465E-0 6	3.5292E-0 6
PCOLCE2	116.69414 3	-1.03302617	0.2395991 6	7.2791E-0 6	1.4507E-0 5
PLTP	45.444748 5	-1.03342965	0.3251056	0.0006277 4	0.0009708 9
ZNF84	203.95301 6	-1.03363428	0.2879303 7	0.0001440 9	0.0002432 1
EZH2	125.30244	-1.03379179	0.3491159 8	0.0012756 9	0.0018946 4
ZBTB33	75.714218 7	-1.03471621	0.5702578 2	0.0223984 7	0.0283172 6
ANTXR1	80.692638 1	-1.03495738	0.2264221	2.1884E-0 6	4.6177E-0 6
COPS3	468.52144	-1.03843147	0.1931314	3.4533E-0 8	8.9029E-0 8
MKLN1	81.972652 2	-1.03884193	0.2565890 8	2.2692E-0 5	4.2536E-0 5
GAPDH	180.13510 4	-1.03888854	0.1878518	1.4579E-0 8	3.9107E-0 8
SHTN1	86.356017 3	-1.0390007	0.3933974 2	0.0032803 6	0.0046184 5
FERMT2	88.342416 1	-1.03938468	0.2208470 1	1.1319E-0 6	2.471E-06
ELOVL4	222.76171 4	-1.04088313	0.1361348 5	9.616E-15	4.64E-14
HK2	1109.1980 3	-1.04138509	0.0916786 5	3.134E-30	4.2403E-2 9
MAD1L1	174.75301 6	-1.04204247	0.1693142 7	3.4458E-1 0	1.0934E-0 9
RNF43	312.06894 7	-1.04266495	0.1030286 1	2.099E-24	2E-23
DENND2C	311.32444	-1.04285648	0.1280366 9	1.7581E-1 6	9.7888E-1 6
ARHGEF18	436.49692 6	-1.04298922	0.2087872 9	2.6355E-0 7	6.1521E-0 7
STRIP2	259.36187 4	-1.04342164	0.1371161 8	1.268E-14	6.0707E-1 4
CNTNAP1	58.950701 2	-1.04344624	0.3151307 7	0.0003909 1	0.0006210 6
SLC25A25	262.61596 4	-1.04370713	0.2024967 5	1.1459E-0 7	2.7845E-0 7
SCHIP1	284.98092 5	-1.04436099	0.2502221 4	1.3135E-0 5	2.5373E-0 5

RNF138	332.52296 2	-1.04436359	0.1140651 8	2.5036E-2 0	1.8153E-1 9
ZNF146	176.73765 1	-1.04496414	0.250226	1.2988E-0 5	2.5132E-0 5
MGLL	221.70049 4	-1.04724514	0.2169814 8	6.1752E-0 7	1.387E-06
MRPS12	87.806859	-1.04749035	0.2471064 6	9.8094E-0 6	1.9257E-0 5
FADS3	1285.0597 6	-1.04803679	0.0724778 8	1.0086E-4 7	3.0734E-4 6
RNF6	245.50623	-1.04987809	0.2415446 4	6.04E-06	1.2172E-0 5
SNAPC4	679.22833 3	-1.05003923	0.1610227 9	3.1645E-1 1	1.1232E-1 0
ZCCHC17	138.93898	-1.05008815	0.3105781 9	0.0003015 3	0.0004869 5
TNFRSF25	120.81986 6	-1.05016965	0.1972635 9	4.5393E-0 8	1.1579E-0 7
IDH3G	164.83426 9	-1.05044447	0.1742116	7.4028E-1 0	2.2681E-0 9
GAREM2	46.809943 5	-1.05079801	0.323618	0.0004817 4	0.0007582 6
DNAJC9	1625.2101 7	-1.05092122	0.0560260 1	7.7818E-7 9	6.9269E-7 7
NUPR1	397.88987 9	-1.05168779	0.1423665 7	6.8256E-1 4	3.0804E-1 3
PORCN	411.91111 9	-1.05332203	0.1649905 4	7.7617E-1 1	2.6346E-1 0
AKIRIN1	1947.1945 7	-1.05585343	0.0776972 4	2.1304E-4 2	5.2029E-4 1
FAM216A	178.50449 1	-1.05590406	0.1956503 4	3.002E-08	7.787E-08
HRH1	93.336469 7	-1.05745239	0.3950173 6	0.0028542 7	0.0040505 9
UTP6	115.16960 7	-1.05846308	0.2544191 5	1.3589E-0 5	2.619E-05
RBBP8	753.51505 9	-1.06189624	0.0950031 7	2.3858E-2 9	3.0743E-2 8
CREM	71.530159 7	-1.06470373	0.2613976 3	1.9553E-0 5	3.6928E-0 5
SLC52A2	606.00584 8	-1.06503814	0.1005552 3	1.4709E-2 6	1.6024E-2 5
SEC61G	62.462182 1	-1.06534953	0.4019399 3	0.0030257 8	0.0042796 1

CD63	32.957869 3	-1.06759044	0.4312863 9	0.0048415 6	0.0066884 2
CCDC137	767.62197 4	-1.06763492	0.0782024	8.842E-43	2.1991E-4 1
SOCS1	50.612589 3	-1.06811237	0.2913816	0.0001014	0.0001746 8
COQ10B	252.04245 3	-1.06840348	0.1182081 7	7.1066E-2 0	4.9768E-1 9
RASSF10	113.80803 4	-1.06858415	0.1723341 5	2.4647E-1 0	7.9476E-1 0
GUK1	218.55187	-1.06934921	0.1748869 5	4.2357E-1 0	1.3297E-0 9
IL1RAP	148.10740 9	-1.06970871	0.2977758 7	0.0001337 7	0.0002266 6
NCBP2	135.70369 3	-1.07084138	0.2802192 1	5.4706E-0 5	9.7339E-0 5
PRKAR1B	607.93816	-1.07257953	0.0856483 8	2.4977E-3 6	4.7067E-3 5
TRAF7	232.58243 7	-1.07428283	0.2848720 9	6.6429E-0 5	0.0001170 3
SLC30A1	956.24050 2	-1.07472105	0.0955863 4	1.1094E-2 9	1.463E-28
SOCS4	399.06762 2	-1.07618734	0.1020657 5	2.3977E-2 6	2.5771E-2 5
ITGB1BP1	79.257295 9	-1.07626614	0.2871749 2	7.2571E-0 5	0.0001273 8
MT2A	4218.72	-1.07792668	0.0909441 1	9.239E-33	1.4109E-3 1
CDC42EP1	2360.7019 6	-1.07795488	0.0715600 4	1.249E-51	4.4238E-5 0
RCAN1	453.45706 7	-1.07806843	0.1417668 4	1.2488E-1 4	5.9833E-1 4
SLC39A3	173.08103 8	-1.07871537	0.1392715 5	4.1598E-1 5	2.0677E-1 4
NOP2	784.19049 8	-1.07873811	0.1422117 5	1.4454E-1 4	6.8955E-1 4
TICAM1	662.55216 2	-1.07933164	0.0888134 8	2.4518E-3 4	4.1055E-3 3
NUDT16L1	306.76865	-1.0796062	0.1510273 4	3.8119E-1 3	1.6097E-1 2
AKR1B1	5519.5963 7	-1.08130618	0.0741372 2	1.5425E-4 8	4.8763E-4 7
CHAC2	93.446452 4	-1.08499767	0.2523637 2	7.0239E-0 6	1.4029E-0 5



FAAP20	84.389768 9	-1.08513223	0.1973832 6	1.6255E-0 8	4.3344E-0 8
PRELID3B	130.34776 4	-1.08561375	0.2009534 3	2.7705E-0 8	7.2031E-0 8
KCNJ15	71.049892	-1.08585086	0.3771623	0.0014847 9	0.0021874 1
MMD	48.139245 1	-1.08725472	0.3131007 9	0.0002020 9	0.0003338 5
PKM	18.978142 9	-1.08739619	0.9454702 2	0.0375045 6	0.0462314 8
C19orf25	305.25633 5	-1.08766927	0.2105666 2	1.0021E-0 7	2.4518E-0 7
ANKRD46	58.904352 8	-1.08921458	0.3303117 9	0.0003759 6	0.0005995 7
NUP62	757.51071 2	-1.08943124	0.089504	1.9096E-3 4	3.2297E-3 3
ITGB6	1257.3523 2	-1.09065572	0.0836118 9	2.9788E-3 9	6.564E-38
ADGRL1	58.719028 9	-1.09207153	0.5224579 3	0.0113520 9	0.0149381 2
GFOD1	75.369126 5	-1.09223382	0.2341948 2	1.2712E-0 6	2.7606E-0 6
CYTH4	9.5938705 9	-1.09422143	0.8219361 9	0.0331566 3	0.0411870 3
CPSF2	102.34809 6	-1.09588858	0.3596201 2	0.0008581	0.0013039 1
EEPD1	193.59058 3	-1.09722943	0.1258522 6	1.201E-18	7.8196E-1 8
DCUN1D3	308.77996 2	-1.0975494	0.0981498 9	2.1317E-2 9	2.7521E-2 8
ADM	1062.1432 1	-1.09823485	0.0879757 2	3.9473E-3 6	7.3161E-3 5
ADGRL2	41.302088 7	-1.09854275	0.6131120 2	0.0193995 9	0.0247882 1
KTN1	795.79561 1	-1.09970647	0.3370636 9	0.0004156 2	0.0006587 8
SPIRE1	448.71339 9	-1.1004596	0.2751564 5	2.5011E-0 5	4.6586E-0 5
THBS1	2030.4810 9	-1.1009993	0.1288952	5.5838E-1 8	3.4528E-1 7
FDX2	165.01051 8	-1.10110254	0.1446879	1.1504E-1 4	5.5273E-1 4
PLEKHB2	430.70420 2	-1.10181466	0.1397001 6	1.3018E-1 5	6.8165E-1 5

RMC1	550.09226 4	-1.102029	0.0799544 6	1.374E-43	3.5613E-4 2
TASOR2	207.63877 4	-1.10254891	0.3484878 9	0.0005777 6	0.0008993 4
DPH2	100.84739 3	-1.10388104	0.4053185 1	0.0022651 1	0.0032513 2
TNFRSF10D	454.90204 6	-1.10408232	0.1269048 7	1.3954E-1 8	9.0162E-1 8
IFI6	379.91370 9	-1.10456487	0.2119791 8	7.6369E-0 8	1.9008E-0 7
BOLA2	350.28320 3	-1.10499302	0.1858526 2	1.1321E-0 9	3.4008E-0 9
CDKN2AIP	153.52271 3	-1.10541559	0.2008137 6	1.5078E-0 8	4.0364E-0 8
MSANTD3	111.87237 5	-1.10626527	0.2863743 9	4.3346E-0 5	7.8196E-0 5
LRRC8E	305.24473 3	-1.10640735	0.2139264 9	9.3694E-0 8	2.3024E-0 7
THAP5	57.813997 9	-1.10776929	0.3857709 8	0.0014507	0.0021410 2
EIF1AD	222.99194 5	-1.10780091	0.2099264 4	5.3056E-0 8	1.3448E-0 7
SUPT20H	54.228923 3	-1.11065518	0.4177594 9	0.0026823 7	0.0038178 5
CTNNAL1	911.97364 4	-1.11127841	0.1518450 5	1.0338E-1 3	4.5952E-1 3
HIVEP2	772.71059 6	-1.11194264	0.4044079 5	0.0020644 5	0.002981
MTF2	82.365546 7	-1.11211206	0.3606125 8	0.0007373 2	0.0011292 6
CHST7	110.85613 1	-1.11285893	0.1682719 4	1.534E-11	5.5975E-1 1
MAP1LC3B	2220.3074	-1.11297349	0.0518176	1.039E-10 2	1.673E-10 0
SBDS	1626.2295 3	-1.11313657	0.0776655 6	5.7589E-4 7	1.6793E-4 5
BORCS5	94.567872	-1.11382655	0.2249618 5	2.9285E-0 7	6.8104E-0 7
MB21D2	168.87092 1	-1.11425868	0.1458518 6	8.9548E-1 5	4.3302E-1 4
PDCD2	220.73666 9	-1.11426691	0.1501074 7	4.6958E-1 4	2.1464E-1 3
UAP1	799.96231 8	-1.11539744	0.1122663 6	1.2126E-2 3	1.0879E-2 2

TRIM39	77.316170 6	-1.11591142	0.4067721 3	0.0020837 7	0.0030082 6
HMOX2	349.59272 9	-1.1159664	0.1545788 9	2.1341E-1 3	9.2782E-1 3
TRIM35	1391.5219 9	-1.11668296	0.0495753 1	9.901E-11 3	2.03E-110
B4GALNT1	91.787843 4	-1.11784528	0.2060187 7	2.2961E-0 8	6.0112E-0 8
ATP6V1D	906.13656 3	-1.11879917	0.0891041 8	1.527E-36	2.9347E-3 5
NKIRAS1	6.6187491 1	-1.11932877	1.8010775 6	0.0402326 5	0.0494232 6
HHEX	134.32110 9	-1.12018503	0.1835702 6	4.1946E-1 0	1.318E-09
OPA1	344.52547 8	-1.12048692	0.2220825 9	1.7798E-0 7	4.2336E-0 7
RBP1	62.111294 1	-1.12072414	0.2590721 6	5.8411E-0 6	1.1797E-0 5
PRKAR1A	65.999401 5	-1.12141404	0.2856348 3	3.2581E-0 5	5.9537E-0 5
MRPL55	121.60764	-1.12216734	0.1804764	2.0176E-1 0	6.5715E-1 0
SCYL2	744.58021	-1.12286512	0.1028667 9	3.9817E-2 8	4.7929E-2 7
CCN3	66.489741 4	-1.12344356	0.2337724 4	5.9932E-0 7	1.3479E-0 6
ASPHD1	29.623390 4	-1.12411098	0.4095839 9	0.0020393 8	0.0029475 6
CLMP	285.72233 9	-1.12495834	0.1118850 4	3.5798E-2 4	3.3269E-2 3
NME4	47.908129 6	-1.1250034	0.3350146 9	0.0002832 2	0.0004593 6
SLC38A2	210.20593 6	-1.12596516	0.2584280 4	5.0275E-0 6	1.0201E-0 5
FOX E1	378.08099 2	-1.12837554	0.0957730 4	1.9756E-3 2	2.9503E-3 1
PDGFB	125.14058 6	-1.12882972	0.2374275 6	7.648E-07	1.7031E-0 6
TRMT61A	590.24671 2	-1.13044728	0.1024088 1	1.0096E-2 8	1.2567E-2 7
MRPL14	39.686046 8	-1.13298859	0.3269896 1	0.0001899 8	0.0003147 7
RILPL1	32.470542 2	-1.13318167	0.4009474 6	0.0015731 5	0.0023115 5

GLRX2	189.24579 1	-1.13370415	0.1377103 7	7.3161E-1 7	4.1697E-1 6
MYO19	43.693467 2	-1.1352615	0.4008144 3	0.0015376 4	0.0022608 4
CDKAL1	32.132884	-1.13657534	0.3807675 1	0.0009611 5	0.0014513 8
SLC25A44	98.416518 8	-1.13719862	0.3208712 6	0.0001407 6	0.0002378 8
NCDN	400.47170 3	-1.13779174	0.1449663 9	1.6625E-1 5	8.625E-15
CLTCL1	13.427823 4	-1.13854834	1.8985820 6	0.0381437 2	0.0469765 7
ANTXR2	40.712952 5	-1.13901846	0.3985378 5	0.0014124 6	0.0020867 6
MELK	474.30453 4	-1.14202954	0.1691275 7	5.6515E-1 2	2.1612E-1 1
ENOSF1	14.903363 1	-1.14407165	1.7542443 4	0.0383870 1	0.0472503 9
SWAP70	203.15626 7	-1.14468523	0.3194992 6	0.00012	0.0002048 5
UBASH3B	521.82043 1	-1.14476938	0.1424684	3.6518E-1 6	1.9859E-1 5
PTPN7	16.410860 3	-1.14612694	1.7907402	0.0381356 7	0.0469752
USP11	1470.6948 4	-1.15033296	0.0761264 4	5.4203E-5 2	1.9609E-5 0
EDF1	496.52305 8	-1.15054312	0.1116752 9	2.6823E-2 5	2.6984E-2 4
HLCS	14.020453 1	-1.15087814	1.9555783 4	0.0368373 3	0.0454669 9
TPM2	560.60879 3	-1.15239077	0.1053215 2	2.845E-28	3.4617E-2 7
CLIP4	93.168299	-1.15251539	0.3014632 5	4.6531E-0 5	8.3585E-0 5
LIMA1	1155.4210 6	-1.1527068	0.1304442 9	3.8161E-1 9	2.5662E-1 8
RNF14	26.670380 7	-1.15376585	1.3396147	0.0353742 5	0.0437409 6
SURF2	156.99931 6	-1.15433201	0.1703847 6	4.7381E-1 2	1.8285E-1 1
AP1S2	85.103453 1	-1.1562642	0.2523005 5	1.6649E-0 6	3.5665E-0 6
REXO4	544.33785 4	-1.15645759	0.0794515 7	2.102E-48	6.5832E-4 7

ADAMTS15	12.809268 8	-1.15840413	1.7622493 3	0.0372369 8	0.0459267 5
ZNF530	145.27952 9	-1.15899132	0.2243622 9	8.8005E-0 8	2.1712E-0 7
MANEAL	107.50175 6	-1.16023773	0.3055418 2	5.0767E-0 5	9.0736E-0 5
NIP7	1601.0603 9	-1.16111521	0.0726658 7	6.9547E-5 8	3.2225E-5 6
ZP3	31.888699 6	-1.16187212	0.7100071 7	0.0197428 1	0.0252095 3
TP53BP2	1048.3651 9	-1.16248695	0.1286221 6	6.0806E-2 0	4.2805E-1 9
SERTAD1	370.61860 2	-1.16341036	0.0978731 9	5.3131E-3 3	8.2316E-3 2
SLC45A3	302.31919 3	-1.16458934	0.1121623 3	1.1299E-2 5	1.1652E-2 4
TIPIN	251.24129	-1.16491533	0.2967169 4	2.9926E-0 5	5.5043E-0 5
ARMC5	45.496703 1	-1.16744336	0.3412650 9	0.0002074 4	0.0003419 5
ATG4A	137.37181	-1.1679931	0.1989726 1	1.5964E-0 9	4.7159E-0 9
AMIGO2	1325.0631 4	-1.1683681	0.180308	3.3939E-1 1	1.1996E-1 0
UPP1	411.87219 8	-1.16860359	0.1128785 8	1.5406E-2 5	1.5696E-2 4
SRPRB	1363.9444 7	-1.16933595	0.0908377 1	2.4368E-3 8	5.1195E-3 7
MYO1B	128.05106 7	-1.17236195	0.3137628 9	6.2942E-0 5	0.0001111 5
VDAC2	58.789530 4	-1.17312652	0.7480468 5	0.0205697 9	0.0261751 9
KBTBD8	32.646263 9	-1.17421548	0.4277046 2	0.0018135 1	0.0026434 9
ITPRID2	54.909630 1	-1.1766455	0.2877909 3	1.4824E-0 5	2.8457E-0 5
LACTB	23.313518 9	-1.176746	0.9594456 4	0.0270711 4	0.0339266 8
RASSF6	73.017467 5	-1.17784073	0.7468922 7	0.0200533 1	0.0255722 3
USP53	13.728850 6	-1.17827783	1.9827797 9	0.0348489 1	0.0431544 7
TFCP2	138.05908 3	-1.17960774	0.4369847 5	0.0020395 5	0.0029475 6

TMEM39B	106.28345 5	-1.18020173	0.2914692 9	1.7392E-0 5	3.3087E-0 5
SESN2	593.98536 7	-1.18176297	0.0873510 6	3.9352E-4 2	9.5078E-4 1
RHOT2	103.81715 9	-1.18385716	0.2305823 5	9.9227E-0 8	2.4304E-0 7
PNO1	545.15728 2	-1.18417005	0.1067359 4	4.9324E-2 9	6.2369E-2 8
AP3M2	206.63328 5	-1.185108	0.2586499 4	1.5817E-0 6	3.4034E-0 6
LUC7L	88.992944 9	-1.18653101	0.9747420 8	0.0264214	0.0331369 6
PCM1	7.3060918 5	-1.18715294	1.7395791 3	0.0350375 1	0.0433642 1
RABEPK	207.62157 8	-1.18838539	0.3960005 6	0.0008145 1	0.0012407 5
BCORL1	148.96147 2	-1.18856384	0.2448941 1	4.1776E-0 7	9.577E-07
ZFAND2A	77.379895 9	-1.18874183	0.2042309 1	2.066E-09	6.0478E-0 9
LIMK2	485.46073 4	-1.1899952	0.1666868 9	3.3617E-1 3	1.433E-12
COL16A1	885.20734 9	-1.19070164	0.1270536 4	2.5907E-2 1	2.0145E-2 0
SZT2	708.28187 3	-1.19073891	0.3049678 1	3.1005E-0 5	5.6857E-0 5
SYNC	33.615271	-1.19309062	0.5669347 5	0.0083511 8	0.0111762 1
NFKBIB	162.62569 8	-1.19365026	0.1611633 5	4.6222E-1 4	2.1142E-1 3
PLEKHG5	602.09212	-1.19427582	0.0961697 4	7.5517E-3 6	1.3734E-3 4
MICAL3	422.17183 6	-1.1946025	0.0989156 5	5.0766E-3 4	8.3155E-3 3
MAPKAP1	244.92043 7	-1.19749291	0.2184081 5	1.4402E-0 8	3.8648E-0 8
FOXD1	290.90203 5	-1.19820621	0.1389038 4	2.2619E-1 8	1.4328E-1 7
ATP2C1	121.86640 4	-1.19853749	0.4851989 4	0.0035832 2	0.0050208 1
KLK5	75.709300 9	-1.19867506	0.4466487 3	0.0020342 1	0.0029417 3
RASAL1	11.282872 8	-1.19877953	1.7127757 2	0.0341186 5	0.0423276 4

ALCAM	90.281676 6	-1.19943228	0.4286892 2	0.0014672 5	0.0021634 5
CCDC71L	258.99096 5	-1.20053421	0.1174470 1	5.6553E-2 5	5.6015E-2 4
ABTB2	1353.2267 8	-1.20069644	0.0585428 9	6.3915E-9 4	8.3151E-9 2
CDC27	18.096315 1	-1.20127598	1.9607848 3	0.0335670 6	0.0416586 2
CKB	146.58832	-1.20202895	0.2398744 2	1.8233E-0 7	4.3326E-0 7
MAP2K3	1120.2234 8	-1.20629469	0.0996518 1	3.5298E-3 4	5.8526E-3 3
GDAP1	253.48293 2	-1.20664286	0.1505420 9	3.84E-16	2.0866E-1 5
MST1R	123.36357 9	-1.2106628	0.3229567 2	5.5373E-0 5	9.8397E-0 5
SLC25A4	279.29033 5	-1.21141207	0.1143282 5	1.0923E-2 6	1.2094E-2 5
BCLAF1	137.06613 8	-1.21142059	0.2712725 1	2.5867E-0 6	5.4025E-0 6
SGMS2	167.01983 6	-1.21198864	0.3944884 2	0.0006149 7	0.0009535 4
PALS1	149.35387	-1.21312915	0.4240608 7	0.0011798 1	0.0017619
OSMR	729.24152 8	-1.21484249	0.1429867 4	6.7664E-1 8	4.1538E-1 7
PLB1	94.057556 2	-1.21597515	0.2154563	5.5434E-0 9	1.5407E-0 8
SMOX	433.74401	-1.21610529	0.1299460 4	2.7988E-2 1	2.1688E-2 0
GPATCH4	904.28929 5	-1.21814956	0.1046361 6	8.7847E-3 2	1.2808E-3 0
BLZF1	923.79238 5	-1.21995271	0.0958543 1	1.4507E-3 7	2.9036E-3 6
DOK7	57.341126 5	-1.22331259	0.2616350 6	9.3506E-0 7	2.0605E-0 6
TGFA	567.22480 3	-1.22419657	0.1799609 7	3.4345E-1 2	1.3446E-1 1
ARNTL2	238.94278 2	-1.22423475	0.3506564 8	0.0001422	0.0002401 9
OPTN	178.37038 3	-1.22442006	0.2434390 9	1.5838E-0 7	3.7806E-0 7
PKN2	159.46147 8	-1.22465099	0.3516766 3	0.0001467 7	0.0002472 3

PPIF	4190.1082 8	-1.22690031	0.0777867 9	1.6534E-5 6	7.2632E-5 5
UNC13D	1284.7077	-1.22794139	0.0600015 4	1.5174E-9 3	1.9369E-9 1
PLPPR2	69.449690 8	-1.23175282	0.3099115 2	2.1331E-0 5	4.0129E-0 5
MIOS	261.144	-1.23227267	0.2280641 3	2.0996E-0 8	5.5246E-0 8
FBXO32	1389.3089 4	-1.23283259	0.1085696 9	2.3611E-3 0	3.2203E-2 9
NSMF	162.5511	-1.2333186	0.3095344 4	2.0405E-0 5	3.8463E-0 5
PPP2R5B	203.66585 5	-1.23408904	0.1602689 1	4.4998E-1 5	2.2285E-1 4
RUBCN	213.70804 2	-1.23483981	0.1905763 4	2.9992E-1 1	1.0662E-1 0
TNIP2	48.302815 8	-1.24026488	0.3625427 5	0.0001766 8	0.0002939 8
CSPG4	173.96762 6	-1.24066843	0.1871550 1	1.0906E-1 1	4.0383E-1 1
PRR13	78.373552	-1.24073653	0.3752532 9	0.0002638 5	0.0004299 1
HAP1	85.679428 1	-1.2419805	0.3327704	5.514E-05	9.8012E-0 5
PLA2G2F	15.076757 8	-1.2440709	0.6796984 9	0.0115420 4	0.0151762 6
LIF	185.96540 1	-1.24486422	0.3063219 7	1.4273E-0 5	2.7453E-0 5
MRPL34	110.60056 1	-1.24527921	0.3608553 1	0.0001569 1	0.0002632 1
GPD2	246.58795 5	-1.24625434	0.3396334 7	6.9589E-0 5	0.0001224 1
ARHGAP17	45.075964 5	-1.24815062	0.5458516 4	0.0048330 7	0.0066780 5
GSTT2B	155.15211 6	-1.24882561	0.1686012 8	4.1448E-1 4	1.901E-13
BNIP1	19.282056 5	-1.25062227	0.8280469 4	0.0168533 5	0.0217002 2
ETV5	839.76096 3	-1.25100249	0.1179204 3	8.8278E-2 7	9.8224E-2 6
PLEKHG4	88.603329 2	-1.25145823	0.4720039 2	0.0019414 6	0.0028148 3
MYBL2	210.94051 4	-1.25164109	0.3480938 4	9.0868E-0 5	0.0001575 8



CYB5R1	2532.7679	-1.251685	0.0644650 2	1.845E-84	1.8629E-8 2
NFKBIE	1063.2701 1	-1.25463521	0.0930280 4	6.1075E-4 2	1.4548E-4 0
NCEH1	1463.9055 8	-1.25670016	0.0805525 3	2.3324E-5 5	9.8005E-5 4
SCNM1	165.87820 3	-1.25674477	0.1949764 6	3.5909E-1 1	1.2652E-1 0
LGALSL	176.50117 1	-1.25801746	0.1480099 1	6.0524E-1 8	3.7324E-1 7
OAF	2467.3123 1	-1.25937666	0.0528623	6.173E-12 6	1.67E-123
C4orf48	79.996760 3	-1.26037343	0.2511258 8	1.5556E-0 7	3.7187E-0 7
ADRA1B	80.971109 8	-1.26261835	0.2532418 1	1.8361E-0 7	4.3598E-0 7
MOCS2	132.53006 8	-1.2637381	0.2061139 8	2.6668E-1 0	8.5582E-1 0
CELF1	12.957720 5	-1.26623783	1.8854271 8	0.0298715 9	0.0372294 2
TSC22D1	36.091141 7	-1.26657421	0.4378125 2	0.0009379 4	0.0014175 9
CHUK	653.52744 8	-1.26708825	0.0771841 6	4.6594E-6 1	2.3523E-5 9
DGAT2	139.34308 6	-1.26840598	0.2835854 4	2.2212E-0 6	4.6796E-0 6
C18orf54	88.953927 3	-1.26985657	0.3642984 9	0.0001306 6	0.0002217 6
ARHGDI1	122.56819 6	-1.27059331	0.2397017 4	3.4104E-0 8	8.7957E-0 8
NATD1	146.47955	-1.27118644	0.1648383 1	3.8215E-1 5	1.9065E-1 4
RAN	221.78908	-1.27174891	0.2104083 8	4.5109E-1 0	1.4128E-0 9
PEA15	140.02231 2	-1.27210265	0.1844260 7	1.6098E-1 2	6.4594E-1 2
GLMP	87.942361 8	-1.27256404	0.3357461 5	4.1011E-0 5	7.4301E-0 5
INTS13	12.032019 8	-1.27286679	1.8812286 7	0.0294849 1	0.0367813 8
LRRC28	30.243023	-1.27427157	0.3809857 7	0.0002134 5	0.0003512 6
TBC1D30	148.33126 3	-1.27482877	0.1707113 6	2.4871E-1 4	1.1604E-1 3

MAP1A	50.109522 7	-1.2749081	0.2923175 7	3.6438E-0 6	7.4903E-0 6
NABP1	386.15441 6	-1.27527698	0.1889088 8	4.44E-12	1.7193E-1 1
TRMT6	544.94315 1	-1.27774208	0.1868239 7	2.3937E-1 2	9.4975E-1 2
DIAPH3	122.23545	-1.27866101	0.4307645 2	0.0007238 3	0.0011096 1
LRRC8B	84.025401	-1.281934	0.3823196 6	0.0002035 2	0.0003360 5
EEF1AKNMT	108.93412 9	-1.28302723	0.2637327 1	3.2486E-0 7	7.5135E-0 7
DERL1	27.154586 2	-1.28394204	0.6684784 7	0.0087773 6	0.0117025 7
SDSL	93.423738 7	-1.2840994	0.2573119 6	1.7132E-0 7	4.0822E-0 7
ITGA1	46.676893 8	-1.28500236	0.2977858 4	4.3853E-0 6	8.9545E-0 6
PTGS1	9.0693042 1	-1.28582674	1.8744985 5	0.0287355 6	0.0358929 2
EFHD2	769.56761	-1.28586445	0.1653164 8	2.2004E-1 5	1.1294E-1 4
ACOT4	134.20886 2	-1.28895014	0.1582204 3	1.1168E-1 6	6.2595E-1 6
PVR	840.68525 1	-1.28929046	0.1293921 8	6.5904E-2 4	5.9925E-2 3
MANBAL	115.55473 5	-1.28996774	0.5001376 3	0.0021150 5	0.0030508 1
FBXO5	141.15085 1	-1.29088069	0.2242124 2	2.4505E-0 9	7.1179E-0 9
THRAP3	124.30484 9	-1.29139358	0.2551131 6	1.1643E-0 7	2.8281E-0 7
CSNK1G3	50.528374 4	-1.29260202	0.3779211 1	0.0001565 2	0.0002626 2
AGMAT	173.23789 5	-1.29591123	0.1685052 6	4.2872E-1 5	2.1294E-1 4
TOP3B	287.71800 6	-1.29735028	0.1920536 4	4.1173E-1 2	1.5989E-1 1
WFDC5	7.1173005 3	-1.29788973	1.2115765 9	0.0216048 6	0.0273958 6
IRAK1	336.97021 3	-1.29854779	0.2722829 9	5.054E-07	1.1469E-0 6
DDX60L	47.506616 3	-1.29972508	0.3527419 5	5.8015E-0 5	0.0001029

KLHL18	337.86897 8	-1.30078456	0.1362501 3	3.9236E-2 2	3.2489E-2 1
TP63	65.329429 5	-1.30159643	0.2771616 1	7.168E-07	1.6004E-0 6
BDKRB1	121.15908 5	-1.30203086	0.2108818 2	1.8806E-1 0	6.1431E-1 0
ACLY	245.83151 1	-1.30241753	0.1703079 2	5.9216E-1 5	2.9071E-1 4
HOXA11	127.86051 1	-1.30253101	0.2356357 2	9.0242E-0 9	2.4656E-0 8
DBN1	665.39615 9	-1.30414919	0.1203572 9	6.8521E-2 8	8.1467E-2 7
SMURF1	8.8266155 6	-1.30520445	1.7818973	0.0273573 3	0.0342726 5
DNAJC10	66.173246 9	-1.30843871	0.4116690 2	0.0003441 4	0.0005519 5
LMNB1	39.876202 4	-1.30855404	1.4032832 4	0.0236861 1	0.0298558 8
TMC8	17.084424	-1.30966916	1.0916338 3	0.0187465 8	0.0239827 2
NCAPG2	229.03940 6	-1.31302033	0.2954857 8	2.3013E-0 6	4.8364E-0 6
PNPLA8	204.51272 3	-1.31305647	0.2118921	1.5928E-1 0	5.2332E-1 0
CCDC88B	129.85810 6	-1.31341962	0.3707202 1	9.5514E-0 5	0.000165
PAK1	12.030679 5	-1.31355455	1.7473067 2	0.0266957 3	0.0334686
MAP6D1	169.55244 8	-1.31364943	0.1429590 6	1.1333E-2 0	8.3792E-2 0
FGD6	1148.8596 3	-1.31371947	0.0746679	7.9665E-7 0	5.5481E-6 8
GALE	94.803053 5	-1.3140072	0.4283303 3	0.0004845 8	0.0007616 5
ENTPD3	93.240066	-1.31535138	0.2583046 6	9.4374E-0 8	2.3174E-0 7
CTPS1	2139.9981 2	-1.31700455	0.0787900 9	2.934E-63	1.6965E-6 1
CD55	641.50639 9	-1.31741155	0.1524542 4	1.5695E-1 8	1.0083E-1 7
TYK2	50.410910 5	-1.31758622	0.9632460 9	0.0156771 8	0.0202745 4
MROH1	264.27010 4	-1.32148614	0.1507974 7	5.3164E-1 9	3.5295E-1 8

YRDC	905.80360 4	-1.3223112	0.0939937 1	1.7034E-4 5	4.7035E-4 4
XRCC3	101.35493 9	-1.32386295	0.3088659 8	4.5674E-0 6	9.3041E-0 6
ELL3	63.766354 3	-1.32602619	0.2447978 4	1.5984E-0 8	4.2672E-0 8
ATAD3B	129.93783 8	-1.32622351	0.3830487 5	0.0001239 8	0.000211
MRPS18A	91.144823 2	-1.32671214	0.2092536 6	6.1785E-1 1	2.1282E-1 0
FUBP3	356.07882 8	-1.3288069	0.1998414 7	7.9392E-1 2	2.9855E-1 1
VSNL1	19.513755 1	-1.32886865	0.6485351 2	0.0060637 5	0.0082770 9
TIMP4	71.374817 4	-1.32944808	0.2807357 5	5.5589E-0 7	1.2552E-0 6
STX3	323.69061 6	-1.32967726	0.1301872 8	4.794E-25	4.7693E-2 4
KDM2B	119.49485 7	-1.33006491	0.3255557 9	1.0737E-0 5	2.0963E-0 5
RPL41	853.19640 8	-1.33084221	0.1309107 6	7.7975E-2 5	7.6671E-2 4
KPNA7	54.648697 5	-1.33197963	0.2964058 4	1.7479E-0 6	3.7293E-0 6
PI4KB	323.76741 6	-1.33302648	0.2366708 7	4.6408E-0 9	1.3016E-0 8
RIT1	15.866292 6	-1.33619811	1.8393182 2	0.0258770 4	0.0324783 3
CHKA	354.30577 9	-1.33672307	0.1103062 6	2.3323E-3 4	3.9151E-3 3
PREX1	149.03123 5	-1.33913113	0.1706372 6	1.1348E-1 5	5.9787E-1 5
MAP4K4	147.57364 4	-1.34176978	0.3113964 7	3.9601E-0 6	8.1231E-0 6
MICALL2	8.4272989 4	-1.34254948	1.8783952 3	0.0256792 6	0.0322360 8
PFKM	29.531996 7	-1.34263743	1.3398329 9	0.0206797 6	0.0262967 2
GRPEL2	1009.9753 9	-1.34334587	0.0672835 1	3.0285E-8 9	3.5378E-8 7
ELOVL1	162.41326 1	-1.34346415	0.2558982 6	3.8328E-0 8	9.8478E-0 8
ZNF860	82.965879 9	-1.34437881	0.2630590 2	8.0342E-0 8	1.9902E-0 7

SLC25A33	326.98914 3	-1.34509427	0.1273224 5	1.1745E-2 6	1.2941E-2 5
CYP1A1	640.57026 5	-1.34591135	0.2055612 3	1.5175E-1 1	5.546E-11
ABLM1	71.223301 7	-1.34720348	0.2959253 4	1.2825E-0 6	2.7825E-0 6
CHIC2	318.12908 6	-1.34821977	0.1177164 5	6.1004E-3 1	8.5267E-3 0
OSTM1	386.54662 1	-1.34841172	0.0992414 9	1.29E-42	3.1849E-4 1
MRPS11	144.12866 9	-1.34855213	0.2269542 7	7.1668E-1 0	2.1998E-0 9
UTP4	279.27625 4	-1.34967644	0.2789230 9	3.1884E-0 7	7.3843E-0 7
ALOX12	436.52220 3	-1.35018486	0.1053632 6	3.654E-38	7.6294E-3 7
PSEN2	189.89894 7	-1.3504248	0.2274034 2	7.2906E-1 0	2.2358E-0 9
VCP	227.26509 1	-1.3521435	0.1889451 7	2.1425E-1 3	9.3031E-1 3
MERTK	285.82068 5	-1.35264692	0.1848764 1	6.5861E-1 4	2.9783E-1 3
MDGA1	171.28676 3	-1.35340673	0.2399898 1	4.2589E-0 9	1.199E-08
RAB13	4.6853790 1	-1.35422145	1.6399843 3	0.0235722 7	0.0297179 3
UST	270.05699 7	-1.35430109	0.1220915 8	3.6173E-2 9	4.6171E-2 8
TMPRSS11E	7.0344024 7	-1.35430215	1.6872582 1	0.0239764 5	0.0302049 7
PLEC	1548.7686 1	-1.35459425	0.1358377 3	5.3207E-2 4	4.8707E-2 3
DKK3	859.90377 9	-1.35546607	0.1893926 9	2.1173E-1 3	9.2174E-1 3
OLR1	1015.4023 7	-1.35628898	0.0932469 7	1.671E-48	5.2579E-4 7
PCDH12	11.318720 2	-1.35887452	0.8070125 2	0.0096269 4	0.0127723 6
GADD45A	95.534723 5	-1.36068591	0.3570681 9	3.0627E-0 5	5.621E-05
COMMD4	51.860718 1	-1.36258869	0.3524633 4	2.4484E-0 5	4.568E-05
CNGB1	68.064631 2	-1.36396632	0.3506867 6	2.2204E-0 5	4.1702E-0 5

PLEKHA4	435.47614 4	-1.36432098	0.1483359 4	9.4158E-2 1	7.0229E-2 0
BMP2	130.09433 4	-1.36479385	0.1737289 7	1.0072E-1 5	5.3356E-1 5
DCAF4	8.2870802 5	-1.36489033	1.8481352 3	0.0244355 4	0.0307432 5
FCMR	42.854819 2	-1.36507955	0.3277036 4	7.0123E-0 6	1.4014E-0 5
SUSD1	115.00223 5	-1.36622846	0.1973821	1.114E-12	4.5234E-1 2
PINLYP	28.495190 9	-1.366236	0.4789791 4	0.0008046 1	0.0012262 1
TAF4B	16.957136 5	-1.3671036	1.9086768 1	0.0245482	0.0308735 1
SELENOF	372.36798 5	-1.36730279	0.1653903 8	3.4777E-1 7	2.0247E-1 6
SLC9A2	55.388175 1	-1.36800337	0.2697640 2	9.3545E-0 8	2.2995E-0 7
STAMBPL1	169.78345 8	-1.36941473	0.1878122 8	7.6494E-1 4	3.4407E-1 3
GRIN2D	275.98187 9	-1.36981602	0.1208842 3	2.3495E-3 0	3.2109E-2 9
ITGAX	27.800853 4	-1.37023223	1.1097595	0.0154238 1	0.0199735 9
BCL2A1	5.3107367 8	-1.3702823	1.6876352 5	0.023119	0.0291682 3
CRYBG2	249.15868	-1.37087133	0.5569151 4	0.0022244 4	0.0031949 7
LZIC	92.398915 9	-1.3708917	0.3467663 9	1.6839E-0 5	3.2089E-0 5
COQ10A	102.75745 1	-1.3735341	0.3281795 7	6.3081E-0 6	1.2693E-0 5
APOC1	65.122638 1	-1.37799212	0.2388748 2	1.8936E-0 9	5.5623E-0 9
SMTN	136.31216 8	-1.37830317	0.3331935 6	7.6842E-0 6	1.5276E-0 5
BAG6	5.6640784 5	-1.38017057	1.7520542 1	0.0231069 2	0.0291584 3
OSGIN1	273.22839 4	-1.38329116	0.1310117 7	1.1536E-2 6	1.2731E-2 5
TM4SF19	53.323200 1	-1.38366122	0.4418896 8	0.0003275 8	0.0005267 5
ARMCX5	66.358631 8	-1.38464361	0.3633663 8	2.8827E-0 5	5.3181E-0 5

TMEM63B	425.59049 3	-1.38640305	0.1957350 3	3.3754E-1 3	1.437E-12
BAD	69.634127 6	-1.38772729	0.2680603 1	5.1175E-0 8	1.2995E-0 7
KRT86	97.992011 8	-1.38867286	0.2045602 1	2.6833E-1 2	1.0597E-1 1
CRY1	122.65297 6	-1.38889903	0.1866578 8	2.3937E-1 4	1.1199E-1 3
RELT	366.22016 2	-1.38944951	0.0949040 2	3.8444E-4 9	1.2444E-4 7
GPR37L1	63.095501 6	-1.39519232	0.3162741 9	2.194E-06	4.6268E-0 6
MAPK11	62.921658 4	-1.39587576	0.2896989 8	3.1651E-0 7	7.3329E-0 7
COMT	366.81649 4	-1.39620095	0.1386645 9	1.8284E-2 4	1.752E-23
SLC39A14	2216.9984	-1.39727834	0.0679995 3	1.9579E-9 4	2.703E-92
GPRIN1	274.82211 9	-1.39996966	0.1203899 4	7.1021E-3 2	1.04E-30
SERPINB8	32.082514	-1.40032688	1.2479710 3	0.0161005	0.0207992 2
TRIM55	37.325877 8	-1.40122159	0.4459075	0.0003006 9	0.0004857 1
LSS	508.90239 7	-1.40152323	0.1945802 2	1.3673E-1 3	6.0496E-1 3
CORO6	105.84710 7	-1.40202658	0.5709209 1	0.0020412 9	0.0029494 4
ROR1	443.37818 3	-1.4044503	0.1429980 6	2.1521E-2 3	1.9081E-2 2
VGLL3	165.01349 9	-1.40641054	0.2315258 5	2.7839E-1 0	8.917E-10
PPP1R35	25.534655 2	-1.40648017	0.4206817 4	0.0001520 9	0.0002555 6
NKX3-1	110.55731	-1.41047785	0.2034138	9.2464E-1 3	3.7818E-1 2
DHRS11	32.689952 2	-1.41086237	0.4898372 6	0.0006504 1	0.0010041 2
RAB5IF	79.746716	-1.41197486	0.3086339 1	9.8681E-0 7	2.1668E-0 6
IKBKG	49.970062 3	-1.41279005	0.4978391 4	0.0007302 5	0.0011189 4
IL32	23.170418 2	-1.41464247	0.9507561 2	0.0102896 4	0.0136062 2

ARID5A	71.194557	-1.41609744	0.3187521 4	1.805E-06	3.8424E-0 6
GDA	104.93220 4	-1.41695301	0.2399888 4	7.6988E-1 0	2.3524E-0 9
SLC8B1	156.80565 9	-1.41782873	0.2787408 1	7.6631E-0 8	1.9066E-0 7
CBWD1	15.064125 4	-1.41890099	1.9598861 4	0.0223500 5	0.0282666
C1orf109	13.132811	-1.42111438	1.6854743 1	0.0205483 4	0.0261541 9
HAS3	722.79983 6	-1.4230015	0.1471661 6	9.2228E-2 3	7.8679E-2 2
PRDM15	15.768154 4	-1.42323435	1.6294217	0.0199040 9	0.0254010 8
TRNP1	313.90551 1	-1.42650852	0.1013385 1	1.2092E-4 5	3.3665E-4 4
UBE2H	305.72518 2	-1.4278616	0.3508143 5	8.9681E-0 6	1.7667E-0 5
TMEM171	66.009651 8	-1.43612317	0.3106587 5	7.4002E-0 7	1.65E-06
KRT6B	2441.9526 5	-1.43839017	0.0945322 1	6.1979E-5 3	2.3424E-5 1
MBD1	38.874571 7	-1.43860345	0.3993092 4	5.5142E-0 5	9.8012E-0 5
TYW3	48.760417 3	-1.43933602	0.3826057 7	3.0126E-0 5	5.5381E-0 5
NFKBIL1	8.2728974 2	-1.43993869	2.0215362	0.021638	0.0274276
AGPAT2	264.98372 4	-1.44126896	0.2027879 4	2.4983E-1 3	1.0758E-1 2
TNFRSF12A	2618.0700 4	-1.44284623	0.0962583 1	1.9062E-5 1	6.6814E-5 0
TMEM120A	48.871484 6	-1.44399969	0.4209580 8	0.0001011 3	0.0001743
YPEL5	135.55329 8	-1.44428991	0.2253448 3	3.0193E-1 1	1.0728E-1 0
BRSK1	19.094527 9	-1.44484371	0.6080815 3	0.0021253 9	0.0030644 3
KLHL21	1557.8995 5	-1.44500828	0.0881156 4	4.2865E-6 1	2.1803E-5 9
CSTA	603.39175 7	-1.44538369	0.0936197 7	1.972E-54	7.8016E-5 3
BICDL1	84.446049 4	-1.449051	0.2531466 7	2.078E-09	6.0804E-0 9



SLC2A9	13.254217 7	-1.45045546	0.7333532	0.0045477 3	0.0063005 1
PDLIM2	108.09513 3	-1.45191184	0.2638556 6	7.3623E-0 9	2.0271E-0 8
EIF5A2	430.67184 9	-1.45210205	0.1341298 1	5.5309E-2 8	6.6224E-2 7
RDH16	69.152513 7	-1.45222396	0.2593622	4.251E-09	1.1973E-0 8
MCM4	188.65859 3	-1.45364844	0.1918234 9	7.2476E-1 5	3.5324E-1 4
AIMP2	116.85974 9	-1.45417126	0.2175303 2	4.6891E-1 2	1.8112E-1 1
TANGO2	8.7106641 9	-1.45440089	1.8931907 6	0.0205764 5	0.0261751 9
TEP1	165.09123 1	-1.45602626	0.4214481 6	8.9578E-0 5	0.0001553 8
MSL3	90.766009	-1.45624539	0.4426207 5	0.0001578 3	0.0002646 8
C12orf75	55.292903 3	-1.45739946	0.2702934 9	1.3469E-0 8	3.6274E-0 8
ANKRD11	167.33361 2	-1.45813442	0.2976593 5	1.8143E-0 7	4.3129E-0 7
PLEKHO2	431.58649 2	-1.46081714	0.0870819 2	7.8876E-6 4	4.64E-62
AP1G2	114.48698 6	-1.4621686	0.2514296 6	1.1743E-0 9	3.5229E-0 9
GOSR2	137.57580 8	-1.46264397	0.1916789 3	4.7258E-1 5	2.337E-14
PLEKHA7	14.230808 7	-1.46536686	2.2020859 4	0.0207655 6	0.0263959 1
ZNF365	170.57230 3	-1.46655773	0.1560022 6	1.1071E-2 1	8.8632E-2 1
HDAC9	60.698062 8	-1.46697348	1.0954897 1	0.0106534 9	0.0140680 9
SLCO4A1	119.02061 6	-1.46959688	0.2829153 3	3.8097E-0 8	9.7959E-0 8
MFSD2A	478.01262 6	-1.47140062	0.1734018 1	4.3061E-1 8	2.6775E-1 7
LIMS1	193.72450 2	-1.47194574	0.3161308 3	5.7515E-0 7	1.2965E-0 6
ASCC3	13.527450 7	-1.47266737	2.0175593 1	0.0203627 3	0.0259374 6
RTKN2	145.12892 3	-1.47389921	0.1877734 3	8.266E-16	4.4101E-1 5

CCNE1	117.25572 6	-1.47517344	0.3144880 6	4.8303E-0 7	1.0988E-0 6
VASN	85.924773 6	-1.47570752	0.2374807 6	9.822E-11	3.3057E-1 0
C1orf122	734.24758 1	-1.47580972	0.0965824 6	2.1221E-5 3	8.065E-52
DMKN	82.910970 1	-1.4787143	0.2969627 3	1.142E-07	2.7759E-0 7
YKT6	31.614614	-1.47966327	0.4797385 5	0.0002853 9	0.0004626 6
NMD3	179.71632	-1.48220976	0.1851821 3	2.3372E-1 6	1.2886E-1 5
MAP7D1	1108.4036 2	-1.48376076	0.2068434	1.3962E-1 3	6.1655E-1 3
RFXANK	65.576118 8	-1.48686319	0.330429	1.1524E-0 6	2.5117E-0 6
CCND3	1778.1564 9	-1.4869497	0.1044005 5	9.919E-47	2.8799E-4 5
ADGRE1	79.061866 8	-1.48703348	0.2228426 3	4.6907E-1 2	1.8112E-1 1
WIPI1	99.891938	-1.4876688	0.2560660 7	1.1392E-0 9	3.4206E-0 9
PMEPA1	1984.8304 7	-1.48799967	0.0846787 4	8.0372E-7 0	5.5481E-6 8
GLIPR1	91.699087 5	-1.4880408	0.2489375 3	4.144E-10	1.3033E-0 9
HMGA2	63.851829 3	-1.48969054	0.4985407 1	0.0003704 9	0.0005914 1
AXL	1182.2125 1	-1.48969979	0.1624302 8	9.0296E-2 1	6.7423E-2 0
USP36	327.12443 2	-1.49287056	0.4333754 7	8.3191E-0 5	0.0001450 9
MON1A	145.78622	-1.49311163	0.1808220 6	2.8257E-1 7	1.6565E-1 6
SPRY4	442.97102 4	-1.49421158	0.1624482 2	6.9674E-2 1	5.2605E-2 0
TAF12	38.352993 9	-1.49469422	0.4131781 7	4.4395E-0 5	7.994E-05
MYO5A	106.70677 5	-1.49586121	0.6796732 2	0.0025777 4	0.0036774 4
KIAA0895	66.435694 8	-1.49642275	0.9451978	0.0071371 6	0.0096276 9
DAXX	124.94106 1	-1.49876686	0.2076562	9.7401E-1 4	4.3378E-1 3

ZMIZ2	77.376257	-1.49977171	2.0288685 5	0.0194018 6	0.0247882 1
SDR16C5	64.365884 7	-1.50014786	0.2747776 3	8.2926E-0 9	2.2731E-0 8
SLC66A1	161.88043 5	-1.50448324	0.2482031 2	2.3727E-1 0	7.6726E-1 0
NCF2	39.037251 3	-1.505087	0.8974169 4	0.0060831	0.0083018 3
SGSH	100.28079	-1.50942265	0.2433819 9	9.7382E-1 1	3.2808E-1 0
TNNC1	26.741722 6	-1.51189094	0.5385525 6	0.0005785 9	0.0009004 3
ESYT3	6.0441867	-1.51321441	1.5625307 4	0.0152643 6	0.0197746 8
SSH2	9.9088979 4	-1.51391706	1.2781808 4	0.0115884 9	0.0152343 8
ZNF274	10.595302 6	-1.5139757	1.9328329 6	0.0184701 8	0.0236514 8
MYBL1	284.66163	-1.51895862	0.1900376 6	2.3364E-1 6	1.2886E-1 5
IRAK2	312.49772 1	-1.52106215	0.1095914 2	1.5514E-4 4	4.1812E-4 3
LY6K	487.85670 1	-1.52106297	0.1127081 2	3.0458E-4 2	7.3853E-4 1
EPHX4	50.246119	-1.52273711	0.292684	3.1697E-0 8	8.2095E-0 8
SLC7A8	268.64612 5	-1.52282078	0.1748440 5	5.4073E-1 9	3.5863E-1 8
BMERB1	55.248872 5	-1.52374419	0.3073632 8	1.1318E-0 7	2.7539E-0 7
PHACTR2	172.96996 1	-1.52489293	0.4342705 5	5.9562E-0 5	0.0001055 1
CLCF1	468.13692 4	-1.52548344	0.1068399 7	5.443E-47	1.6009E-4 5
CENPT	110.84332 2	-1.52674121	0.3148053 7	1.928E-07	4.5701E-0 7
DVL1	830.36210 7	-1.53077796	0.1443688 6	5.0886E-2 7	5.7469E-2 6
GPAT3	165.27123 6	-1.53084563	0.2107836 1	6.4462E-1 4	2.9189E-1 3
UPF3B	11.991858 5	-1.53206585	1.2400455 6	0.0104078 1	0.0137571
NT5C2	28.636899 1	-1.53345664	1.5211965 2	0.0140107 6	0.0182488 6

GRAMD2B	50.055677 5	-1.53363049	1.0429979 3	0.0075190 6	0.0101106
PGAP3	40.784661 8	-1.53390045	0.5006698 1	0.0002552 6	0.0004166
TNPO1	268.49724 2	-1.53446628	0.2883538 2	1.6194E-0 8	4.3215E-0 8
WDR74	96.221671 3	-1.53572168	0.2392902 6	2.2684E-1 1	8.1714E-1 1
GCNT2	6.0534680 4	-1.53585542	1.7397212	0.0162343 8	0.0209550 8
ITGA5	7085.0084 4	-1.53594982	0.0732561 7	2.361E-98	3.63E-96
MCCC2	5.1673277 5	-1.53710625	1.8776949 6	0.0172941 8	0.0222382
FCHSD1	28.858076 6	-1.53720235	1.1529163 2	0.0090067 3	0.0119918 4
WDR53	133.16952 3	-1.53888472	0.2936562 1	2.4786E-0 8	6.4715E-0 8
ARG2	121.69736 5	-1.53928126	0.1840055 6	1.0146E-1 7	6.1456E-1 7
CCDC93	59.531183 6	-1.54050699	0.2868347 3	1.2169E-0 8	3.2915E-0 8
PPP1R15A	5775.6948 4	-1.54073047	0.1201454 8	2.1025E-3 8	4.4447E-3 7
ATP5MF	29.662590 6	-1.5416295	0.4303491 5	4.3777E-0 5	7.8936E-0 5
ZNF678	21.496479 1	-1.54172221	1.9487744 3	0.0175715 7	0.0225648 6
CTSL	527.55516 5	-1.54307277	0.1337998 1	1.5565E-3 1	2.2309E-3 0
ENTR1	361.02412 1	-1.54633728	0.1761929	2.823E-19	1.9174E-1 8
PQBP1	346.59971 8	-1.54689158	0.2082110 4	1.7828E-1 4	8.44E-14
ZNF317	110.60874 9	-1.55271953	0.3670516	3.1922E-0 6	6.6024E-0 6
TRAPPC3	303.29900 1	-1.5537023	0.1205341 3	8.6414E-3 9	1.8797E-3 7
PDGFC	17.575141 5	-1.55526564	2.0750173 8	0.0176766 3	0.0226868 5
CSRP2	36.216234 3	-1.55591686	0.7092243 4	0.0021208 9	0.0030585 8
TPCN1	19.144703 4	-1.56049634	2.1672236 6	0.0177361 6	0.0227589 3

OSBPL2	109.95239 4	-1.56061746	0.2874743 6	8.3559E-0 9	2.2895E-0 8
ZBTB8OS	20.842485 7	-1.56529497	0.5263721 4	0.0003005 6	0.0004856 1
PTK6	271.41932 4	-1.57003663	0.2410768 2	1.109E-11	4.1042E-1 1
KIF23	28.596535 8	-1.57063048	0.7304922 5	0.0021970 8	0.0031590 3
DLX2	21.455894	-1.57103452	0.5053598 4	0.0001961 7	0.0003243 9
NAV3	6.3185188 8	-1.57136585	1.9325027 4	0.0164757 7	0.0212504 5
CXCL3	17.345490 8	-1.57164061	0.6490060 2	0.0012354	0.0018372 1
SPP1	30.790271 9	-1.57191565	0.4762061 5	0.0001056 4	0.0001813 9
ELL2	486.16717 8	-1.57225685	0.2368697 5	4.7756E-1 2	1.8408E-1 1
AMPD3	407.64658 9	-1.57504964	0.1752005 6	3.8494E-2 0	2.7499E-1 9
PEX10	167.37995 6	-1.57892189	0.2126760 7	1.7057E-1 4	8.0917E-1 4
GOLGA7	89.766613 3	-1.57900401	0.2746252 5	1.271E-09	3.7927E-0 9
NFATC2IP	130.82520 9	-1.58245924	0.4070575 3	1.2058E-0 5	2.3414E-0 5
MET	248.89823 3	-1.58274543	0.4125162 1	1.4708E-0 5	2.8243E-0 5
ZNRD2	79.806495 1	-1.58391978	0.2957424 5	1.1692E-0 8	3.1638E-0 8
TUBB2A	559.30804 5	-1.58858936	0.1192112 9	2.5369E-4 1	5.8976E-4 0
MOSPD1	110.7035	-1.59587872	0.3531593 2	7.7026E-0 7	1.713E-06
ANKLE2	555.30790 8	-1.59738073	0.2370109	2.2263E-1 2	8.8438E-1 2
AK1	266.47786 5	-1.59800899	0.1297494	1.1162E-3 5	2.0082E-3 4
IP6K1	7.5661510 3	-1.59981663	1.9300641 3	0.0155473 1	0.0201258 2
EFNB2	1327.1781	-1.59988956	0.0636974 3	4.967E-14 0	1.769E-13 7
ORMDL1	187.90044 3	-1.60361675	0.2035715 5	4.7385E-1 6	2.5686E-1 5

CAPN2	143.05369 9	-1.60518605	0.2589896 5	7.7038E-1 1	2.6163E-1 0
XRCC6	118.47550 7	-1.60572518	0.2905014 1	4.2282E-0 9	1.1922E-0 8
DEDD2	66.482953 7	-1.60732564	0.5220386 5	0.0001895 6	0.0003141 6
PLD6	103.48648 5	-1.61360347	0.2120333 7	3.7555E-1 5	1.875E-14
GDF15	1280.5665 4	-1.61747356	0.1350103 2	6.4247E-3 4	1.0398E-3 2
PDE8A	14.700877 9	-1.61971567	2.3439925 2	0.0162286 3	0.0209516 5
ACADVL	381.46565 5	-1.62027964	0.1799859 3	3.0501E-2 0	2.1975E-1 9
CDC25A	570.47753 5	-1.62059845	0.1722962 8	7.147E-22	5.7973E-2 1
C3orf52	812.45047 4	-1.62190101	0.0980398	2.5643E-6 2	1.399E-60
SPRR2D	6.4067492 6	-1.62295103	1.6827849 9	0.0127551 4	0.0166934 6
ARFIP2	70.201275 6	-1.62635101	0.4460912 7	2.6298E-0 5	4.8768E-0 5
DDIT3	38.472775 9	-1.62723701	0.5474929 9	0.0002428	0.0003975 2
TNFAIP8L3	23.519840 7	-1.62754558	0.4833584 8	7.0002E-0 5	0.0001230 7
HRAS	114.25280 2	-1.63083057	0.2115239 5	1.6492E-1 5	8.5627E-1 5
UBE2F	19.701420 8	-1.63172285	0.7583017 3	0.0017747 4	0.0025908 8
PAQR5	16.191283 6	-1.64144637	0.6137750 5	0.0005217 6	0.0008166 9
PIGT	236.75115 1	-1.64147828	0.2729750 3	2.1835E-1 0	7.0947E-1 0
AFAP1L1	76.003970 4	-1.64238632	0.2359262 7	4.1855E-1 3	1.7576E-1 2
CHCHD3	22.281789 2	-1.64340015	0.5241092 7	0.0001400 6	0.0002368 2
PGF	73.153167 4	-1.64493079	0.3134677 5	1.7503E-0 8	4.6562E-0 8
FSD1	53.662900 6	-1.64611698	0.2871826 3	1.1588E-0 9	3.4779E-0 9
DCAF5	19.985655 2	-1.6468862	0.5088489 6	0.0001005 5	0.0001733 5

NLRP1	21.717982 2	-1.64902328	2.1005033 8	0.0150179 9	0.0194928 5
PLPP5	7.4905664 3	-1.6553217	1.8530779 3	0.0133266	0.0174144 3
KLK11	27.831761 7	-1.65597582	0.5287535 2	0.0001354	0.0002292 8
YDJC	184.33464 2	-1.65702677	0.2912759 2	1.4402E-0 9	4.277E-09
AREG	1184.2163 3	-1.65739518	0.1604995 9	6.7576E-2 6	7.0657E-2 5
TNIP1	1147.4812 8	-1.65923255	0.1381166 3	3.8537E-3 4	6.3586E-3 3
ODC1	4392.6574	-1.66253682	0.0929036 3	1.6527E-7 2	1.2153E-7 0
YIF1A	186.84136 2	-1.66469214	0.2359105 6	1.9938E-1 3	8.7021E-1 3
IL1RN	2635.2706 7	-1.6655699	0.1147190 9	1.168E-48	3.7098E-4 7
SLC12A4	9.6964154	-1.66696472	2.0801926 2	0.0144493 7	0.0187800 2
ULBP2	1064.1066 1	-1.66824844	0.0971043 7	4.7496E-6 7	3.0601E-6 5
UBAP1	38.923937 2	-1.67160424	1.3057597 4	0.0072508	0.0097751 4
PREB	33.580841 3	-1.6727079	0.4824982 7	4.2415E-0 5	7.665E-05
ANXA6	12.196856 8	-1.67488518	1.0424698 3	0.0041963	0.0058399 4
CAPN8	20.129859 2	-1.6801555	0.6850728 3	0.0007803	0.0011907 7
SLC6A11	72.914887 9	-1.68129931	0.2878290 6	5.4565E-1 0	1.6933E-0 9
CCNE2	755.30004 6	-1.68694187	0.1352431 5	1.2314E-3 6	2.3801E-3 5
TRABD2A	22.706168	-1.68709939	0.5067515 4	6.4184E-0 5	0.0001132 8
HIP1	620.13262 7	-1.68710557	0.4777427 6	3.2098E-0 5	5.8719E-0 5
MATN3	55.801306 5	-1.69009581	0.2809617	1.8568E-1 0	6.0711E-1 0
TMEM265	478.69923 5	-1.69010076	0.0993605 3	8.2725E-6 6	5.1818E-6 4
ZBTB8B	17.224100 5	-1.69337993	0.6296164 1	0.0004146 4	0.0006575 3

ADIPOR1	107.96052 2	-1.69367593	0.4002047 1	2.01E-06	4.2573E-0 6
KHDC1L	61.955540 7	-1.69553891	0.2966337 3	1.0903E-0 9	3.2812E-0 9
DAPP1	1001.7574 2	-1.69560918	0.0828546 9	5.2236E-9 4	6.9289E-9 2
AEN	431.43713 5	-1.69591899	0.1700465 9	2.2484E-2 4	2.1333E-2 3
LAMC2	43118.054 8	-1.70531339	0.0958928 1	1.0824E-7 1	7.8739E-7 0
EPOP	131.00060 9	-1.70773141	0.1812274 2	4.7285E-2 2	3.8963E-2 1
ARHGEF28	389.07221	-1.71362759	0.1457882 7	7.3053E-3 3	1.1206E-3 1
DNAJB2	804.87803 4	-1.71365145	0.0751506 4	4.821E-11 6	1.125E-11 3
KLHDC7B	118.99902 8	-1.7136996	0.2224536 5	1.3559E-1 5	7.0887E-1 5
CLSPN	333.08819 6	-1.71759904	0.3153762 6	4.6957E-0 9	1.3165E-0 8
MLLT11	607.83339 3	-1.719089	0.0927561 1	1.2195E-7 7	1.0185E-7 5
SYT14	31.06388	-1.72093677	0.4752045 3	2.0524E-0 5	3.8664E-0 5
GCH1	223.40557	-1.72121988	0.1927701 3	4.4275E-2 0	3.1495E-1 9
NES	62.900809 1	-1.72265103	0.4168050 3	2.7605E-0 6	5.7443E-0 6
TRPM2	63.663740 9	-1.73250443	0.2946717 3	3.6833E-1 0	1.1649E-0 9
C1orf112	63.150128 1	-1.73397635	1.6330989 1	0.0092788 8	0.0123396 2
SAMD4B	16.308763 1	-1.73515178	2.2727141 2	0.0134778 1	0.0175984 2
CFLAR	28.062449 2	-1.73694641	1.4828451 2	0.0076986	0.0103396 9
KRT23	558.10671 2	-1.7418578	0.1497343 3	2.7957E-3 2	4.1567E-3 1
HMGA1	2907.1325 4	-1.74284085	0.0746190 7	1.221E-12 1	3.059E-11 9
INHBA	119.87376 2	-1.74353501	0.2986210 3	4.5265E-1 0	1.4164E-0 9
TAF13	520.06045 3	-1.75537778	0.1200994 1	2.1638E-4 9	7.0716E-4 8



TAF9	65.8783017	-1.75795529	0.28636293	6.9323E-11	2.3781E-10
ZFP1	14.477403	-1.75838022	2.20085389	0.01275433	0.01669346
FZD9	19.844187	-1.75952669	0.50343712	2.7818E-05	5.1404E-05
NT5E	1000.06934	-1.76415014	0.16625357	2.4372E-27	2.7804E-26
ZNF26	97.3134247	-1.76684264	0.62850969	0.00022771	0.00037371
KDM4A	251.621158	-1.76767138	0.36583153	9.773E-08	2.3963E-07
ADAM8	3703.95985	-1.77122324	0.12073376	9.2516E-50	3.068E-48
FMNL1	164.443825	-1.77904732	0.15934287	5.3575E-30	7.1912E-29
DUSP14	164.644423	-1.78037138	1.26632258	0.00469542	0.00650113
FAM214B	71.8244	-1.78039544	0.47994602	1.1846E-05	2.3008E-05
STYK1	57.7909801	-1.7834105	0.701791	0.00043407	0.00068722
ZNF324	112.72081	-1.78565862	0.25536388	2.1366E-13	9.2831E-13
JCAD	591.845686	-1.78628096	0.09213791	8.9225E-85	9.1456E-83
SPATA33	53.5126746	-1.79057784	0.36823568	7.7252E-08	1.9206E-07
AAAS	46.9396866	-1.7914444	0.35062723	2.2098E-08	5.8011E-08
TMEM248	205.760589	-1.79216216	0.27544758	5.8258E-12	2.2204E-11
SLC25A19	115.727965	-1.79254904	0.275329	5.6585E-12	2.1627E-11
ATP5MJ	36.5178845	-1.79284831	0.35296945	2.5664E-08	6.693E-08
MAPK3	75.5427716	-1.79488474	0.30146253	1.8979E-10	6.1905E-10
RAB3IL1	89.309422	-1.7953459	0.25641696	1.9378E-13	8.4629E-13
BHLHA15	56.0402468	-1.79558261	0.33066363	3.9066E-09	1.1058E-08
MLX	247.720344	-1.79804546	0.12455095	2.6088E-48	8.1331E-47

DPY19L3	17.9283	-1.79847164	2.2568022 7	0.0121103 7	0.0158772 6
SOD2	2754.8432 6	-1.79919011	0.4145937 8	8.5596E-0 7	1.8917E-0 6
TMEM40	155.28741 3	-1.80090414	0.1714003 5	6.5586E-2 7	7.3459E-2 6
STAT5A	76.652110 5	-1.8098279	0.3493744 2	1.4249E-0 8	3.8266E-0 8
PLK3	999.86163 9	-1.81035431	0.0975310 8	5.4376E-7 8	4.7161E-7 6
ATF5	638.69112 2	-1.81216083	0.1145355 3	1.8021E-5 7	8.1274E-5 6
TUBB3	480.80915 8	-1.81315119	0.1136686 7	2.2829E-5 8	1.0953E-5 6
TJP2	2740.6387	-1.8162218	0.1142110 5	4.9359E-5 8	2.3351E-5 6
BSCL2	43.826902 2	-1.81698159	0.5467603 7	3.9812E-0 5	7.2206E-0 5
ACOT7	89.903194	-1.82169048	0.2405148 1	2.5831E-1 5	1.3158E-1 4
GDF11	153.55006 4	-1.82336531	0.1692867 9	3.5966E-2 8	4.3448E-2 7
CNOT10	52.678956 6	-1.82632686	0.3616713 3	2.6344E-0 8	6.8625E-0 8
RETREG1	24.379171 6	-1.83025793	0.5996918	8.9059E-0 5	0.0001545 6
IER3	2696.9607 2	-1.8314352	0.1299973 6	3.4186E-4 6	9.7994E-4 5
ZNF777	79.606313 4	-1.83347563	0.6918398 7	0.0002736 8	0.0004451 6
SFXN4	142.82902 9	-1.83498196	0.2609983 7	1.3701E-1 3	6.0582E-1 3
CDIPT	229.99404 5	-1.83595172	0.2073003 9	5.8227E-2 0	4.1032E-1 9
VNN1	17.071237 8	-1.83744325	0.7168040 2	0.0003379	0.0005423 2
FAM222B	11.449207 6	-1.8415428	2.0730581 7	0.0104156 6	0.0137647 8
PLCXD2	16.946282 8	-1.8434679	2.4728282 8	0.0117243 7	0.0153950 6
PDZK1	124.59661 4	-1.84367574	0.3202027 1	5.0822E-1 0	1.5815E-0 9
SH2D5	9.0813920 7	-1.84846838	2.3093025 8	0.0113194 7	0.014901

THSD1	83.316973	-1.85024568	0.3674037	2.5741E-08	6.7106E-08
TP53I3	138.116217	-1.85292293	0.20035288	1.5276E-21	1.2123E-20
TOLLIP	149.801059	-1.85528948	0.17793885	1.2721E-26	1.3993E-25
HMOX1	699.754608	-1.85959578	0.12091178	1.5596E-54	6.2429E-53
TCF7	54.1308338	-1.8621231	0.84377544	0.00073886	0.00113112
MCRIP1	17.0064384	-1.86673712	0.9272196	0.00112785	0.00168916
LIPG	266.589024	-1.87043611	0.14611447	1.0662E-38	2.3044E-37
DLD	35.4043061	-1.87426435	0.65545338	0.00013227	0.00022438
DNLZ	92.7301485	-1.87507782	0.22333643	2.7988E-18	1.7629E-17
STX2	12.0728843	-1.87560721	2.03242307	0.00952242	0.0126436
PSMA5	56.8368897	-1.8761929	0.31384134	1.2078E-10	4.019E-10
FBXO27	165.489548	-1.88032522	0.16157967	1.6808E-32	2.5324E-31
PIGV	161.982594	-1.88266786	0.24435943	7.54E-16	4.0451E-15
BCL2L13	258.755865	-1.89986427	0.16891433	1.3901E-30	1.9153E-29
MTX1	91.6787868	-1.90284454	0.37919629	2.278E-08	5.9707E-08
COMMD5	39.8874063	-1.90697323	0.45857717	1.2028E-06	2.6172E-06
IFRD1	1021.20765	-1.90829359	0.09137383	4.4236E-98	6.6502E-96
REEP4	63.6813044	-1.91117354	0.59219023	3.733E-05	6.7941E-05
ANKRD33B	126.939644	-1.91279404	0.35233511	2.4891E-09	7.2207E-09
SLAMF7	204.223151	-1.91891631	0.2084556	1.7799E-21	1.4034E-20
PLAUR	161.683545	-1.924946	0.19584763	4.383E-24	4.0507E-23
ADPGK	75.2409756	-1.92670791	0.32591702	1.4684E-10	4.8434E-10

SNAI1	182.78768 7	-1.93152772	0.2287315 8	1.4863E-1 8	9.567E-18
ZNF469	401.89782	-1.93461415	0.1254348 6	6.059E-55	2.4692E-5 3
STAU1	92.846462 3	-1.93873524	0.4052018 6	6.222E-08	1.5642E-0 7
TPST1	147.07769 1	-1.93981977	0.3066402 9	1.0664E-1 1	3.953E-11
NUAK2	531.08658	-1.94488476	0.1034158 6	3.4601E-8 0	3.121E-78
PTGR1	296.59522 8	-1.9463717	0.2252885 3	2.6054E-1 9	1.7786E-1 8
FGFR2	12.574131 9	-1.94730663	2.3739626 9	0.0098567 2	0.0130541 7
SH3D21	38.848791 7	-1.95014083	0.5689611 9	1.6298E-0 5	3.1128E-0 5
PTGES2	72.806054 5	-1.95371797	0.7212459 4	0.0001508 4	0.0002536 5
GNAZ	50.404734 1	-1.95405081	0.3371365 7	2.5939E-1 0	8.3441E-1 0
SMPD1	281.86976 6	-1.95460984	0.1323960 7	1.2341E-5 0	4.1955E-4 9
FHIP2B	22.500812 8	-1.95594942	2.3451311 2	0.0096366 9	0.0127802 8
RGS19	62.653124 4	-1.95723867	0.3074882 4	7.6982E-1 2	2.8981E-1 1
FAM222A	37.653505 3	-1.95849273	0.4837945 6	1.5208E-0 6	3.2786E-0 6
TRIM62	119.23003 5	-1.95869546	0.3749959 7	6.1974E-0 9	1.712E-08
ARID3B	306.68284	-1.96538567	0.1788330 8	1.9204E-2 9	2.5032E-2 8
CHST3	394.23250 8	-1.96709251	0.3046604 7	4.0767E-1 2	1.5841E-1 1
SH3KBP1	198.83136 1	-1.96802894	0.3716883 5	4.0638E-0 9	1.1484E-0 8
SERPINE1	5419.8476 4	-1.97161135	0.2902950 6	4.2314E-1 3	1.7747E-1 2
TATDN1	16.279461 9	-1.97552637	2.2245062 7	0.0088685 4	0.0118125
MFHAS1	123.31158 9	-1.98205827	0.4466980 5	2.594E-07	6.0616E-0 7
MRPL9	178.10760 8	-1.9861394	0.1987688 5	6.6795E-2 5	6.5966E-2 4

NEDD1	9.2825166 2	-1.98781893	2.3940147 3	0.0093124 8	0.0123794 3
TAGLN3	45.948782 6	-1.98863602	0.4602114 9	4.207E-07	9.6313E-0 7
WIZ	132.29318 1	-2.00547267	0.2714501 2	5.0743E-1 5	2.5042E-1 4
MXD1	18.116222 1	-2.00691502	2.2589648 2	0.0085529 4	0.0114191 2
SLC41A1	1928.1399 4	-2.00796063	0.1310888 6	2.3022E-5 4	9.0548E-5 3
AP3B2	12.826391	-2.00989168	0.8361959 7	0.0002865 2	0.0004642 7
CD44	1265.3261 3	-2.01139206	0.3960924 8	1.0417E-0 8	2.8312E-0 8
ITGAV	496.9553	-2.01540056	0.2529676 6	5.4395E-1 7	3.1291E-1 6
FRMD8	316.77245 2	-2.02011992	0.3510205 3	2.4518E-1 0	7.9095E-1 0
STOML1	19.480422 2	-2.02190759	2.3018421 3	0.0085145 4	0.0113723 3
TRMU	83.783460 8	-2.02465366	0.4009210 8	1.1313E-0 8	3.0662E-0 8
ICAM1	3926.1417 9	-2.02491124	0.0799653 6	6.871E-14 3	2.734E-14 0
PSMC3IP	194.29764 2	-2.02692608	0.2171354 1	3.3716E-2 2	2.7986E-2 1
S100A16	420.8633	-2.0425592	0.1616302 7	4.3524E-3 8	9.0596E-3 7
NRIP3	441.46459 4	-2.04607477	0.0943412 2	9.133E-10 6	1.584E-10 3
TIGAR	188.46926 5	-2.05537162	0.1768165 8	9.5345E-3 3	1.4527E-3 1
MMP9	33.782206 8	-2.05637943	0.5767893 8	6.4059E-0 6	1.2882E-0 5
NEDD4	70.735137 4	-2.05664171	0.3609624 6	2.8767E-1 0	9.1839E-1 0
TMCC1	84.212262 6	-2.05777251	0.3749587 2	9.3709E-1 0	2.839E-09
HSPB8	1082.1110 1	-2.06028937	0.0594198 8	6.497E-26 5	1.465E-26 1
EDN1	37.288494 1	-2.06088926	1.2504463 7	0.0016553 2	0.0024254 3
MAPK8IP2	14.117567 5	-2.06301083	2.3200054	0.0080276 3	0.0107687 8

KRT31	15.054799 9	-2.06460776	1.0659309 5	0.0008163 6	0.0012430 1
AKT1	124.96673 1	-2.06923658	0.3879304 6	2.0603E-0 9	6.0364E-0 9
SCNN1G	51.505146 1	-2.08160634	0.3879143	1.6307E-0 9	4.811E-09
SLC43A3	323.25015 2	-2.0859536	0.3453810 1	3.2761E-1 1	1.1604E-1 0
AVEN	125.66763 1	-2.09181722	0.2133917 4	2.7271E-2 4	2.573E-23
DNM1L	557.77510 2	-2.09383505	0.1735816 2	4.2962E-3 5	7.5687E-3 4
KRTAP2-3	6.3405193 5	-2.09405982	2.0167315 1	0.0061147 8	0.0083366 6
USB1	257.02331	-2.09428796	0.1345735 1	3.501E-56	1.5182E-5 4
RNH1	118.11163 9	-2.10386428	1.3608716 1	0.0019635 8	0.0028438 4
FILIP1L	374.09167 2	-2.10940192	0.1657782 9	1.0459E-3 8	2.2677E-3 7
TUBG2	7.4982690 4	-2.11470303	2.1711699 8	0.0067085 3	0.0090930 1
MISP	1048.5423 5	-2.11716384	0.0747374 4	3.887E-17 8	2.922E-17 5
SLC39A4	140.15256 5	-2.12144664	0.1840327 7	2.1356E-3 2	3.1823E-3 1
PLIN2	76.504593 6	-2.12811569	0.2669484 4	3.0289E-1 7	1.7725E-1 6
AK2	123.02855 1	-2.14191232	0.2112268 7	7.1213E-2 6	7.4346E-2 5
CLTRN	53.543424 9	-2.14640478	0.4481220 5	2.3075E-0 8	6.0389E-0 8
CPSF3	25.329795	-2.14995832	0.6455705 5	1.0125E-0 5	1.9839E-0 5
C12orf4	20.871387 4	-2.15139276	2.4918735 1	0.0075154 9	0.0101078 1
IL6R	452.47744 6	-2.1566665	0.4766907 7	7.7391E-0 8	1.9234E-0 7
GAPVD1	16.024397 2	-2.15912896	2.3341344 8	0.0069127 9	0.0093436 6
INAFM2	19.361281 1	-2.15996722	0.7149690 9	2.7925E-0 5	5.1586E-0 5
ZC3H14	8.2221063 6	-2.16023931	2.2667847 5	0.0066232	0.0089863 5

SUN1	9.3802076 1	-2.16218874	2.1899658 4	0.0062486 3	0.0085088 6
CEMIP	233.69063 3	-2.17425846	0.2042308 5	3.0138E-2 8	3.6538E-2 7
SERPINE2	75.978917	-2.17690852	0.2894432	7.9568E-1 6	4.2518E-1 5
NDOR1	66.546571	-2.19012337	1.7326509	0.0034177 1	0.0048041 1
ETFDH	18.150364 3	-2.19148707	1.5500621 1	0.0023903 5	0.0034238 3
NIBAN2	1094.6507 5	-2.19510632	0.3094919	1.7034E-1 4	8.0867E-1 4
CYP27B1	187.05112 8	-2.19767983	0.1754575 2	8.1644E-3 8	1.6636E-3 6
SPHK1	270.54039 4	-2.20501959	0.1805089 2	3.6918E-3 6	6.8803E-3 5
GPS1	15.571207 4	-2.20679831	1.9003076 5	0.0042338 9	0.0058886 2
TGM2	35.738826	-2.20811091	0.7830184 5	4.5605E-0 5	8.2009E-0 5
N4BP3	176.83393 3	-2.21065316	0.1882186 8	1.0338E-3 3	1.6494E-3 2
TENT5B	165.18118 8	-2.21351598	0.1938655 1	4.6052E-3 2	6.8022E-3 1
TRMT2B	16.667545 8	-2.21376497	2.2464489 4	0.0059568 8	0.0081410 7
NLRP10	71.419747 7	-2.21430037	0.3017308 8	2.5438E-1 5	1.2968E-1 4
FLYWCH1	48.609240 2	-2.21829965	0.7509775 8	2.8541E-0 5	5.2682E-0 5
ARHGAP25	66.069889 4	-2.22546228	0.3144725 4	1.6108E-1 4	7.6631E-1 4
ZNF44	30.316147	-2.22858468	0.4953162 5	6.1472E-0 8	1.5459E-0 7
EHBP1L1	22.841943 2	-2.23065871	0.8315927 6	6.5894E-0 5	0.0001161 5
HSD17B2	72.806636 7	-2.23659504	0.3247800 7	5.8031E-1 4	2.6312E-1 3
CENPK	7.4256629 4	-2.23675907	2.1385302	0.0052210 8	0.0071877 5
PRRG1	13.284278 3	-2.23849677	0.8586627 8	8.1557E-0 5	0.0001423 8
DPF1	68.533452 8	-2.24090205	0.3410077 4	4.849E-13	2.0261E-1 2

CDKN1A	3959.3475 4	-2.24105805	0.0408298 6	0	0
BCL2L1	107.04168 4	-2.24168954	0.3968820 9	1.4813E-1 0	4.8834E-1 0
ZDHHC21	59.686562 9	-2.25621903	1.0163699 4	0.0002493 8	0.0004076
NFKB2	233.26742 9	-2.25815051	0.3045811 4	1.129E-15	5.9527E-1 5
ZNF263	11.951085	-2.26516679	2.3274224 5	0.0057861	0.0079140 7
CAB39	179.10007 9	-2.26662867	0.3591223 1	2.2913E-1 2	9.0967E-1 2
LAMB3	21118.811 2	-2.27873232	0.0969073 3	2.887E-12 4	7.512E-12 2
LYPLA1	29.450957 8	-2.27908753	0.9601766	0.0001502 4	0.0002529
RNF185	76.180682 9	-2.28458094	0.8023605 1	3.3023E-0 5	6.0297E-0 5
CHAC1	448.03160 2	-2.28478464	0.1535787 7	4.2816E-5 2	1.5573E-5 0
PHLDA2	576.37387 9	-2.29678084	0.1985918 2	5.0579E-3 3	7.8659E-3 2
L1CAM	53.847558 3	-2.29819499	0.3747245 2	5.9352E-1 2	2.2595E-1 1
ZBED2	152.27579 5	-2.3040895	0.2076615 3	1.0242E-3 0	1.417E-29
EEF1A2	50.263932 3	-2.30747845	0.4310415 3	5.4704E-1 0	1.6968E-0 9
NEURL3	14.184248 6	-2.31265204	1.2649574 9	0.0006854	0.0010545 2
PLEKHM1	13.091875 5	-2.334851	2.4321044 6	0.0055352 4	0.0075847 5
PRSS22	57.314161 8	-2.34293602	0.5622456	1.6379E-0 7	3.9058E-0 7
TNFAIP3	537.52332 9	-2.3537208	0.2467407 9	7.8583E-2 4	7.1071E-2 3
SNAP23	129.65424 1	-2.35544219	0.4570358 7	1.2553E-0 9	3.7542E-0 9
ATM	64.781387 9	-2.35847441	2.6177440 3	0.0058564 1	0.0080053 7
CD177	37.530726 4	-2.35942094	0.5118032 4	1.9538E-0 8	5.1569E-0 8
STARD3NL	14.384924 3	-2.36250963	2.4256666 5	0.0052817 1	0.0072638 3



ALAS1	299.99935 4	-2.36499555	0.1663745 3	3.9869E-4 8	1.2316E-4 6
SH2D3A	9.0674223 9	-2.36507018	2.0231148 3	0.0035858 9	0.0050235 1
SNTA1	16.797177 7	-2.36645333	2.3786657 4	0.0050863 5	0.0070079 8
SUPT7L	165.46037	-2.3834527	0.2535666 2	2.4518E-2 3	2.1653E-2 2
NKX1-2	317.46470 9	-2.38480718	0.1242865 7	2.2439E-8 4	2.2E-82
ABL2	1172.2764 5	-2.39655045	0.3246143 2	6.1852E-1 6	3.3288E-1 5
SEH1L	10.200496 4	-2.40247106	2.4171803 5	0.0049348 5	0.0068117 3
SDCBP2	315.32041 8	-2.40451203	0.1855292 4	8.3039E-4 1	1.8978E-3 9
IL1B	2798.2113 8	-2.40781407	0.1467382 6	6.6552E-6 3	3.7209E-6 1
GPR137	30.552012 7	-2.41005439	1.3247028 4	0.0006132 6	0.0009511
RPP40	74.697375	-2.41820213	0.7844056 5	9.8635E-0 6	1.9352E-0 5
KIAA0513	62.683963 1	-2.41901215	0.3044530 9	6.7448E-1 8	4.1443E-1 7
CD2BP2	26.277388 1	-2.42020482	1.1080064 6	0.0002025 1	0.0003344 7
TMEM217	15.966804 4	-2.42579299	1.3690632 6	0.0006894 5	0.0010600 3
MPI	23.450874 4	-2.42796302	0.8602616	2.4407E-0 5	4.5548E-0 5
MFSD8	49.578709	-2.44339704	3.0230368 6	0.0057757 2	0.0079014 7
TRAPPC2L	12.591705 8	-2.44452926	1.3575303 2	0.0006198 4	0.0009604 3
RAB3B	78.208071 7	-2.44977837	0.3140452 6	1.7634E-1 7	1.052E-16
SPRR1A	18.970312 7	-2.45219701	1.3663992 3	0.0006251 3	0.0009675 1
DLL4	11.341006 2	-2.46011299	1.7130160 7	0.0016957 7	0.0024809 5
GSDMC	30.148254 6	-2.46162145	0.8745789 5	2.3149E-0 5	4.3333E-0 5
GNL2	422.29848 5	-2.46342515	0.1876246 8	5.8932E-4 2	1.4087E-4 0

FAM83A	30.133395	-2.46559992	0.4817636 4	8.8098E-1 0	2.675E-09
SULT2B1	186.42881 1	-2.48552146	0.1867187 3	4.4494E-4 3	1.1232E-4 1
KDM6A	19.948010 9	-2.4897224	2.6815291 8	0.0050227 5	0.0069245 8
CLTB	78.860635 8	-2.50117437	0.2654199 6	8.8249E-2 4	7.9495E-2 3
APTX	43.606932 6	-2.51039466	1.0459327 1	8.6963E-0 5	0.0001511 6
ZNF562	34.103298 3	-2.51523675	3.0153467 4	0.0053209 9	0.0073120 1
LY96	14.581511 3	-2.51834713	0.8234188 4	8.3269E-0 6	1.6481E-0 5
ACP7	69.668757 9	-2.52293731	0.4854918 1	4.3846E-1 0	1.3745E-0 9
KPNA1	227.17262 7	-2.53690309	0.2018234 9	4.7353E-3 9	1.0401E-3 7
ENOX2	16.144444 2	-2.54408943	2.7837556 8	0.0048642 5	0.0067170 2
RNASE7	488.59382	-2.54417165	0.1634203 8	1.7122E-5 7	7.7738E-5 6
KRT8	376.46850 8	-2.55120096	0.2689494 3	3.4559E-2 4	3.2247E-2 3
CPNE5	7.2101605	-2.55146891	2.2980721 1	0.0035057 5	0.0049204 2
LAMA3	14860.328	-2.55646322	0.0926959 5	2.536E-17 0	1.56E-167
NAB2	227.41791 9	-2.55811272	0.3015822	3.1195E-2 0	2.2451E-1 9
CDSN	13.196650 8	-2.57081027	1.4234711 4	0.0005308 4	0.0008299 4
MIA2	9.3166717 8	-2.57292217	2.3307292 1	0.0034947 2	0.0049059 6
RAET1L	74.360183 3	-2.57667019	0.3513467 6	2.994E-16	1.636E-15
LAPTM5	178.79124 5	-2.5794244	0.2080246 3	2.939E-38	6.1555E-3 7
MRPL52	73.071110 1	-2.58136457	0.3996745 3	1.4816E-1 3	6.5255E-1 3
NCR3LG1	68.613992 3	-2.58611803	0.3651994 8	1.843E-15	9.5101E-1 5
SPRR2E	10.478574 8	-2.59713177	1.9301864 8	0.0019306 1	0.0028009

ZNF260	19.594913 9	-2.59967253	2.7197926 5	0.0044110 3	0.0061186 4
IGFL1	25.716688 6	-2.6068068	0.7329480 2	9.1562E-0 7	2.0189E-0 6
SUN3	6.2539861 9	-2.60878083	2.2385270 3	0.0029802	0.0042186 8
ADAM19	315.24310 6	-2.61671578	0.2544946 6	7.6448E-2 8	9.0415E-2 7
CD274	578.02061 6	-2.62019875	0.1104594 6	1.664E-12 7	4.69E-125
CPA4	633.25723 5	-2.6257705	0.1054870 7	6.579E-14 0	2.225E-13 7
FAM25A	55.809493 7	-2.62903328	0.3928349 5	2.3427E-1 4	1.0975E-1 3
SFXN5	109.40744 8	-2.63055684	0.8729041	7.766E-06	1.542E-05
BDH1	70.332421 3	-2.65823066	0.3246371 3	2.0689E-1 9	1.4181E-1 8
FSTL3	515.80066 9	-2.66301663	0.1368725 2	1.4163E-8 7	1.5969E-8 5
NEFM	46.096192 2	-2.66305782	0.6482640 4	6.7213E-0 8	1.6829E-0 7
NOCT	320.10701 1	-2.66567088	0.1430637 9	9.4274E-8 1	8.6184E-7 9
ARC	29.925557 9	-2.69605132	0.6141902 3	1.5683E-0 8	4.1968E-0 8
SDR9C7	14.289807 5	-2.70438467	1.2700462 7	0.0001666 8	0.0002784 1
CAMK1G	8.421765	-2.71135015	2.1545136 2	0.0022287 7	0.0032005 2
METTL26	99.786642 6	-2.71367129	0.2907684 2	5.3189E-2 4	4.8707E-2 3
OTUD5	12.080251 8	-2.72287002	2.7379100 4	0.0037842 3	0.0052915 1
IGF2BP2	63.473189 6	-2.73105227	0.5841014 8	3.3003E-0 9	9.4206E-0 9
ATG13	11.801709 5	-2.74916204	2.5623304	0.0032617 2	0.0045941 1
SSR3	222.90165 2	-2.75609124	0.3053221 3	7.4408E-2 3	6.3961E-2 2
KMO	24.515822 7	-2.76258407	0.8197965 6	1.4564E-0 6	3.1438E-0 6
IQCE	21.548771 7	-2.76355444	2.6906111 9	0.0034911 7	0.0049019 9

PTGES3L	9.7090048 1	-2.77270371	1.8575686 8	0.0011464 2	0.0017150 7
ZBTB38	15.850257 8	-2.77981093	2.7194832 4	0.0034755 1	0.0048810 1
IFFO1	16.233997 2	-2.78450965	0.8955576 4	4.1348E-0 6	8.4662E-0 6
FOSL1	493.91335 6	-2.78930685	0.2264510 4	1.9793E-3 8	4.2107E-3 7
MPO	7.8824564 1	-2.79072655	2.1396280 8	0.0018892 7	0.0027456 3
ANKRD22	258.13804 3	-2.79563488	0.1863372 1	1.6247E-5 4	6.4654E-5 3
EMP3	488.57557	-2.81276775	0.2343407 7	8.3377E-3 7	1.6162E-3 5
PDCD1LG2	44.168020 9	-2.8218966	0.4582175	3.9436E-1 3	1.6601E-1 2
FMNL2	71.427739 4	-2.83468577	0.5677874	4.5605E-1 0	1.4263E-0 9
IRF3	175.14288 2	-2.83980387	0.2610319 6	3.3582E-3 1	4.7329E-3 0
FHOD3	9.2492011 2	-2.85671037	2.2177089 3	0.0018922	0.0027493
TRPV3	63.486003 6	-2.85815389	0.8922837 4	2.5646E-0 6	5.3614E-0 6
GGCT	14.813686 9	-2.86291374	1.1686894	4.7616E-0 5	8.5444E-0 5
UCN2	213.94871	-2.86869266	0.1743013	1.0712E-6 4	6.4701E-6 3
CXCL1	589.98689 5	-2.89160794	0.1866276 6	5.189E-58	2.4378E-5 6
ZNF544	35.250445	-2.89583175	1.2239538 1	6.2802E-0 5	0.0001109 3
SRRT	78.482145 8	-2.91383187	0.6580209 5	8.1211E-0 9	2.2279E-0 8
LCK	36.439375 1	-2.91674044	0.7461352	1.0456E-0 7	2.5528E-0 7
PLEKHN1	52.022603	-2.92077491	1.6864432 3	0.0005167 1	0.0008091 6
SIRPB2	89.675876 7	-2.93610334	0.3133806 4	1.4268E-2 4	1.3809E-2 3
SAA2	24.298379 1	-2.93767002	1.0178934 1	8.6191E-0 6	1.6999E-0 5
ZCCHC8	8.2831654 8	-2.94891875	2.4584364 5	0.0022111 1	0.0031778 5

PLGRKT	28.935817 9	-2.95652371	0.6461246	3.5632E-0 9	1.0128E-0 8
PRDM1	135.63158 4	-2.96258266	0.2489546 1	1.583E-36	3.0337E-3 5
CEACAM19	286.85704 3	-2.96966571	0.3336044 2	1.0697E-2 2	9.1027E-2 2
GGT1	47.431646 6	-2.98026521	1.2108237 4	4.224E-05	7.6405E-0 5
TNFRSF9	135.69366 3	-2.99686405	0.2703025	1.9572E-3 2	2.9293E-3 1
ZNF211	24.425870 4	-3.00532385	2.882371	0.0028602 2	0.0040581 7
IL1A	2410.8591 7	-3.01859337	0.2303158 2	3.2541E-4 3	8.3071E-4 2
NACAD	6.4703239 2	-3.03453664	2.3107523 2	0.0016124	0.0023661 4
NOX5	9.7154481 1	-3.03586467	1.8851066 9	0.0007085 9	0.0010874 9
EXOG	51.638926 4	-3.04926325	0.7988754	1.4475E-0 7	3.4811E-0 7
ABCA12	67.913954 8	-3.08098671	0.7026562 5	8.807E-09	2.4082E-0 8
LOC10065304 9	6.6497421 1	-3.11048386	2.3415961 1	0.0014947 6	0.0021997
PLAU	325.93039 9	-3.15645001	0.2216720 9	5.2535E-5 0	1.7682E-4 8
TMEM52B	40.181369 5	-3.16444519	0.7692482 1	3.4069E-0 8	8.79E-08
GFPT2	67.883120 6	-3.21451573	0.3831024 3	1.0219E-2 0	7.5802E-2 0
ANKRD1	35.791640 7	-3.23905877	0.5934698 9	2.3169E-1 1	8.3415E-1 1
PPCDC	96.952875 7	-3.24680063	0.7131351 6	3.7764E-0 9	1.0712E-0 8
IL36RN	213.15252 7	-3.24847552	0.3943822 5	4.1157E-2 0	2.9308E-1 9
HBEGF	2970.0816 2	-3.27691295	0.2237602 5	2.0861E-5 2	7.6697E-5 1
CCL20	14.559806 9	-3.28944082	1.7771991 2	0.0003107 2	0.0005010 8
NFATC2	42.924241 9	-3.31259609	2.9796253 6	0.0021011 7	0.0030327 3
C11orf96	11.269235 2	-3.31899305	1.8488532 7	0.0003674 6	0.0005871 1

MCAM	40.699826 2	-3.32959827	0.6336126 9	8.5657E-1 1	2.8988E-1 0
LAT2	23.914039 6	-3.34883379	1.9301126 7	0.0004386 3	0.0006939 6
SHISAL1	10.570398 4	-3.35570481	2.4119829 8	0.0011447 6	0.0017129 7
TEDC2	50.233590 8	-3.36913978	0.6619282 9	2.3309E-1 0	7.5555E-1 0
PFKFB4	75.850218 1	-3.37648231	0.4428780 9	9.067E-18	5.536E-17
ALOXE3	79.821470 3	-3.38685655	0.9851358 4	8.3207E-0 7	1.8437E-0 6
IL4I1	86.100292	-3.40483578	0.4339569 7	1.6979E-1 8	1.0856E-1 7
TMEFF1	42.753917 5	-3.46394129	0.5277790 6	3.0075E-1 4	1.3916E-1 3
TNF	31.538563 1	-3.49715697	0.8601937 6	5.4773E-0 8	1.3857E-0 7
RND1	71.934048 3	-3.56424247	0.4092186 8	2.3972E-2 1	1.8705E-2 0
IL2RG	39.339138 2	-3.57228917	0.6012327 9	2.4526E-1 2	9.7257E-1 2
TRIM36	34.457053	-3.59852584	0.7892489 5	5.8789E-0 9	1.6286E-0 8
ECM1	26.104614 2	-3.60055021	1.3969377 1	2.672E-05	4.9497E-0 5
SEMA7A	90.876987 8	-3.60427688	0.5193372	3.6656E-1 5	1.8315E-1 4
CRCT1	14.519700 1	-3.60765028	1.5927892	7.8714E-0 5	0.0001376 7
CNOT7	17.224342 4	-3.61364064	2.8458107 9	0.0013416 4	0.0019860 4
SPRED3	21.482645 4	-3.6217815	2.6615874 7	0.0011035 6	0.0016557 1
PRAME	10.374242 5	-3.66852124	2.3591335 9	0.0006752 5	0.0010404 5
FKBP9	633.90494 3	-3.6982575	0.6905426 7	1.1252E-1 0	3.7516E-1 0
DISP1	14.027765 2	-3.71310829	2.9345178 7	0.0012889 5	0.0019132 6
KRT75	18.265189 4	-3.71660327	1.3292143 5	1.2766E-0 5	2.4724E-0 5
RNF223	267.06148 8	-3.72523005	0.2017795 1	1.7046E-7 8	1.4976E-7 6

PI3	182.60456 3	-3.76879419	0.3100427 1	2.0995E-3 6	4.0121E-3 5
CXCL8	1085.3382 3	-3.77115929	0.1497847 6	5.052E-14 2	1.899E-13 9
COL9A2	10.930234 1	-3.77209152	2.6521322 5	0.0009050 3	0.0013718 4
PHLPP2	19.379625 2	-3.81858076	2.8245233 3	0.0010352	0.0015579 8
MBNL1	16.062952 5	-3.84444715	2.7560813 2	0.0009354 4	0.0014147 6
CST6	382.69461 1	-3.85258573	0.1729357 3	7.88E-112	1.568E-10 9
STIM1	13.640554 1	-3.86608489	2.4722123 4	0.0006253 3	0.0009676
RABGEF1	30.679107 1	-3.91979907	1.7839444 2	0.0001022 5	0.0001761
CXCL2	135.61871 6	-3.95131284	0.3159155	9.8805E-3 8	1.9953E-3 6
XRCC4	8.4554827 8	-3.9664501	2.4575659 7	0.0005374	0.0008396 1
NDRG3	15.166864 4	-3.97396625	2.8939165	0.0009283 3	0.0014052 7
MSX1	14.093442 7	-3.97413916	1.4930970 5	2.3212E-0 5	4.3437E-0 5
RAP1GAP	11.024221 5	-3.98219479	2.3779033 7	0.0004587 1	0.0007236 9
SERPINB2	111.50569 6	-3.99727959	0.3651535 2	1.0543E-2 9	1.3931E-2 8
PAX8	18.962817	-4.00178159	1.2307714 5	2.9964E-0 6	6.2179E-0 6
GIPR	11.547155 1	-4.03100762	2.4766597 7	0.0005114 6	0.0008014 9
ACAD8	13.324084 1	-4.04781884	2.5915211 2	0.0005972 6	0.0009277 7
CALD1	43.444819 5	-4.07382465	3.0571441 9	0.0009604 6	0.0014506 6
SPRR1B	174.40793 3	-4.10897436	0.3806120 7	1.0075E-2 8	1.2567E-2 7
CGB8	21.406688 5	-4.11852997	1.1878306 8	1.5337E-0 6	3.3054E-0 6
MITF	22.989983 2	-4.11874015	2.5053179 6	0.0004812	0.0007577 5
MCOLN3	13.251522 5	-4.1511514	1.9614661 8	0.0001339 4	0.0002268 6

GTF2IRD1	13.284313 7	-4.18574993	2.3227070 2	0.0003185 6	0.0005128 7
GSDME	44.300964 1	-4.19518939	0.8250471	1.9247E-0 9	5.6512E-0 9
IL6	80.691386 1	-4.23970331	0.4682551 8	4.6998E-2 1	3.5885E-2 0
KDM1B	10.636074 7	-4.24445175	2.474088	0.0003929 7	0.0006239
IL11	334.88404	-4.24615892	0.1971136	7.708E-10 4	1.272E-10 1
EFCAB1	14.883317 2	-4.25236372	2.9041472 3	0.0006923 1	0.0010639 4
TDRKH	15.135166 9	-4.26444632	2.3579304 9	0.0003101 1	0.0005002 1
SLC28A3	45.608238 4	-4.27033329	0.6511332 2	7.5893E-1 3	3.1268E-1 2
CSGALNACT1	14.381777 1	-4.27232022	2.1900702 5	0.0002133 3	0.0003511 4
PAG1	69.778948 6	-4.28228138	1.0691156 5	2.506E-07	5.8662E-0 7
RPUSD1	15.411959 2	-4.31471626	1.9213331 7	9.4155E-0 5	0.0001629
C4BPB	8.1343402 7	-4.32737728	2.4565158 1	0.0003455 8	0.000554
STXBP1	11.731082 4	-4.37602582	2.3077679 5	0.0002446 5	0.0004003 6
TRIML2	33.740869 7	-4.42301584	1.2681929 2	2.0099E-0 6	4.2573E-0 6
CNPPD1	18.344369 9	-4.42587359	2.3232709 9	0.0002381 6	0.0003902
TNFRSF1B	60.256260 3	-4.43568022	1.1039835 2	3.0355E-0 7	7.0496E-0 7
IL23A	176.22398 8	-4.4522137	0.3717532 4	6.5121E-3 4	1.0514E-3 2
UNC13A	23.772430 6	-4.45601054	2.1411940 3	0.0001503 4	0.0002529 9
EBI3	53.505256 9	-4.46027879	0.7016982 3	4.8194E-1 2	1.8567E-1 1
PRKCZ	19.630977 9	-4.47573637	2.7947597 3	0.0004825 3	0.0007591 4
MAP3K7CL	9.4575752 5	-4.49559388	2.0555526 8	0.0001133 4	0.0001938 2
GTF2H3	10.894254 6	-4.51349979	2.4411132	0.0002710 9	0.0004411 7



RCHY1	11.329807 8	-4.51977958	2.3862549	0.0002425	0.0003971 2
DUSP18	12.459557 5	-4.54613605	2.6451464 1	0.0003659 4	0.0005848 3
ABLM2	10.117624 3	-4.56512798	2.5230132 7	0.0002956 2	0.0004780 3
SBSN	52.553964	-4.6257298	1.0240369	5.9948E-0 8	1.511E-07
IRF7	73.839733	-4.66370047	0.6828975 3	4.6828E-1 3	1.9579E-1 2
ACSL4	22.138419	-4.68004267	2.7784119 4	0.0003813 8	0.0006074 9
DNASE1	16.368133 4	-4.75711063	2.3168701 2	0.0001607 5	0.0002691 8
ZNF419	16.710526 6	-4.75765531	2.3271609	0.0001642 7	0.0002747 2
NGF	17.869243 6	-4.75809621	1.3211794 3	1.9405E-0 6	4.1164E-0 6
CEP72	14.659500 2	-4.76456007	2.4373910 3	0.0002036 8	0.0003362 4
OFD1	11.715377 3	-4.78085142	2.2446894 7	0.0001329 5	0.0002254 8
MEMO1	16.133565 3	-4.80615177	2.3672113 7	0.0001694 2	0.0002825
MANBA	27.794184 9	-4.83680276	2.1345648 6	9.4595E-0 5	0.0001635 8
NRM	22.374535 7	-5.0302003	2.3233201 3	0.0001212 2	0.0002066 2
SGPP2	29.781633	-5.14837919	1.4387641 1	2.8884E-0 6	6.003E-06
FLNC	199.02456 4	-5.18334083	0.4279590 2	3.1877E-3 4	5.3116E-3 3
SPRR2A	50.869898	-5.19787286	1.1961163 9	2.4981E-0 7	5.8497E-0 7
MYLK	15.632482 6	-5.2109981	2.5654888 1	0.0001611	0.0002696 3
KRIT1	24.664163 4	-5.25232321	1.8717643 1	2.5569E-0 5	4.7534E-0 5
ZC3H12C	23.891066 9	-5.25254894	2.6368774 2	0.0001739 6	0.0002895 8
CSPG5	12.097762 8	-5.31750566	2.0515044 5	4.4015E-0 5	7.9308E-0 5
ZNF124	11.995338 3	-5.3781624	2.1214403 6	5.0675E-0 5	9.0621E-0 5

AMDHD2	14.297529 3	-5.38516625	2.068236	4.3067E-0 5	7.7713E-0 5
SRRM1	33.063630 6	-5.38709832	2.8404843 3	0.0002051 3	0.0003384 7
RNF212	8.6971909	-5.39792507	1.7115855 2	1.0847E-0 5	2.1159E-0 5
CCSER2	40.777132 8	-5.40614436	2.5149650 8	0.0001211 3	0.0002065 6
CSF2	656.71415 3	-5.42810325	0.2490037 4	8.945E-10 6	1.584E-10 3
ZMAT3	32.767382 3	-5.43361018	2.6323596	0.0001444 7	0.0002437 3
SPATS2	12.290647 7	-5.43574942	2.1845238 6	5.6664E-0 5	0.0001006 1
EVI2B	19.185908	-5.46300651	1.5892406 8	5.1825E-0 6	1.0509E-0 5
ZBTB21	14.999672 8	-5.49325812	2.0005306 1	3.0974E-0 5	5.6816E-0 5
MBNL2	20.992585 1	-5.58115229	2.1824950 5	4.8438E-0 5	8.6804E-0 5
APOE	13.839325 8	-5.58778411	1.7742257 9	1.1625E-0 5	2.2612E-0 5
OSBPL8	19.176476 4	-5.60621044	2.3757278 8	7.5118E-0 5	0.0001317 5
POC5	22.121647 1	-5.61909005	1.9096161 5	1.9595E-0 5	3.6986E-0 5
VEZT	21.609436 6	-5.64095121	2.6203670 2	0.0001157 4	0.0001977 3
FLG	116.72579 5	-5.64798173	0.4469930 7	4.5576E-3 7	8.8853E-3 6
GZF1	18.978069 4	-5.64799243	2.1790320 3	4.4768E-0 5	8.0589E-0 5
SLC44A3	11.812948 9	-5.65578251	1.8707567 3	1.6183E-0 5	3.0917E-0 5
MROH6	74.110397	-5.69272022	0.6556854 4	1.1191E-1 8	7.3008E-1 8
NR1H2	13.964325 1	-5.73848346	1.8177550 9	1.1811E-0 5	2.2953E-0 5
CSF3	21.197951 9	-5.8260577	1.4284276	9.5292E-0 7	2.0978E-0 6
NLRP3	9.0009521 6	-5.84068762	1.8005017 9	9.696E-06	1.904E-05
CLEC16A	15.354589 8	-5.86951817	2.1478194 4	3.2568E-0 5	5.9531E-0 5

ISG20	21.767781 9	-6.00437795	1.7222852 3	5.4028E-0 6	1.0943E-0 5
SLMAP	21.321371 7	-6.0051467	2.4549394 5	5.9627E-0 5	0.0001056
STON2	12.470910 7	-6.07077729	1.7831786 3	6.732E-06	1.3478E-0 5
RHOBTB2	20.247951 7	-6.1080898	2.0396477 9	1.8016E-0 5	3.4169E-0 5
GRHL3	15.98333	-6.11687788	1.9521818 7	1.3072E-0 5	2.5266E-0 5
IL36G	22.177906 5	-6.12153028	1.3412458 2	2.1367E-0 7	5.0505E-0 7
BROX	43.898322 7	-6.13484342	3.1607142 2	0.0001514 9	0.0002546 8
C1S	14.056238 3	-6.17085676	1.5108580 2	1.0539E-0 6	2.3066E-0 6
SEMA6B	22.812349 3	-6.22601573	1.7927547 7	5.7665E-0 6	1.1655E-0 5
ANGPTL4	109.61916 9	-6.23321849	0.6888709 7	3.6362E-2 0	2.6058E-1 9
ARHGEF10	17.716374 5	-6.24092388	1.3943302 1	3.0099E-0 7	6.9923E-0 7
PMAIP1	19.701901 4	-6.37250641	1.2720928 3	3.998E-08	1.0256E-0 7
KCNG1	27.184786 4	-6.43277424	1.2357248 8	1.7023E-0 8	4.5339E-0 8
UBE2E1	15.781953 5	-6.44322877	1.3226267 4	7.0933E-0 8	1.7714E-0 7
TUT7	26.391198	-6.45034446	2.2343539 5	2.2321E-0 5	4.1899E-0 5
GPR132	21.455471 2	-6.46932572	1.4216286 8	2.3972E-0 7	5.6252E-0 7
RBP4	22.493377 1	-6.55369903	1.5756152 1	8.8186E-0 7	1.9471E-0 6
CCDC68	17.743362 8	-6.59200248	1.5330067 5	5.658E-07	1.2759E-0 6
APOBEC3A	37.453835 8	-6.59611952	1.2335009 9	8.7045E-0 9	2.3821E-0 8
PISD	14.140009 2	-6.60675547	1.5996192 1	9.6542E-0 7	2.1239E-0 6
ARMC10	29.088047 8	-6.61319425	1.4107267 7	1.4557E-0 7	3.4971E-0 7
PLEKHA5	14.491378	-6.62747264	1.3519121 8	6.2599E-0 8	1.5725E-0 7

KANK1	23.296023 8	-6.65543968	1.5269396 3	4.6656E-0 7	1.062E-06
HSD11B1	57.414031 1	-6.69152657	1.2785597 1	1.4646E-0 8	3.927E-08
FGFR1	20.383064 4	-6.78025614	1.5693386 5	5.2554E-0 7	1.1891E-0 6
TULP4	20.178897 2	-6.783205	1.4338916	1.2195E-0 7	2.9569E-0 7
TRPM4	21.007988 5	-6.89813845	1.5238146 3	2.5538E-0 7	5.9738E-0 7
ZNF12	32.559760 1	-6.93446138	1.8040017 1	2.1493E-0 6	4.5381E-0 6
SLC4A11	30.436296 6	-6.95346191	1.3516114 8	2.0606E-0 8	5.424E-08
HECTD2	29.426354 9	-6.96538878	1.8830240 7	3.1452E-0 6	6.5107E-0 6
STK32C	25.027013 3	-6.98096766	1.3933393 4	3.7114E-0 8	9.5504E-0 8
TBC1D1	35.722708 1	-7.03440856	1.8322602 9	2.1395E-0 6	4.5189E-0 6
PSMD2	21.603447 5	-7.03756245	1.5627132 7	2.697E-07	6.2915E-0 7
DAB2	25.395187 9	-7.07899615	1.2703287 2	2.3916E-0 9	6.9558E-0 9
HLA-E	221.88914 6	-7.10325158	0.6301470 1	2.7203E-3 0	3.6953E-2 9
DPH7	29.762137 5	-7.16177614	1.4787143 5	7.0608E-0 8	1.7639E-0 7
LETM2	68.101050 6	-7.22227714	2.4232044 9	1.5572E-0 5	2.9818E-0 5
PFKFB3	26.798901 2	-7.23230465	1.9549336	2.9634E-0 6	6.1552E-0 6
GEM	31.918553 7	-7.26266102	1.2758262 4	1.1294E-0 9	3.3944E-0 9
MLH1	31.872930 5	-7.26899183	1.6011147 4	2.2023E-0 7	5.1929E-0 7
ARRB2	32.418053 2	-7.27029245	1.7418183 6	7.5999E-0 7	1.6935E-0 6
GLMN	26.370952 1	-7.41973657	1.5332805 3	6.3973E-0 8	1.6059E-0 7
APCDD1L	27.400351 1	-7.45622443	1.5292459 8	5.3786E-0 8	1.3618E-0 7
SLC12A9	45.193175 2	-7.46801465	1.9556241 6	2.011E-06	4.2579E-0 6

TMEM255B	28.479097	-7.47437379	1.2159517 3	6.9357E-1 1	2.3781E-1 0
XPO4	41.300561 2	-7.47715479	1.3054716 9	8.0006E-1 0	2.4413E-0 9
SCML1	48.238286 8	-7.50063931	1.2363423 9	1.1023E-1 0	3.6825E-1 0
RCBTB2	28.889587	-7.56483283	1.3039795 2	4.9302E-1 0	1.5356E-0 9
UNC5B	47.183495 6	-7.72222405	1.6708562 7	1.299E-07	3.1384E-0 7
IL1R2	44.066096	-7.77056018	1.4987589 2	1.0736E-0 8	2.9142E-0 8
EXO1	40.444232 8	-7.78498617	1.6867911 1	1.2822E-0 7	3.1024E-0 7
RNGTT	43.799566 7	-7.80032807	1.5675037 3	2.7782E-0 8	7.2204E-0 8
DBNDD2	40.873901 7	-7.8358239	1.2078327	5.7839E-1 2	2.2069E-1 1
NEURL1	49.609640 9	-7.83708068	1.2719506 1	4.5652E-1 1	1.5919E-1 0
EGFR	62.057854 2	-7.84559965	2.0028447 2	1.3103E-0 6	2.8383E-0 6
SERPINB7	48.484637 2	-7.85272784	1.2393894 5	1.5086E-1 1	5.5167E-1 1
ZER1	70.831790 2	-7.90972572	1.5686417	1.887E-08	4.9886E-0 8
APOLD1	47.924297 3	-7.98371642	1.7358074 4	1.1976E-0 7	2.906E-07
PKP1	48.020875	-8.06480693	1.4683036	1.7222E-0 9	5.0787E-0 9
SPATS2L	46.790100 3	-8.13898986	1.2680958 6	6.5663E-1 2	2.4886E-1 1
DROSHA	50.464161 3	-8.16760403	1.5216176 1	3.0101E-0 9	8.6395E-0 9
HIVEP1	56.622179 6	-8.20587797	1.5852659 1	7.6561E-0 9	2.1037E-0 8
DCTN4	68.338817 5	-8.35298148	1.3003085 3	4.9498E-1 2	1.9047E-1 1
SLC9A3R2	98.545523 9	-8.79960417	1.7401041 4	7.5734E-0 9	2.0835E-0 8
DNAL1	96.161244 5	-8.95905825	1.2717943 7	3.2983E-1 4	1.522E-13
ZDHHC16	102.43203 3	-8.97387069	1.2495023 1	1.1968E-1 4	5.7419E-1 4

IL1RL1	85.083859 4	-9.14041078	1.2164989 5	7.9783E-1 6	4.2599E-1 5
GGA1	85.113405 7	-9.40253269	1.2847490 9	2.3958E-1 5	1.2251E-1 4
VOPP1	623.75470 6	-10.0026011	1.1046226 5	5.1668E-2 2	4.2513E-2 1
SF1	200.41095	-10.2421935	1.2589642 8	1.1673E-1 8	7.6075E-1 8
ETV4	209.49249 4	-10.6941615	1.2574381 3	2.8472E-2 0	2.0557E-1 9
GPT2	41.738064 2	-20.561357	4.4879149 2	1.4954E-0 7	3.5847E-0 7
FAM111A	27.513287 7	-21.3477124	2.3635165 9	5.491E-20	3.8816E-1 9
HPCAL1	18.922393 8	-26.1626626	3.6228911 8	1.1996E-1 3	5.3217E-1 3
GRB7	17.177284 8	-26.5855827	3.8092507 8	6.5153E-1 3	2.6951E-1 2
ATRX	18.692909 5	-28.0129311	3.6456772 4	3.0982E-1 5	1.5595E-1 4
IDE	23.302538 2	-29.9572934	4.1114874	4.9712E-1 4	2.2631E-1 3
ARHGAP32	35.123367	-30.7069423	4.1117989 6	1.1653E-1 4	5.595E-14

Table 1: Gene expression alterations following berberine chloride and 5-FU combined treatment ( $|\log_2\text{FoldChange}| \geq 1$ )

gene_id	baseMean	log2FoldChange	lfcSE	pvalue	padj
GEN1	48.2752989	20.8943281	4.24144051	1.0682E-07	2.7901E-06
DICER1	28.2093486	20.5661335	4.26459779	1.63E-07	4.0391E-06
HERC2	94.7505987	10.6079368	6.43176134	9.9333E-05	0.00103065
UCKL1	37.3119761	7.23842503	1.57922352	7.4945E-07	1.5893E-05
ANO9	72.1606188	6.93306611	2.54808808	2.2167E-05	0.00028294
TFEB	15.4725759	4.24713248	4.22097968	0.00041848	0.00345671
MKNK1	20.9678984	4.22458737	4.13263282	0.00040111	0.00335419
S100A7	190.797286	2.74745397	0.28539428	1.7887E-23	4.8404E-21
PFKM	29.5319967	2.43992092	2.16802246	0.00023151	0.00208263
S100A9	1462.91681	2.36771158	0.17431243	1.4111E-44	2.3865E-41
S100A8	192.497983	2.15315597	0.23650511	8.6266E-23	2.1614E-20
UBA2	127.690237	2.12148489	0.36994698	1.0413E-11	6.1257E-10
PDZK1IP1	158.213471	1.87546227	0.27185086	5.0934E-15	5.6486E-13
APOBEC3A	37.4538358	1.8533181	0.48614899	8.661E-08	2.3251E-06
SPRR2A	50.869898	1.83764164	0.5219884	2.4404E-07	5.8752E-06
ADAM10	328.808713	1.76781828	0.36420722	1.0399E-09	4.4246E-08
ARHGEF11	13.9116538	1.74979311	3.1840304	0.00199263	0.01252804
ZNF808	11.2060697	1.65756281	2.96279735	0.0018939	0.01206423
MMP24OS	86.0229648	1.64743691	0.32405996	3.7868E-10	1.7427E-08
CXCL8	1085.33823	1.54955332	0.11450455	3.2077E-44	4.34E-41
SSBP1	52.4529367	1.52301313	3.31474968	0.00315573	0.01810732
PLAT	474.916071	1.36026227	0.148456	1.1567E-22	2.6983E-20
EBI3	53.5052569	1.26033267	0.38325301	9.7517E-07	1.9518E-05
CXCL1	589.986895	1.23804361	0.1647561	1.0142E-16	1.4294E-14
GBP2	468.748519	1.21664692	0.15416096	5.2547E-18	8.4638E-16
ZNF276	210.35578	1.18072593	0.32426752	3.5344E-07	8.1044E-06
SPRR1B	174.407933	1.17313078	0.28785774	6.9083E-08	1.9111E-06
BTBD19	49.7724835	1.15226314	1.91347266	0.00145739	0.00974232
TNFRSF9	135.693663	1.12017738	0.16836546	5.7649E-14	5.2702E-12
RABGGTA	64.200942	1.10619301	0.23241638	3.8923E-09	1.4468E-07
RASA4	134.19646	1.09474624	0.27339655	1.1151E-07	2.885E-06
SNAI1	182.787687	1.07756689	0.21094717	7.3678E-10	3.2366E-08
GCNT3	37.3254066	1.06199118	0.39668577	9.3771E-06	0.00014035
LRG1	560.690483	1.05999442	0.12133522	5.5027E-21	1.1633E-18
NCCRP1	83.6492264	1.05997647	0.25254379	5.6323E-08	1.581E-06
HEXD	77.9152801	1.02456264	0.44136015	2.5561E-05	0.00031787
PAQR8	194.455645	1.00069861	0.17060183	1.4673E-11	8.412E-10
MPRIIP	648.506425	-1.02073328	0.16047822	6.0078E-13	4.7815E-11
ZNF692	19.2062808	-1.03879386	1.93643998	0.00205688	0.01284841
FER	13.1910257	-1.04477383	2.40287111	0.00374087	0.0206218
CHM	17.7260053	-1.05240587	2.53096837	0.00420685	0.02271297
SLC6A9	852.69058	-1.07346055	0.14627319	4.9138E-16	6.1559E-14

PRPSAP2	90.2188245	-1.08955773	0.25304688	3.249E-08	9.7255E-07
SWT1	13.3880671	-1.10840413	2.46640126	0.0034156	0.01930368
RAPGEF2	26.5203623	-1.13427292	2.49566675	0.00331137	0.01884056
PHGDH	5928.46182	-1.17055365	0.0783282	2.8249E-53	9.5554E-50
CHAC1	448.031602	-1.20693611	0.14265172	4.6854E-20	8.8047E-18
RUFY2	74.2374797	-1.21424222	0.30467434	9.0836E-08	2.4289E-06
TMEM116	10.97262	-1.24609025	2.27079795	0.00194237	0.01225863
KLHL3	19.3897664	-1.31230925	2.59185391	0.00246439	0.01492536
WDR44	13.0785369	-1.32478025	2.25547644	0.00159419	0.0105114
CAMKK2	125.952857	-1.38802998	0.56991644	8.3736E-06	0.00012758
ATAT1	11.3229054	-1.41739946	2.69026438	0.00221419	0.01365449
ULBP1	122.952744	-1.43349474	0.26929902	1.4123E-10	7.1299E-09
ATP11A	35.6784858	-1.47825727	2.19371558	0.00105986	0.00759531
PSAT1	105.063878	-1.53000237	0.45528443	5.0186E-07	1.1095E-05
STC2	1515.36903	-1.53868109	0.12176487	4.1699E-39	3.1344E-36
ZNF195	14.9792906	-1.54730381	2.79403236	0.00193744	0.01225612
ASNS	328.011923	-1.55014975	0.14136498	1.564E-30	5.8781E-28
DEPDC1B	10.8103552	-1.59522416	2.56115991	0.0013777	0.00931081
ZNF487	13.953818	-1.61732557	2.65160367	0.00147141	0.00979731
MAST3	9.71938311	-1.64077109	2.622952	0.00136759	0.00927959
CTH	518.874606	-1.68229619	0.13209734	7.5692E-40	6.4007E-37
SLC7A11	980.278401	-1.69195692	0.13453276	5.4645E-39	3.6967E-36
ZNF695	7.61326915	-1.72081083	2.52927263	0.00106795	0.00764516
GLT8D1	61.7497246	-1.77023058	0.61995641	1.9344E-06	3.6451E-05
ZSWIM9	16.8120236	-1.92669499	3.08742389	0.00141594	0.00952168
NUPR1	397.889879	-2.02369767	0.15553742	7.2613E-42	7.0176E-39
GRAMD2A	13.0650717	-2.1308511	3.22677673	0.00122314	0.00853048
POLK	47.0288926	-2.34684381	2.71572065	0.00055548	0.00437978
SH2D4A	11.2267486	-2.40376861	2.91148094	0.00064821	0.00502307
ARHGAP33	18.2387136	-2.4078109	2.26390567	0.00028007	0.00246383
RDH13	8.02336108	-2.5130272	2.72186786	0.00046237	0.00372817
ALDH1L2	958.58583	-2.53036466	0.20530541	5.9229E-37	3.0822E-34
ZNF182	16.150144	-2.57158776	3.47385267	0.00091176	0.00667536
KIF20B	52.6864488	-2.59275734	3.83695349	0.00116558	0.00818811
DGKA	19.0144869	-2.70012108	3.45597246	0.00078952	0.00592375
ZNF41	15.5246401	-2.899403	3.02767635	0.00043899	0.003578
CYP1A1	640.570265	-3.14272035	0.25871223	1.3718E-34	6.6289E-32
WAC	384.601562	-3.20515211	1.26693438	1.1697E-05	0.000168
WSB1	78.3846497	-3.44816944	4.12494162	0.00067477	0.00519907
ZNF320	22.1123781	-3.62495965	3.66619823	0.00042958	0.00353114
SEC16A	117.72324	-3.66161226	4.48882017	0.00071692	0.0054864
PLSCR3	10.7078474	-3.78635011	2.94733147	0.00019833	0.00182542
MTMR10	22.7355376	-3.98430076	4.07640852	0.00045011	0.00364267



N4BP2L1	11.2972157	-4.20172796	2.93721623	0.00014961	0.00144796
RPGRIP1L	16.7664243	-4.21379858	2.32295416	6.8307E-05	0.00075016
CASP1	50.048387	-4.22611172	0.61933419	4.8971E-12	3.1854E-10
KANSL1	27.8076208	-4.26552748	3.13194604	0.00017576	0.0016632
PAN2	20.1507872	-4.45299279	2.30384657	5.7558E-05	0.0006436
DENND4A	27.0400727	-4.47015306	3.88417799	0.00029234	0.00255842
SCAPER	34.5911319	-4.50698224	0.761762	1.5922E-09	6.4113E-08
USP45	10.1795321	-4.80901017	2.74235163	8.4542E-05	0.00089363
PIH1D2	8.92628094	-4.9186265	2.64816363	7.1074E-05	0.00077526
SLC10A7	36.4497011	-4.92532781	1.82904862	1.8361E-05	0.00024213
SLC52A1	18.4271801	-4.95368275	2.53387948	6.0229E-05	0.00067125
GPANK1	11.939964	-5.03977213	2.73054552	7.3649E-05	0.00079718
MCTP2	72.9327528	-5.05283116	3.26621421	0.00012817	0.00126755
FRYL	106.72738	-5.174693	1.4934299	5.8886E-06	9.2859E-05
RBM38	22.9584112	-5.68708726	1.74824286	9.1301E-06	0.00013756
UBXN2B	56.4573335	-5.7114001	1.02833685	1.4527E-08	4.7707E-07
PNISR	111.063942	-5.82758214	3.70820442	0.00012694	0.00126103
CPLANE1	18.2679937	-5.85642357	1.51745845	3.4729E-06	6.0396E-05
SYTL3	19.4748415	-5.94026641	1.94525222	1.2752E-05	0.00017935
MRPL4	25.2017225	-6.12234093	2.56135374	3.4205E-05	0.0004081
NAP1L4	46.9591135	-6.15889589	2.49029017	3.0357E-05	0.00036936
RBM23	16.0229287	-6.32106869	1.49163237	1.7422E-06	3.3106E-05
ORC3	27.121763	-6.47242921	2.18291472	1.5262E-05	0.00020609
DTL	18.6418634	-6.6249049	2.18769573	1.4069E-05	0.00019374
ENTPD5	49.5499976	-6.69387787	1.90706081	6.8375E-06	0.00010585
ZNF236	38.7699095	-6.79495475	1.32181275	1.0225E-07	2.7022E-06
TANC1	33.5421074	-6.8703944	1.77925113	3.816E-06	6.5521E-05
SIN3A	63.464879	-6.87734188	1.91565276	6.0737E-06	9.5556E-05
INTS14	22.3652055	-6.911465	2.20895785	1.2337E-05	0.0001746
RPS6KC1	20.2627515	-6.92565503	2.2110051	1.2281E-05	0.00017418
NEDD4L	33.3351037	-7.16862616	2.20282492	1.0349E-05	0.00015187
SLC7A1	71.4215509	-7.31201095	2.62206728	2.0339E-05	0.0002641
RO60	26.4894193	-7.61762675	2.25662049	8.6828E-06	0.00013141
ZMYND11	36.1866023	-7.63476427	1.47151371	7.3987E-08	1.9941E-06
EFR3A	28.7007022	-7.79417069	1.85505576	1.944E-06	3.6531E-05
FBXL5	47.7331899	-7.86543495	1.41104003	9.71E-09	3.3009E-07
PPT2	48.6287044	-8.04598115	1.93483961	2.1183E-06	3.9368E-05
VRK2	40.951873	-8.0840614	1.65531498	2.5395E-07	6.0706E-06
BRD1	142.73165	-8.35943268	2.09063937	2.9219E-06	5.1744E-05
RAB35	43.9133392	-8.69526528	1.46980953	1.089E-09	4.6044E-08
RAF1	14.627801	-14.8943232	4.27158914	5.5589E-06	8.8803E-05
GATD1	53.4473333	-21.4063974	2.51004498	3.5858E-18	5.9166E-16
TCF3	34.1135967	-21.4367481	2.26913965	8.8007E-22	1.9846E-19

AHCTF1	38.9610598	-26.4677167	4.11872931	2.3282E-11	1.2702E-09
NSD2	33.7333104	-27.0987022	4.1143758	7.7562E-12	4.6456E-10

Table 2: Compared with 5-FU treatment, gene expression alterations following berberine chloride and 5-fu combined treatment ( $|\log_2\text{FoldChange}| \geq 1$ )